AD-F300038

AD A114950

AD

MEMORANDUM REPORT ARBRL-MR-03164

EXPERIMENTAL VALIDATION FOR THE UNIQUENESS OF THE DIFFERENTIAL PRESSURE-MAXIMUM PRESSURE SENSITIVITY CURVE FOR CHARGE SAFETY ASSESSMENT

Carl R. Ruth
Albert W. Horst

April 1982

US ARMY ARMAMENT RESEARCH AND DEVELOPMENT COMMAND
BALLISTIC RESEARCH LABORATORY
ABERDEEN PROVING GROUND, MARYLAND

DTIC FILE COPY

UNCLASSIFIED

SECURITY CLASSIFICATION OF THIS PAGE *(When Data Entered)*

REPORT DOCUMENTATION PAGE

READ INSTRUCTIONS BEFORE COMPLETING FORM

1. REPORT NUMBER Memorandum Report ARBRL-MR-03164	2. GOVT ACCESSION NO. AD-A114950	3. RECIPIENT'S CATALOG NUMBER
4. TITLE *(and Subtitle)* Experimental Validation for the Uniqueness of the Differential Pressure-Maximum Pressure Sensitivity Curve for Charge Safety Assessment		5. TYPE OF REPORT & PERIOD COVERED Memorandum Report 1 Oct 78 - 30 Sep 80 6. PERFORMING ORG. REPORT NUMBER
7. AUTHOR(s) Carl R. Ruth and Albert W. Horst		8. CONTRACT OR GRANT NUMBER(s)
9. PERFORMING ORGANIZATION NAME AND ADDRESS U.S. Army Ballistic Research Laboratory ATTN: DRDAR-BLI Aberdeen Proving Ground, MD 21005		10. PROGRAM ELEMENT, PROJECT, TASK AREA & WORK UNIT NUMBERS 1L162618AH80
11. CONTROLLING OFFICE NAME AND ADDRESS U.S. Army Armament Research & Development Command U.S. Army Ballistic Research Laboratory (DRDAR-BL) Aberdeen Proving Ground, MD 21005		12. REPORT DATE April 1982 13. NUMBER OF PAGES 126
14. MONITORING AGENCY NAME & ADDRESS *(if different from Controlling Office)*		15. SECURITY CLASS. *(of this report)* Unclassified 15a. DECLASSIFICATION/DOWNGRADING SCHEDULE

16. DISTRIBUTION STATEMENT *(of this Report)*

Approved for public release; distribution unlimited

17. DISTRIBUTION STATEMENT *(of the abstract entered in Block 20, if different from Report)*

18. SUPPLEMENTARY NOTES

19. KEY WORDS *(Continue on reverse side if necessary and identify by block number)*

Interior ballistics
Pressure waves
Guns
155-mm Howitzer

delta P sub i

P sub max

20. ABSTRACT *(Continue on reverse side if necessary and identify by block number)*

jmk

One of the most used indicators of the level of longitudinal pressure waves in the gun environment is $-\Delta P_i$, the first negative minimum of the pressure difference curve measured between the breech and forward ends of the chamber. A current procedure for propelling charge safety assessment by the U.S. Army employs the correlation between $-\Delta P_i$ and P_{max}, the maximum chamber pressure, in order to project the expected probability of exceeding a given pressure limit. Major concerns exist both in terms of how to generate a P_{max} vs. $-\Delta P_i$ sensitivity

DD FORM 1473 1 JAN 73 EDITION OF 1 NOV 65 IS OBSOLETE

UNCLASSIFIED

SECURITY CLASSIFICATION OF THIS PAGE *(When Data Entered)* curve and whether the curve is unique for a given charge/weapon interface. This study addresses one aspect of the problem, that of uniqueness, and hence the applicability of a curve generated by means of intentionally faulted igniter systems with respect to the broader and more ill-defined class of failures experienced over many firings in the field. Within the limits of reasonable occasion-to-occasion differences and possible experimental errors, the existence of significantly different P_{max} vs. $-\Delta P_i$ curves for a given charge/weapon combination was not demonstrated in this study. However, apparent differences were revealed in the ease with which one could generate substantial pressure waves in similar charge configurations using different propellant production lots. These results suggest that variations in propellant associated with different production lots may impact overall charge safety, and that current charge safety assessment procedures employing test results from a single lot of propelling charges (and hence a single propellant lot) may not be adequate for the prediction of failure rates.

TABLE OF CONTENTS

LIST OF ILLUSTRATIONS

LIST OF ILLUSTRATIONS (Continued)

LIST OF TABLES

I. INTRODUCTION

Safety must always be one of the major concerns of the propelling charge designer. Any candidate charge design must ultimately be shown to be safe to produce, handle, ship, store, load, fire, and eventually demilitarized. In this study, we confine our interest to safety during the firing operation and, in particular, to problems resulting from overpressures, which may be related to pressure waves in the gun chamber. As pointed out by Budka and Knapton[1], "researchers have revealed one common characteristic associated with the occurrence of unexpected high pressure excursions--namely, the existence of strong pressure waves in the gun system." Yet many weapons with excellent safety records exhibit pressure waves, some at substantial amplitudes. Techniques for distinguishing between acceptable and unacceptable amplitudes of pressure waves are based on philosophies that range all the way from "she ain't blown yet, so why worry now?" to "all pressure waves are unacceptable!" While both views may be considered impractical, the more conservative approach finds its origin in the costly experiences of numerous catastrophic gun malfunctions[2-7], where large pressure waves served as precursors to the overpressure or premature functioning of the payload. Further motivation arises from our lack of understanding of the detailed phenomenology of such failures, as articulated nearly three

---

[1] *A. J. Budka and J.D. Knapton, "Pressure Wave Generation in Gun Systems: A Survey," Ballistic Research Laboratory, Aberdeen Proving Ground, MD, Memorandum Report 2567, December 1975. (AD #B008893L)*

[2] *D. W. Culbertson, M. C. Shamblen, and J. S. O'Brasky, "Investigation of 5"/38 Gun In-Bore Ammunition Malfunctions," Naval Weapons Laboratory, Dahlgren, VA, TR-2624, December 1971.*

[3] *M. C. Shamblen and J. S. O'Brasky, "Investigation of 8"/55 Close Aboard Malfunctions," Naval Weapons Laboratory, Dahlgren, VA, TR-2753, April 1973.*

[4] *P. J. Olenick, "Investigation of the 76-mm/62 Caliber Mark 75 Gun Mount Malfunctions," Naval Surface Weapons Center, Dahlgren, VA, TR-3411, October 1975.*

[5] *E. V. Clarke, Jr. and I. W. May, "Subtle Effects of Low-Amplitude Pressure Wave Dynamics on the Ballistics Performance of Guns," 11th JANNAF Combustion Meeting, CPIA Publication 261, Vol. 1, pp. 141-156, December 1974.*

[6] *A. W. Horst, I. W. May, and E. V. Clarke, Jr., "The Missing Link Between Pressure Waves and Breechblows," USA ARRADCOM, Ballistic Research Laboratory, Aberdeen Proving Ground, MD, Memorandum Report 02849, July 1978. (A058354)*

[7] *K. H. Russel and H. M. Goldstein, "Investigation and Screening of M17 Propellant Production for Lots Subject to Poor Low Temperature Performance, Picatinny Arsenal, Dover, NJ, DB-TR-7-61, June 1961.*

decades ago by the British interior ballistician Lockett[8], "It might be pertinent to point out...that there is always some uncertainty in the interpretation of what might be dismissed as minor irregularities in the pressure-time curve. We have by bitter experience learned to regard such irregularities with a degree of suspicion...because of the apparent ease with which such minor flaws can turn over to major irregularities by some mechanism not yet understood."

The problem of breechblows is of most concern to the U.S. Army with respect to the design of high performance artillery bag charges. A typical layout for such a charge is presented schematically in Figure 1. Principal

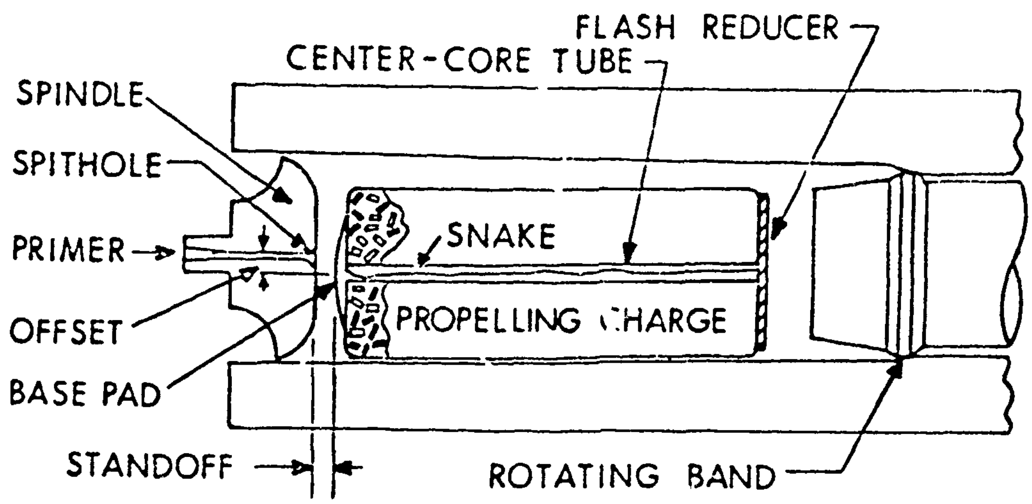

Figure 1. Typical Centercore-Ignited Artillery Propelling Charge

components of the charge include a basepad igniter (usually containing black powder or CBI*), a centercore igniter tube (containing additional igniter material), and a main charge (typically multi-perforated, triple-base, granular propellant). A cloth bag is employed to contain the charge, and other components such as a flash inhibitor or wear-reducing additive may be present. We postulate functioning of the charge to be described by the following sequence of events. The basepad igniter is initiated by the impingement of hot combustion products from a percussion primer. The basepad then ignites the centercore charge, and together they ignite nearby propellant grains. Combined igniter and propellant gases penetrate the propellant bed, convectively heating the grains and resulting in flamespread. During this process, the pressure gradient and interphase drag forces tend to accelerate the propellant grains, largely in the forward direction,

---

[8] *N. Lockett, "British Work on Solid Propellant Ignition,"* *__Bulletin of the First Symposium on Solid Propellant Ignition__, Solid Propellant Information Agency, Silver Spring, MD, September 1953.*

* *"Clean Burning Igniter," a nitrocellulose-based ignition material.*

thrusting them and any intervening elements against the projectile base. Upon stagnation, a reflected compression wave in the gas phase may be formed, its magnitude being subject to the combined effects of reduction in free volume (due to bed compaction) and combustion in this low-porosity region.

If the charge functions as intended, smooth pressure-time curves as shown in Figure 2 are obtained. A pressure-difference history, formed by subtracting the pressure measured by a gage in the chamber wall near the initial position of the projectile base (hereafter identified as the chamber mouth) from the breech pressure as a function of time, reveals only the normal forward-facing gradient associated with motion of the projectile down the tube. On occasion, however, pressure-time histories as shown in Figure 3 are obtained. High-amplitude, longitudinal pressure waves are clearly

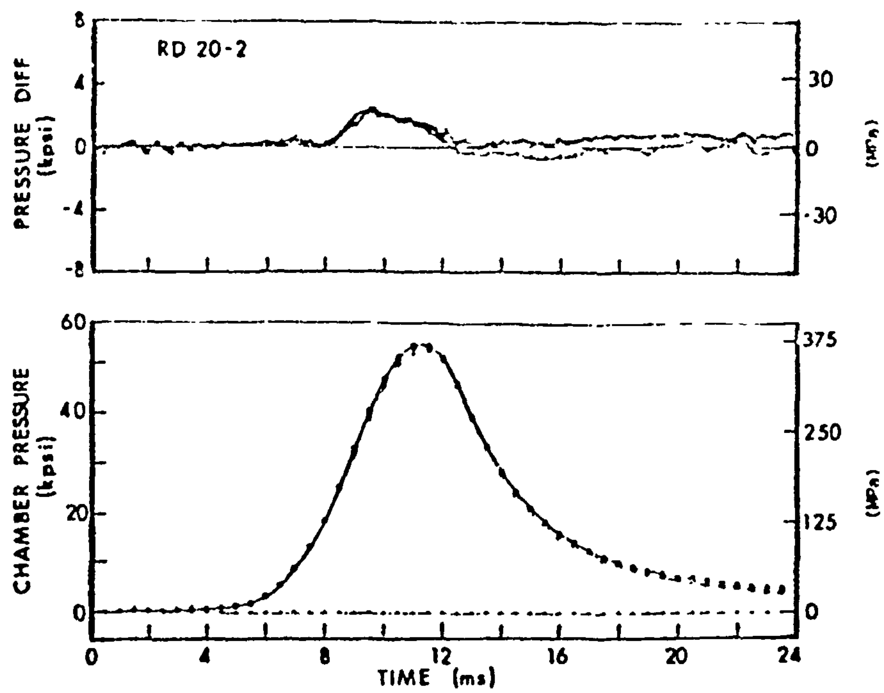

Figure 2. Pressure-Time and Pressure-Difference Profiles for a Properly-Ignited, High-Performance Charge

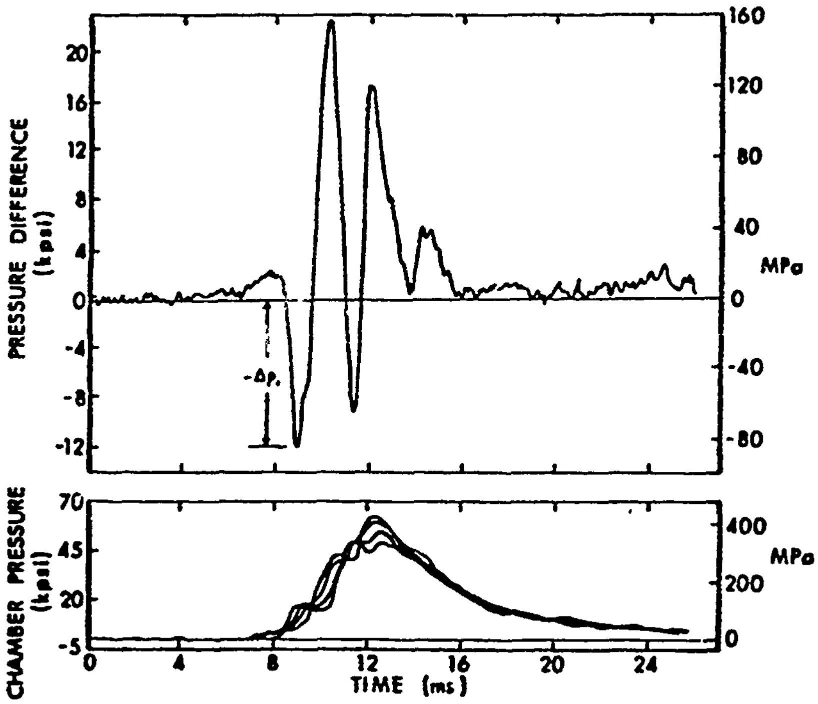

Figure 3. Pressure-Time and Pressure-Difference Profiles, Localized Base Ignition

manifested in the pressure-difference plot. Such phenomena have been traditionally associated with localized ignition of the propellant bed and thus may imply non-functioning or at least late functioning of the centercore charge. Whether this wave dissipates or grows is dependent on a complex interplay of events including gas production rates, ullage, bed permeability and projectile motion. Thus, other factors in addition to proper functioning of the ignition train may be of importance. Finally, increases in maximum chamber pressure may or may not accompany such increases in pressure-wave dynamics. The extreme cases which generate large pressure waves may result in breechblows (see Figure 4).

In this study, we address the validity of a fundamental assumption on which is based the procedure currently used by the U.S. Army to evaluate the influence of pressure waves on those aspects of system safety related to maximum chamber pressure.

II. TECHNICAL DISCUSSION

A. Current Procedure

As one facet of the overall safety assessment procedure for new propelling charges for artillery, the Ballistic Research Laboratory (BRL)

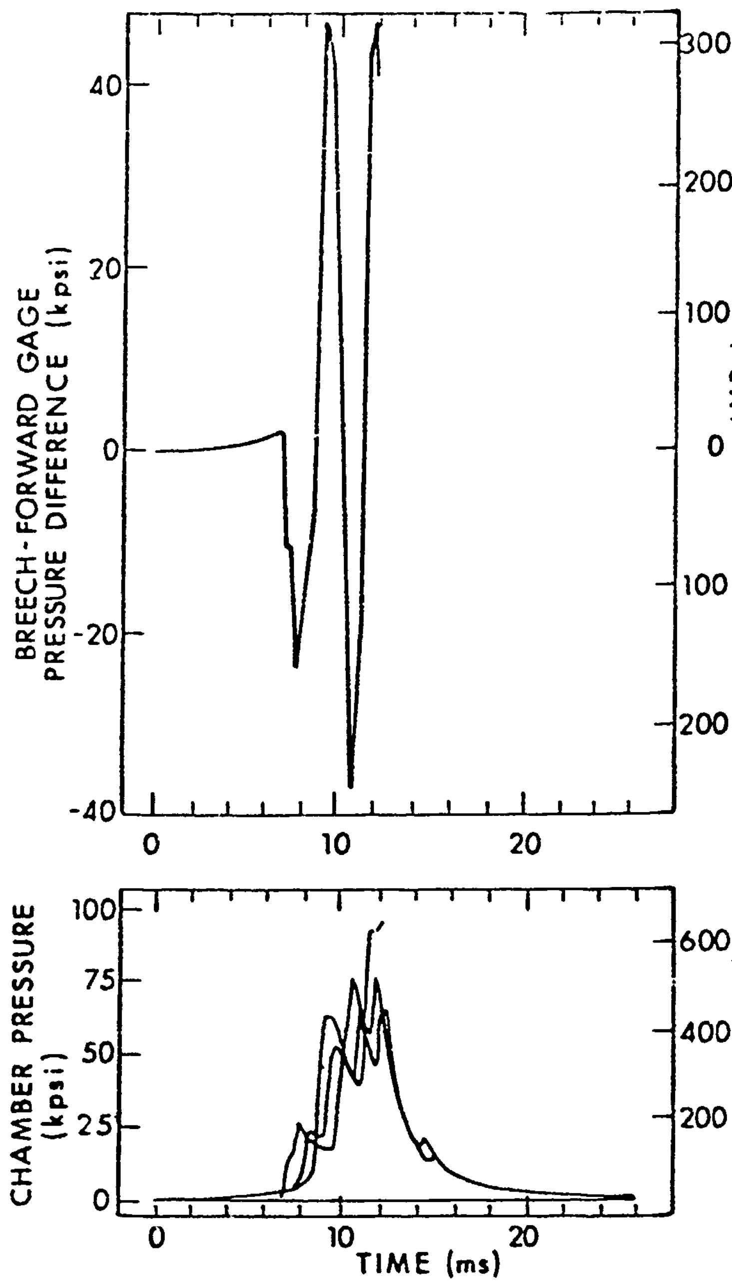

Figure 4. Catastrophic Pressure-Wave Dynamic Behavior Observed in a 175-mm Gun Firing (APG FR P-82501)

is often asked to comment on safety of the charge, particularly with respect to any deleterious effects of pressure waves. While problems arising from transient loads on the projectile base (both gas and solid phase) associated with the presence of pressure waves will not be addressed in this report, the influence of pressure waves on maximum chamber pressure can be assessed in the following manner:

(1) Charge design sensitivity firings are conducted to determine the relationship between $-\Delta P_i$ and maximum chamber pressure for the charge/weapon combination. Intentionally-altered centercore or base-ignited charges may be included to assure that data from a localized ignition will result in a large $-\Delta P_i$ for a reasonable number of tests. More recent assessments of base-ignited charges have included sensitivity testing with special charges in which faster-burning igniter materials have been substituted for the standard material.

(2) A failure criterion is identified, usually in terms of some maximum chamber pressure, dictated most often by breech or payload failure levels.

(3) This failure level is reinterpreted in terms of a $-\Delta P_i$ level, determined from the sensitivity curve developed in Step (1).

(4) A sample population of firing data is then obtained which is believed to be representative of "real-world" propelling charges, typical of those to be fielded for use. One or more statistical distributions are fit to these data.

(5) The probability of failure (as defined in Step (3)) can then be statistically determined with respect to the distribution of $-\Delta P_i$ values from Step (4).

An alternate form of this procedure is possible if the sample population of firing data described in step (4) is available prior to sensitivity testing. Based on this population, the $-\Delta P_i$ value to be associated with the highest, acceptable probability for failure can be statistically projected, and sensitivity testing to determine the corresponding chamber pressure need not be continued beyond that point. In this fashion, while we do not necessarily determine the $-\Delta P_i$ value corresponding to the maximum pressure failure criterion, we do ensure that this pressure limit is not exceeded at that $-\Delta P_i$ level projected to occur at a frequency equal to the highest allowable probability for failure. This alternate plan, in some cases, may significantly reduce the risk of catastrophic overpressure during sensitivity testing.

Application of the basic procedure can be demonstrated with respect to a data base available for the 175-mm, M107 gun. The relationship between $-\Delta P_i$

and maximum chamber pressure for M86A2, Zone 3 charges fired in the M107 gun, based on charge design sensitivity firings, is presented in Figure 5. A $-\Delta P_i$ failure criterion can also be identified on this curve, corresponding to a known breech failure pressure level. Figure 6 then presents the cumulative distribution of $-\Delta P_i$ levels for a data base considered to represent a typical population of "real-world" M86A2, Zone 3 charges. The probability of achieving the $-\Delta P_i$ failure level, as determined using Kolmogorov-Smirnov statistics and two different population distribution functions, is presented in Figure 7. The prediction of one failure in about half a million firings compares quite favorably with historical data of half a dozen breechblows in some two and one-half million firings to date. This agreement, although satisfying, must be considered somewhat fortuitous.

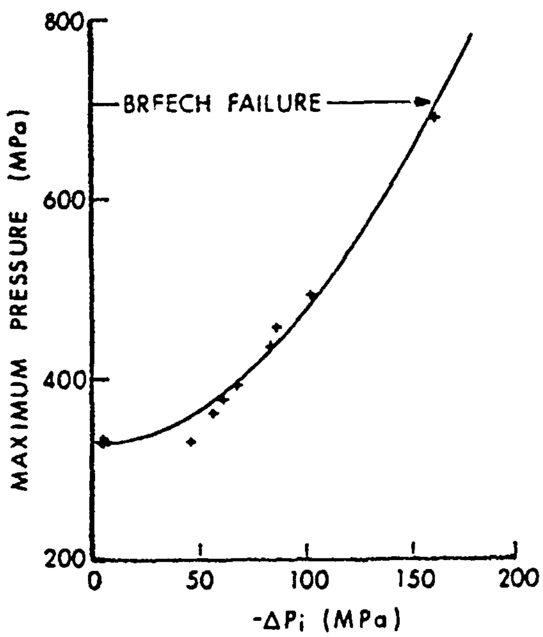

Figure 5. Pressure-Wave Sensitivity for a 175-mm, M107 Gun (M86A2 (Zone 3) Propelling Charge)

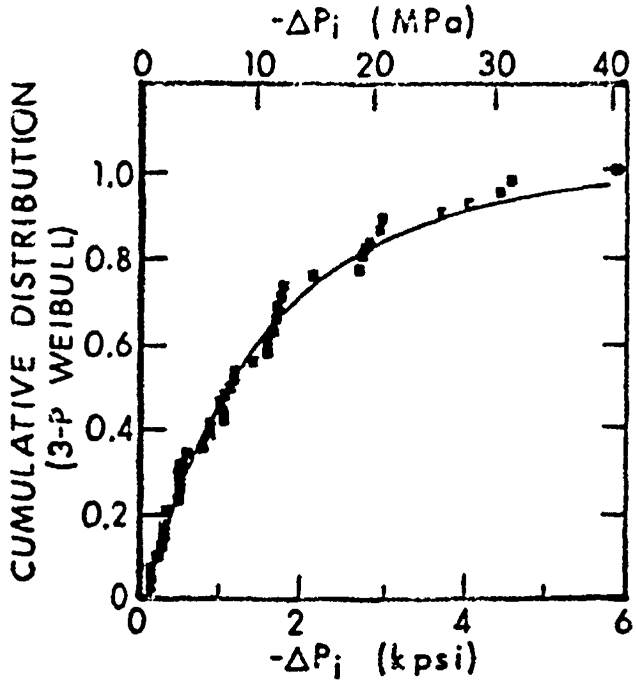

Figure 6. Distribution of Pressure-Wave Amplitudes for the 175-mm, M107 Gun (M86A2 (Zone 3) Propelling Charge)

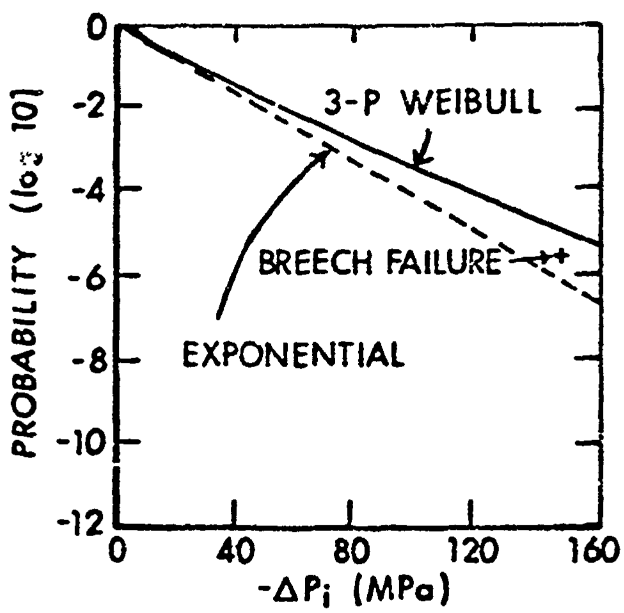

Figure 7. Probability of High-Amplitude Pressure Waves for the 175-mm, M107 Gun (M86A2 (Zone 3) Propelling Charge)

B. Problem Areas.

There exists, unfortunately, a number of areas of concern associated both with the physical foundation for and application of the assessment procedures just described. Treating the latter first, many times it is impossible to achieve good fits of statistical distribution functions to the experimentally obtained populations of $-\Delta P_i$ data. This may be, in part, a consequence of the fact that $-\Delta P_i$ is not the most physically well-motivated parameter of interest; this possibility is under separate investigation. In addition, use of the Kolmogorov-Smirnov statistic to provide an extrapolation to failure levels well outside the range of experimental data leads to extremely broad confidence bands associated with the prediction.

The current study, however, was not motivated by these or any related concerns. Rather, it deals with the major physical assumption on which the assessment procedure is based, that being the existence of a unique relationship between $-\Delta P_i$ and P_{max} for a given propelling charge/weapon combination. The uniqueness of this relationship is essential first to allow generation of the sensitivity curve via intentionally-altered ignition systems and second to assume applicability of a curve so generated to the much broader class of failures that occur over many years of fielded uses of production charges.

Having said this, we immediately weaken the requirement to "nearly unique." It is clear that a detailed analysis of the chemically reacting, two-phase flow processes leading to pressure waves in guns and linking their presence to increases in peak pressure will lead us to the conclusion that in the limit this relationship cannot be unique. Moreover, if these processes include such mechanisms as mechanical failure of propellant grains, one should expect some variation in performance even for virtually identical firing conditions. The key question then becomes whether or not the P_{max} vs $-\Delta P_i$ relationship is near enough to being unique to be useful.

Since the early systematic studies of May and Clarke[5], much has been learned about the nature of this relationship. One major factor influencing the sensitivity curve is the initial temperature of the propelling charge. If one ascribes pressure increases accompanying high levels of pressure waves to grain fracture, as suggested by Horst et al.[6], the increasing sensitivity of peak pressure to pressure waves for cold-conditioned charges is not surprising, as an increased brittleness of propellant grains at cold temperatures has been demonstrated experimentally[7]. This complicating feature of the P_{max} vs $-\Delta P_i$ relationship merely requires performing the described safety assessment procedures at both hot and cold temperature extremes.

As the failure pressure for the system may also be temperature-dependent, the role of initial temperature will have to be considered throughout the analysis. Similar though smaller corrections may be, at least conceptually, applied for any influence on P_{max} vs $-\Delta P_i$ sensitivity imparted by projectile type, wear state of the gun, recoil system, etc..

In the area of ignition system modifications, however, no such correction is possible and hence the requirement for approximate uniqueness is absolute. Since modifications to the ignition system are intentionally introduced to assure the generation of large-amplitude pressure waves with reasonably few firings, we assume that the curve so generated would not have been different had we selected another set of igniter modifications for testing. While different faults may or may not lead to different pressure-wave levels, a single sensitivity curve must be defined by all such $-\Delta P_i$, P_{max} data pairs. It is with this fundamental assumption that the following study deals.

III. 155-mm HOWITZER FIRINGS

Since major concerns exist both in terms of how to generate a P_{max} vs $-\Delta P_i$ sensitivity curve and whether such a curve, once generated, is unique and universally applicable to a given charge/weapon interface, an experimental investigation was undertaken to quantify the effects of deliberately induced high-amplitude pressure waves on the peak chamber pressure exhibited by a high-performance artillery charge. The parameters varied to induce the waves were charge diameter, charge standoff, and ignition train characteristics (configuration, interfaces, basepad composition, etc.).

A. Charge Design and Construction

Standard 155-mm, M203 Propelling Charges, Lots IND-78H-069806, IND-78F-069805, and IND-79K-069960 were obtained for testing from Project Manager, Cannon Artillery Weapons System. The M203 Charge is the top zone (8S) for the U.S. Army 155-mm, M198 Towed Howitzer. Depicted in Figure 8, this charge employs M30A1 triple-base propellant, ignited by a basepad and centercore ignition system employing Class 1, Black Powder. The test charges were fabricated by unloading the standard M203 charges, making the desired changes to the igniter tube, snake, basepad, etc., and then reloading the standard 7-perforation propellant. Since the possibility of catastrophic failure of the gun or breech exists with tests of this nature, the charge weight for all tests was reduced from the standard 11.80 kg to 10.89 kg. Fabrication of the full-bore charges was accomplished by modifying the bag by inserting a tapered wedge of cloth to form a sleeve wherein the spindle end was larger in diameter than the forward chamber end. The standard 7-perforation propellant was then reloaded into the full-bore bags. The excess material caused by the downloading of the charges was removed and the front end-cover was sewn back on. The reassembled charges were then each secured in a lacing jacket to give the charge rigidity and maintain component integrity. All charge modifications (loading, bag sewing, basepad

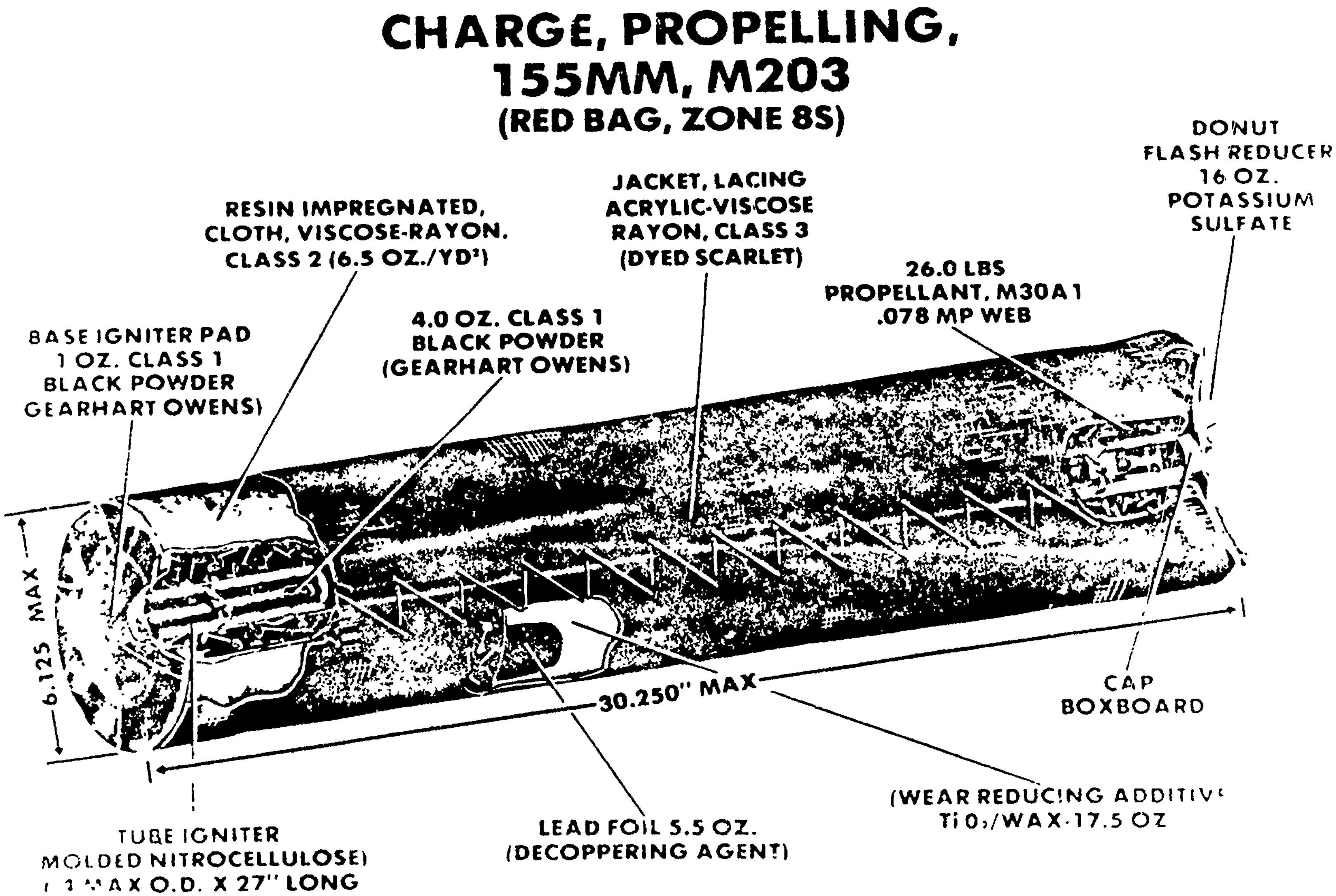

Figure 8. Standard M203 Propelling Charge (Zone 8).

and centercore revamping, etc.) were done either at the BRL or the Material Testing Directorate (MTD). Table 1 provides a general outline of the charge types tested in this study. All charges were conditioned at a temperature of 295-300 K for at least 24 hours prior to firing. The charges were loaded into the cannon chamber at varying stand-offs (distance from spindle face to base of propellant basepad) depending on the requirements of the test. Standard M101, inert-loaded projectiles, Lot E-SXH-2-6-57, available at the BRL, were used for all firings. The weight of the projectiles (43.63 ± .04 kg) was accurately monitored by using on-post MTD loading facilities.

B. Test Procedure

All firings were conducted at the BRL Sandy Point Firing Facility (R-18) in an M185 Cannon, modified to provide a chamber configuration similar to that of the M199 Cannon (see Figure 9). Multiple station pressure-time data, differential pressures, and projectile velocities were recorded by the Ballistic Data Acquisition System (BALDAS), under the control of a PDP11/45 minicomputer. Pressures were measured using Kistler 607C3 piezoelectric transducers, and projectile velocity was measured by solenoid coils approximately 20 and 35 meters from the muzzle. Ignition delays were recorded by measuring the interval between the time the firing pulse was sent to the gun to the time a pressure of 10 MPa was first detected on the spindle gage. A backup analog magnetic tape system also recorded all data.

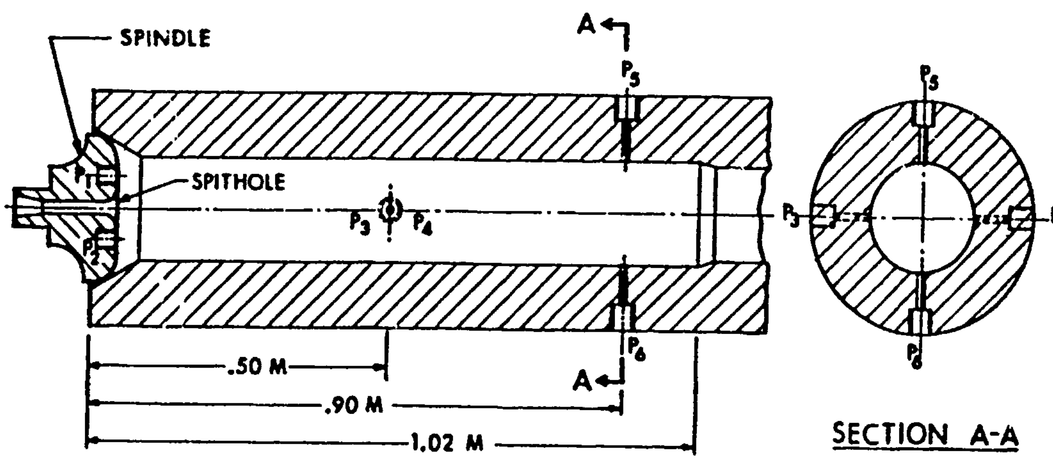

Figure 9. Locations of Pressure Taps in the Modified, M185 Cannon (Range 18)

TABLE 1. CHARGE FABRICATION PARAMETERS*

Propellant Lot	Series	Charge Diameter	Basepad	Nitrocellulose Centercore	Black Powder Snake	Comments
RAD-77H-069806**	1	Std	Std	Std	Std	Series 1 is the "standard" for comparison in these tests.
	2-3-4	"	"	"	None	Black powder (BP) snake removed from nitrocellulose (NC) centercore
	7-8	"	"	"	Modified	1/2 BP snake removed. Remainder (56 g) at front end of NC tube.
	11-12	"	"	"	"	BP removed from snake and placed at front of NC tube (112 g). Wad of cottonwaste held BP inplace in NC tube.
	9-10	"	"	None	None	Base-Ignited
	5-6	Full-Bore	"	"	"	Base-Ignited
RAD-79E-069960	13	"	Modified	"	"	Two Part:*** 28 g BP, Class 5 Basepad 56 g CBI
	14	"	"	"	"	Basepad: 84 g BP, Class 1
	15	Std	"	"	"	Basepad: 84 g BP, Class 3
RAD-77G-069805	16	Full-Bore	"	"	"	Two Part:*** 28 g BP, Class 5 Basepad 56 g CBI
	17	"	"	"	"	Two Part:*** 28 g BP, Class 5 Basepad 56 g CBI Propellant: Bottom 1/3 stacked
	18	"	"	"	"	Basepad: 84 g CBI
	19	"	"	"	"	Basepad: 84 g BP, Class 5

* All charges weighed 10.89 kg. Series 1 is the "standard" series. Reduced charge weight shortened length of charge and NC tube.

** Basepad for Test Series 1-12 was 28 g BP, Class 1.

*** Basepad divided into two concentric circles. The center circle contained BP; the remaining area contained CBI.

C. Firing Results

Nineteen series of test firings, encompassing many experimental parameters, were fired over a two-year period. Results will be discussed, not in chronological order of firing, but according to the three propellant lots into which all the series fall. Table 1 nomenclature will be employed throughout the discussion. Averaged firing data for each series are tabulated in tables throughout the report with computer-generated plots of selected data channels (spindle and forward pressure vs. time, pressure-difference vs. time) included as the Appendix.

1. Propellant Lot RAD-77H-069806.

a. Standard-Diameter Charge, Standard Centercore; Series 1. Centercore-ignited, standard-diameter charges, with no changes to the ignition system and downloaded to 10.89 kg of propellant, were tested at zero standoff from the spindle face. Past data[6] suggested that no standoff between the spindle face and propelling charge promoted the formation of pressure waves. Baseline firing data for this loading condition were required to ensure that pressures and pressure waves with this charge weight would be at safe levels. A four-round series yielded average values for P_{max} and $-\Delta P_i$ of 262 MPa and 13 MPa respectively, with a maximum individual $-\Delta P_i$ of 26 MPa. Average values for projectile velocity and ignition delay were 758 m/s and 44 ms, respectively. Since these data were considered at a safe level, all subsequent series discussed will be at this charge weight.

b. Standard Diameter Charge, No Black Powder Snake in Nitrocellulose Centercore; Series 2-3-4. Centercore-ignited, standard-diameter charges with the black powder snake removed from the nitrocellulose (NC) centercore tube were tested at zero, 2.5-cm and maximum standoff (24.0 cm). Table 2 summarizes the firing results for these three series. As expected, the removal of the black powder snake caused local base ignition of the charges as indicated by the large $-\Delta P_i$. The ignition delay increased as the charge standoff increased. Although P_{max} and $-\Delta P_i$ were essentially the same for the three series, the standard deviation at maximum standoff for $-\Delta P_i$ was considerably higher than at zero or 2.5-cm standoff.

TABLE 2. SUMMARY OF FIRING DATA* FOR STANDARD-DIAMETER CHARGES, NO BLACK POWDER SNAKE IN NITROCELLULOSE CENTERCORE (PROPELLANT LOT RAD-77H-069806).

Series	Charge Standoff (cm)	Projectile Velocity (m/s)	P_{max} (MPa)	$-\Delta P_i$ (MPa)	Ignition Delay (ms)
2	0	759.	280.	54.	66.
	(0.0)	(1.2)	(2.7)	(2.2)	(4.6)
4	2.5	762.	278.	50.	132.
	(0.0)	(3.6)	(10.4)	(3.6)	(121.5)
3	24.0	764.	280.	57.	348.
	(0.8)	(7.1)	(11.2)	(11.8)	(107.4)

* Values shown are averages for 4 firings; sample standard deviations are shown in parentheses.

c. Standard-Diameter Charge, Half Black Powder Snake in Nitrocellulose Centercore; Series 7-8. Centercore-ignited, standard-diameter charges with modified black powder snakes were tested at 2.5-cm and maximum standoff. The black powder snake was modified by reducing its length by half and repositioning the reduced snake at the front of the NC centercore. This left a gap of about 30 cm between the black powder basepad and the snake. Firing results are summarized in Table 3. Pressure and velocity were similar to Series 1, the "standard" wherein no changes were made to the ignition system. The substantial reductions in $-\Delta P_i$ and ignition delay for both charge standoffs from those noted in Series 2-3-4 were attributed to the additional 56 g of black powder (half-length black powder snake) which partly served to function as a normal, full-length snake.

TABLE 3. SUMMARY OF FIRING DATA* FOR STANDARD-DIAMETER CHARGES, HALF BLACK POWDER SNAKE IN NITROCELLULOSE CENTERCORE (PROPELLANT LOT RAD-77H-069806)

Series	Charge Standoff (cm)	Projectile Velocity (m/s)	P_{max} (MPa)	$-\Delta P_i$ (MPa)	Ignition Delay (ms)
7	2.5	759.	259.	2.5	93.
	(0.0)	(1.9)	(4.2)	(1.7)	(9.4)
8	20.9	762.	262.	3.5*	156.
	(0.4)	(3.6)	(6.5)		(123.9)

* Values shown are averages for 4 firings (Series 8, $-\Delta P_i$, is for 2 rounds); sample standard deviations are shown in parentheses.

d. Standard-Diameter Charge, Black Powder in Nitrocellulose Centercore, No Snake; Series 11-12. Centercore-ignited, standard-diameter charges were modified by removing the black powder from the cloth snake and reloading the 112 g of black powder directly into the forward section of the nitrocellulose tube. The powder was prevented from falling back on the basepad by inserting a 3-cm thick wad of cotton waste forward into the centercore until it contacted the black powder. This left a large gap between the basepad and the wad of cotton waste and significally reduced the porosity of the black powder. Firing results are summarized in Table 4.

TABLE 4. SUMMARY OF FIRING DATA* FOR STANDARD-DIAMETER CHARGES, BLACK POWDER IN NITROCELLULOSE CENTERCORE, NO SNAKE (PROPELLANT LOT RAD-77H-069806)

Series	Charge Standoff (cm)	Projectile Velocity (m/s)	P_{max} (MPa)	$-\Delta P_i$ (MPa)	Ignition Delay (ms)
11	2.5 (0.0)	765. (4.7)	267.* (10.6)	34.* (23.9)	803* (636)
12	26.2 (0.2)	762. (2.3)	252. (11.8)	6. (1.7)	68. (6.1)

* Values shown are averages for 4 firings (Series 11, P_{max}, $-\Delta P_i$, and ignition delay are for three rounds); sample standard deviations are shown in parentheses.

Results for these two series were inconsistent from previous firings. Pressure for both series and ignition delay for Series 12 were similar to Series 1 which had a standard black powder snake in the NC centercore. The $-\Delta P_i$'s for Series 11 and 12, although greatly different from each other, were smaller than those noted for Series 2-3-4 which had no black powder in the NC centercore. The individual ignition delays for Series 11 which were extremely large and variable (1078, 1255, and 76 ms) as well as the large standard deviation in $-\Delta P_i$ suggest that ignition for the 2.5-cm standoff may have depended on whether the ignition products from the 28 g of black powder basepad penetrated the wad of cotton waste in the NC tube and ignited the 112 g of black powder (short delay, low $-\Delta P_i$) or simply spot-ignited the NC tube (long delay, high $-\Delta P_i$). The short and consistent ignition delays for Series 12 as well as the character of the $-\Delta P_i$ traces (Appendix) strongly suggest ignition for this series occurred at the front of the charge where the black powder in the NC centercore was concentrated. Apparently, for Series 12, the effects of charge standoff, location of black powder and parasitic obstruction in the NC tube combined to produce stable burning and small pressure waves.

e. Standard-Diameter Charge, Base-Ignited; Series 9-10. Base-ignited, standard-diameter charges were fabricated from standard charges by removing the black powder snake and NC centercore and fired at two charge standoffs. Table 5 summarizes the firing results.

TABLE 5. SUMMARY OF FIRING DATA* FOR STANDARD-DIAMETER CHARGES, BASE-IGNITED (PROPELLANT LOT RAD-77H-069806)

Series	Charge Standoff (cm)	Projectile Velocity (m/s)	P_{max} (MPa)	$-\Delta P_i$ (MPa)	Ignition Delay (ms)
9	2.5	755.	252.	46.	1270.
	(0.0)	(3.7)	(3.9)	(3.7)	(798.7)
10	27.4	758.	257.	42.	1322.
	(0.2)	(1.8)	(3.8)	(4.5)	(973.7)

* Values shown are averages for 4 firings; sample standard deviations are shown in parentheses.

The decrease in macroscopic propellant bed porosity by elimination of the centercore contributed greatly to the nonsimultaneous ignition of the propellant grains as indicated by the large $-\Delta P_i$ and the very large ignition delays for both standoff conditions. The range of the delay for Series 9 from 382 to 1987 ms and Series 10 from 382 to 2258 ms indicate serious problems in ignition and flamespreading. Apparently, the 28 g of Class 1, Black Powder in the basepad was barely sufficient in conjunction with the large annular and axial ullage to ignite the charge.

f. Full-Bore Charge, Base-Ignited; Series 5-6. Base-ignited, full-bore charges were fabricated and fired at two charge standoffs. This configuration was considered the most severe for inducing pressure waves since all annular ullage was eliminated between the charge and the chamber wall. Firing results are shown in Table 6.

TABLE 6. SUMMARY OF FIRING DATA* FOR FULL-BORE CHARGES, BASE-IGNITED (PROPELLANT LOT RAD-77H-069806)

Series	Charge Standoff (cm)	Projectile Velocity (m/s)	P_{max} (MPa)	$-\Delta P_i$ (MPa)	Ignition Delay (ms)
5	2.5	772.	270.	54.	162.
	(0.0)	(8.1)	(13.8)	(10.7)	(47.4)
6	27.9	771.	262.*	46.*	129.
	(0.0)	(5.2)	(-)	(-)	(22.1)

* Values shown are averages for 4 firings (Series 6, P_{max} and $-\Delta P_i$ are for 2 firings; Series 6, ignition delay is for 3 firings); sample standard deviations are shown in parentheses.

As expected, this series did produce large-ΔP_i's, but not larger than experienced with some of the other series. The substantial reduction in ignition delay over the standard-diameter, base-ignited charges (Series 9-10) is attributed to the elimination of annular ullage. Hot ignition gases, constrained from expanding into this ullage and thus forced to penetrate the propellant bed, quickly ignited the charge. The large $-\Delta P_i$'s attest to the nonsimultaneity of the ignition process.

g. Summary of Firings with Propellant Lot RAD-77H-069806. The experimental firings, which were divided into six groups based on charge configuration and further divided into 4-round series based on charge standoff, were devised to promote nonuniform ignition leading to pressure-wave formation. Within each group the effect of charge standoff on each measured parameter (pressure, $-\Delta P_i$, velocity, etc.) has been discussed. The averaged data for all 12 series are plotted on Figures 10, 11, and 12. Dotted lines connect each series within a group. The effect of standoff within or across a group has essentially no effect on projectile velocity, which averaged 762 m/s (Figure 10), even though standoff for Series 11 and 12 and charge configuration, in general, produced significant changes in $-\Delta P_i$ level. P_{max} was inconsistently affected by charge standoff: namely, independent for Series 2-3-4, 7-8, and 9-10 and decreasing for Series 11-12 and 5-6 with increasing standoff (Figure 11). In general, as $-\Delta P_i$ increased, P_{max} remained around 260 MPa until $-\Delta P_i$ reached 50 MPa; as $-\Delta P_i$ increased above 50 MPa, the P_{max} showed an increase (Series 2-3-4). Velocity did not increase with increasing P_{max} (Figure 12), even though P_{max} varied from 252 to 280 MPa.

2. Propeilant Lot RAD-79E-069960. Three base-ignited, 5-round series, one of standard diameter and two of full-bore configuration, were tested with this lot of propellant. Basepad composition was the primary mechanism for inducing large $-\Delta P_i$'s, with charge diameter and standoff providing tradeoff parameters to ensure against excessive waves that might damage the tube. Data for the three series, as chronologically fired, are shown in Table 7. When the experimental condition (basepad composition, charge standoff) consisted of three or more rounds, the data are shown as an average; otherwise, the individual firings are presented.

All the rounds for Series 13 were fired at zero standoff in order to induce large $-\Delta P_i$'s with the relatively slow burning CBI/black powder basepad. As the basepad composition became more energetic, (Series 15 faster than 14 which was faster than 13), the charge standoff was changed from the "worst" no standoff condition to standoffs less likely to cause catastrophic pressure waves. The Class 3, Black Powder used in Series 15 was considered too fast to use in full-bore charges; therefore, standard-diameter, base-ignited charges were used for this series.

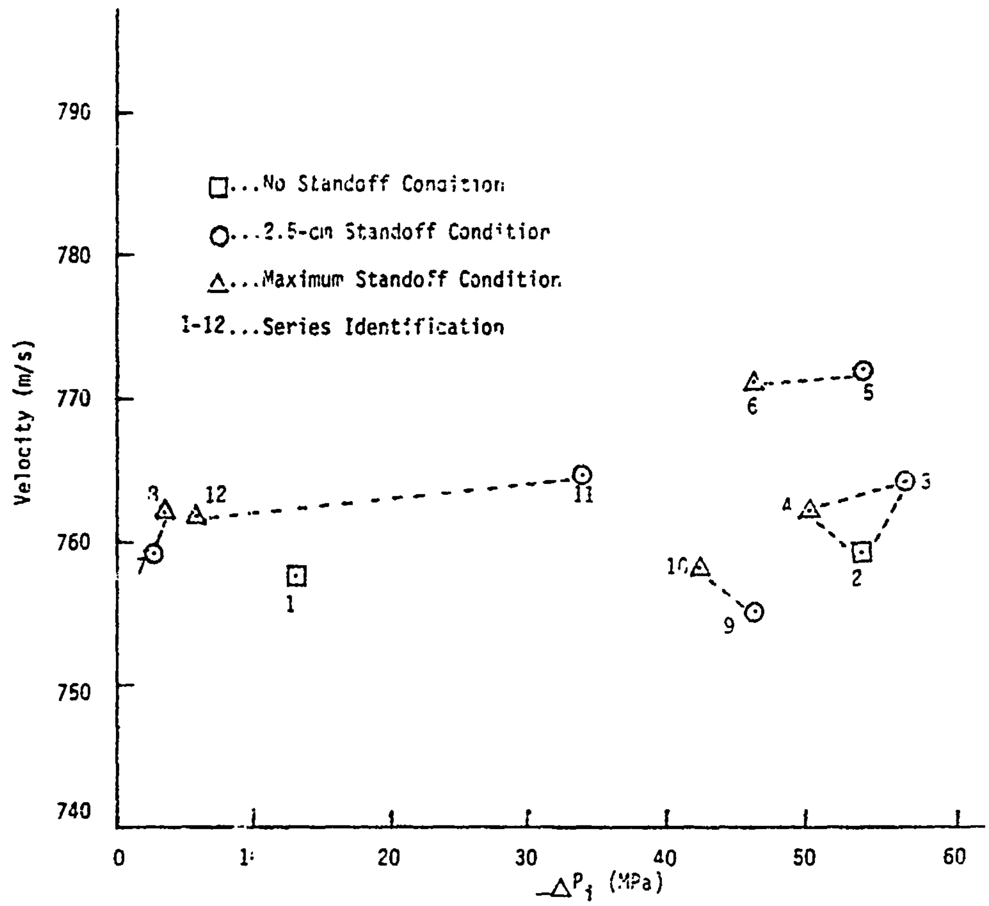

Figure 10. Velocity versus $-\Delta P_i$ (Propellant Lot Rad-77H-069806)

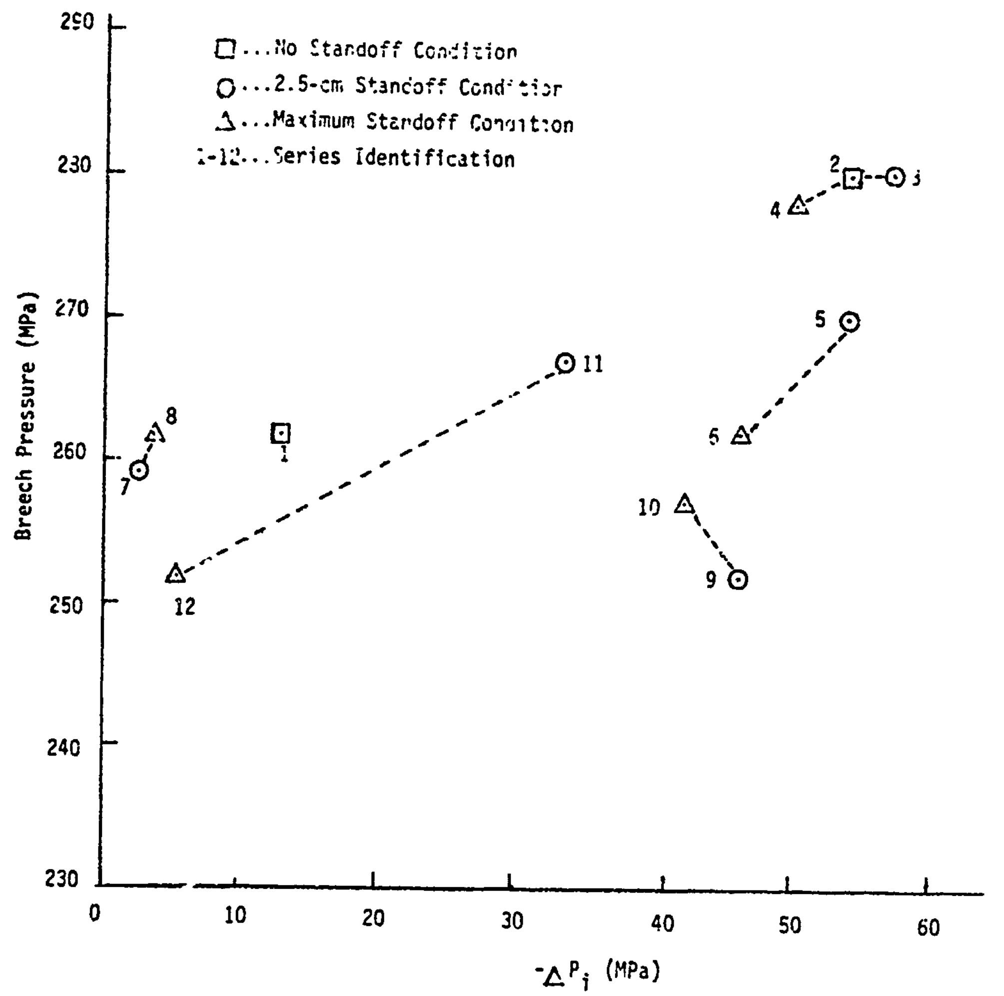

Figure 11. Breech Pressure versus $-\Delta P_i$ (Propellant Lot Rad-77H-069806)

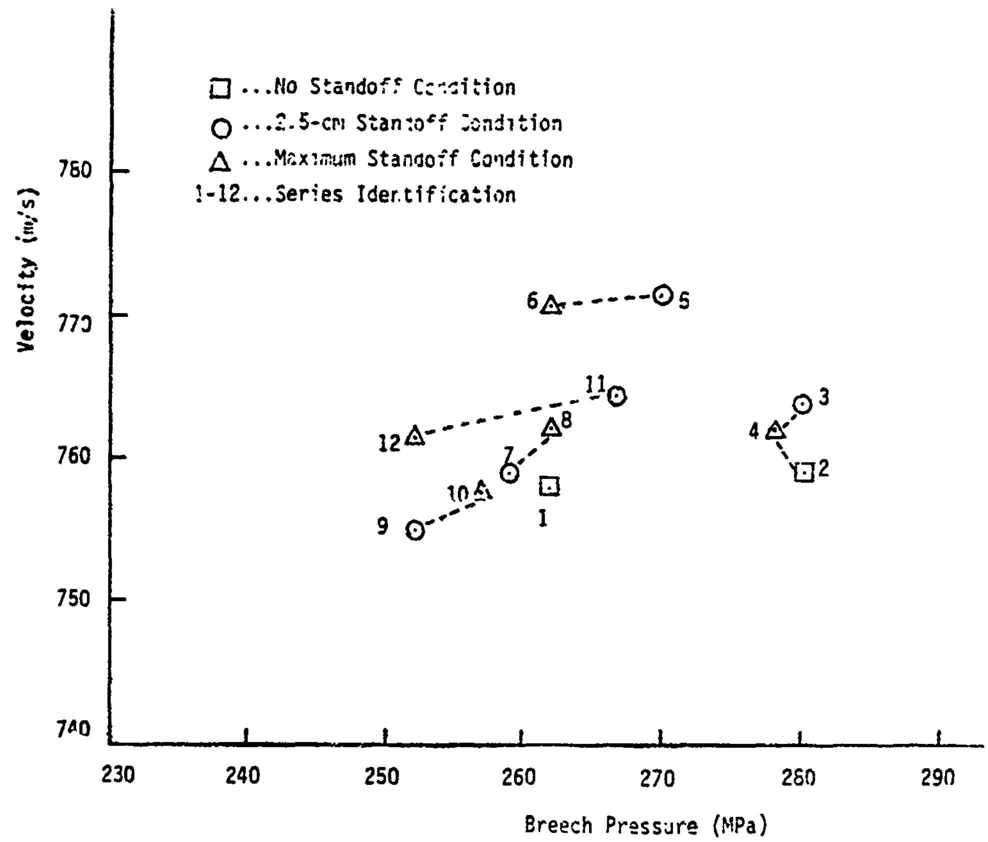

Figure 12. Velocity versus Breech Pressure (Propellant Lot Rad-77H-069806)

TABLE 7. SUMMARY OF FIRING DATA* FOR STANDARD AND FULL-BORE CHARGES, BASE-IGNITED (PROPELLANT LOT RAD-79E-069960)

Series	No. Rds.	Charge Standoff (cm)	Charge Diameter	Muzzle Velocity (m/s)	P_{max} (MPa)	$-\Delta P_i$ (MPa)	Ignition Delay (ms)	Basepad Type
13	5	0	Full Bore	791.	292.	68.	18.	Two Part Basepad:**
		(0.0)		(3.9)	(10.6)	(7.8)	(8.3)	28 g BP, Class 5
								56 g CBI
14	3	2.5	"	772.	260.	50.	24.	Basepad:
		(0.0)		(3.6)	(6.3)	(3.6)	(10.4)	84 g BP, Class 1
	1	7.6	"	791.	303.	75.	39.	
	1	12.7	"	776.	261.	59.	41.	
15	1	2.5	Std. Diam.	773.	259.	54.	31.	Basepad:
	1	0	"	774.	261.	57.	21.	84 g BP, Class 3
	1	7.6	"	772.	255.	58.	89.	
	1	12.7	"	770.	250.	48.	62.	
	1	20.3	"	774.	258.	65.	56.	

* Sample standard deviation is shown in parentheses; basepad weight is 84 g.

** Basepad divided into two concentric circles. The center circle contained Class 1 black powder; the remaining area contained CBI.

The effect of charge standoff (Table 7) on P_{max}, $-\Delta P_i$, and muzzle velocity is minimal for the standard-diameter charges (Series 15). Apparently the increase in annular ullage from full-bore to standard-diameter configurations offset the effects of both charge standoff and the faster burning black powder igniter, thus keeping the $-\Delta P_i$'s from building to catastrophic levels. Ignition delay was inconsistent, showing a maximum at an intermediate charge standoff.

In Series 14, P_{max}, $-\Delta P_i$, and muzzle velocity have the same nominal values at 2.5-cm and 12.7-cm standoffs with a maximum occurring at the intermediate 7.6-cm standoff. Ignition delay increased as charge standoff increased. More rounds would have to be fired to establish if charge standoff is one of the conditions for inducing large $-\Delta P_i$'s for this series as well as for Series 13 which was fired at only one standoff.

The data for all the rounds in the three series are plotted as shown on Figures 13, 14, and 15. In addition, the averaged value for the five rounds in each of Series 13 and 15 and four rounds of Series 14 are superimposed on the plots. The data for the 7.6-cm standoff (Series 14) were not included in the average of this series because the abnormally large P_{max} and $-\Delta P_i$ were not typical for the charge standoff. Series 15 with the same range of standoffs and using a more energetic basepad for ignition did not exhibit wide variations in P_{max} and $-\Delta P_i$. Figures 13 and 14 show, respectively, that the dependence of velocity and P_{max} on $-\Delta P_i$ is divided, roughly, into two groups, delineated by a $-\Delta P_i$ of 65 MPa. Below this value, fairly large excursions in $-\Delta P_i$ produce relatively small "average" changes in P_{max} and velocity. When $-\Delta P_i$ increases beyond -65 MPa, a fairly large increase in P_{max} and velocity is noted. Velocity dependence on P_{max} even with large $-\Delta P_i$'s, is fairly linear, increasing with increasing P_{max} (Figure 15).

3. Propellant Lot RAD-77G-069805. Four full-bore diameter, base-ignited series were tested with this lot of propellant. Basepad composition, charge standoff and charge diameter were again varied to encourage and control the formation of large pressure waves. The goal remained to generate similarly high levels of pressure waves via different mechanisms to determine whether or not correspondingly similar increases in maximum chamber pressure occurred. Table 8 gives a summary of the data. The standard deviation is shown in parenthesis if more than three rounds were fired at one condition (standoff, etc.).

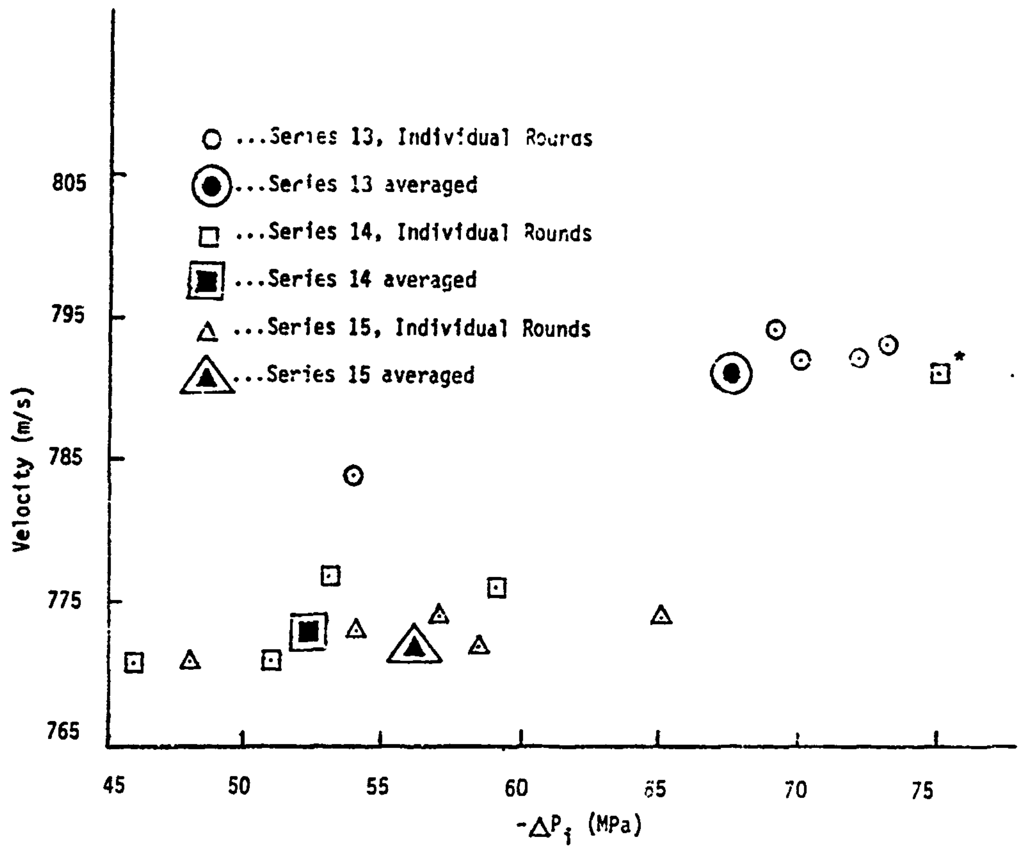

Figure 13. Velocity versus $-\Delta P_i$ (Propellant Lot Rad-79E-069960)
*This round from Series 14 was not included in the series average.

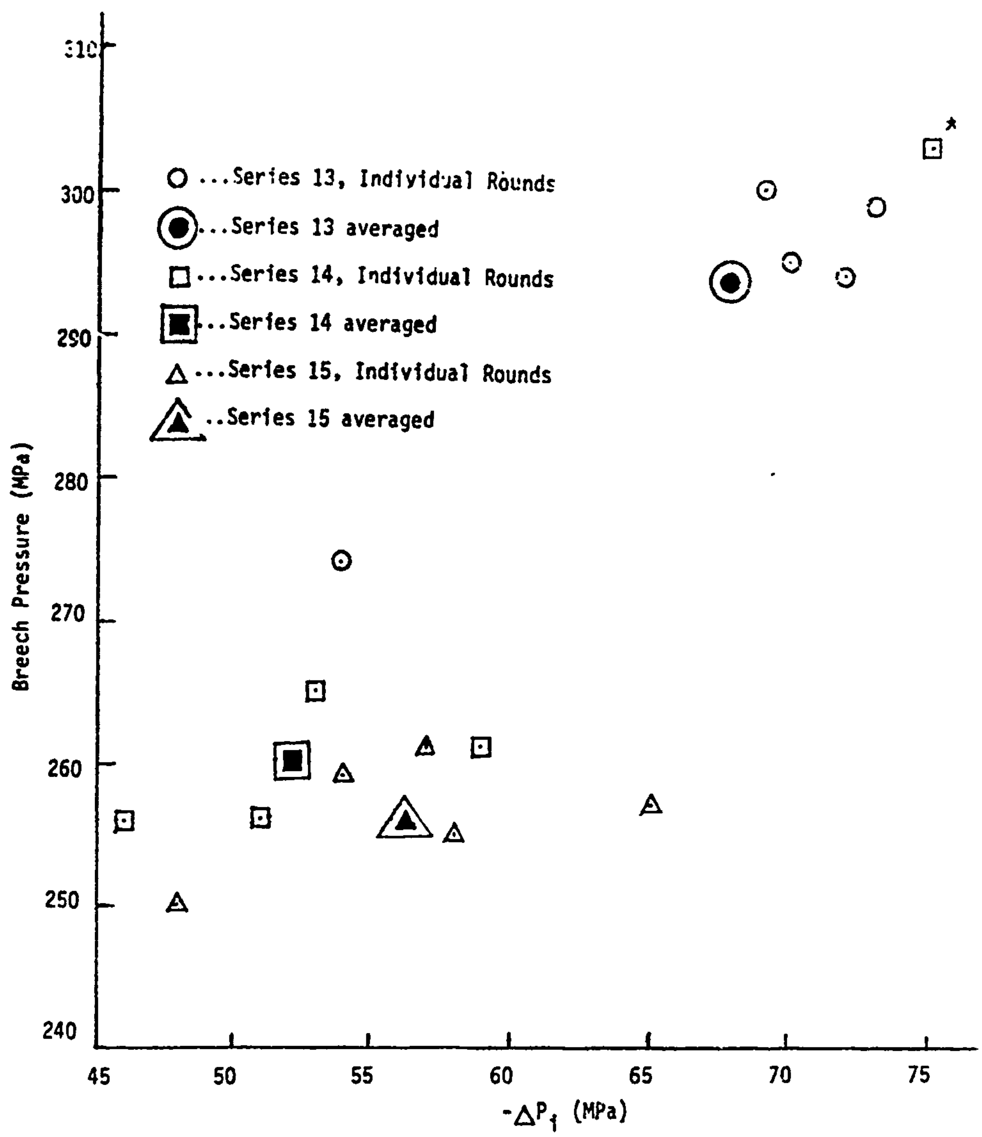

Figure 14. Breech Pressure versus $-\Delta P_i$ (Propellant Lot Rad-79E-069960)
*This round from Series 14 was not included in the series average.

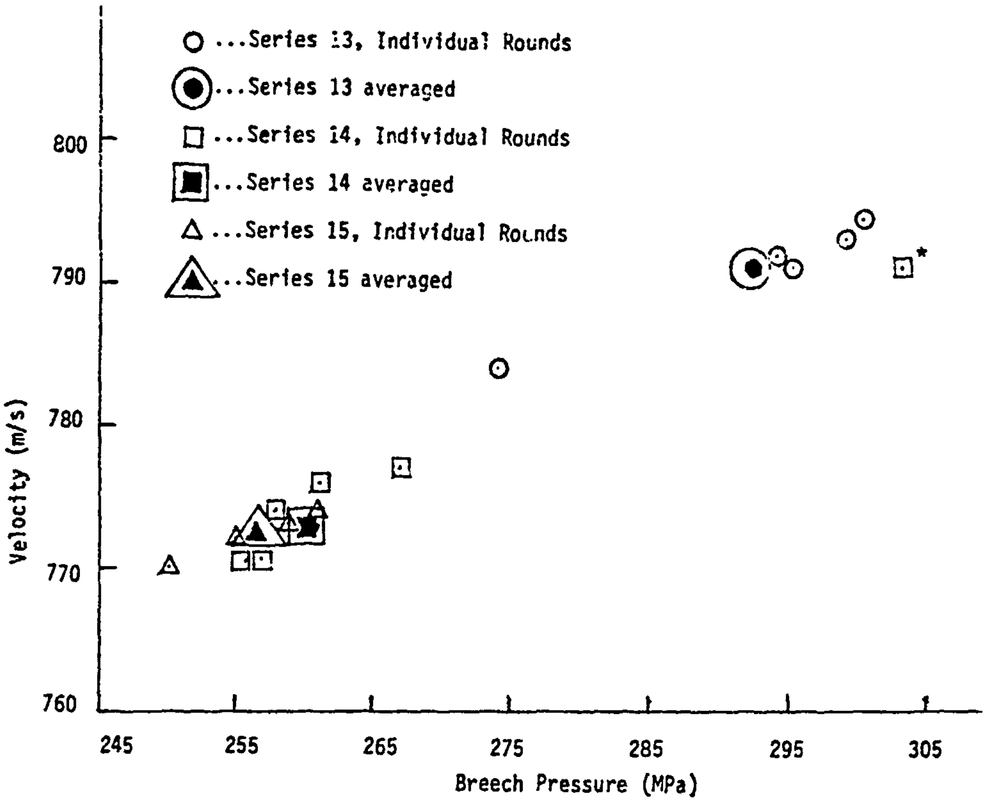

Figure 15. Velocity versus Breech Pressure (Propellant Lot Rad-79E-069960)
*This round from Series 14 was not included in the series average.

TABLE 8. SUMMARY OF FIRING DATA* FOR FULL-BORE CHARGES, BASE-IGNITED (PROPELLANT LOT RAD-77G-069805)

Series	No. Rds.	Charge Standoff (cm)	Charge Diameter & Type	Muzzle Velocity (m/s)	P_{max} (MPa)	$-\Delta P_i$ (MPa)	Ignition Delay (ms)	Basepad Type
16	5	0 (0.0)	Full-Bore Random-loaded	796. (18.5)	340. (31.9)	87. (17.4)	37. (22.8)	Two Part Basepad:** 28 g BP, Class 5 56 g CBI
17***	2	0	Full-Bore 1/3 stacked	797.	300.	60.	25.	Two Part Basepad:** 28 g BP, Class 5 56 g CBI Propellant: Bottom 1/3 stacked
	1	0		823.	404.	116.	12.	
18	1	2.5	Full-Bore Random-Loaded	795.	336.	99.	92.	Basepad: 84 g CBI
	4	0 (0.0)		801. (4.7)	355. (21.9)	99. (6.5)	153. (23.9)	
19	1	2.5	Full-Bore Random-Loaded	825.	468.	112.	16.	Basepad: 84 g BP, Class 5

* Sample standard deviation is shown in parentheses for three or more rounds; total basepad weight is 84 g.

** Basepad divided into 2 concentric circles. The center circle contained Class 5 Black Powder; the remaining area contained CBI.

*** One round of this series listed separately because of very large P_{max} and $-\Delta P_i$.

All the rounds for Series 16-17 were fired with the two-part basepad composition at no standoff in order to induce large $-\Delta P_i$'s. Because of the extremely high $-\Delta P_i$ for one round of Series 17, both basepad composition and charge standoff were changed for the first round of Series 18. After ascertaining the functioning of this basepad configuration did not induce excessive $-\Delta P_i$'s, the remainder of Series 18 was fired at no standoff. The first round of Series 19 with a Class 5, Black Powder basepad and 2.5-cm standoff produced such a large pressure and $-\Delta P_i$ that no further rounds were done in fear of damaging the tube.

The data for all the rounds of Series 16-19 are plotted as shown in Figures 16, 17, and 18. In addition, the "averaged" values for all rounds in Series 16 and 18 and two rounds of Series 17 are superimposed on the plots. The third round of Series 17 (extremely high P_{max} and $-\Delta P_i$ is shown as an individual point. Except for Series 19 and the first round of Series 18, this data represents a zero-standoff condition. The P_{max} and $-\Delta P_i$ are the highest for the three lots of propellant used in these tests. Ignition delay varies directly with the quickness of the basepad being the slowest for CBI alone and the fastest for Class 5, Black Powder. Although the data scatter is large, projectile velocity (Figure 16) and P_{max} (Figure 17) increase with increasing $-\Delta P_i$. P_{max} is especially sensitive to the high $-\Delta P_i$'s, ranging from 300 to 400 MPa as $-\Delta P_i$ goes from 60 to 115 MPa. Velocity is directly dependent on P_{max}, increasing as the pressure increases (Figure 18).

4. <u>All Propellant Lots</u>. As previously noted, three different propellant lots, as well as various charge diameters, charge lengths, ignition systems (base vs centercore), charge standoffs, charge propellant porosity (random vs stacked propellant), and igniter brisance (black powder vs CBI) were employed to induce pressure-wave formation in the 155-mm howitzer. The average value of P_{max} and $-\Delta P_i$ for each of the nineteen series aforementioned is shown on Figure 19. As $-\Delta P_i$ ranged from 2 to 116 MPa, P_{max} increased from 250 to 468 MPa.

IV. CONCLUSIONS

Although several of the series previously discussed were of insufficient size to ascertain standoff effects of different charge configurations, and round-to-round variation within series at the same standoff were somewhat large, several conclusions from the firings on the P_{max} vs $-\Delta P_i$ sensitivity curve can be made.

1. The methods of inducing pressure waves produced a broad range of data with $-\Delta P_i$ (2 MPA to 116 MPa) increases generally accompanied by increases in P_{max} (250 MPa to 468 MPa). Within the limits of reasonable

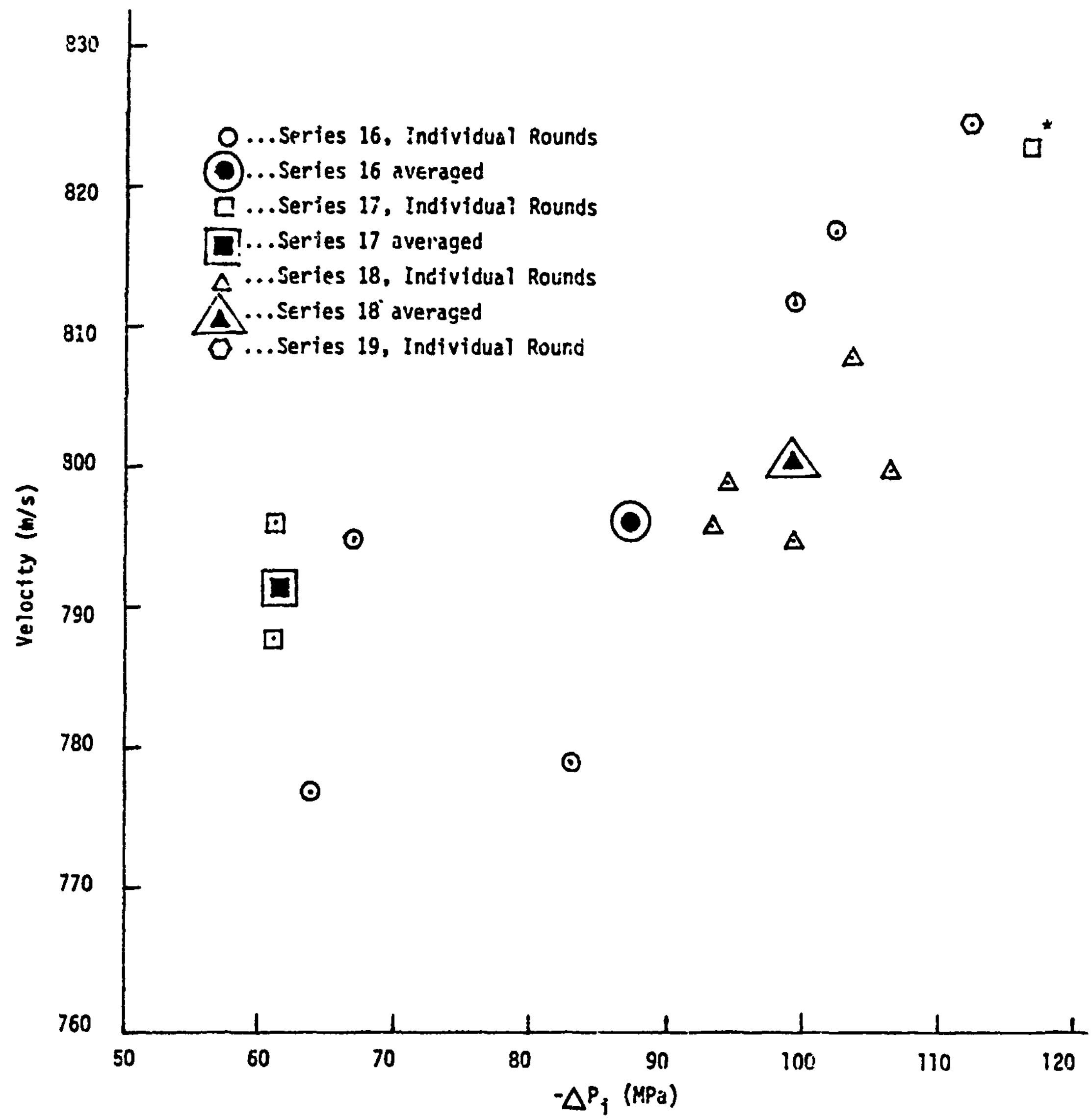

Figure 16. Velocity versus $-\Delta P_i$ (Propellant Lot Rad-77G-069805)
*This round from Series 17 was not included in the series average.

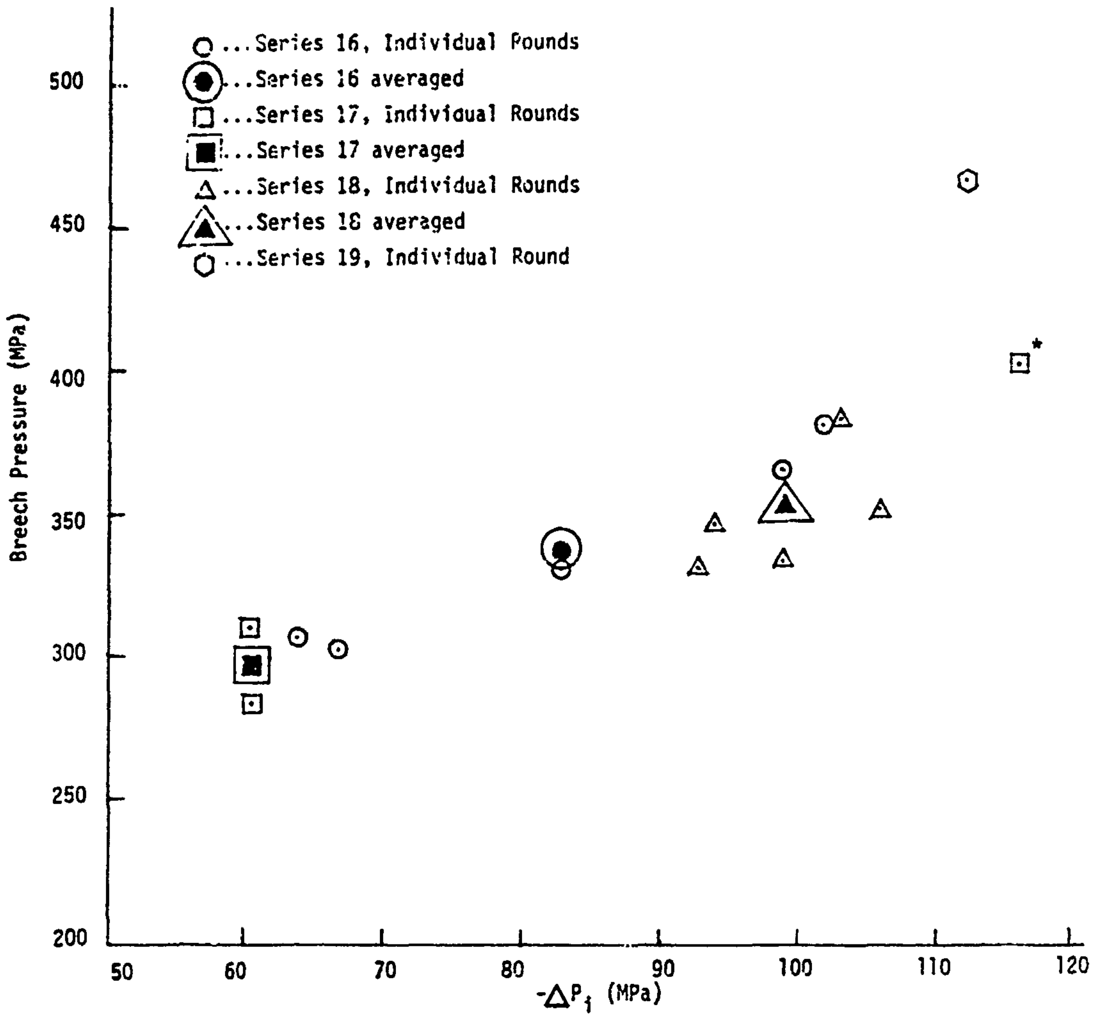

Figure 17. Breech Pressure versus $-\Delta P_i$ (Propellant Lot Rad-77G-069805)
*This round from Series 17 was not included in the series average.

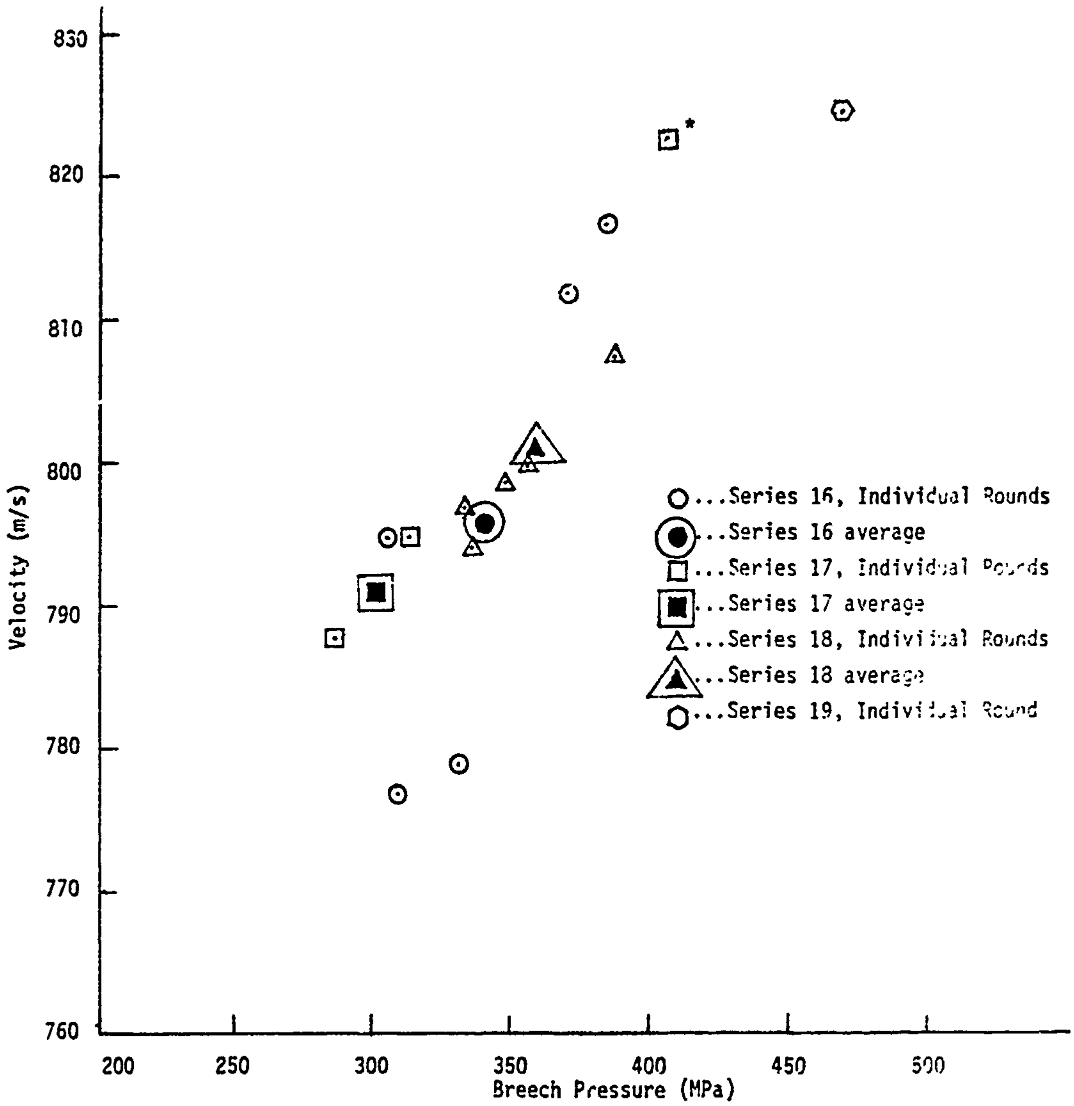

Figure 18. Velocity versus Breech Pressure (Propellant Lot Rad-77G-069805)
*This round from Series 17 was not included in the series average.

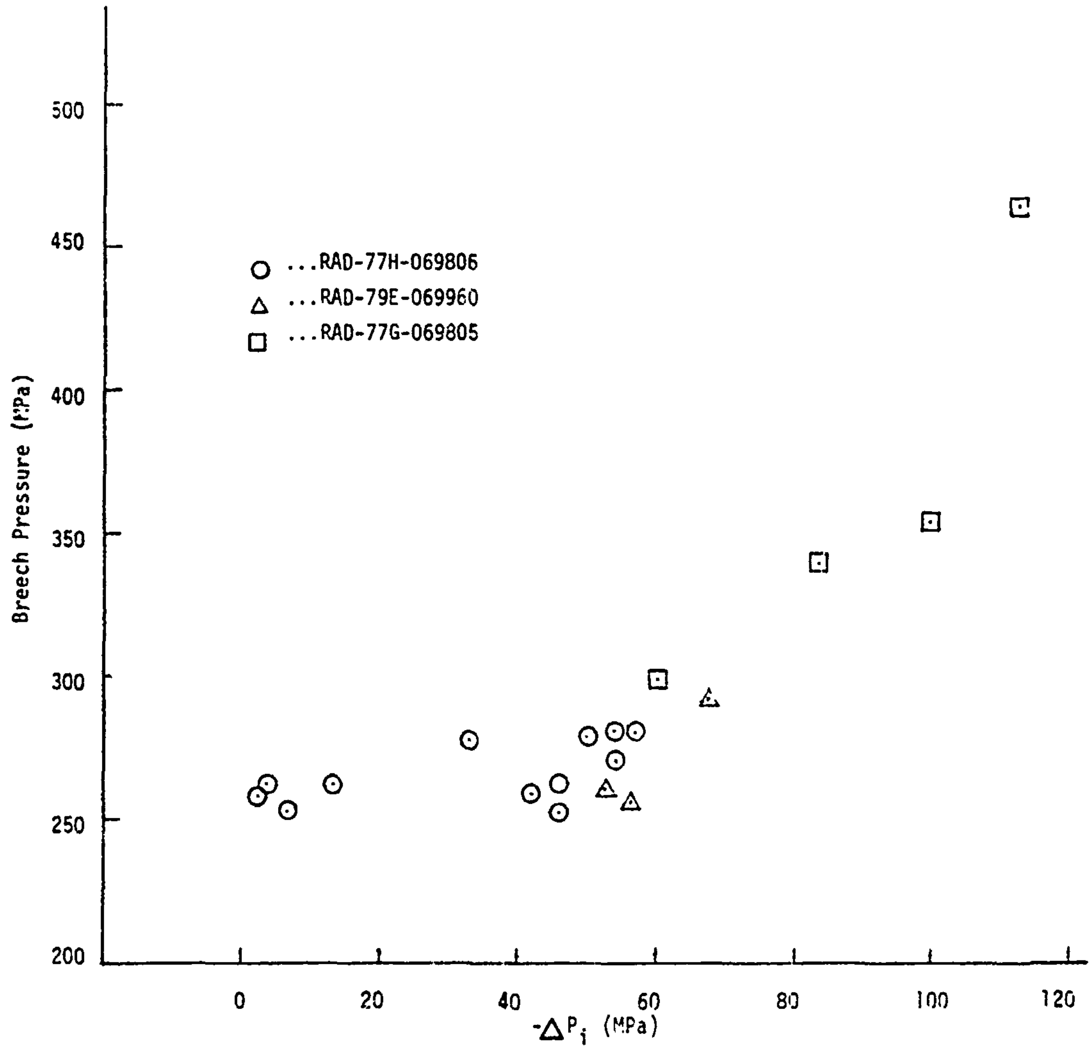

Figure 19. Breech Pressure versus $-\Delta P_i$ for Each of the 19 Series. (Propellant Lot Rad-77H-069806, RAD-79E-069960, RAD-77G-069805)

occasion-to-occasion differences and possible experimental errors, the existence of significantly different P_{max} vs $-\Delta P_i$ curves for this charge/weapon combination could not be demonstrated.

2. A serious concern is raised by the apparent differences in the ease with which one could generate substantial pressure waves in similar charge configurations using different propellant production lots. Current safety assessment procedures usually employ a single propellant lot. If yet undefined lot-to-lot propellant differences can influence the propensity of a given charge design to exhibit large pressure waves, then projected failure rates based on an expected population of firing data consisting of firings with only one propelling charge lot may well be inappropriate for different propellant charge lots.

REFERENCES

1. A.J. Budka and J.D. Knapton, "Pressure Wave Generation in Gun Systems: A Survey," Ballistic Research Laboratory, Aberdeen Proving Ground, MD, Memorandum Report 2567, December 1975. (AD #B008893L)

2. D.W. Culbertson, M.C. Shamblen, and J.S. O'Brasky, "Investigation of 5"/38 Gun In-Bore Ammunition Malfunctions," Naval Weapons Laboratory, Dahlgren, VA, TR-2624, December 1971.

3. M.C. Shamblen and J.S. O'Brasky, "Investigation of 8"/55 Close Aboard Malfunctions," Naval Weapons Laboratory, Dahlgren, VA, TR-2753, April 1973.

4. P.J. Olenick, "Investigation of the 76-mm/62 Caliber Mark 75 Gun Mount Malfunctions," Naval Surface Weapons Center, Dahlgren, VA, TR-3411, October 1975.

5. E.V. Clarke, Jr. and I.W. May, "Subtle Effects of Low-Amplitude Pressure Wave Dynamics on the Ballistics Performance of Guns," 11th JANNAF Combustion Meeting, CPIA Publication 261, Vol. 1, pp. 141-156, December 1974.

6. A.W. Horst, I.W. May, and E.V. Clarke, Jr., "The Missing Link Between Pressure Waves and Breechblows," USA ARRADCOM, Ballistic Research Laboratory, Aberdeen Proving Ground, MD, Memorandum Report 02849, July 1978. (A058354)

7. K.H. Russel and H.M. Goldstein, "Investigation and Screening of M17 Propellant Production for Lots Subject to Poor Low Temperature Performance, Picatinny Arsenal, Dover, NJ, DB-TR-7-61, June 1961.

8. N. Lockett, "British Work on Solid Propellant Ignition," Bulletin of the First Symposium on Solid Propellant Ignition, Solid Propellant Information Agency, Silver Spring, MD, September 1953.

APPENDIX

Computer-Generated Plots of Selected Data Channels
[Spindle (solid line) and Forward (dotted line) Pressure vs
Time, Pressure Difference vs Time]

APPENDIX INDEX

DELTA P STUDY (STD IGNITION SYSTEM)
18 MAY 79; ID T02A

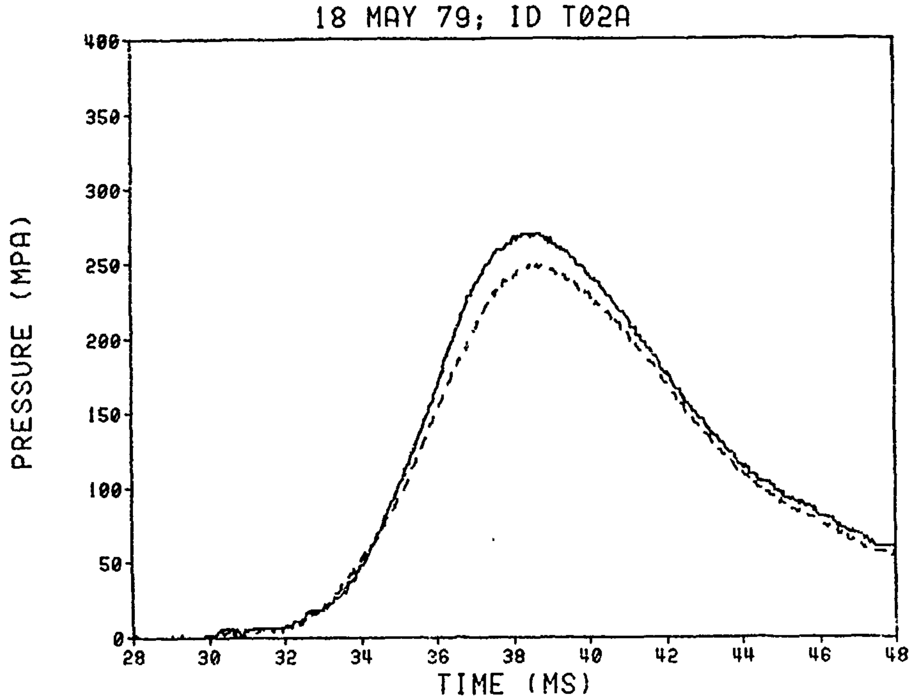

DELTA P STUDY (STD IGNITION SYSTEM)
18 MAY 79; ID T02A

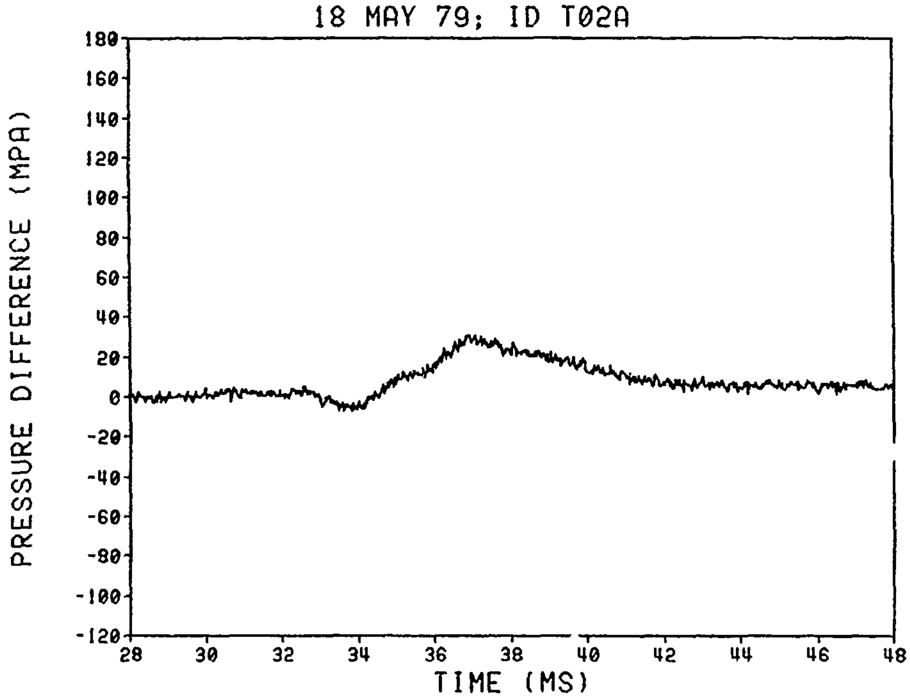

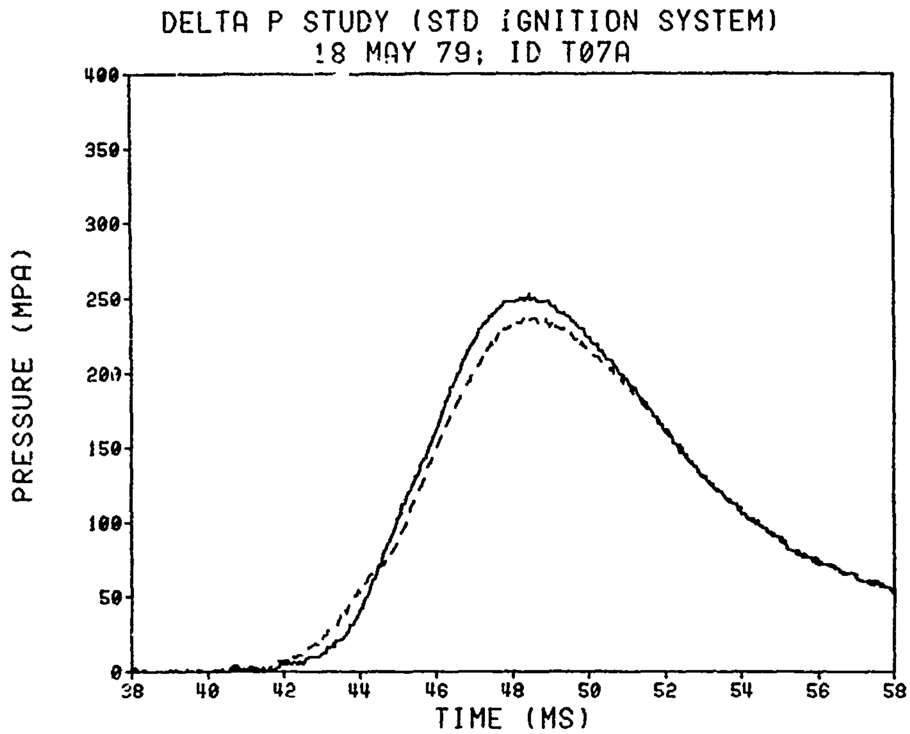

DELTA P STUDY (STD IGNITION SYSTEM)
18 MAY 79; ID T07A
PRESSURE (MPA)
400
350
300
250
200
150
100
50
0
38
40
42
44
46
48
50
52
54
56
58
TIME (MS)

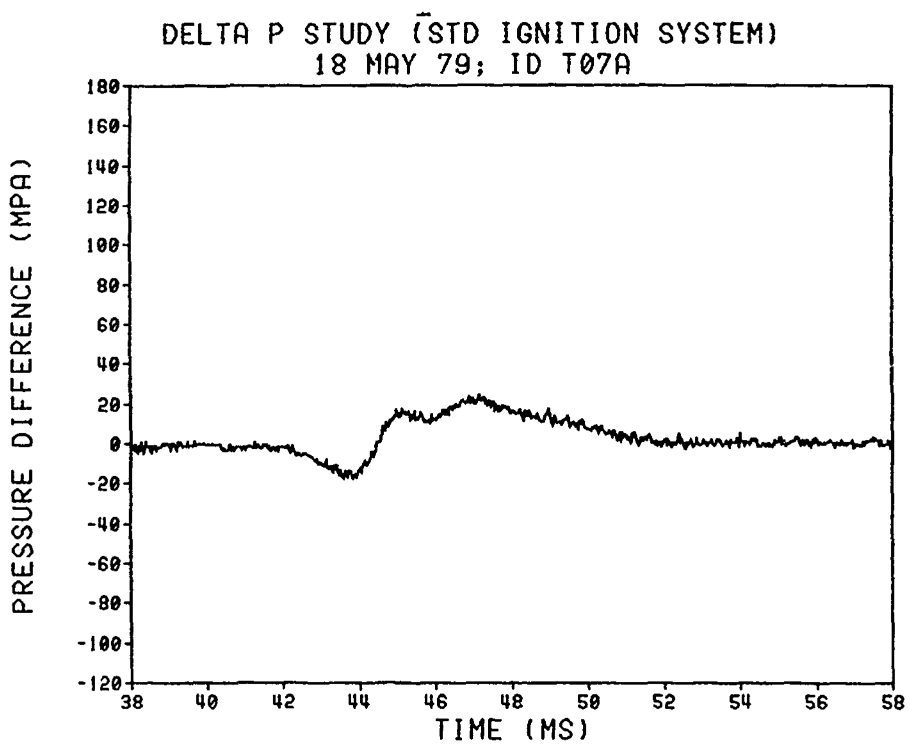

DELTA P STUDY (STD IGNITION SYSTEM)
18 MAY 79; ID T07A
PRESSURE DIFFERENCE (MPA)
180
160
140
120
100
80
60
40
20
0
-20
-40
-60
-80
-100
-120
38
40
42
44
46
48
50
52
54
56
58
TIME (MS)

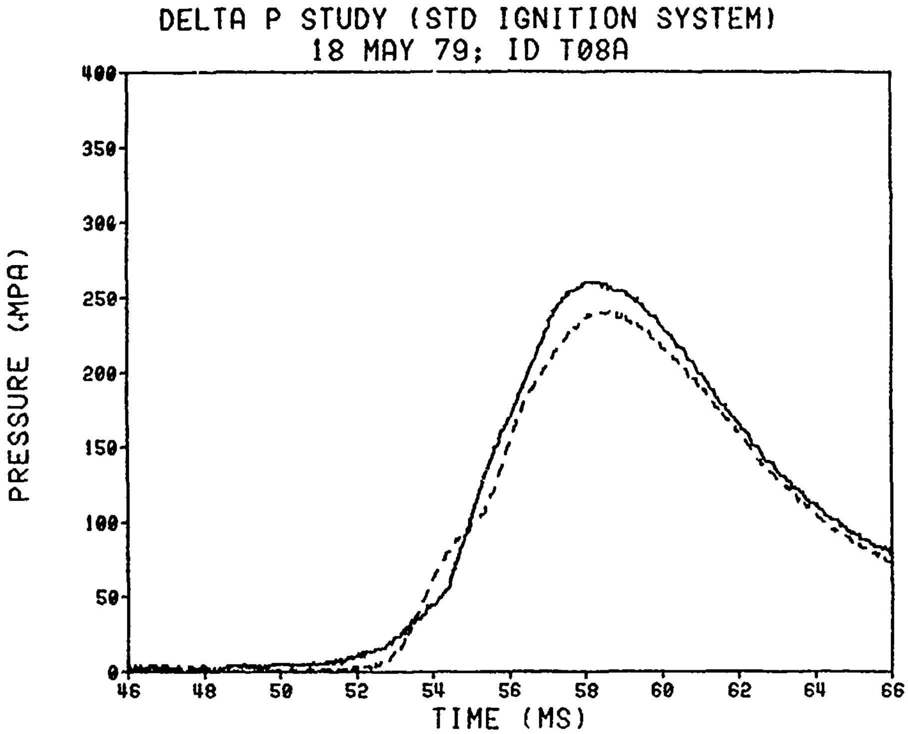

DELTA P STUDY (STD IGNITION SYSTEM)
18 MAY 79; ID T08A
PRESSURE (MPA)
400
350
300
250
200
150
100
50
0
46
48
50
52
54
56
58
60
62
64
66
TIME (MS)

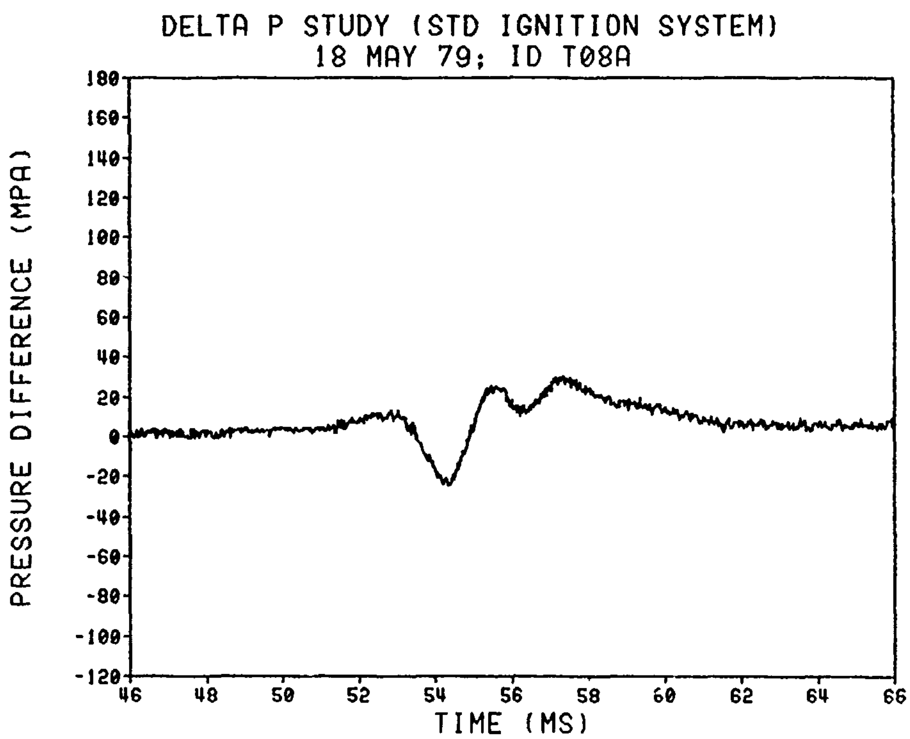

DELTA P STUDY (STD IGNITION SYSTEM)
18 MAY 79; ID T08A
PRESSURE DIFFERENCE (MPA)
180
160
140
120
100
80
60
40
20
0
-20
-40
-60
-80
-100
-120
46
48
50
52
54
56
58
60
62
64
66
TIME (MS)

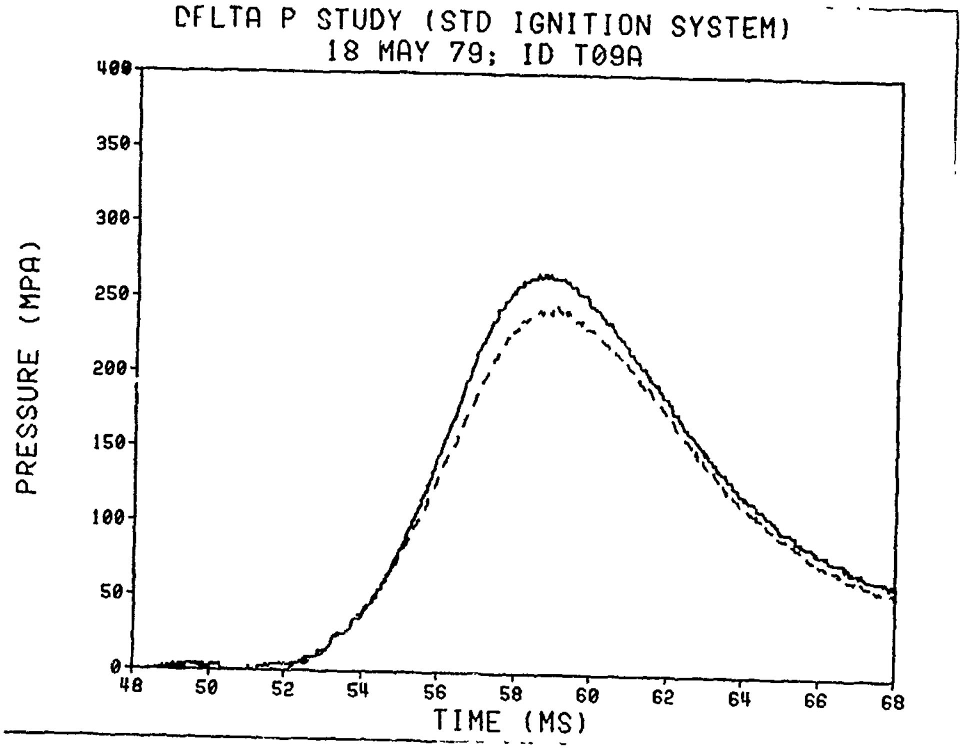
DFLTA P STUDY (STD IGNITION SYSTEM)
18 MAY 79; ID T09A
PRESSURE (MPA)
TIME (MS)
0
50
100
150
200
250
300
350
400
48
50
52
54
56
58
60
62
64
66
68

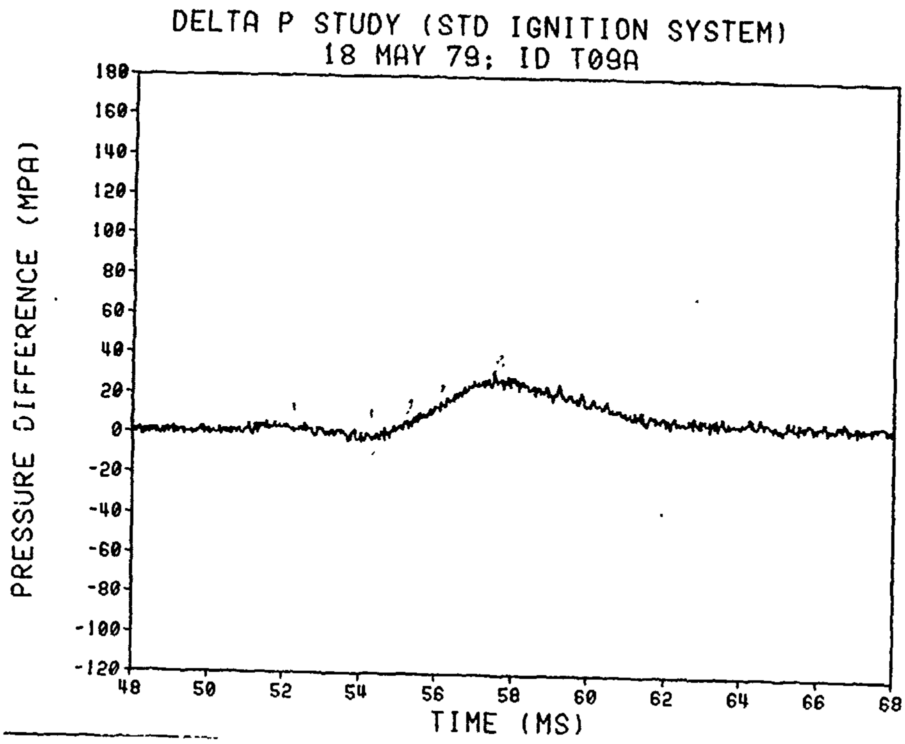
DELTA P STUDY (STD IGNITION SYSTEM)
18 MAY 79; ID T09A
PRESSURE DIFFERENCE (MPA)
TIME (MS)
180
160
140
120
100
80
60
40
20
0
-20
-40
-60
-80
-100
-120
48
50
52
54
56
58
60
62
64
66
68

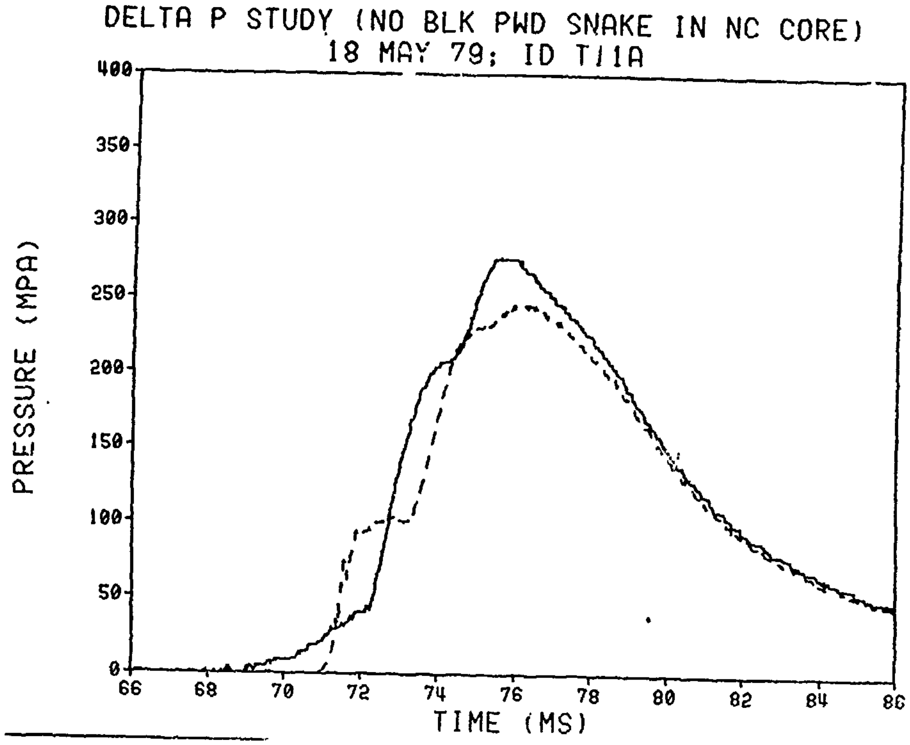

DELTA P STUDY (NO BLK PWD SNAKE IN NC CORE)
18 MAY 79; ID T11A
PRESSURE (MPA)
400
350
300
250
200
150
100
50
0
66
68
70
72
74
76
78
80
82
84
86
TIME (MS)

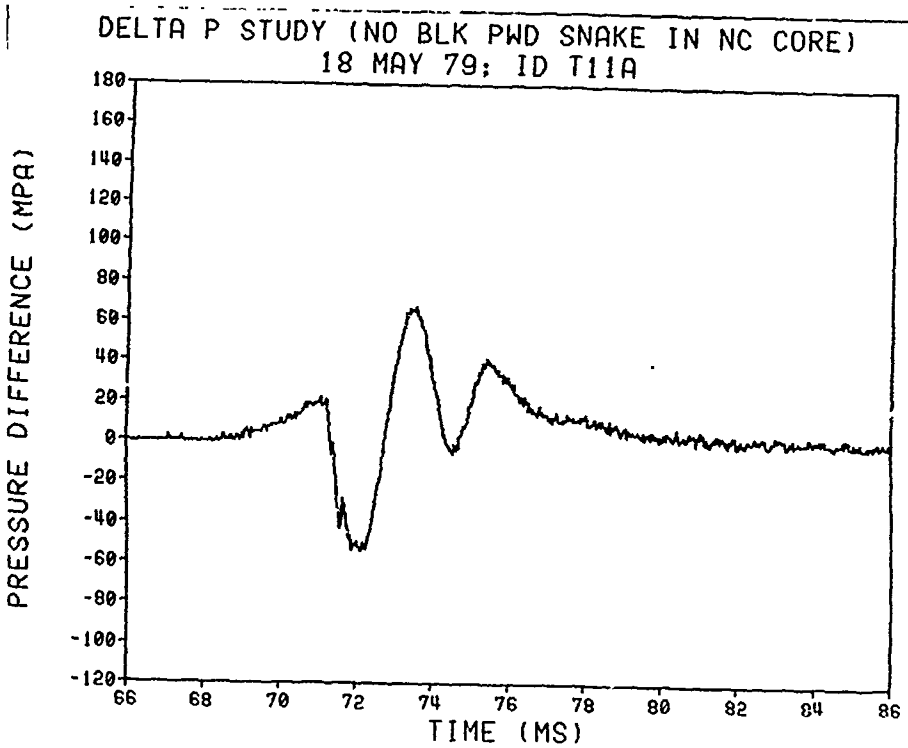

DELTA P STUDY (NO BLK PWD SNAKE IN NC CORE)
18 MAY 79; ID T11A
PRESSURE DIFFERENCE (MPA)
180
160
140
120
100
80
60
40
20
0
-20
-40
-60
-80
-100
-120
66
68
70
72
74
76
78
80
82
84
86
TIME (MS)

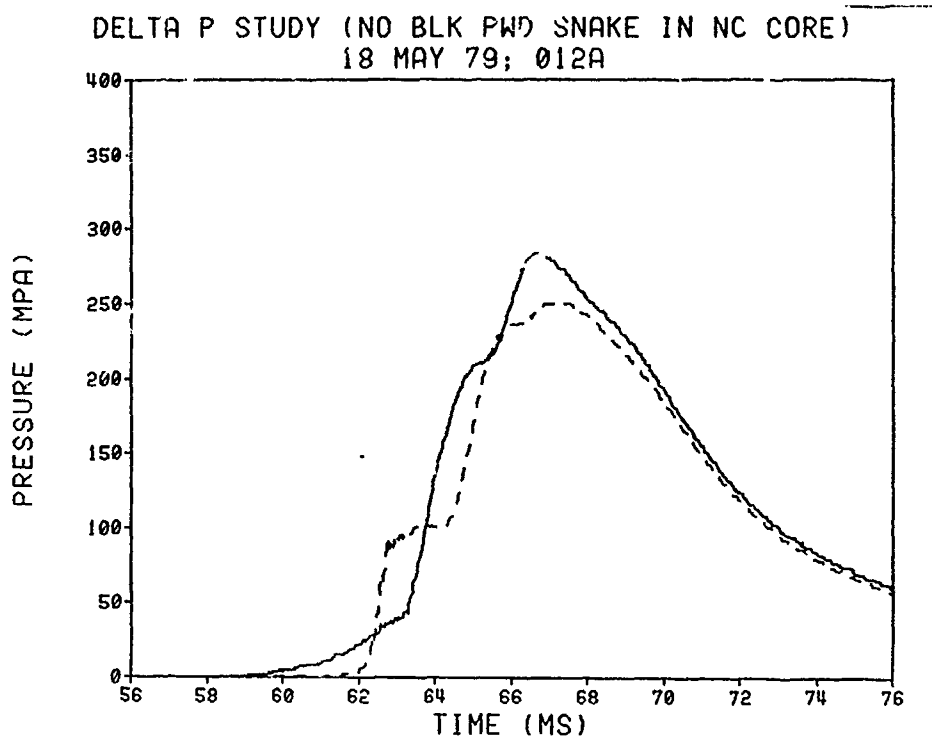
DELTA P STUDY (NO BLK PWD SNAKE IN NC CORE)
18 MAY 79; 012A
PRESSURE (MPA)
TIME (MS)
400
350
300
250
200
150
100
50
0
56
58
60
62
64
66
68
70
72
74
76

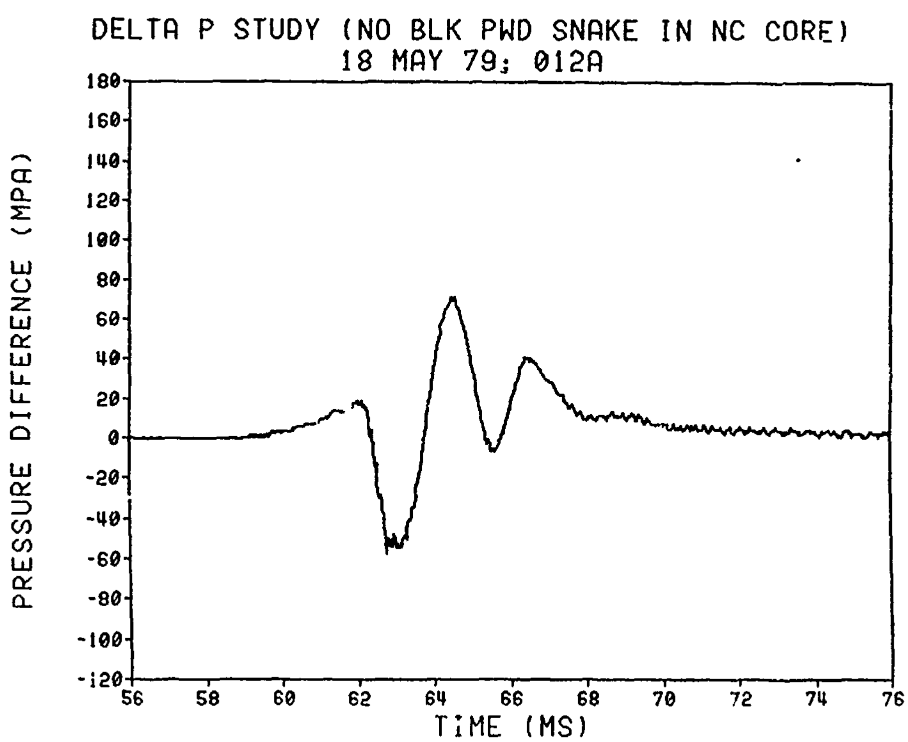
DELTA P STUDY (NO BLK PWD SNAKE IN NC CORE)
18 MAY 79; 012A
PRESSURE DIFFERENCE (MPA)
TIME (MS)
180
160
140
120
100
80
60
40
20
0
-20
-40
-60
-80
-100
-120
56
58
60
62
64
66
68
70
72
74
76

DELTA P STUDY (NO BLK PWD SNAKE IN NC CORE)
18 MAY 79; 013A

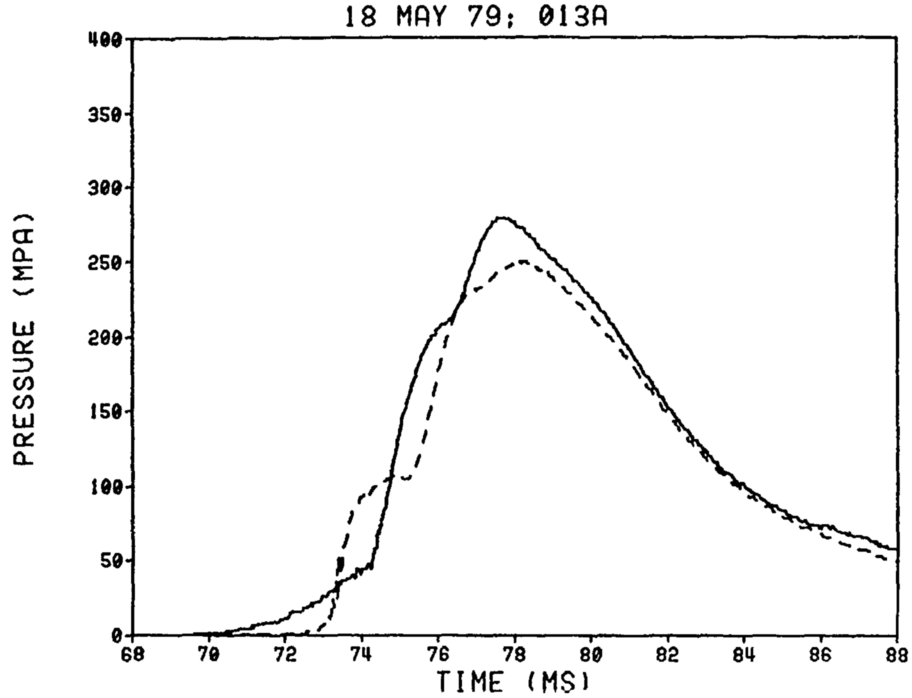

DELTA P STUDY (NO BLK PWD SNAKE IN NC CORE)
18 MAY 79; 013A

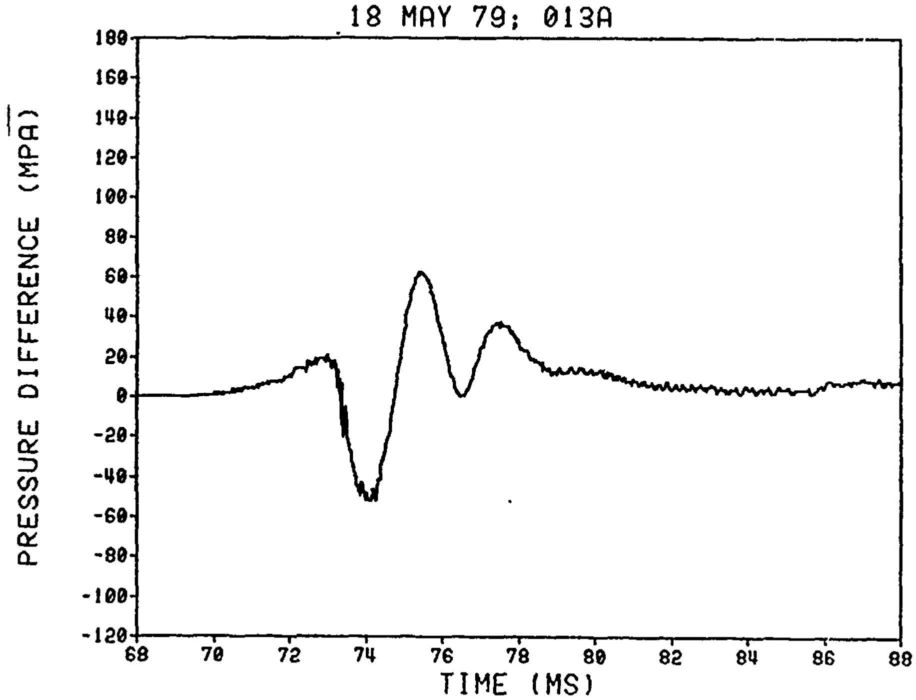

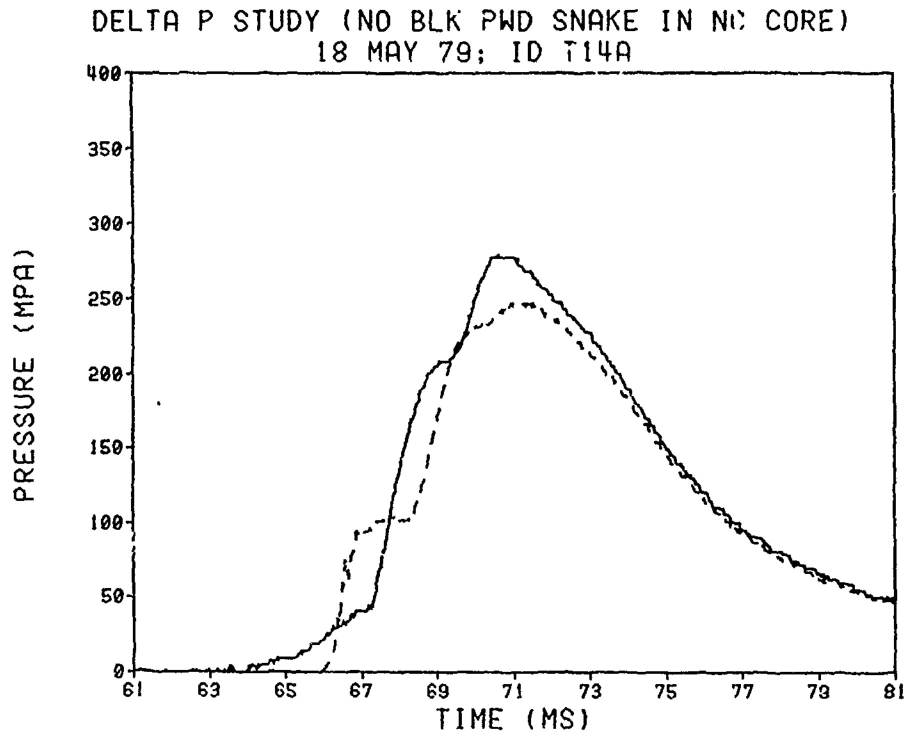
DELTA P STUDY (NO BLK PWD SNAKE IN NC CORE)
18 MAY 79; ID T14A
PRESSURE (MPA)
400
350
300
250
200
150
100
50
0
61
63
65
67
69
71
73
75
77
79
81
TIME (MS)

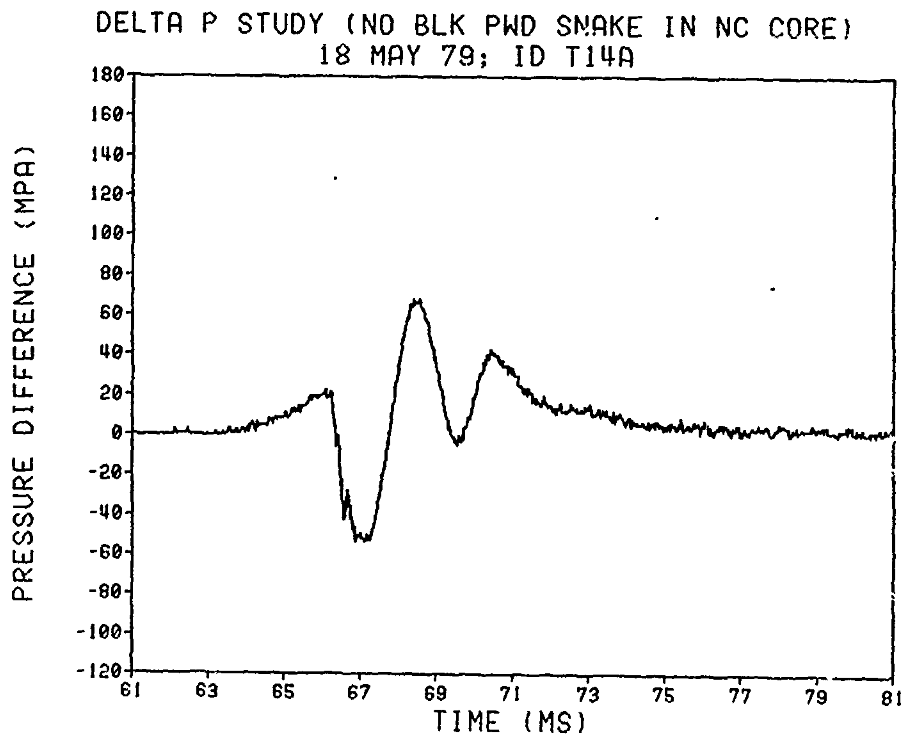
DELTA P STUDY (NO BLK PWD SNAKE IN NC CORE)
18 MAY 79; ID T14A
PRESSURE DIFFERENCE (MPA)
180
160
140
120
100
80
60
40
20
0
-20
-40
-60
-80
-100
-120
61
63
65
67
69
71
73
75
77
79
81
TIME (MS)

DELTA P STUDY (NO BLK PWD SNAKE IN NC CORE)
22 MAY 79; ID T17A

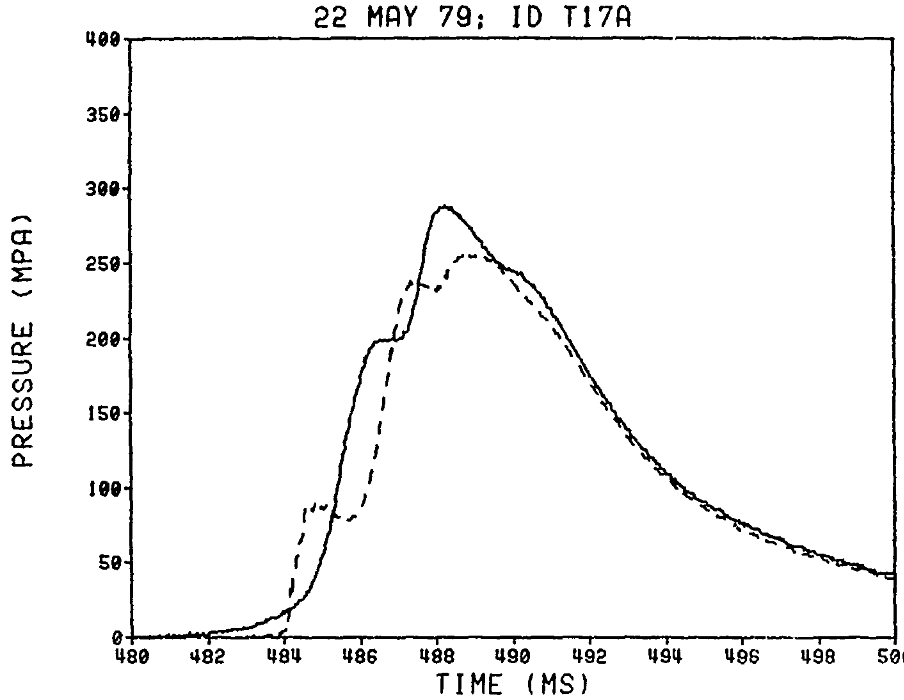

DELTA P STUDY (NO BLK PWD SNAKE IN NC CORE)
22 MAY 79; ID T17A

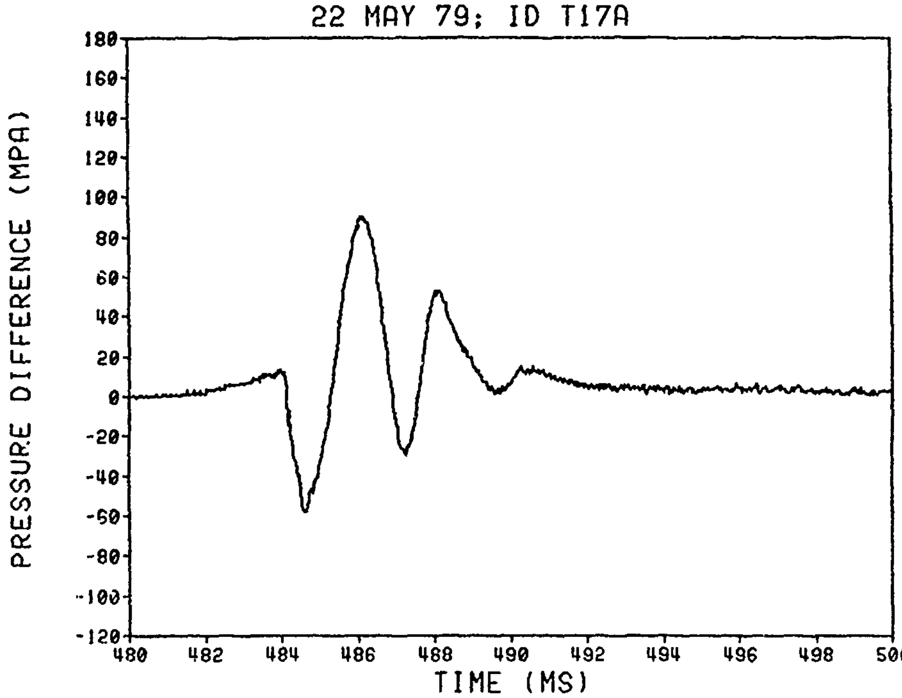

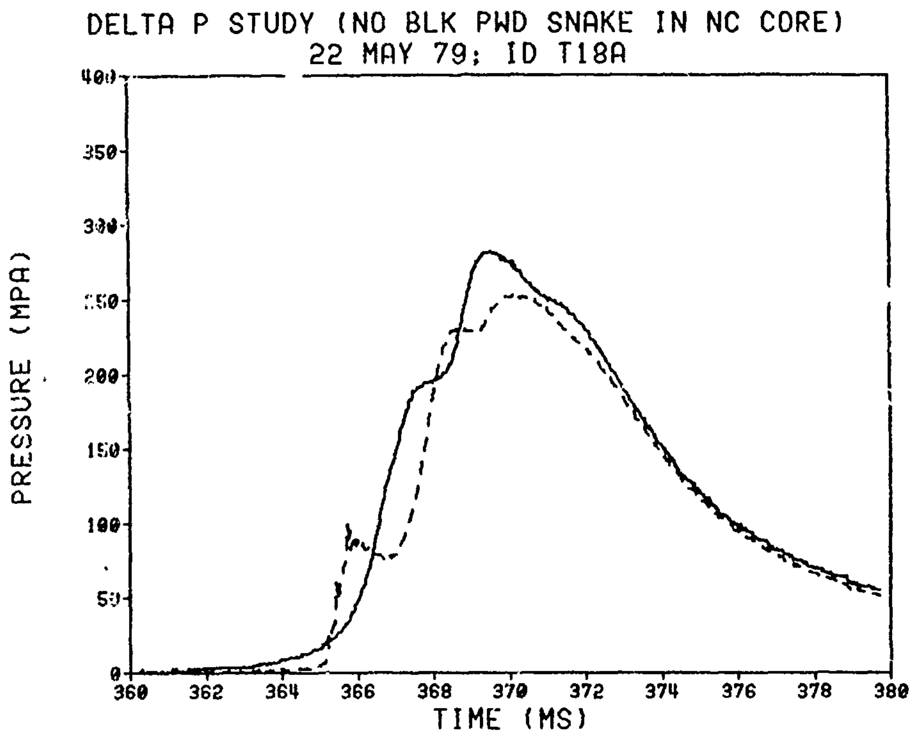
DELTA P STUDY (NO BLK PWD SNAKE IN NC CORE)
22 MAY 79; ID T18A
PRESSURE (MPA)
TIME (MS)
0
50
100
150
200
250
300
350
400
360
362
364
366
368
370
372
374
376
378
380

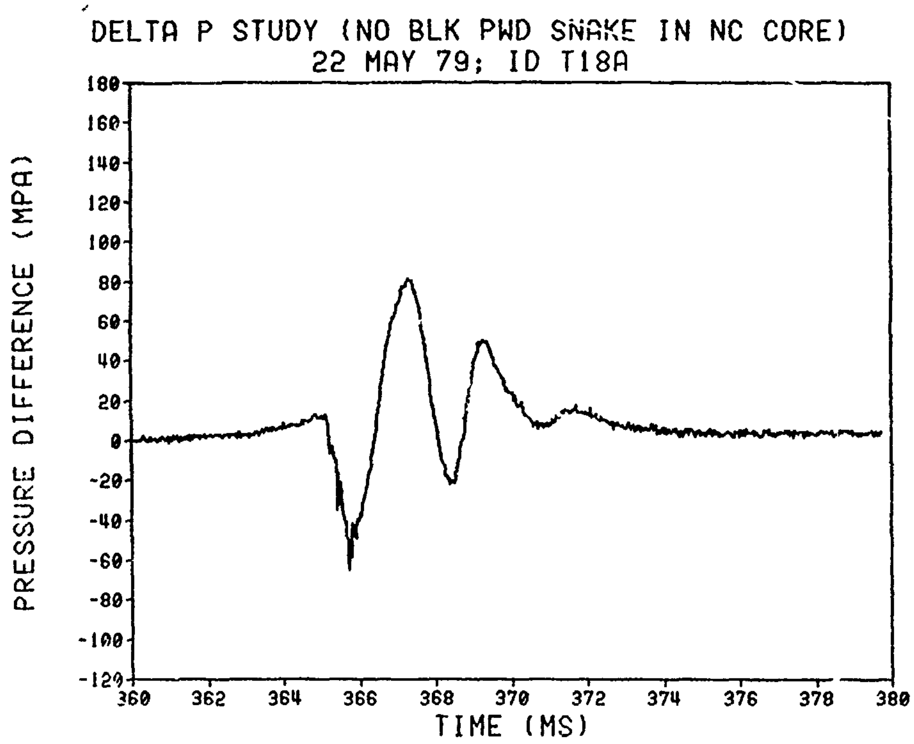
DELTA P STUDY (NO BLK PWD SNAKE IN NC CORE)
22 MAY 79; ID T18A
PRESSURE DIFFERENCE (MPA)
TIME (MS)
180
160
140
120
100
80
60
40
20
0
-20
-40
-60
-80
-100
-120
360
362
364
366
368
370
372
374
376
378
380

DELTA P STUDY (NO BLK PWD SNAKE IN NC CORE)
22 MAY 79; ID T19A

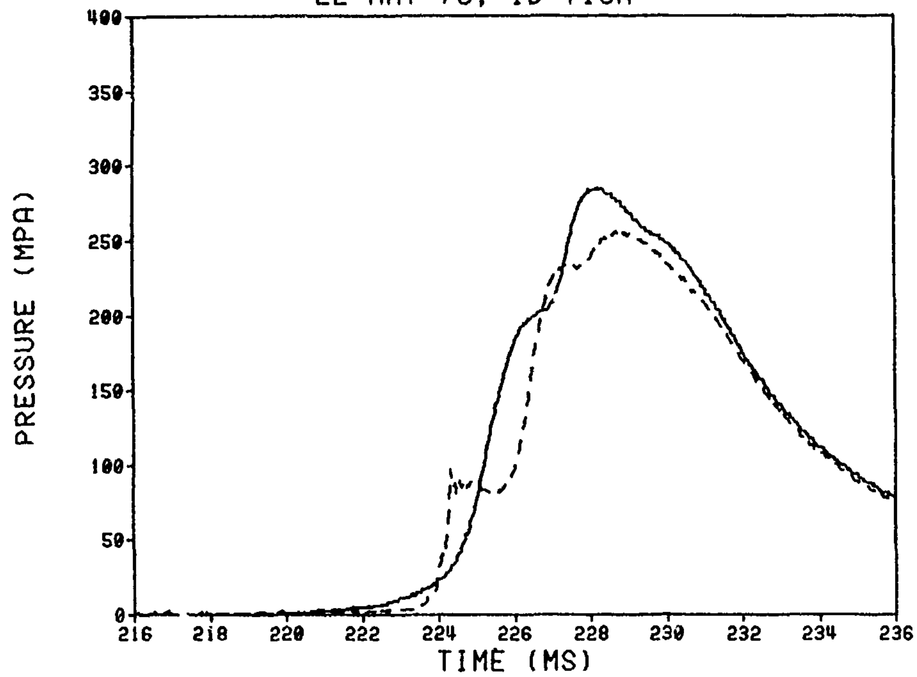

DELTA P STUDY (NO BLK PWD SNAKE IN NC CORE)
22 MAY 79; ID T19A

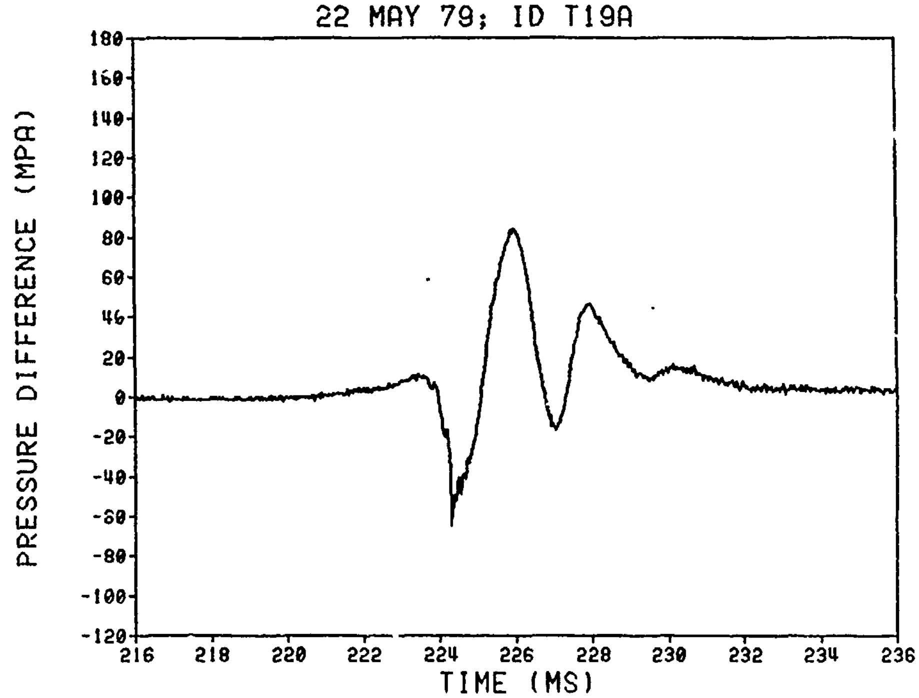

DELTA P STUDY (NO BLK PWD SNAKE IN NC CORE)
22 MAY 79; ID T20A

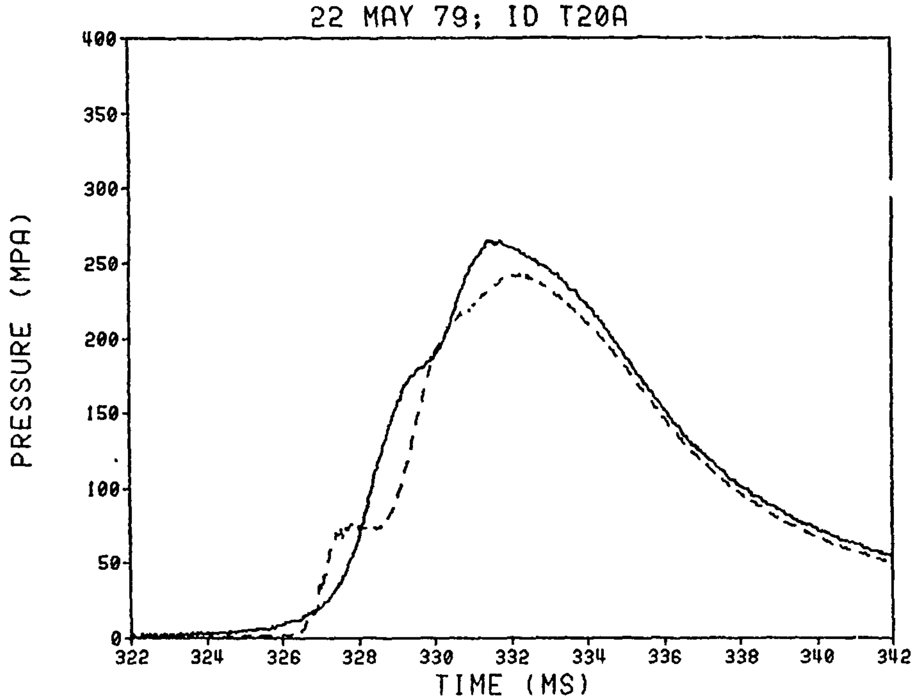

DELTA P STUDY (NO BLK PWD SNAKE IN NC CORE)
22 MAY 79; ID T20A

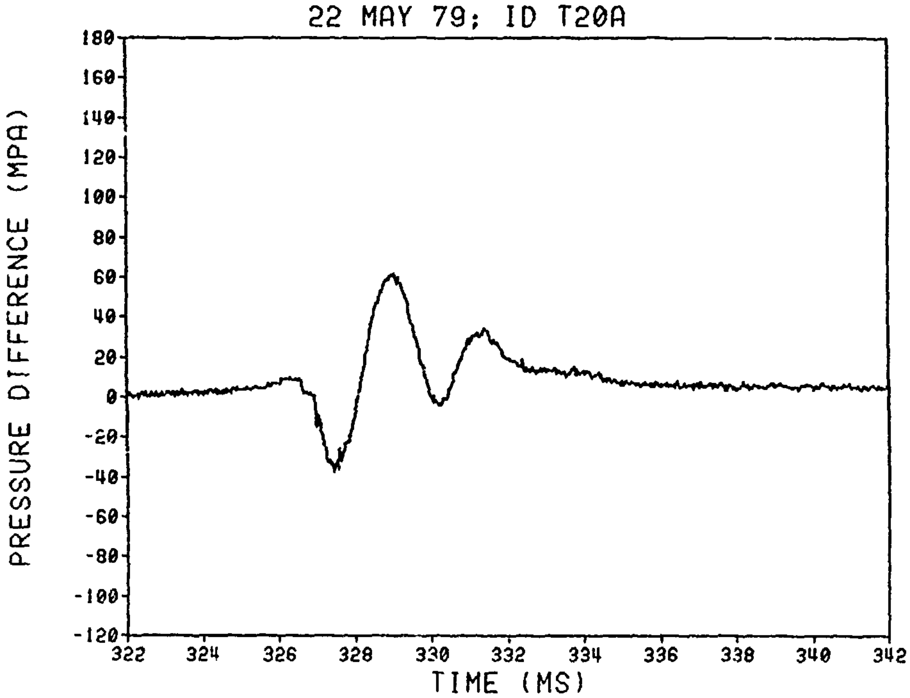

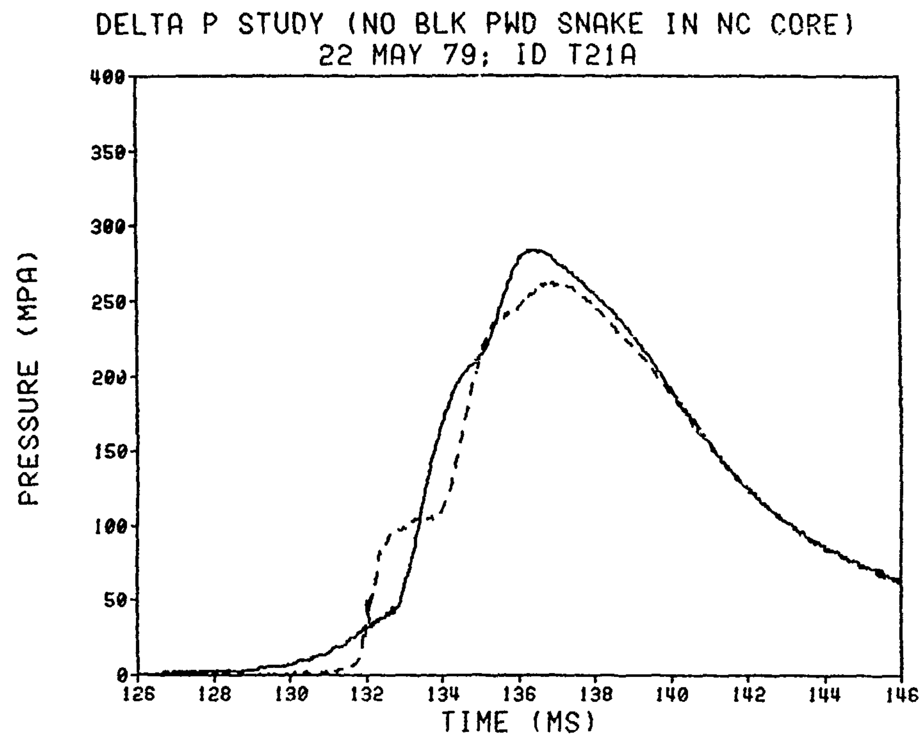
DELTA P STUDY (NO BLK PWD SNAKE IN NC CORE)
22 MAY 79; ID T21A
PRESSURE (MPA)
TIME (MS)
0
50
100
150
200
250
300
350
400
126
128
130
132
134
136
138
140
142
144
146

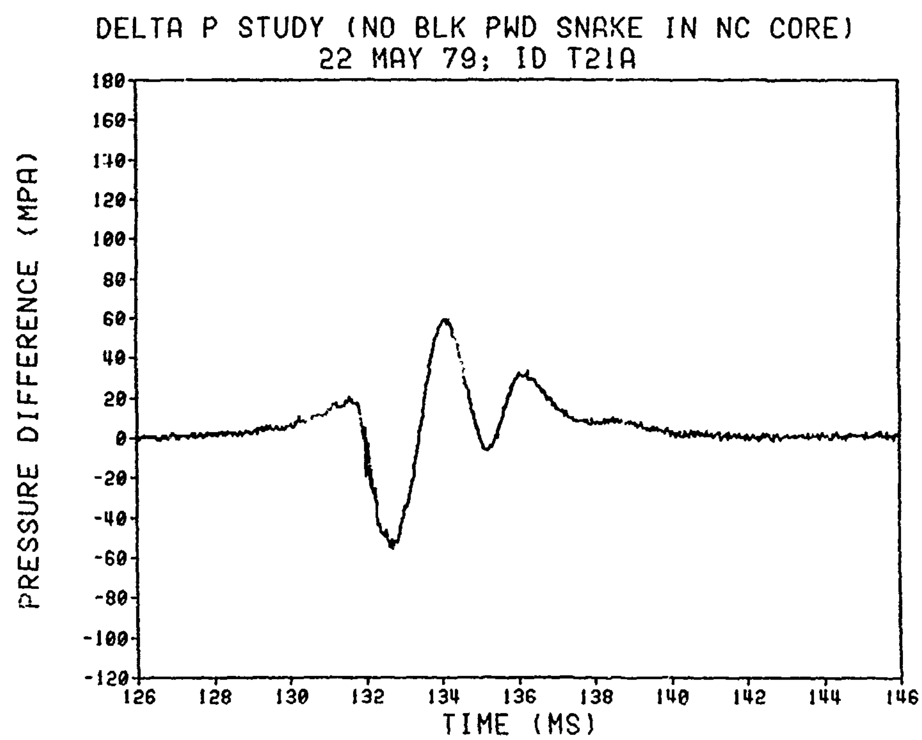
DELTA P STUDY (NO BLK PWD SNAKE IN NC CORE)
22 MAY 79; ID T21A
PRESSURE DIFFERENCE (MPA)
TIME (MS)
180
160
140
120
100
80
60
40
20
0
-20
-40
-60
-80
-100
-120
126
128
130
132
134
136
138
140
142
144
146

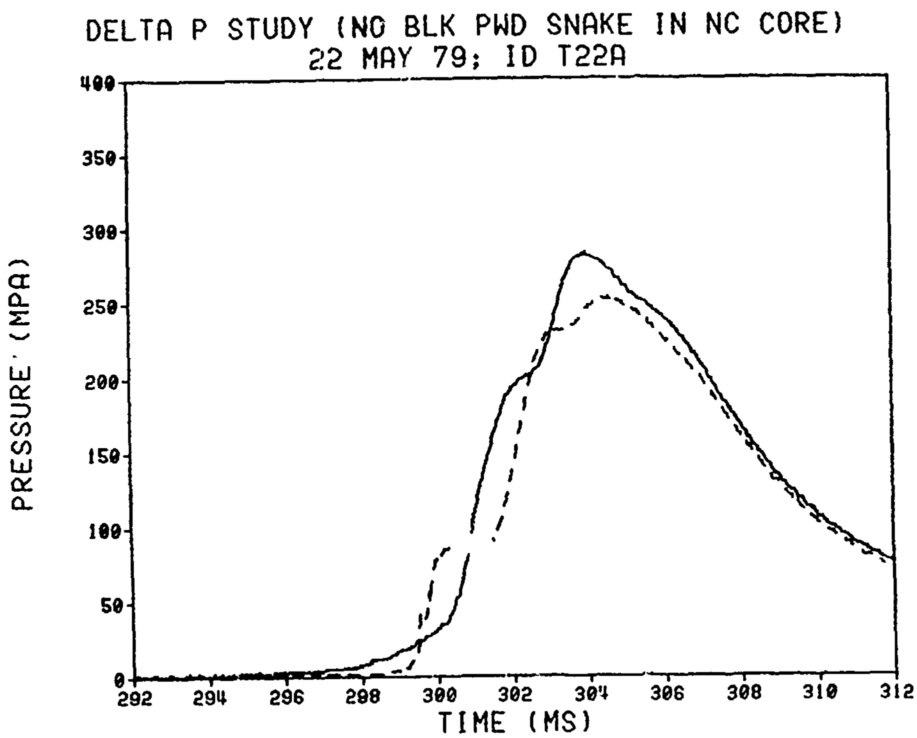
DELTA P STUDY (NO BLK PWD SNAKE IN NC CORE)
22 MAY 79; ID T22A
PRESSURE (MPA)
TIME (MS)
400
350
300
250
200
150
100
50
0
292
294
296
298
300
302
304
306
308
310
312

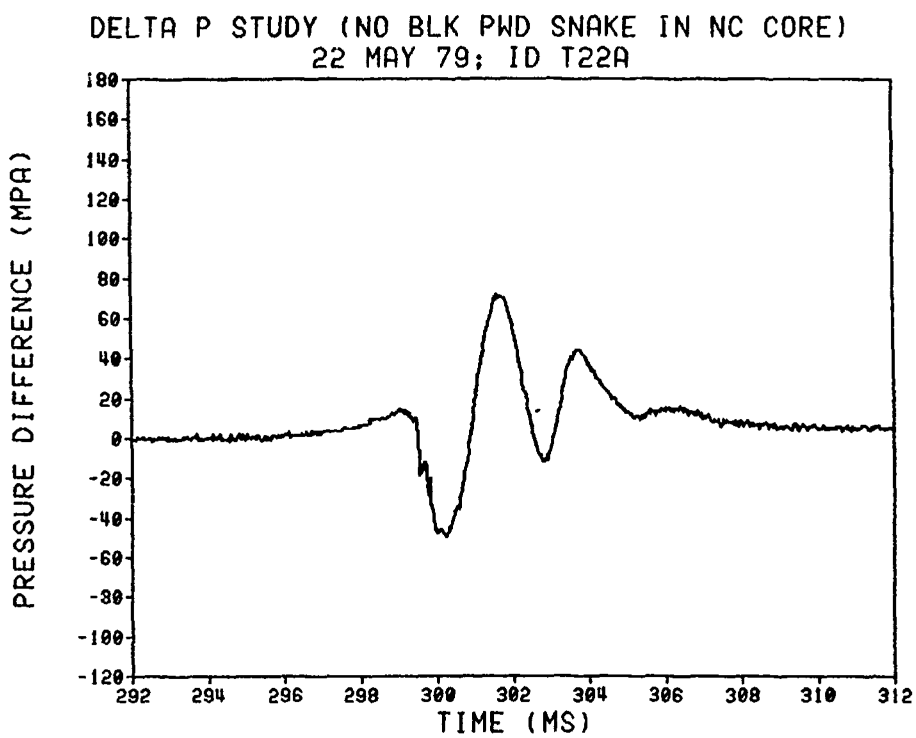
DELTA P STUDY (NO BLK PWD SNAKE IN NC CORE)
22 MAY 79; ID T22A
PRESSURE DIFFERENCE (MPA)
TIME (MS)
180
160
140
120
100
80
60
40
20
0
-20
-40
-60
-80
-100
-120
292
294
296
298
300
302
304
306
308
310
312

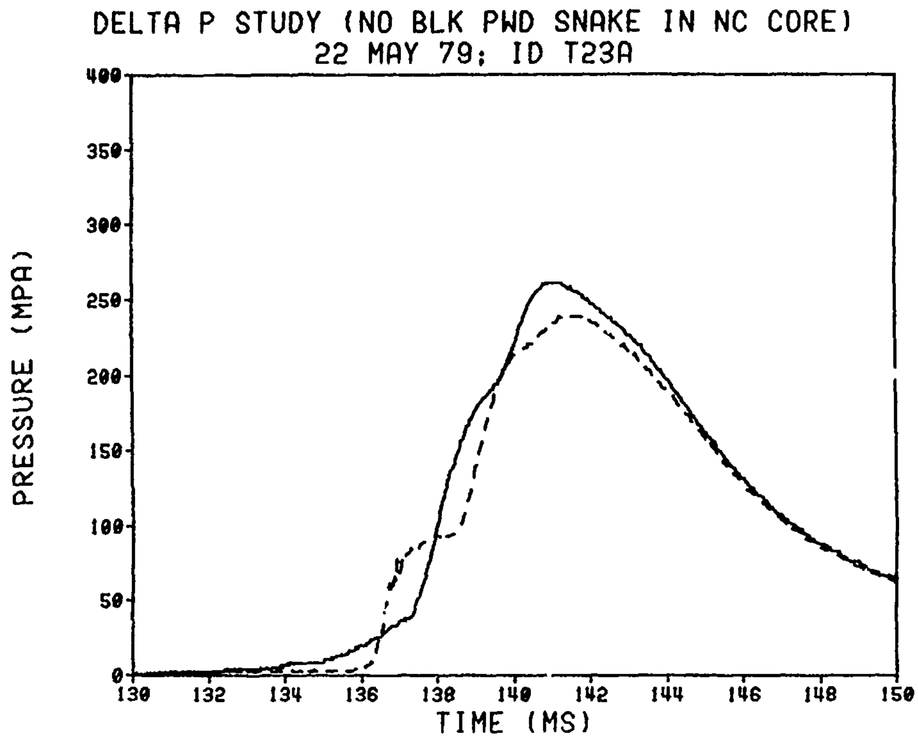

DELTA P STUDY (NO BLK PWD SNAKE IN NC CORE)
22 MAY 79; ID T23A
PRESSURE (MPA)
400
350
300
250
200
150
100
50
0
130
132
134
136
138
140
142
144
146
148
150
TIME (MS)

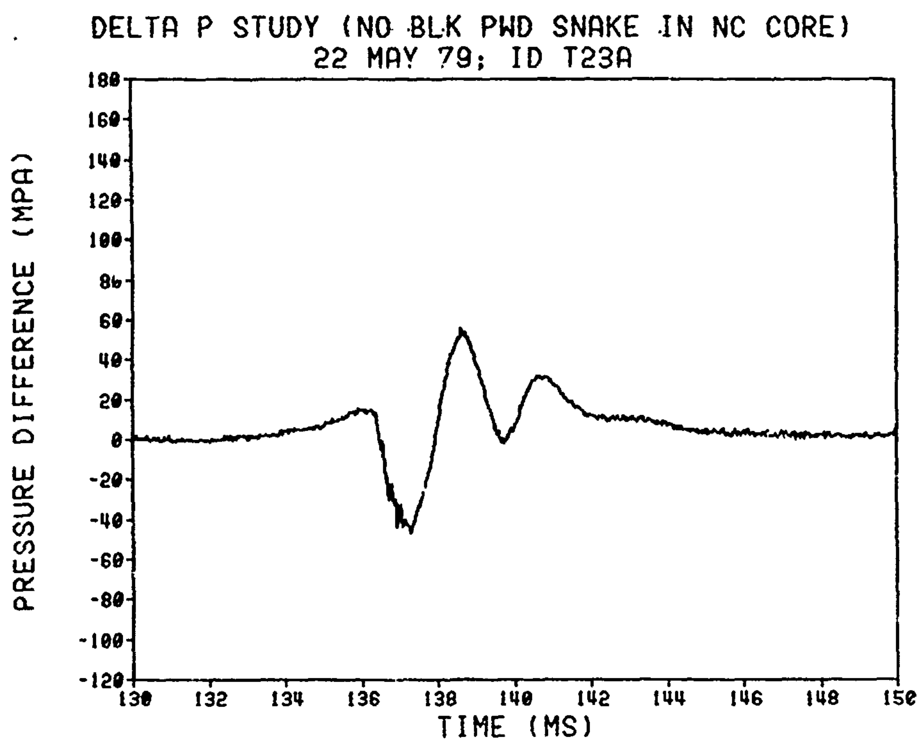

DELTA P STUDY (NO BLK PWD SNAKE IN NC CORE)
22 MAY 79; ID T23A
PRESSURE DIFFERENCE (MPA)
180
160
140
120
100
80
60
40
20
0
-20
-40
-60
-80
-100
-120
130
132
134
136
138
140
142
144
146
148
150
TIME (MS)

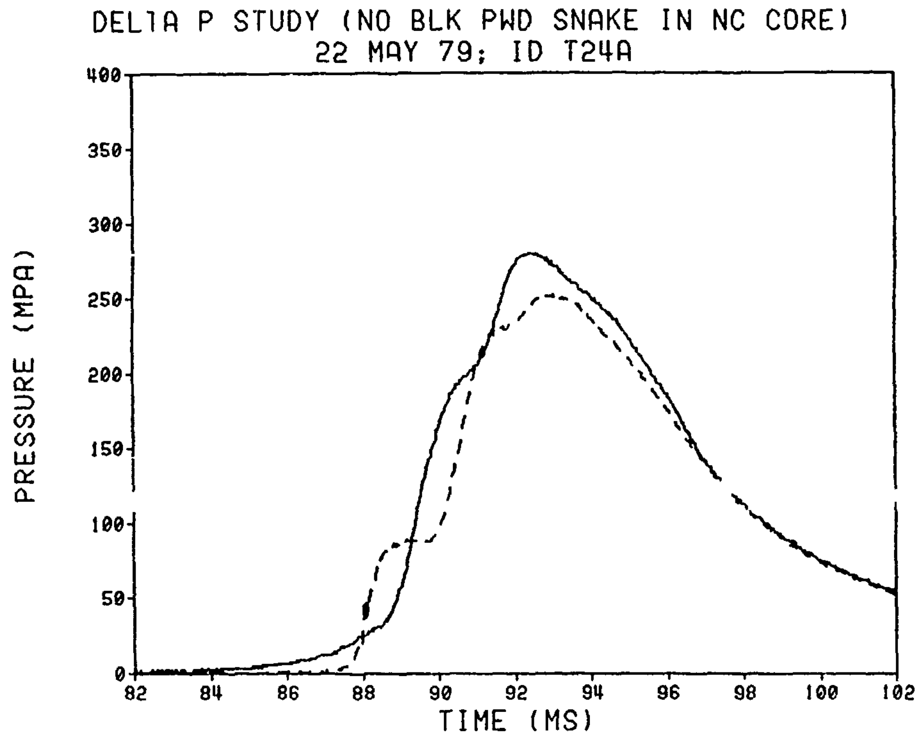
DELTA P STUDY (NO BLK PWD SNAKE IN NC CORE)
22 MAY 79; ID T24A
PRESSURE (MPA)
TIME (MS)
400
350
300
250
200
150
100
50
0
82
84
86
88
90
92
94
96
98
100
102

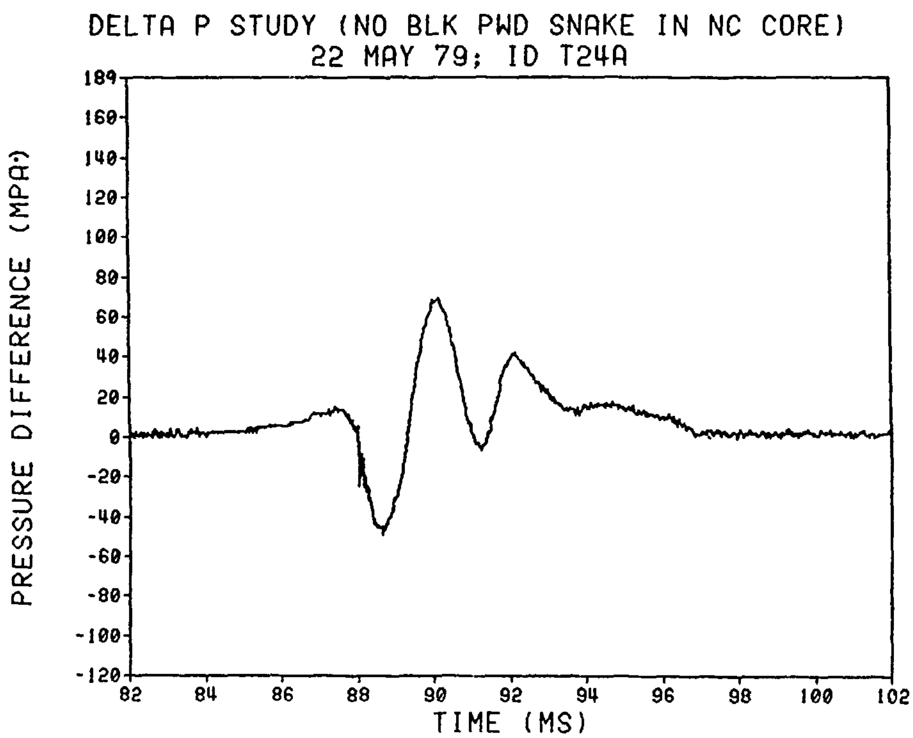
DELTA P STUDY (NO BLK PWD SNAKE IN NC CORE)
22 MAY 79; ID T24A
PRESSURE DIFFERENCE (MPA)
TIME (MS)
180
160
140
120
100
80
60
40
20
0
-20
-40
-60
-80
-100
-120
82
84
86
88
90
92
94
96
98
100
102

DELTA P STUDY (MODIFIED BLK PWD SNAKE IN NC CORE)
31 JULY 79; ID 033A

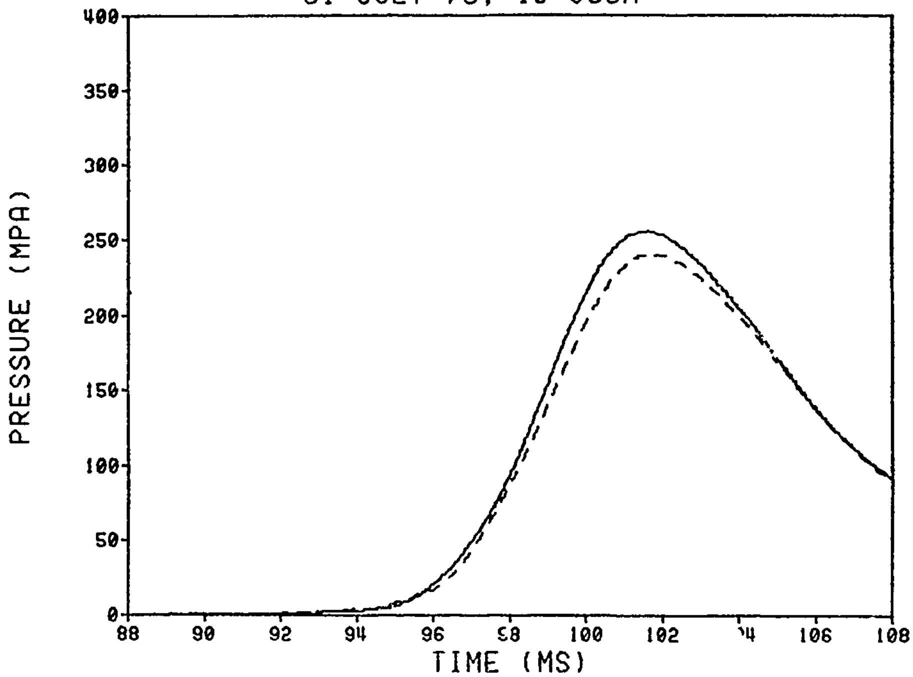

DELTA P STUDY (MODIFIED BLK PWD SNAKE IN NC CORE)
31 JULY 79; ID 033A

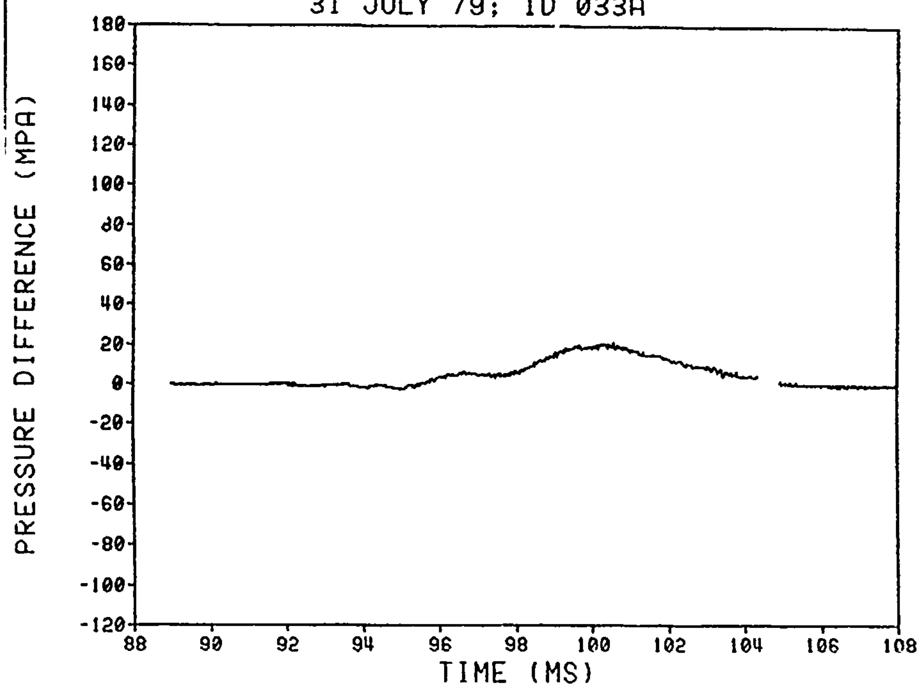

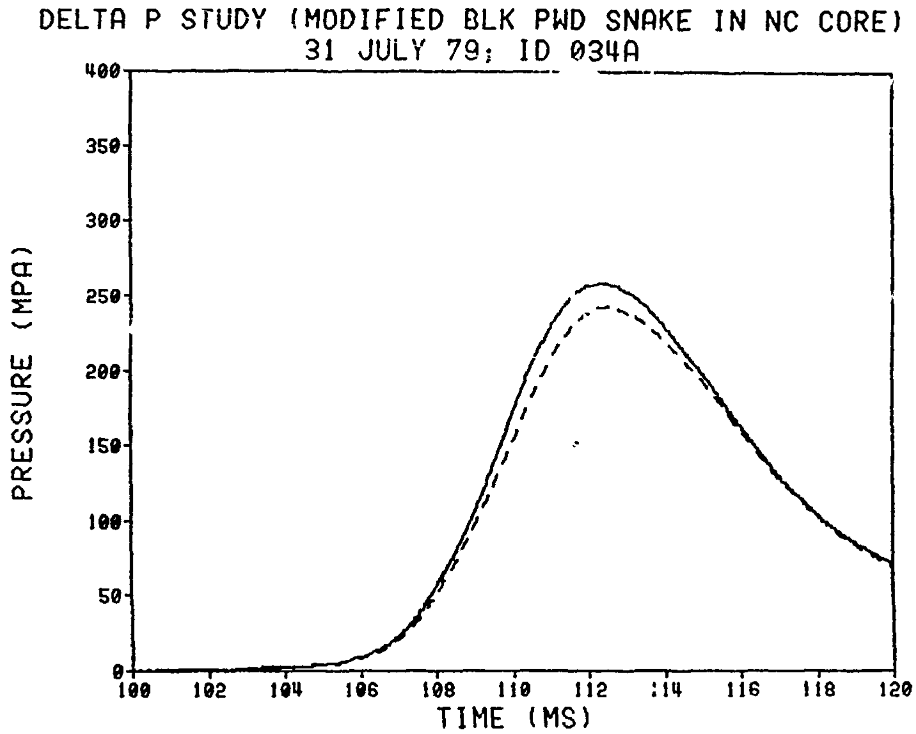
DELTA P STUDY (MODIFIED BLK PWD SNAKE IN NC CORE)
31 JULY 79; ID 034A
PRESSURE (MPA)
TIME (MS)
0
50
100
150
200
250
300
350
400
100
102
104
106
108
110
112
114
116
118
120

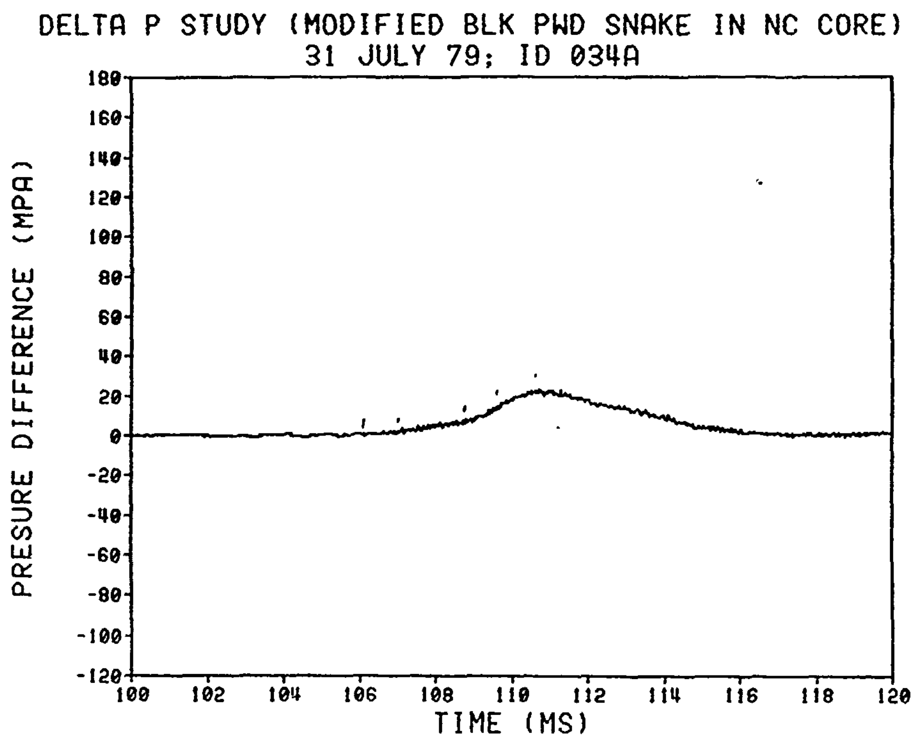
DELTA P STUDY (MODIFIED BLK PWD SNAKE IN NC CORE)
31 JULY 79; ID 034A
PRESURE DIFFERENCE (MPA)
TIME (MS)
180
160
140
120
100
80
60
40
20
0
-20
-40
-60
-80
-100
-120
100
102
104
106
108
110
112
114
116
118
120

DELTA P STUDY (MODIFIED BLK PWD SNAKE IN NC CORE)
31 JULY 79; ID 035A

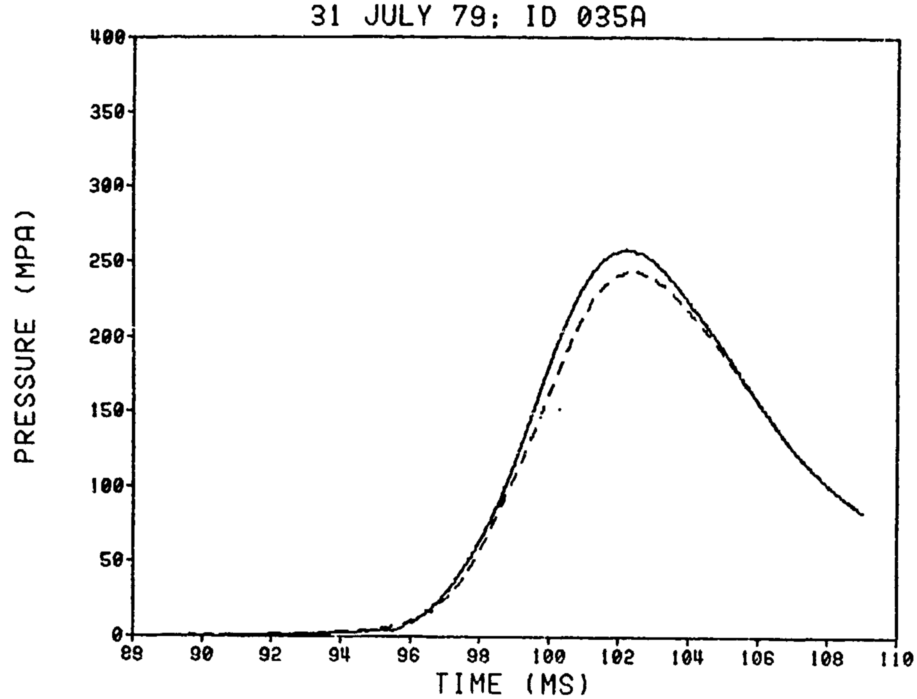

DELTA P STUDY (MODIFIED BLK PWD SNAKE IN NC CORE)
31 JULY 79; ID 035A

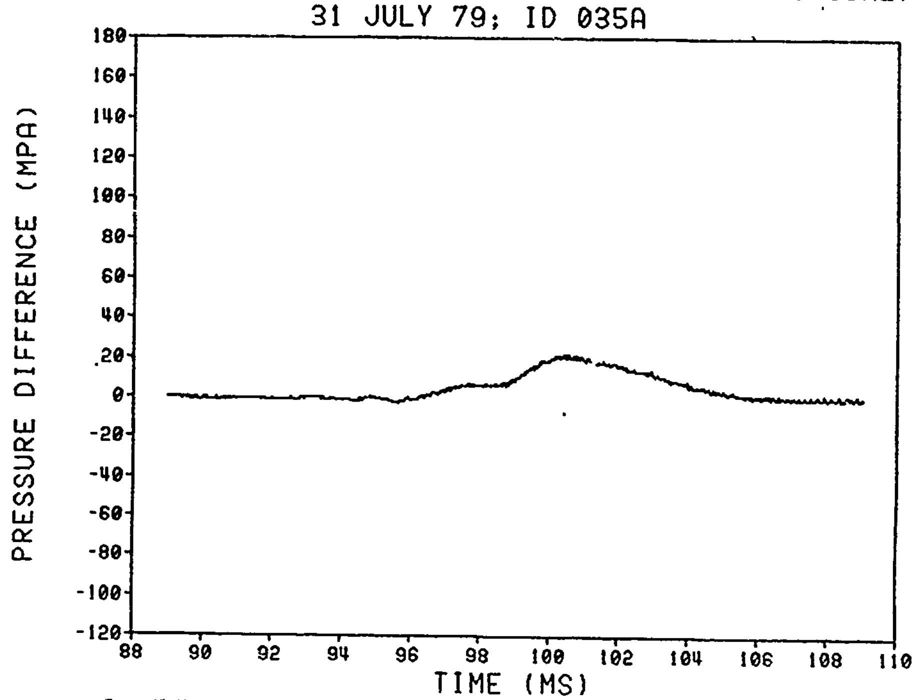

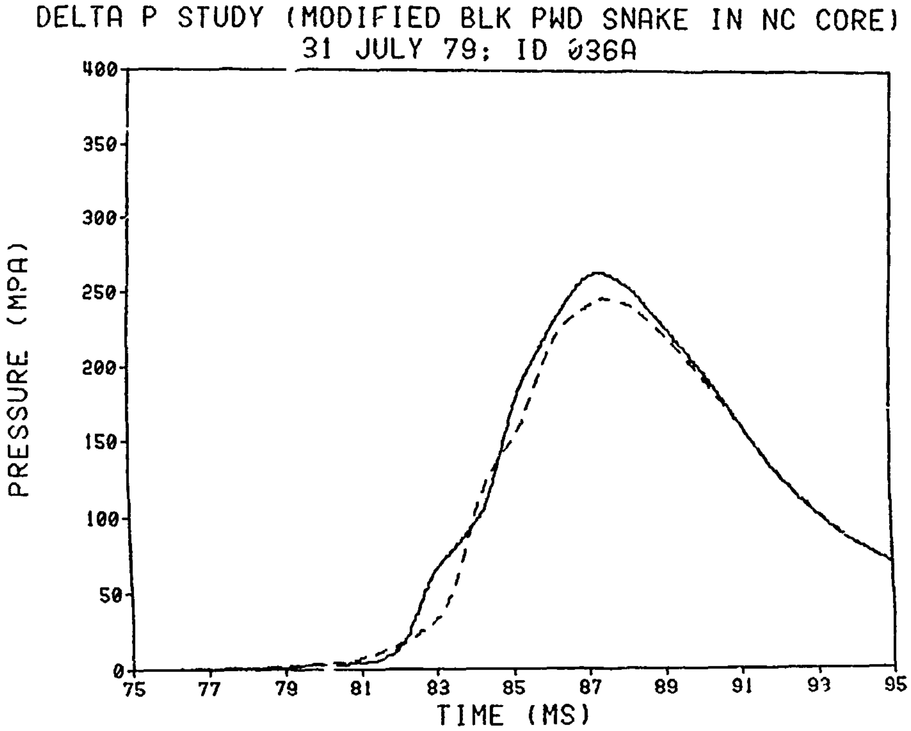
DELTA P STUDY (MODIFIED BLK PWD SNAKE IN NC CORE)
31 JULY 79; ID 036A
PRESSURE (MPA)
TIME (MS)

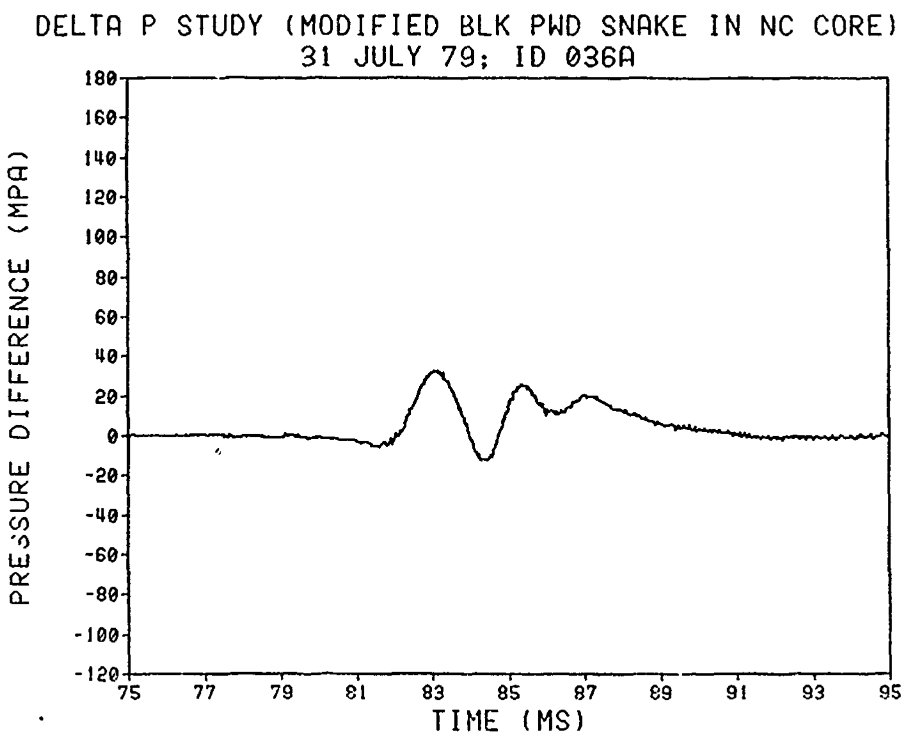
DELTA P STUDY (MODIFIED BLK PWD SNAKE IN NC CORE)
31 JULY 79; ID 036A
PRESSURE DIFFERENCE (MPA)
TIME (MS)

DELTA P STUDY (MODIFIED BLK PWD SNAKE IN NC CORE)
1 AUG 79; ID 041A

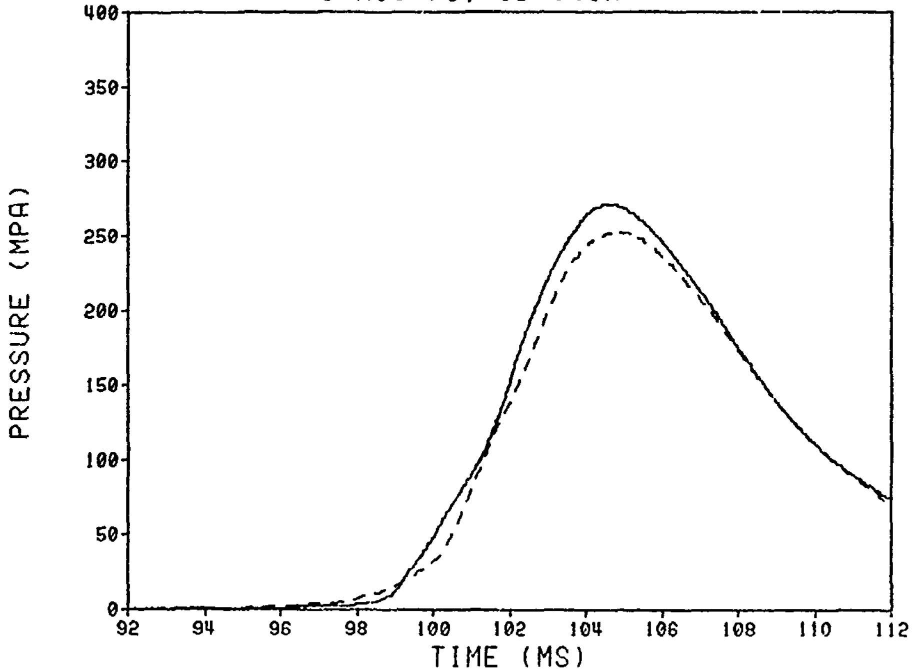

DELTA P STUDY (MODIFIED BLK PWD SNAKE IN NC CORE)
1 AUG 79; ID 041A

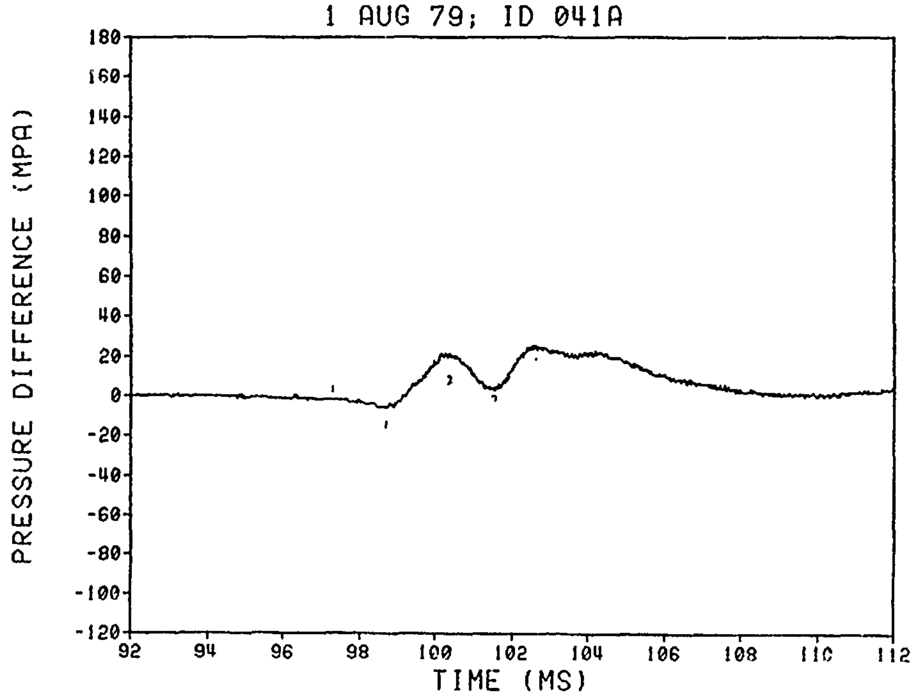

DELTA P STUDY (MODIFIED BLK PWD SNAKE IN NC CORE)
1 AUG 79; ID 042A

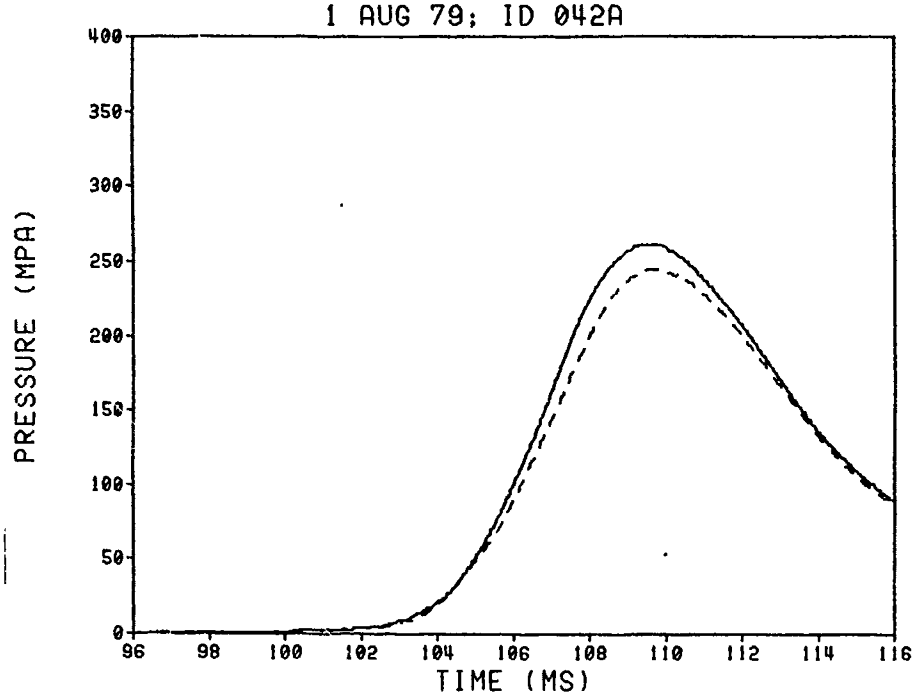

DELTA P STUDY (MODIFIED BLK PWD SNAKE IN NC CORE)
1 AUG 79; ID 042A

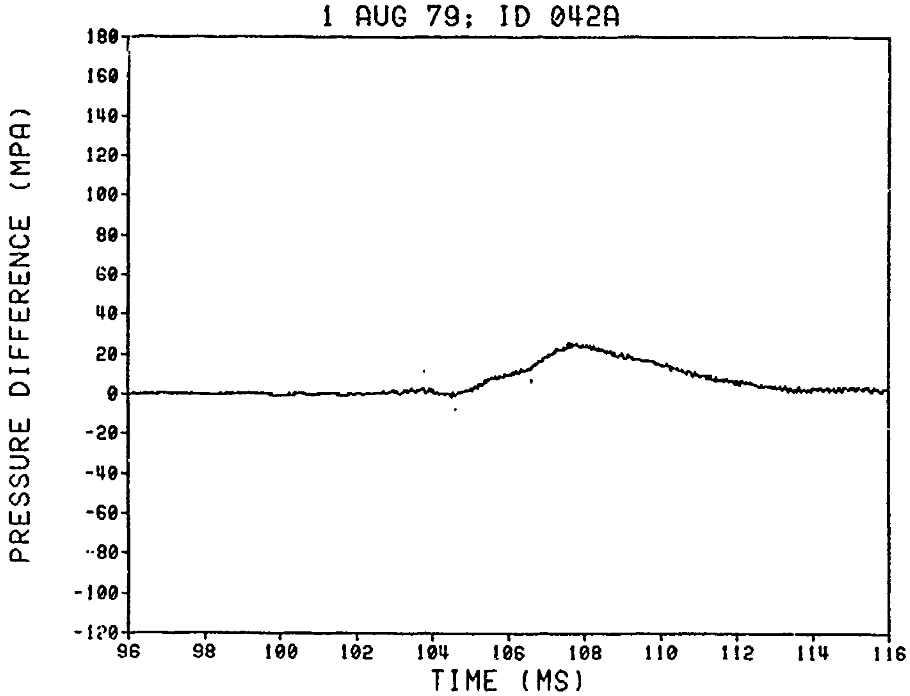

DELTA P STUDY (MODIFIED BLK PWD SNAKE IN NC CORE)
1 AUG 79; ID T43A

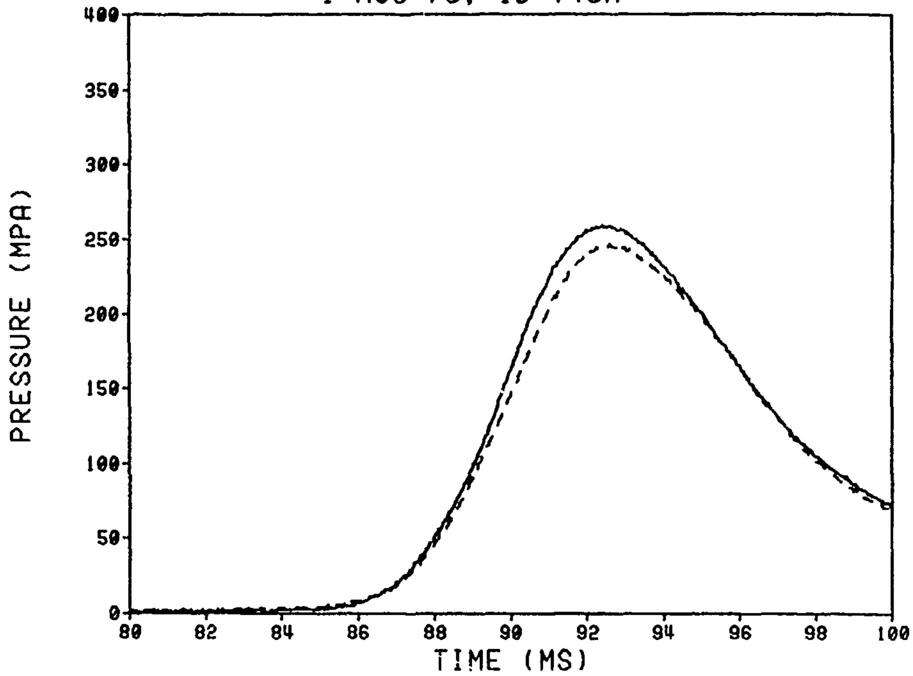

DELTA P STUDY (MODIFIED BLK PWD SNAKE IN NC CORE)
1 AUG 79; ID T43A

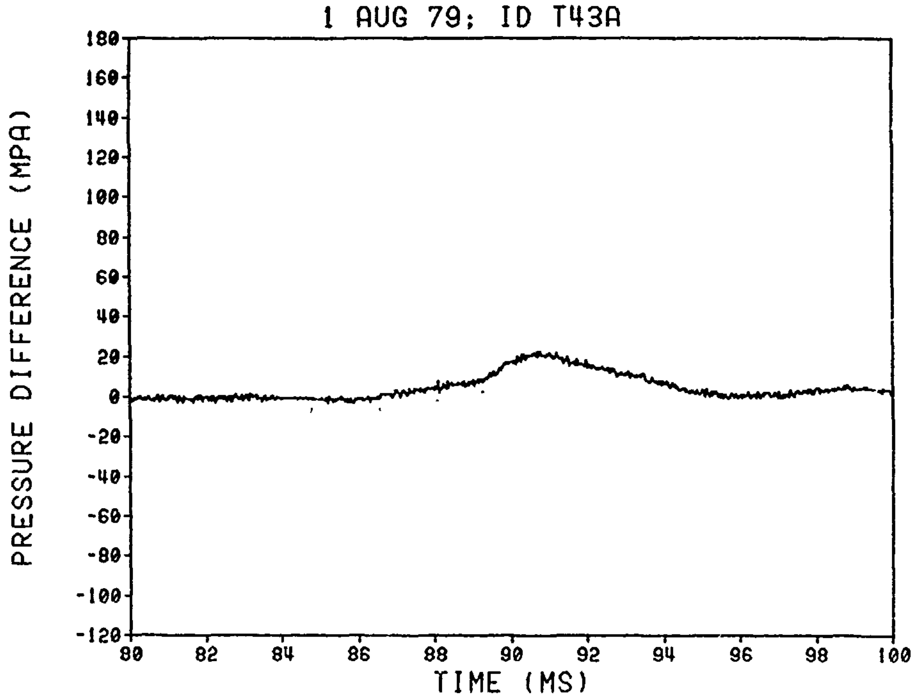

DELTA P STUDY (MODIFIED BLK PWD SNAKE IN NC CORE)
1 AUG 79; ID 044A

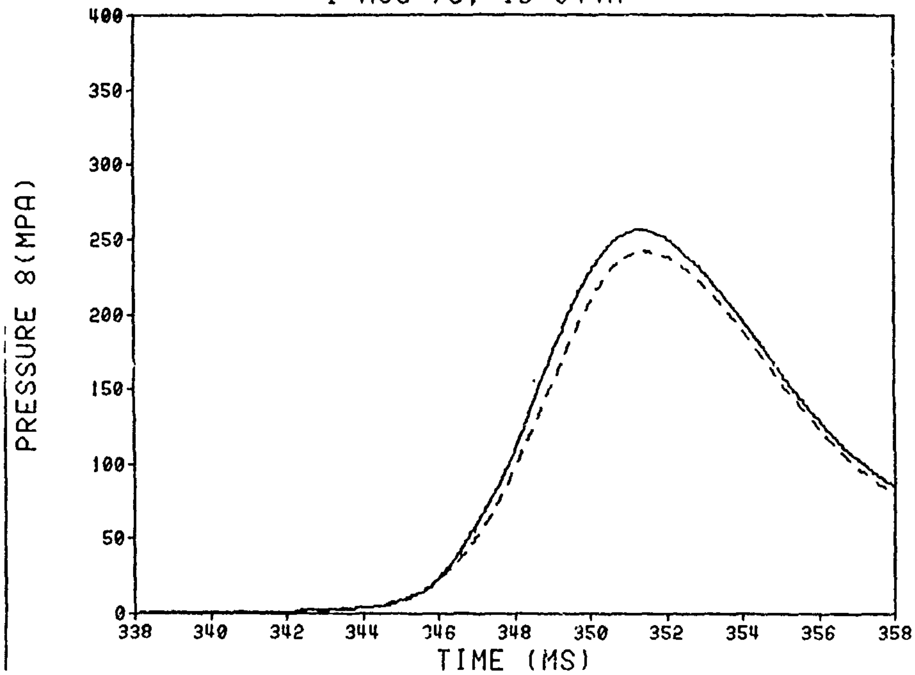

DELTA P STUDY (MODIFIED BLK PWD SNAKE IN NC CORE)
1 AUG 79; ID 044A

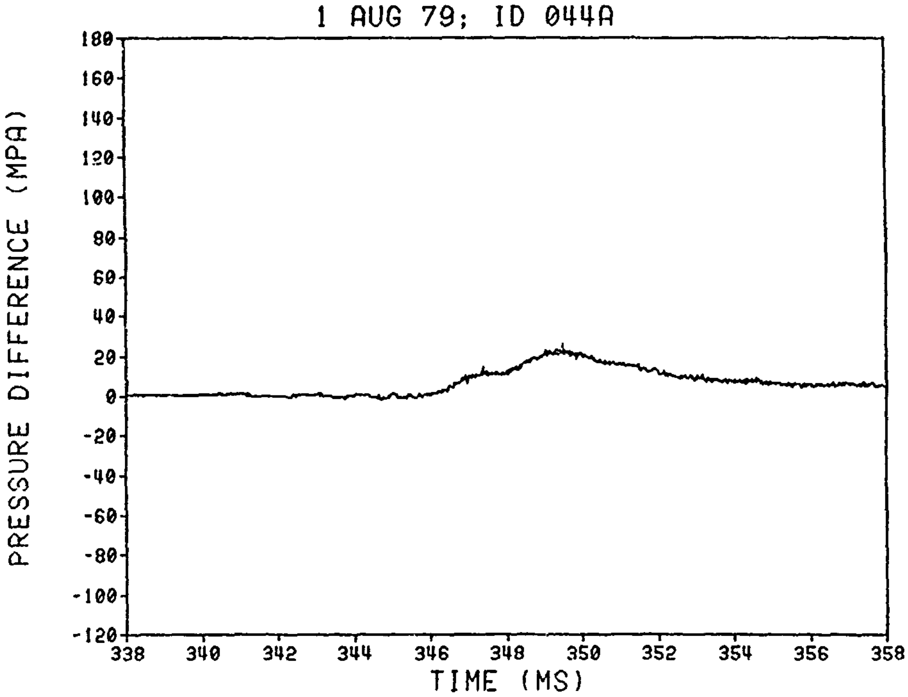

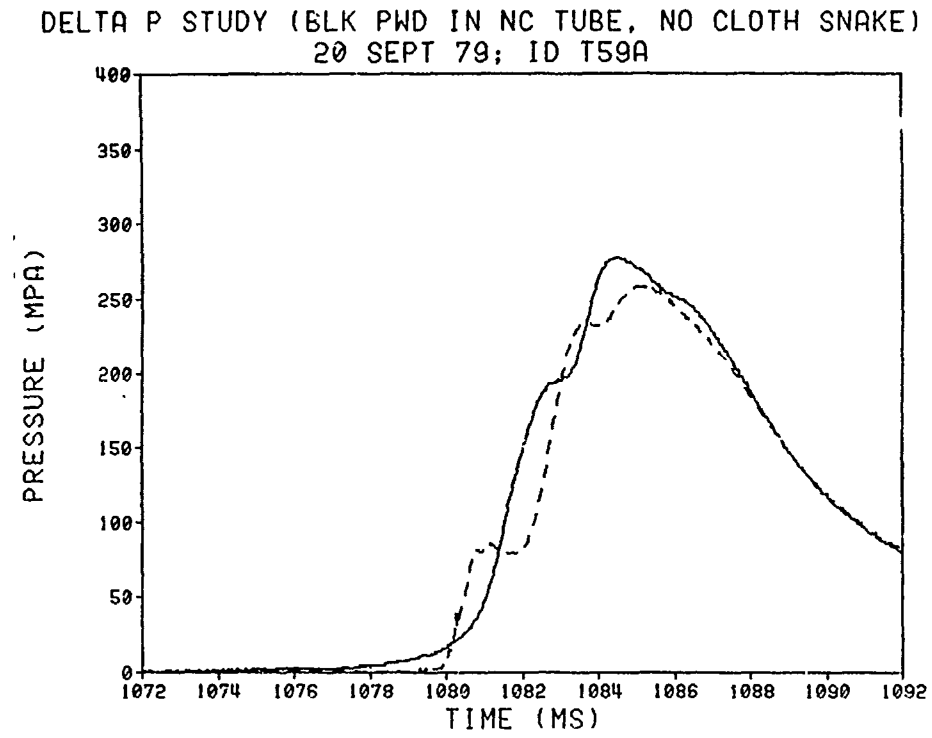
DELTA P STUDY (BLK PWD IN NC TUBE, NO CLOTH SNAKE)
20 SEPT 79; ID T59A
PRESSURE (MPA)
TIME (MS)
0
50
100
150
200
250
300
350
400
1072
1074
1076
1078
1080
1082
1084
1086
1088
1090
1092

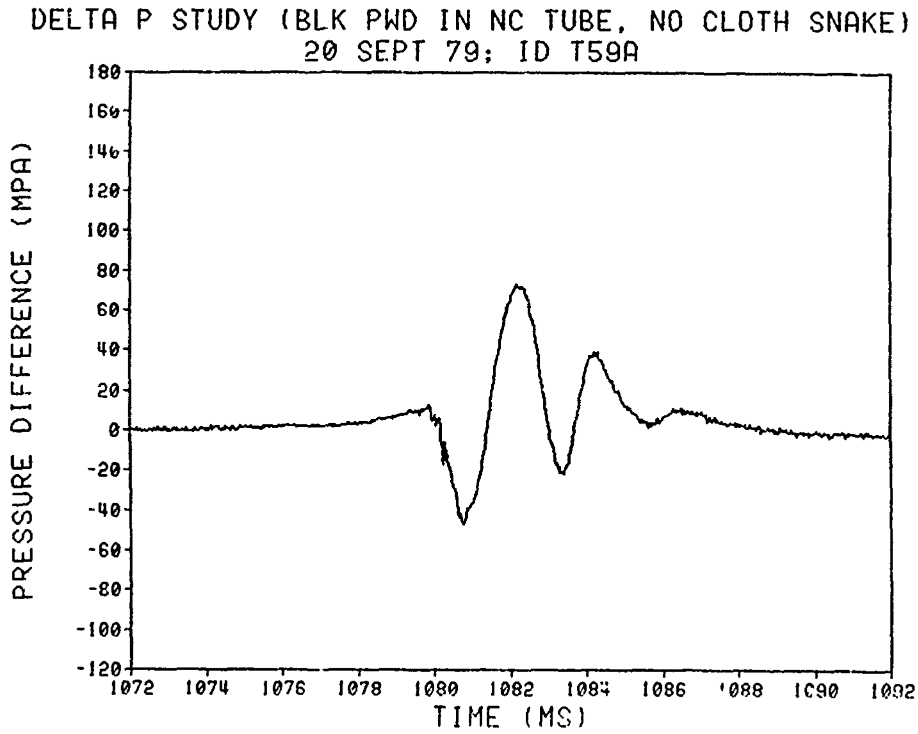
DELTA P STUDY (BLK PWD IN NC TUBE, NO CLOTH SNAKE)
20 SEPT 79; ID T59A
PRESSURE DIFFERENCE (MPA)
TIME (MS)
180
160
140
120
100
80
60
40
20
0
-20
-40
-60
-80
-100
-120
1072
1074
1076
1078
1080
1082
1084
1086
1088
1090
1092

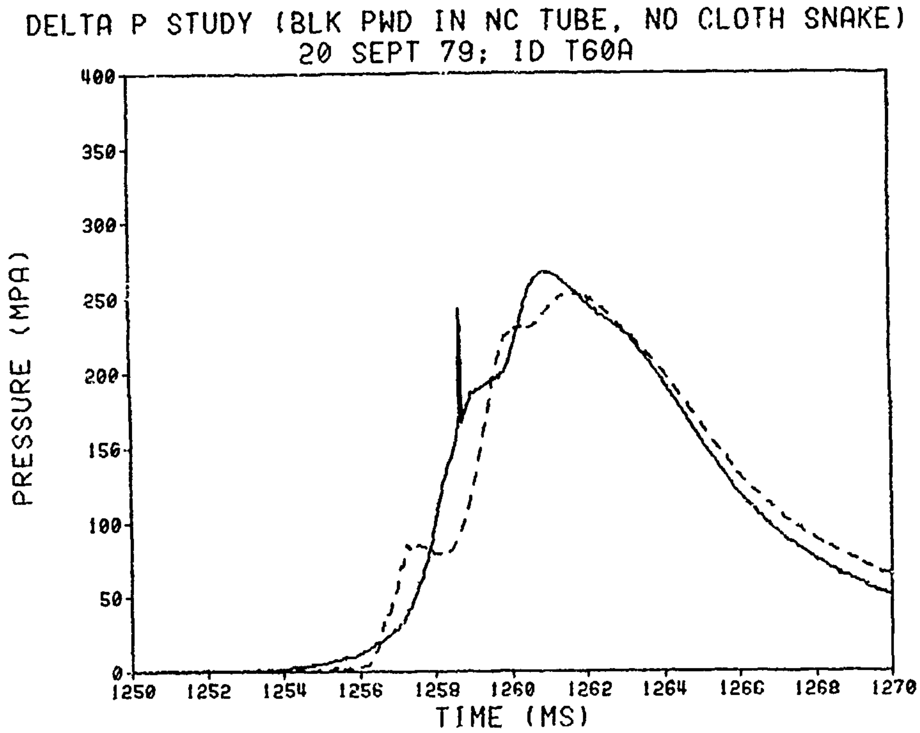
DELTA P STUDY (BLK PWD IN NC TUBE, NO CLOTH SNAKE)
20 SEPT 79; ID T60A
PRESSURE (MPA)
TIME (MS)
400
350
300
250
200
150
100
50
0
1250
1252
1254
1256
1258
1260
1262
1264
1266
1268
1270

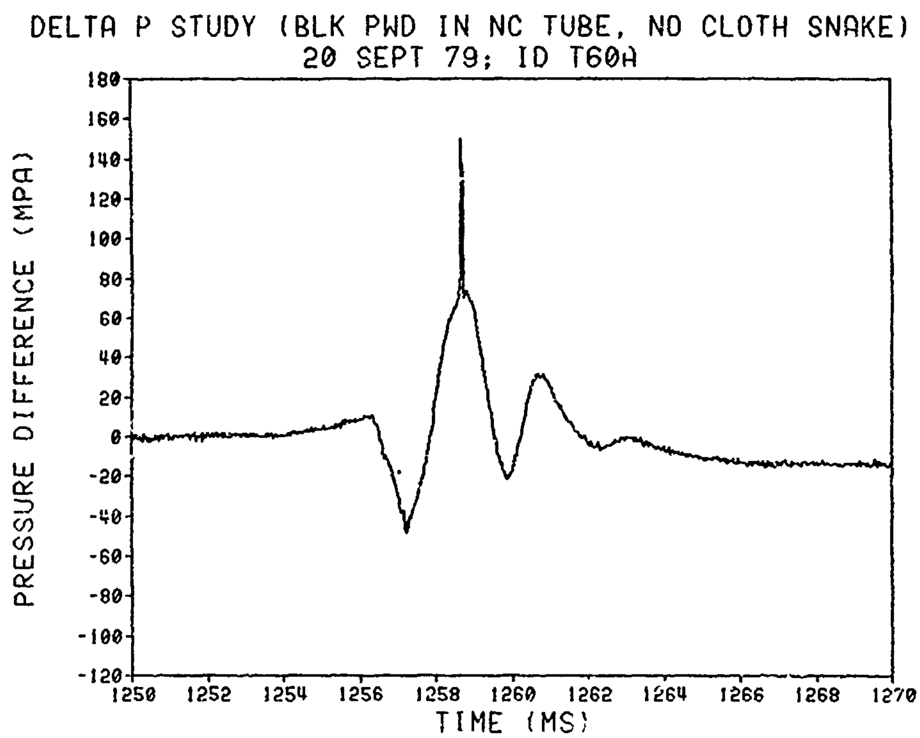
DELTA P STUDY (BLK PWD IN NC TUBE, NO CLOTH SNAKE)
20 SEPT 79; ID T60A
PRESSURE DIFFERENCE (MPA)
TIME (MS)
180
160
140
120
100
80
60
40
20
0
-20
-40
-60
-80
-100
-120
1250
1252
1254
1256
1258
1260
1262
1264
1266
1268
1270

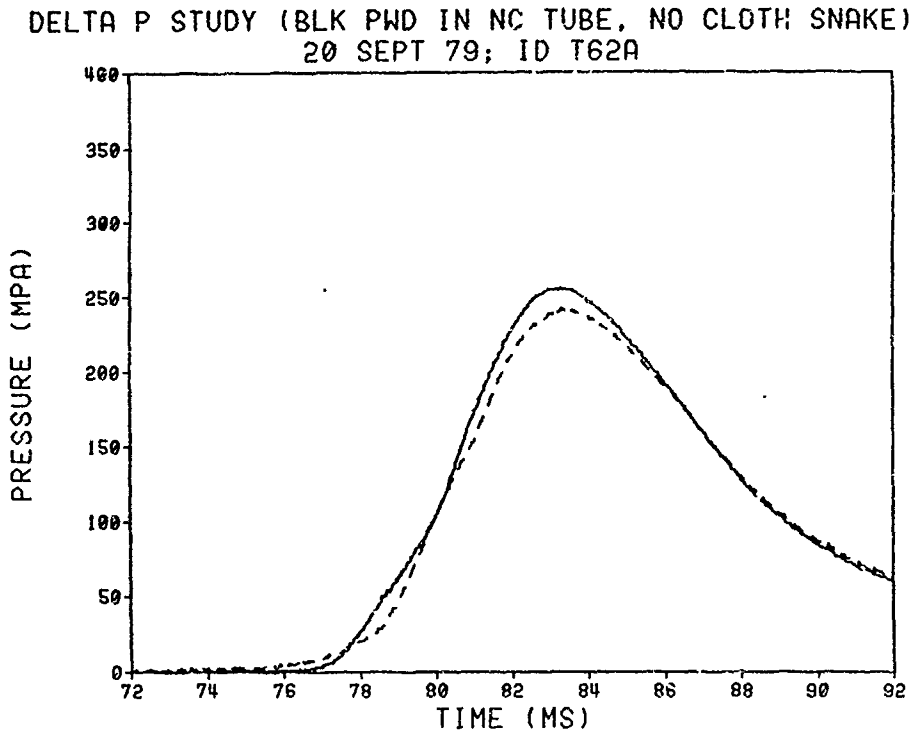
DELTA P STUDY (BLK PWD IN NC TUBE, NO CLOTH SNAKE)
20 SEPT 79; ID T62A
PRESSURE (MPA)
TIME (MS)
0
50
100
150
200
250
300
350
400
72
74
76
78
80
82
84
86
88
90
92

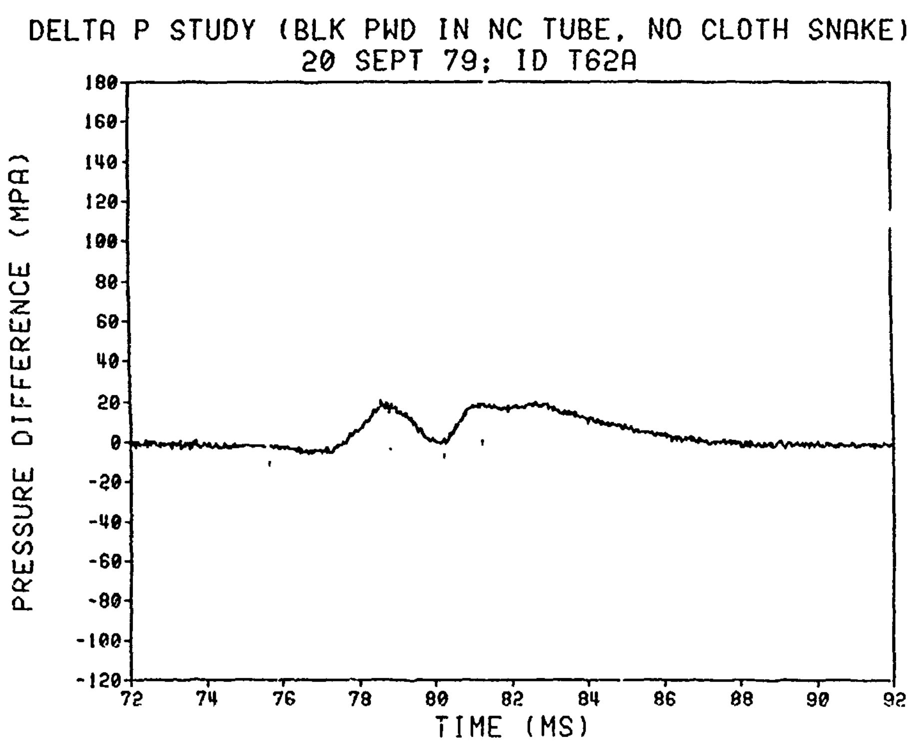
DELTA P STUDY (BLK PWD IN NC TUBE, NO CLOTH SNAKE)
20 SEPT 79; ID T62A
PRESSURE DIFFERENCE (MPA)
TIME (MS)
180
160
140
120
100
80
60
40
20
0
-20
-40
-60
-80
-100
-120
72
74
76
78
80
82
84
86
88
90
92

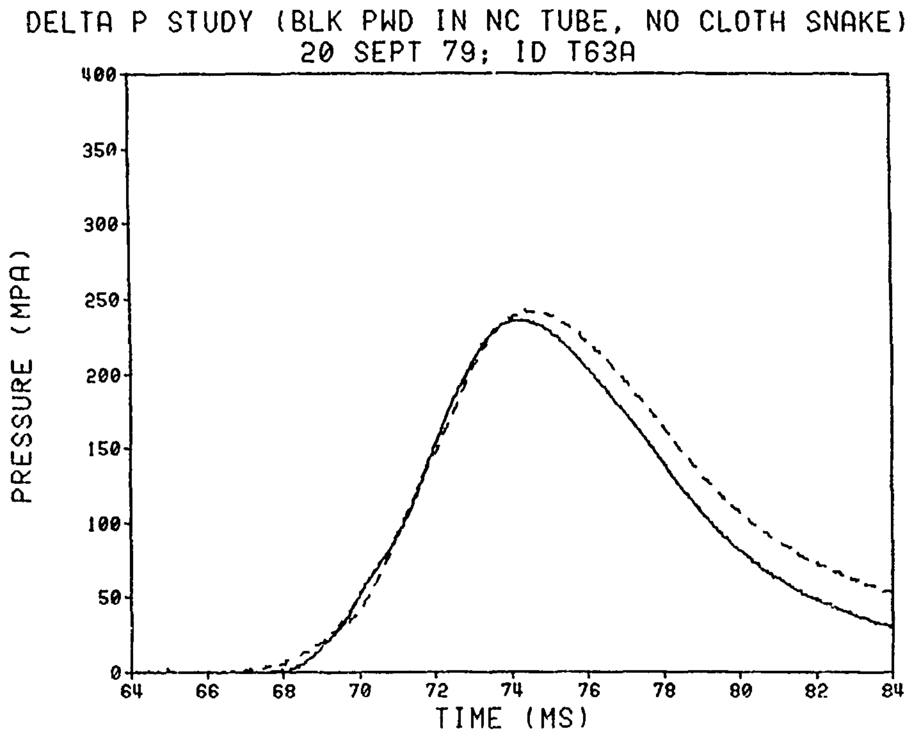
DELTA P STUDY (BLK PWD IN NC TUBE, NO CLOTH SNAKE)
20 SEPT 79; ID T63A
PRESSURE (MPA)
400
350
300
250
200
150
100
50
0
64
66
68
70
72
74
76
78
80
82
84
TIME (MS)

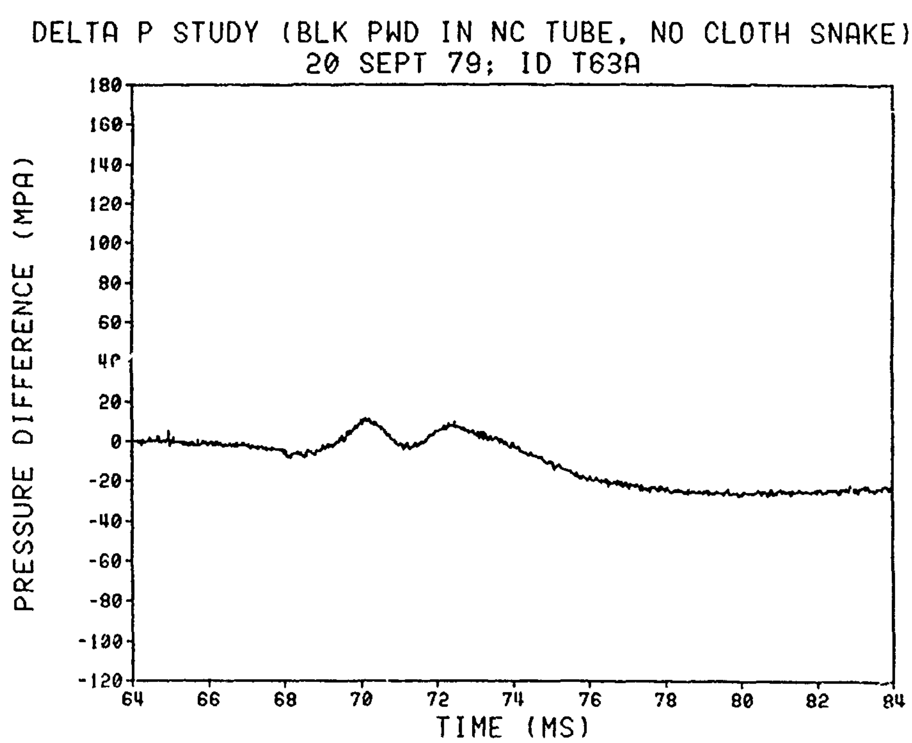
DELTA P STUDY (BLK PWD IN NC TUBE, NO CLOTH SNAKE)
20 SEPT 79; ID T63A
PRESSURE DIFFERENCE (MPA)
180
160
140
120
100
80
60
20
0
-20
-40
-60
-80
-100
-120
64
66
68
70
72
74
76
78
80
82
84
TIME (MS)

DELTA P STUDY (BLK PWD IN NC CORE, NO CLOTH SNAKE)
20 SEPT 79; ID T64A

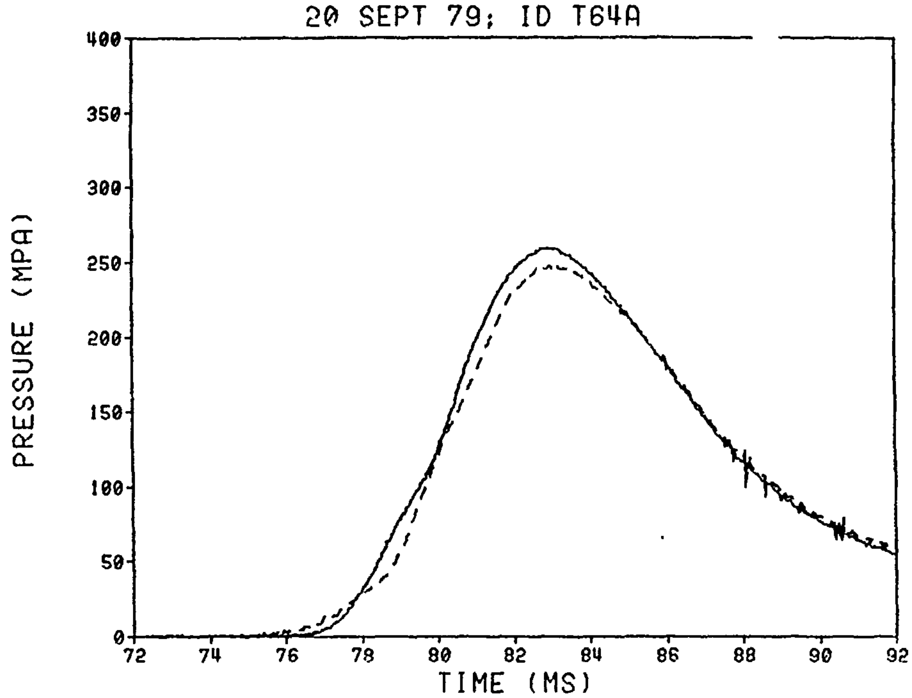

DELTA P STUDY (BLK PWD IN NC CORE, NO CLOTH SNAKE)
20 SEPT 79; ID T64A

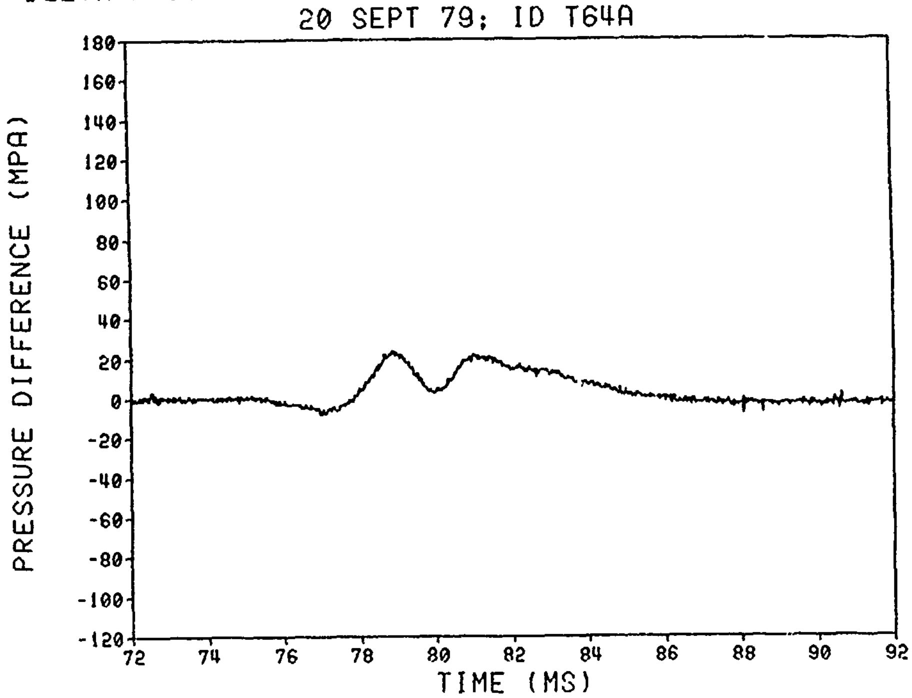

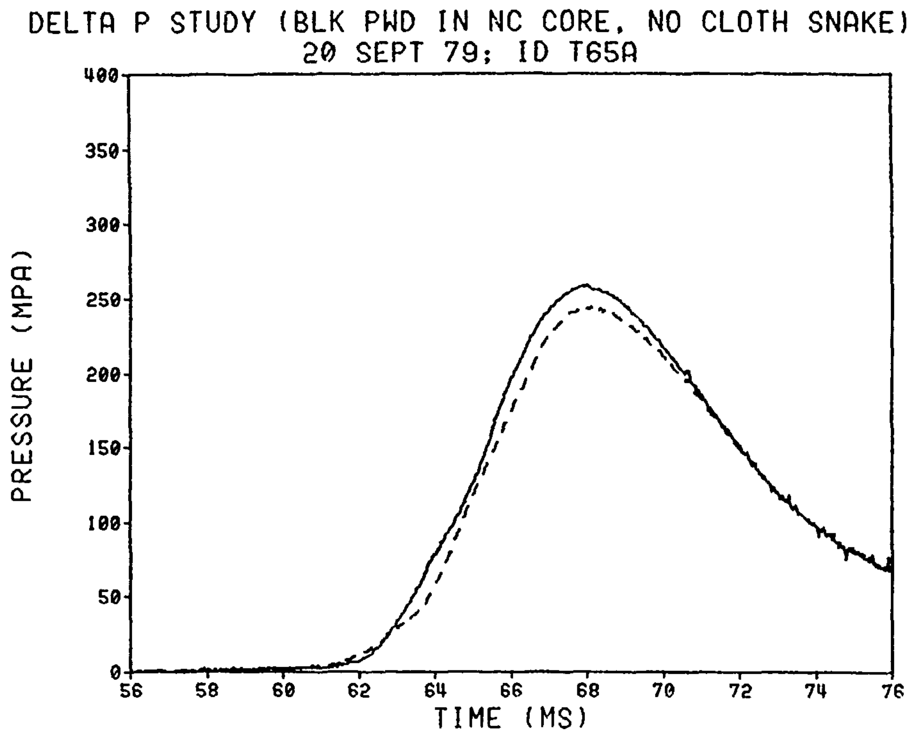
DELTA P STUDY (BLK PWD IN NC CORE, NO CLOTH SNAKE)
20 SEPT 79; ID T65A
PRESSURE (MPA)
TIME (MS)
400
350
300
250
200
150
100
50
0
56
58
60
62
64
66
68
70
72
74
76

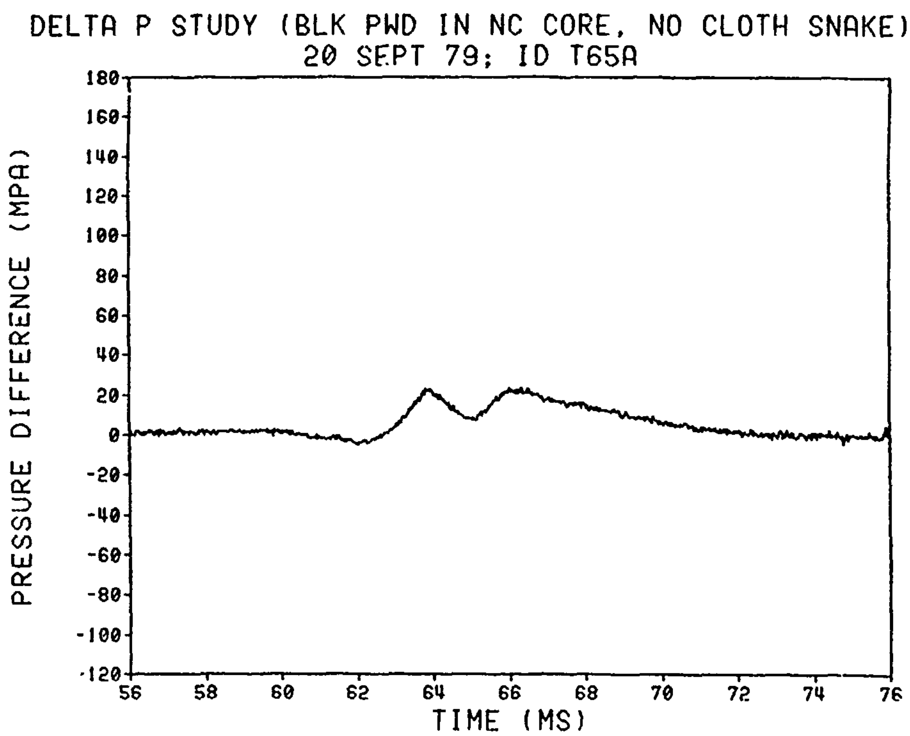
DELTA P STUDY (BLK PWD IN NC CORE, NO CLOTH SNAKE)
20 SEPT 79; ID T65A
PRESSURE DIFFERENCE (MPA)
TIME (MS)
180
160
140
120
100
80
60
40
20
0
-20
-40
-60
-80
-100
-120
56
58
60
62
64
66
68
70
72
74
76

DELTA P STUDY (BLK PWD IN NC CORE, NO CLOTH SNAKE)
20 SEPT 79; ID T66A

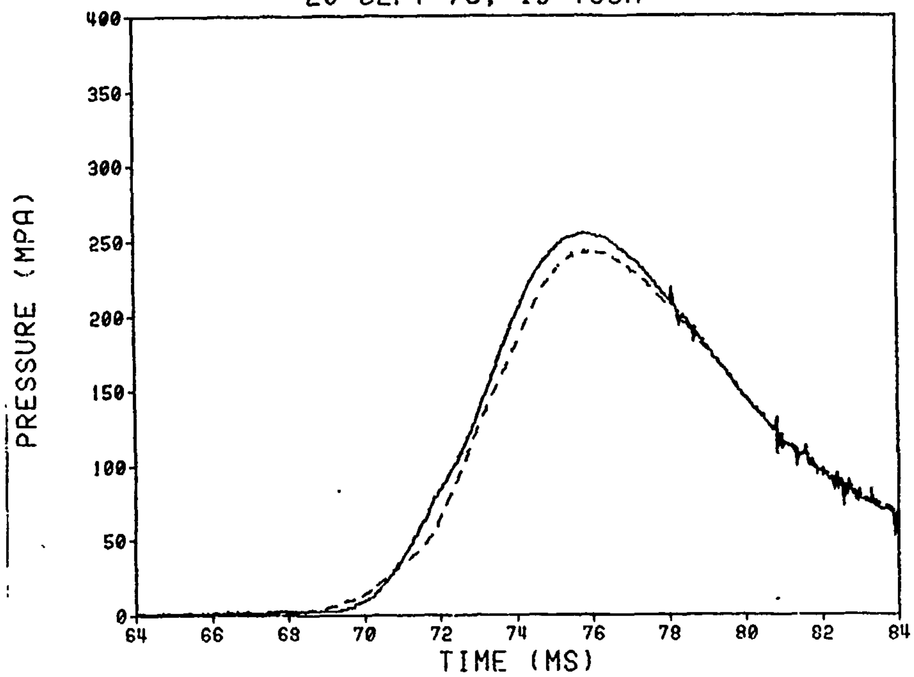

DELTA P STUDY (BLK PWD IN NC CORE, NO CLOTH SNAKE)
20 SEPT 79; ID T66A

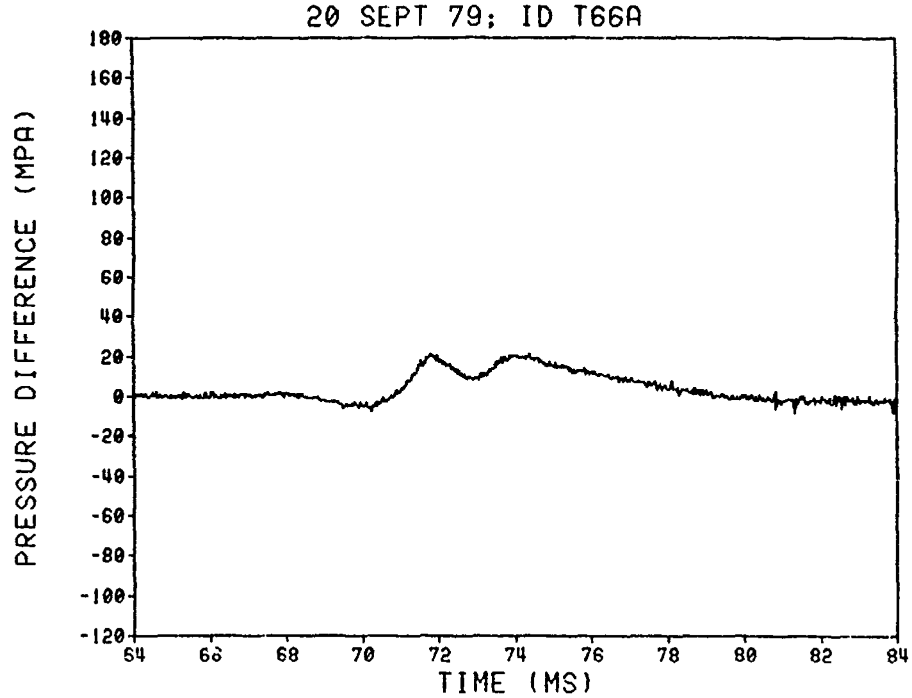

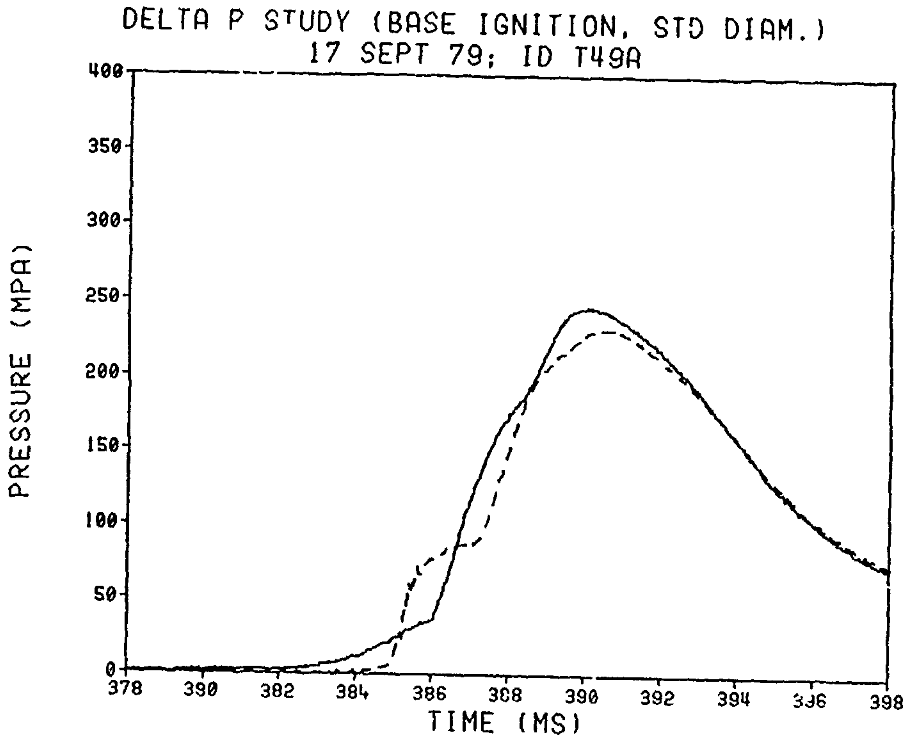
DELTA P STUDY (BASE IGNITION, STD DIAM.)
17 SEPT 79; ID T49A
PRESSURE (MPA)
400
350
300
250
200
150
100
50
0
378
390
382
384
386
368
390
392
394
396
398
TIME (MS)

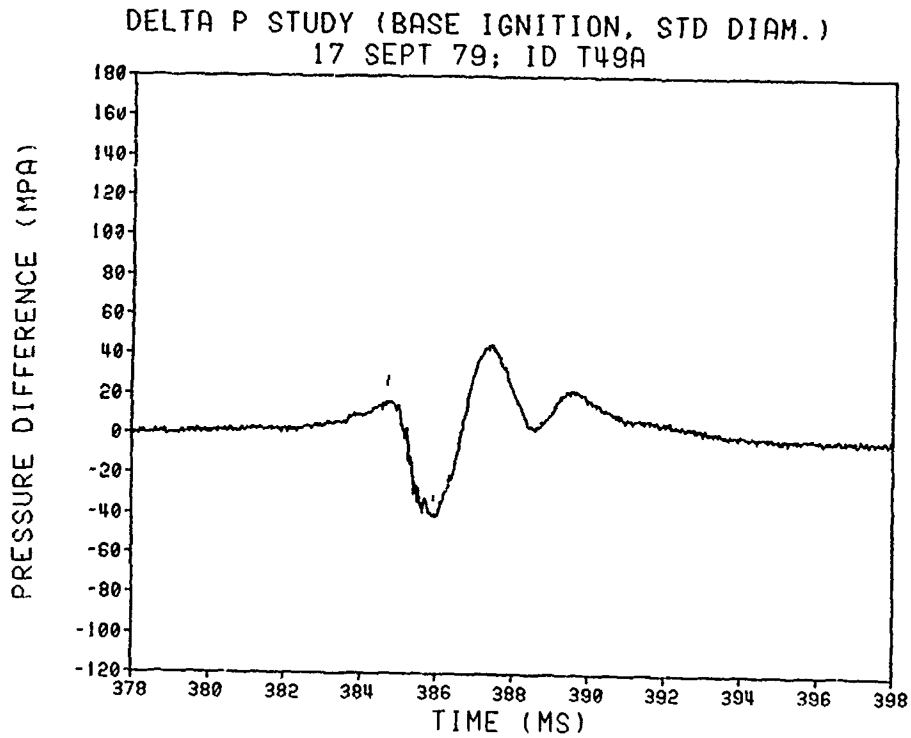
DELTA P STUDY (BASE IGNITION, STD DIAM.)
17 SEPT 79; ID T49A
PRESSURE DIFFERENCE (MPA)
180
160
140
120
100
80
60
40
20
0
-20
-40
-60
-80
-100
-120
378
380
382
384
386
388
390
392
394
396
398
TIME (MS)

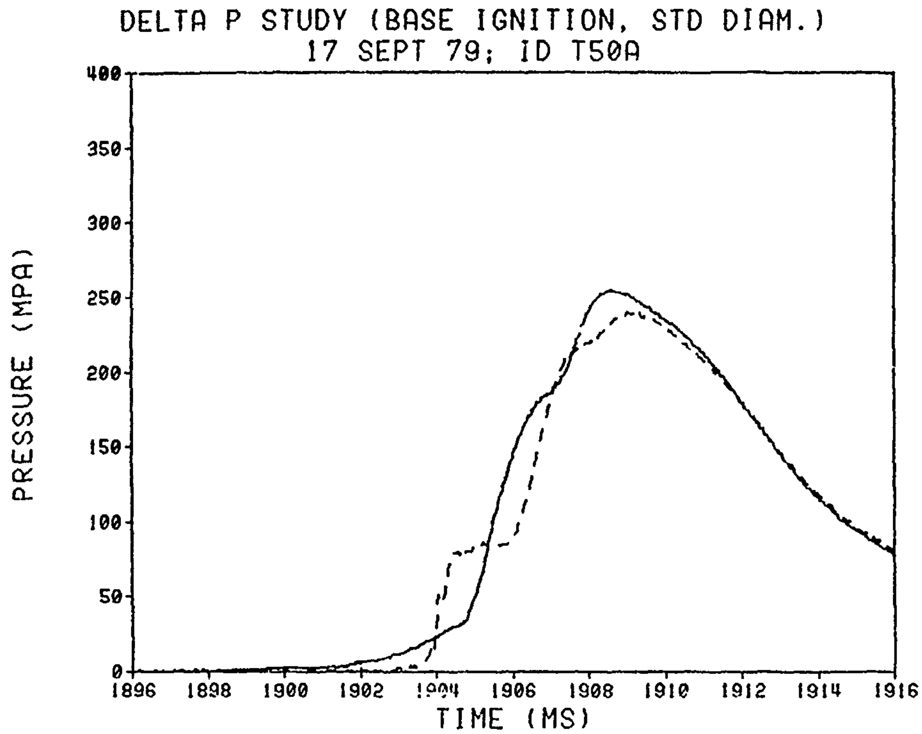
DELTA P STUDY (BASE IGNITION, STD DIAM.)
17 SEPT 79; ID T50A
PRESSURE (MPA)
TIME (MS)
400
350
300
250
200
150
100
50
0
1896
1898
1900
1902
1904
1906
1908
1910
1912
1914
1916

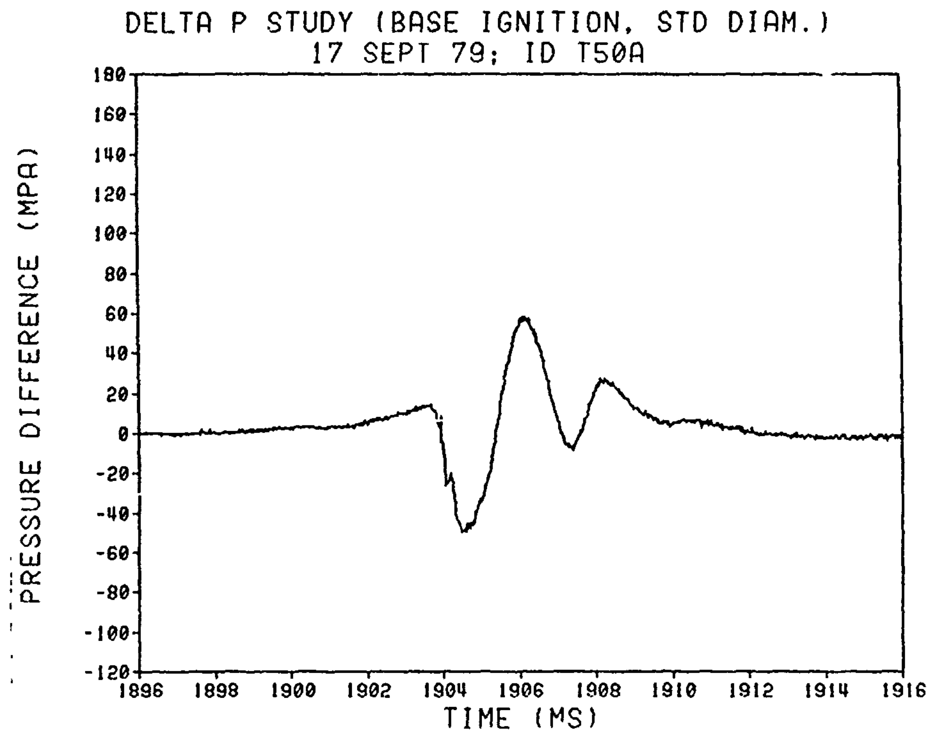
DELTA P STUDY (BASE IGNITION, STD DIAM.)
17 SEPT 79; ID T50A
PRESSURE DIFFERENCE (MPA)
TIME (MS)
180
160
140
120
100
80
60
40
20
0
-20
-40
-60
-80
-100
-120
1896
1898
1900
1902
1904
1906
1908
1910
1912
1914
1916

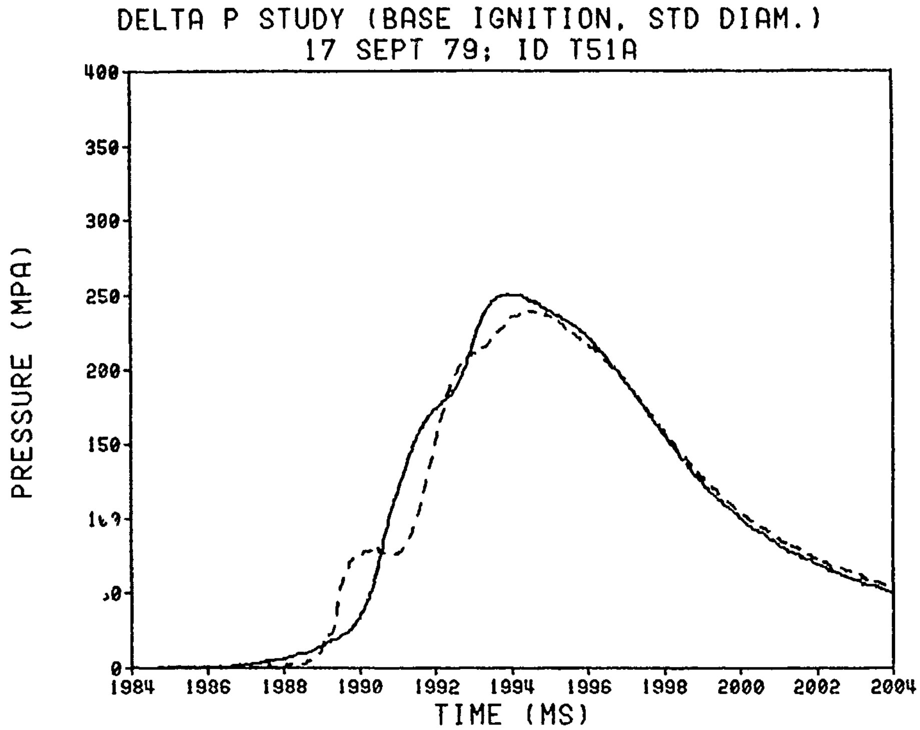
DELTA P STUDY (BASE IGNITION, STD DIAM.)
17 SEPT 79; ID T51A
PRESSURE (MPA)
TIME (MS)
400
350
300
250
200
150
0
1984
1986
1988
1990
1992
1994
1996
1998
2000
2002
2004

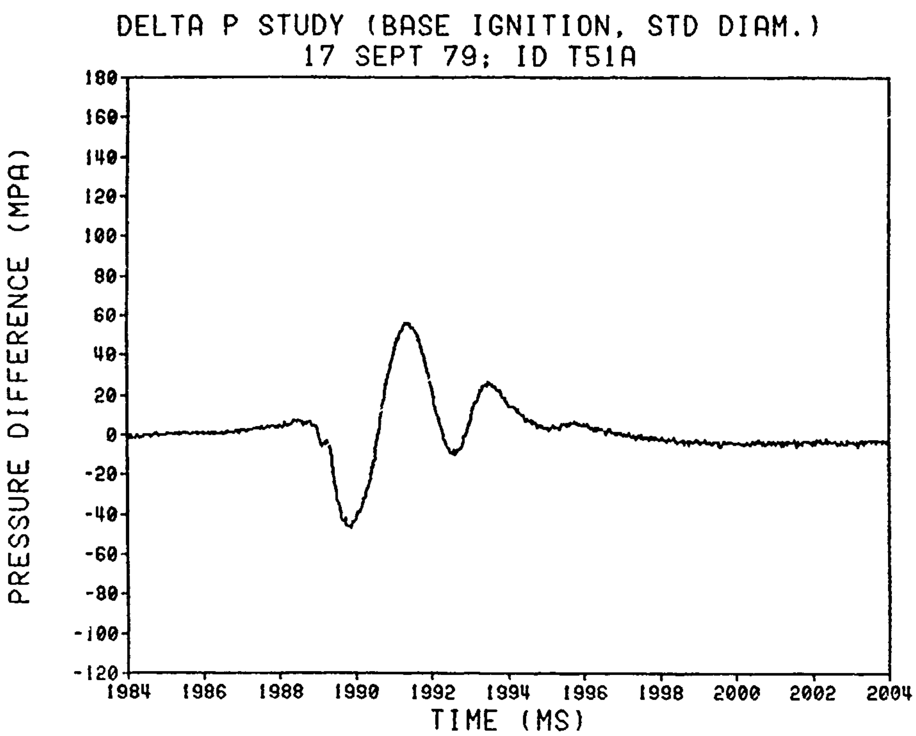
DELTA P STUDY (BASE IGNITION, STD DIAM.)
17 SEPT 79; ID T51A
PRESSURE DIFFERENCE (MPA)
TIME (MS)
180
160
140
120
100
80
60
40
20
0
-20
-40
-60
-80
-100
-120
1984
1986
1988
1990
1992
1994
1996
1998
2000
2002
2004

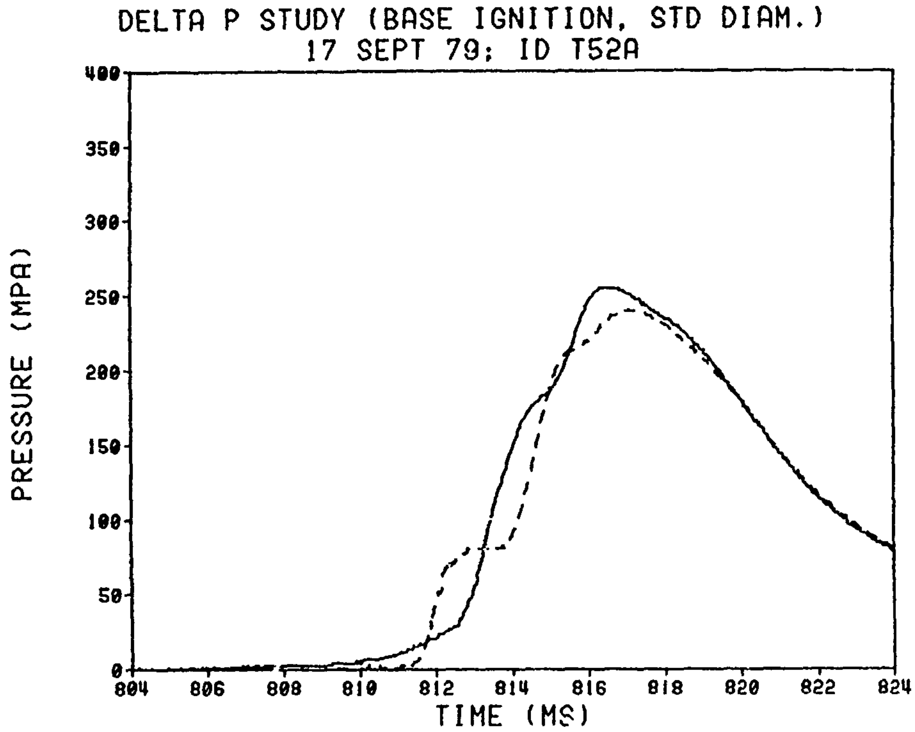

DELTA P STUDY (BASE IGNITION, STD DIAM.)
17 SEPT 79; ID T52A
PRESSURE (MPA)
400
350
300
250
200
150
100
50
0
804
806
808
810
812
814
816
818
820
822
824
TIME (MS)

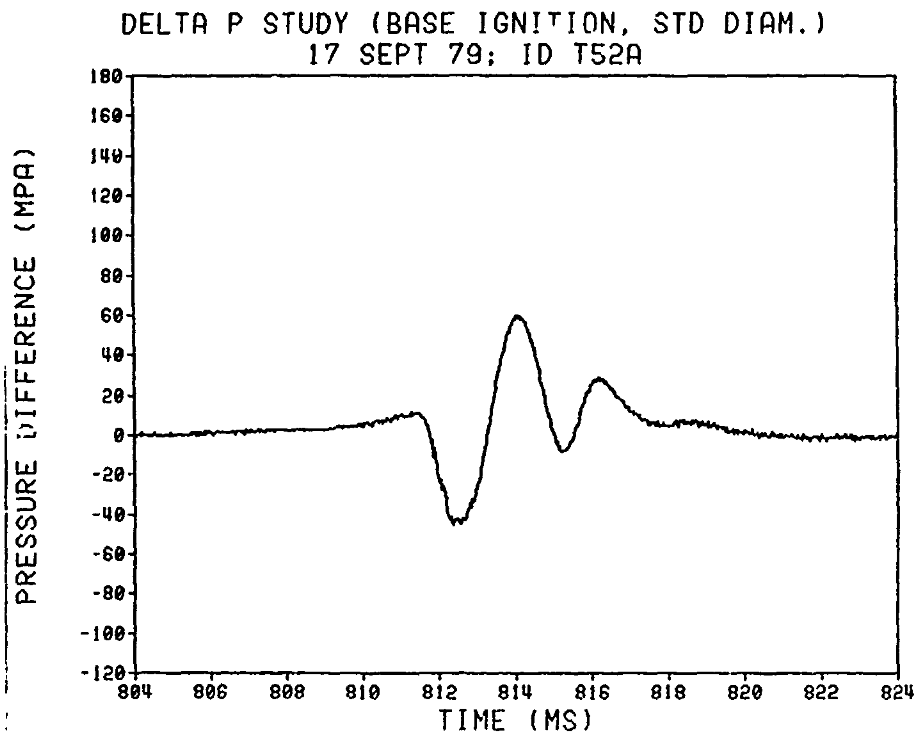

DELTA P STUDY (BASE IGNITION, STD DIAM.)
17 SEPT 79; ID T52A
PRESSURE DIFFERENCE (MPA)
180
160
140
120
100
80
60
40
20
0
-20
-40
-60
-80
-100
-120
804
806
808
810
812
814
816
818
820
822
824
TIME (MS)

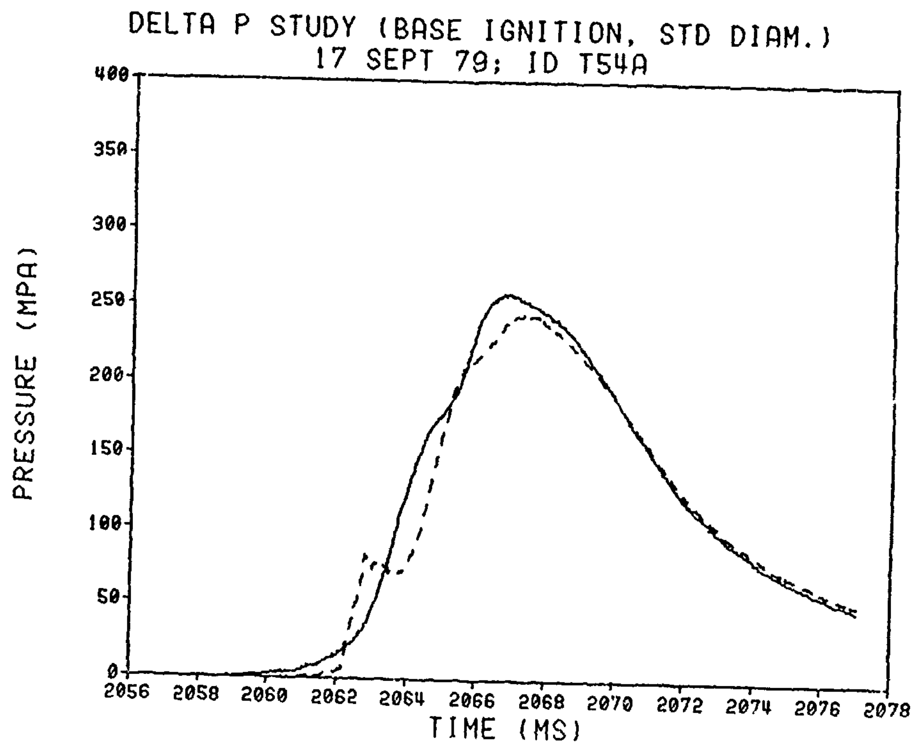
DELTA P STUDY (BASE IGNITION, STD DIAM.)
17 SEPT 79; ID T54A
PRESSURE (MPA)
0
50
100
150
200
250
300
350
400
2056
2058
2060
2062
2064
2066
2068
2070
2072
2074
2076
2078
TIME (MS)

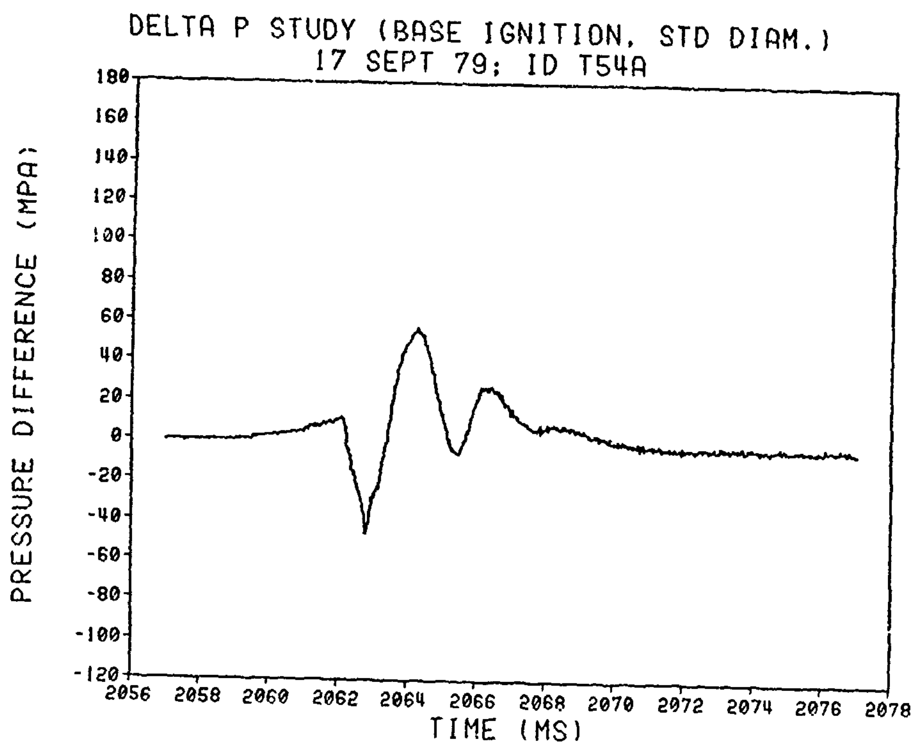
DELTA P STUDY (BASE IGNITION, STD DIAM.)
17 SEPT 79; ID T54A
PRESSURE DIFFERENCE (MPA)
180
160
140
120
100
80
60
40
20
0
-20
-40
-60
-80
-100
-120
2056
2058
2060
2062
2064
2066
2068
2070
2072
2074
2076
2078
TIME (MS)

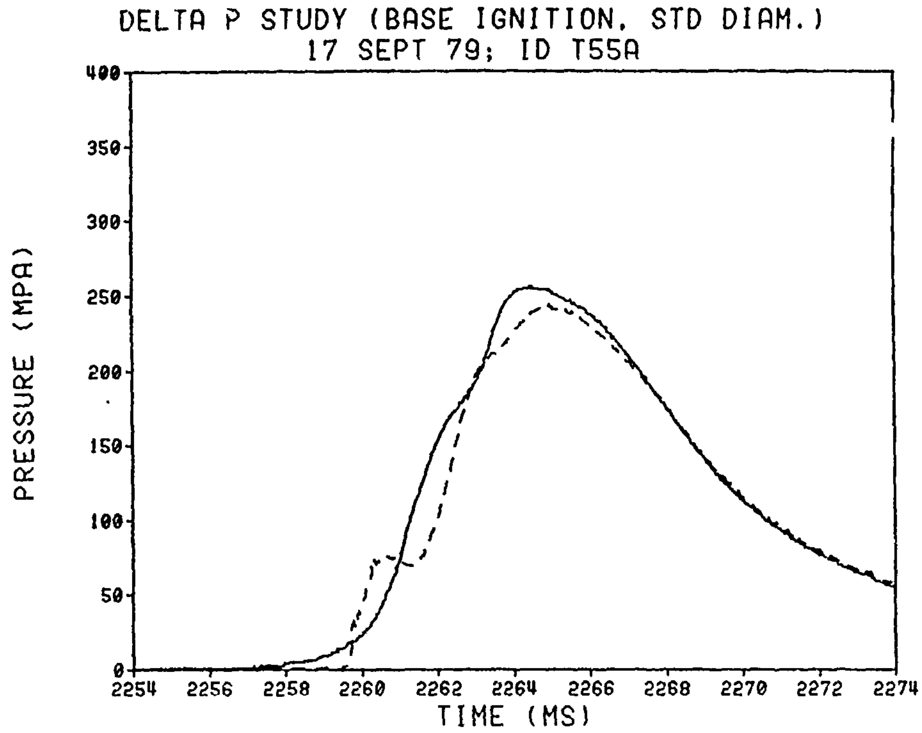
DELTA P STUDY (BASE IGNITION, STD DIAM.)
17 SEPT 79; ID T55A
PRESSURE (MPA)
400
350
300
250
200
150
100
50
0
2254
2256
2258
2260
2262
2264
2266
2268
2270
2272
2274
TIME (MS)

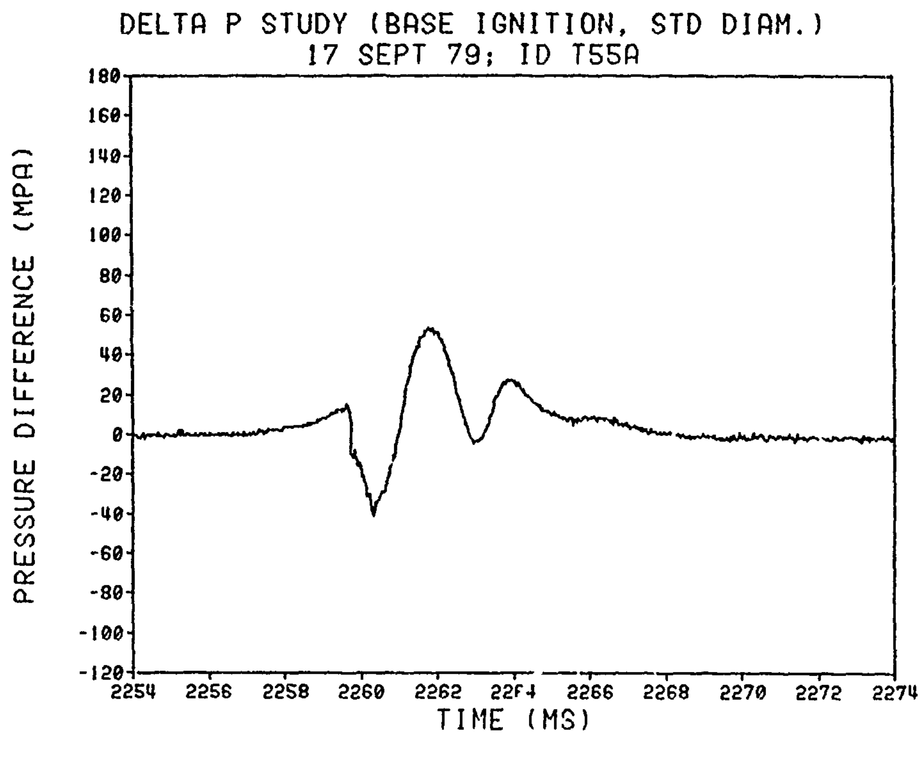
DELTA P STUDY (BASE IGNITION, STD DIAM.)
17 SEPT 79; ID T55A
PRESSURE DIFFERENCE (MPA)
180
160
140
120
100
80
60
40
20
0
-20
-40
-60
-80
-100
-120
2254
2256
2258
2260
2262
22F4
2266
2268
2270
2272
2274
TIME (MS)

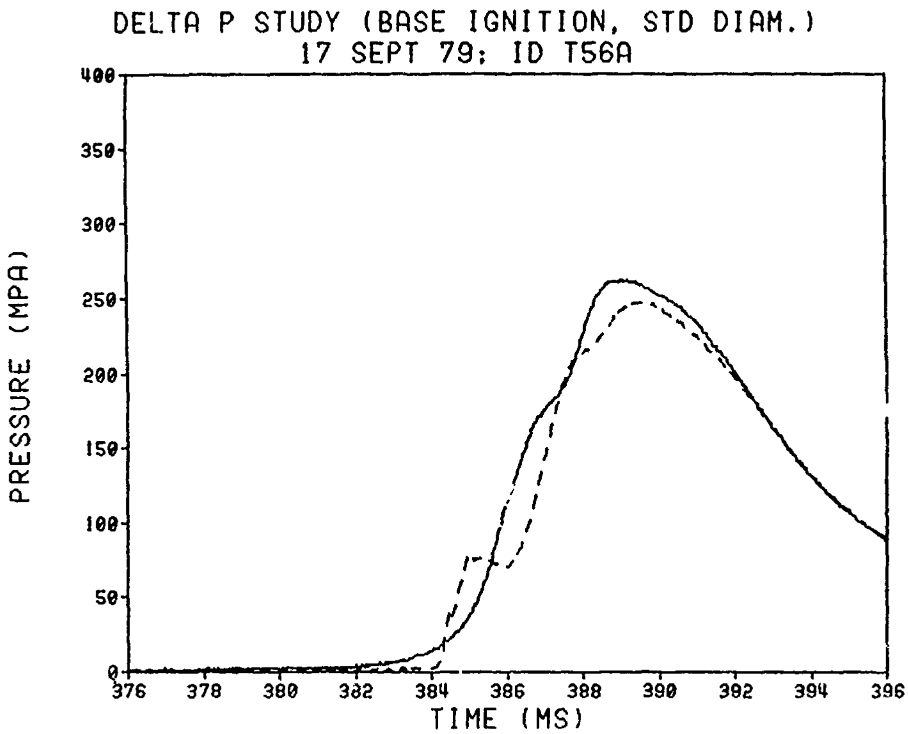
DELTA P STUDY (BASE IGNITION, STD DIAM.)
17 SEPT 79; ID T56A
PRESSURE (MPA)
TIME (MS)
400
350
300
250
200
150
100
50
0
376
378
380
382
384
386
388
390
392
394
396

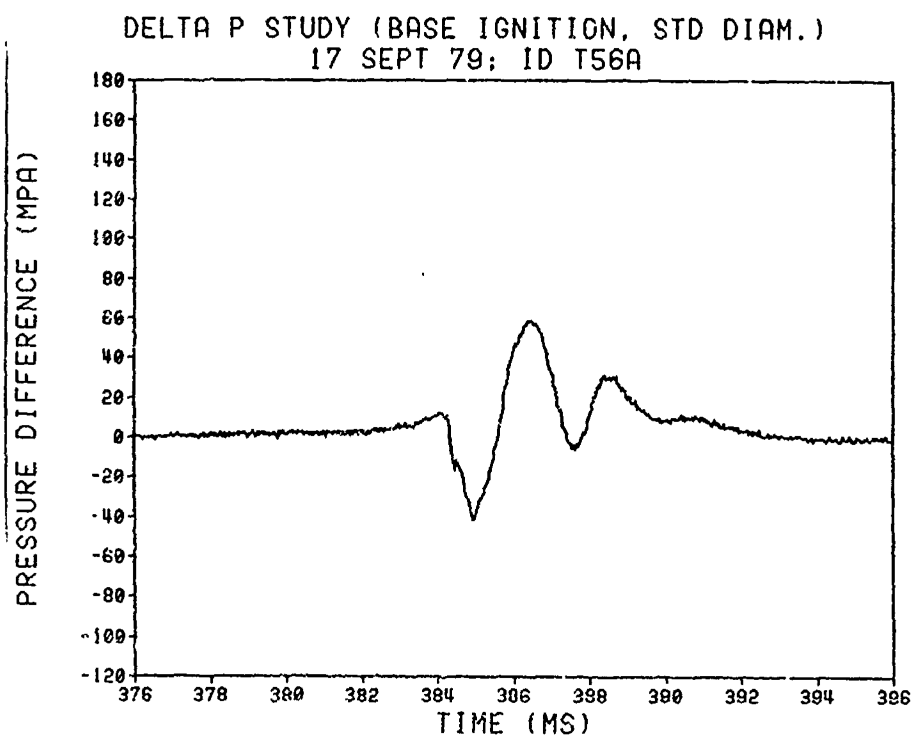
DELTA P STUDY (BASE IGNITION, STD DIAM.)
17 SEPT 79; ID T56A
PRESSURE DIFFERENCE (MPA)
TIME (MS)
180
160
140
120
100
80
60
40
20
0
-20
-40
-60
-80
-100
-120
376
378
380
382
384
386
388
390
392
394
396

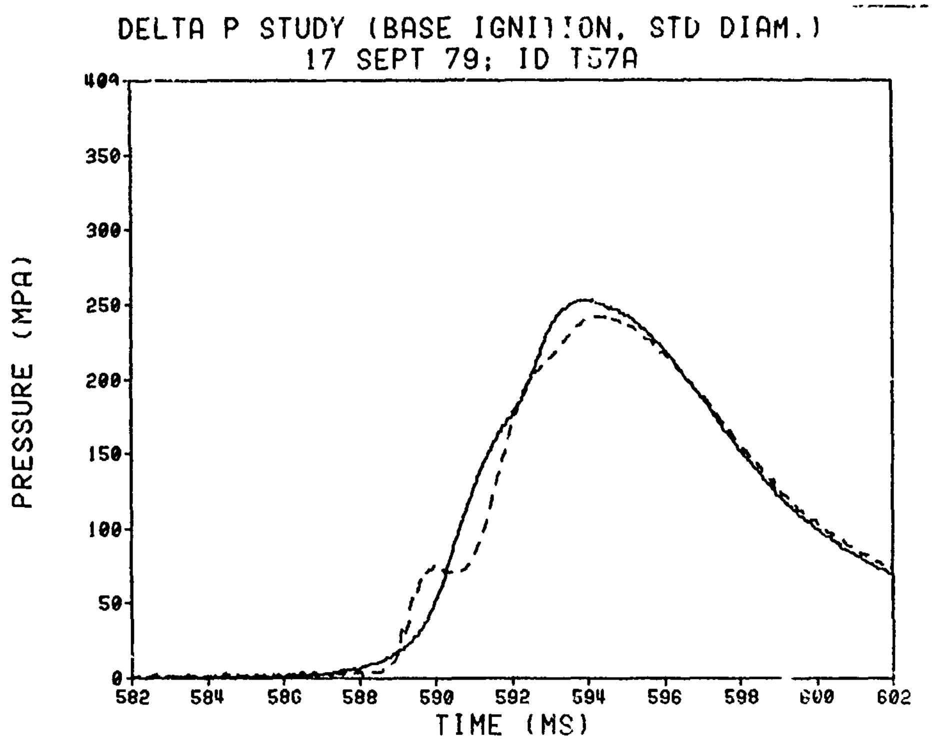
DELTA P STUDY (BASE IGNITION, STD DIAM.)
17 SEPT 79; ID T57A
PRESSURE (MPA)
0
50
100
150
200
250
300
350
400
582
584
586
588
590
592
594
596
598
600
602
TIME (MS)

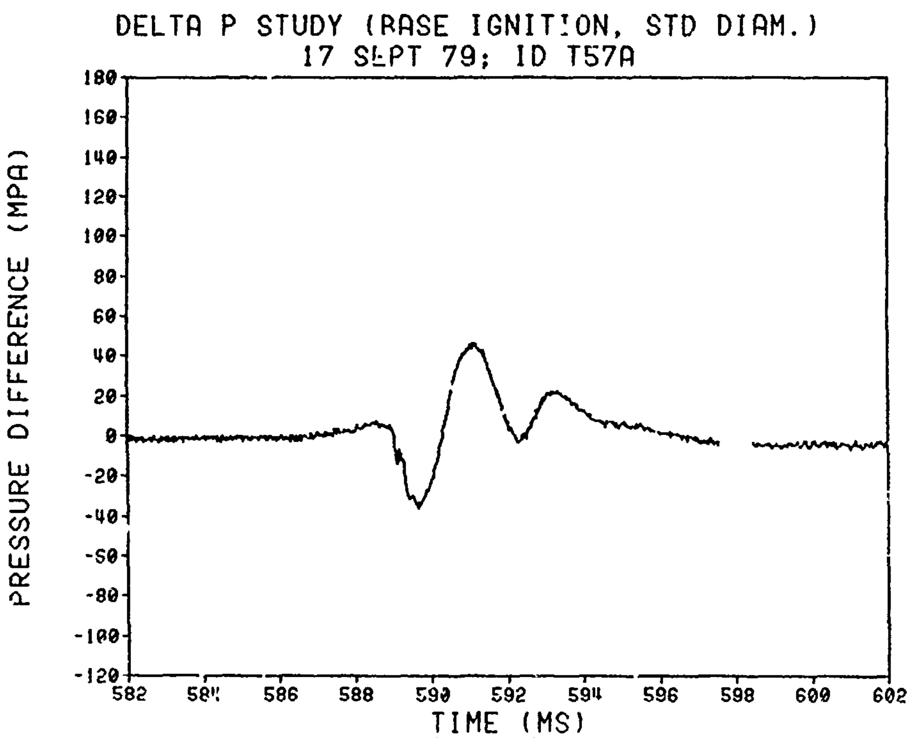
DELTA P STUDY (BASE IGNITION, STD DIAM.)
17 SEPT 79; ID T57A
PRESSURE DIFFERENCE (MPA)
180
160
140
120
100
80
60
40
20
0
-20
-40
-60
-80
-100
-120
582
584
586
588
590
592
594
596
598
600
602
TIME (MS)

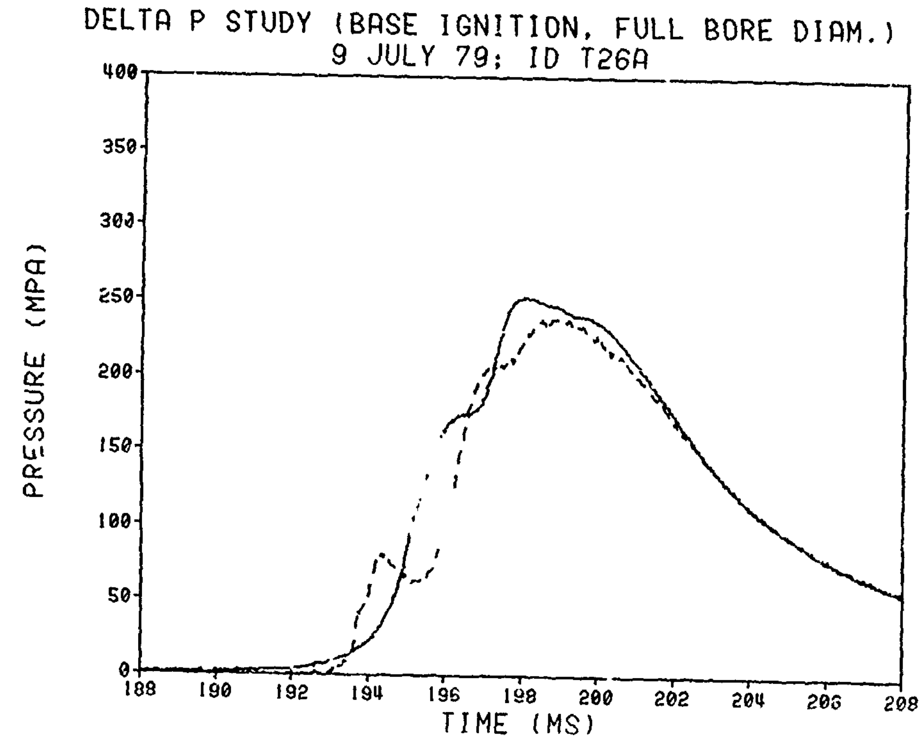
DELTA P STUDY (BASE IGNITION, FULL BORE DIAM.)
9 JULY 79; ID T26A
PRESSURE (MPA)
TIME (MS)
400
350
300
250
200
150
100
50
0
188
190
192
194
196
198
200
202
204
206
208

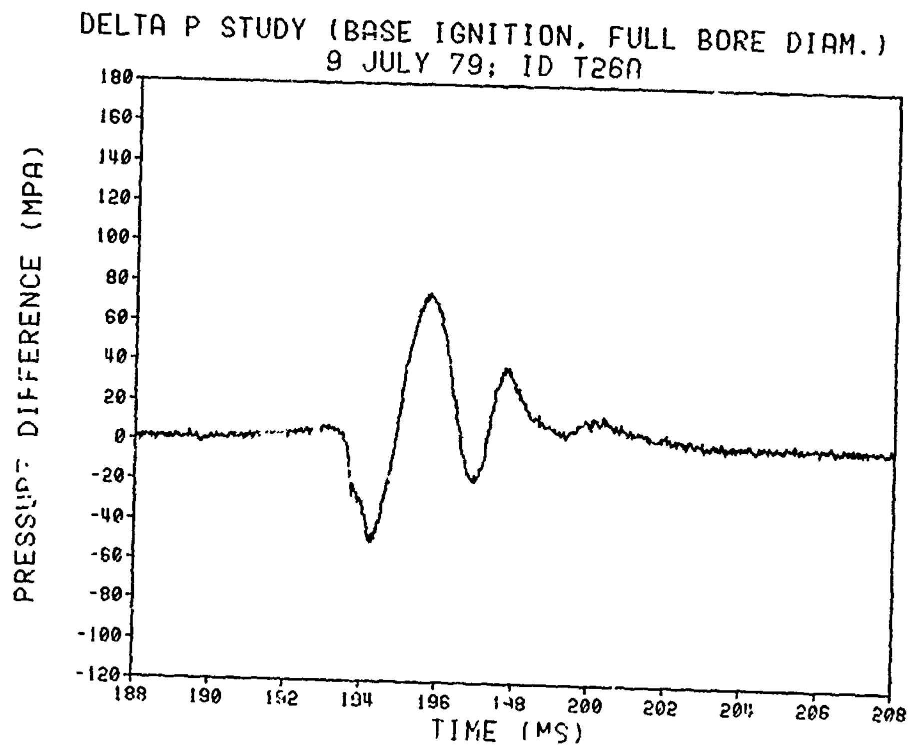
DELTA P STUDY (BASE IGNITION, FULL BORE DIAM.)
9 JULY 79; ID T26A
PRESSURE DIFFERENCE (MPA)
TIME (MS)
180
160
140
120
100
80
60
40
20
0
-20
-40
-60
-80
-100
-120
188
190
192
194
196
198
200
202
204
206
208

DELTA P STUDY (BASE IGNITION, FULL BORE DIAM.)
9 JULY 79; ID T27A

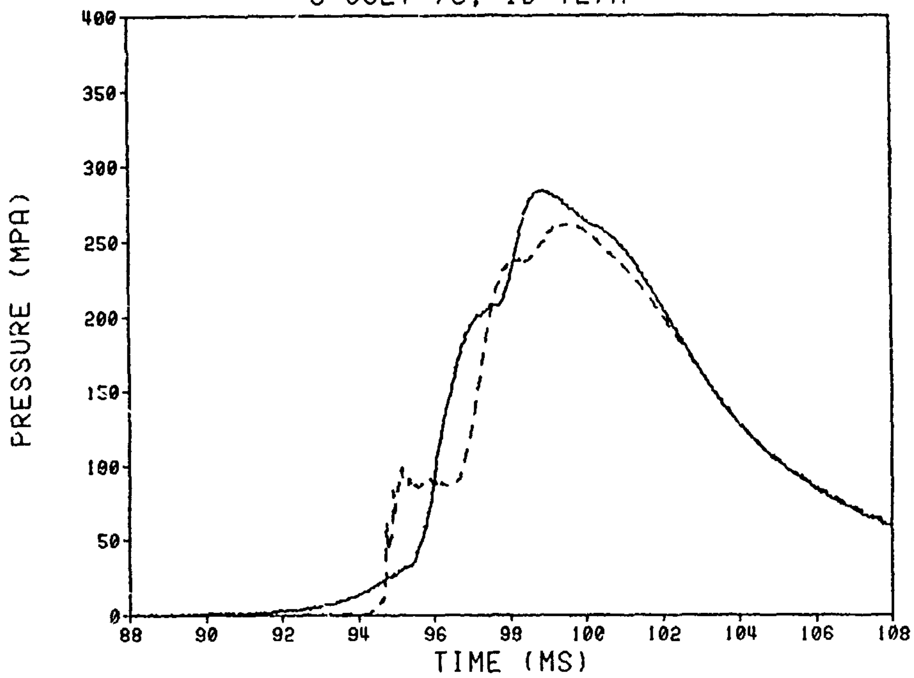

DELTA P STUDY (BASE IGNITION, FULL BORE DIAM.)
9 JULY 79; ID T27A

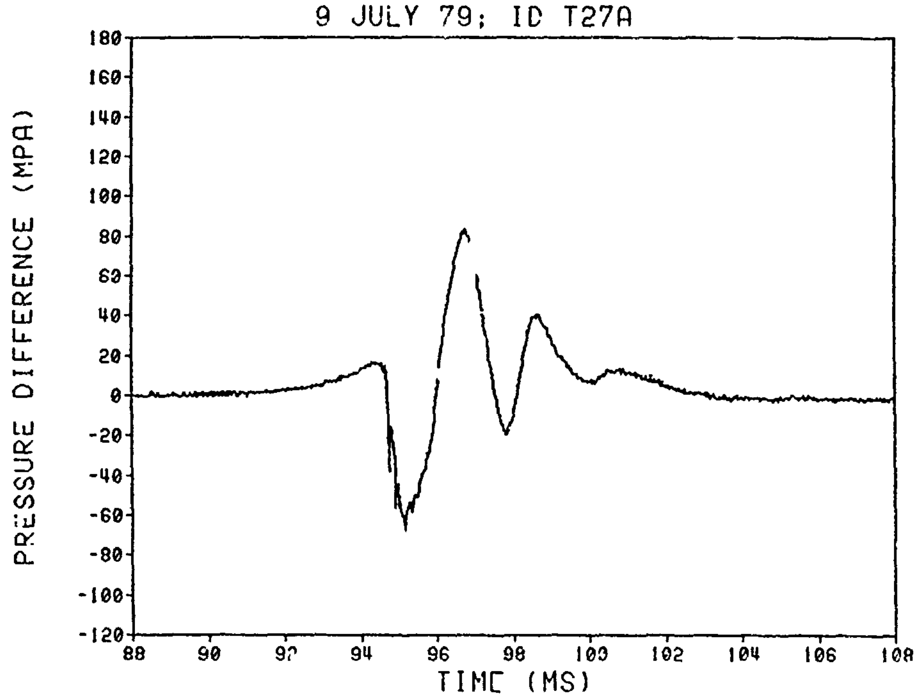

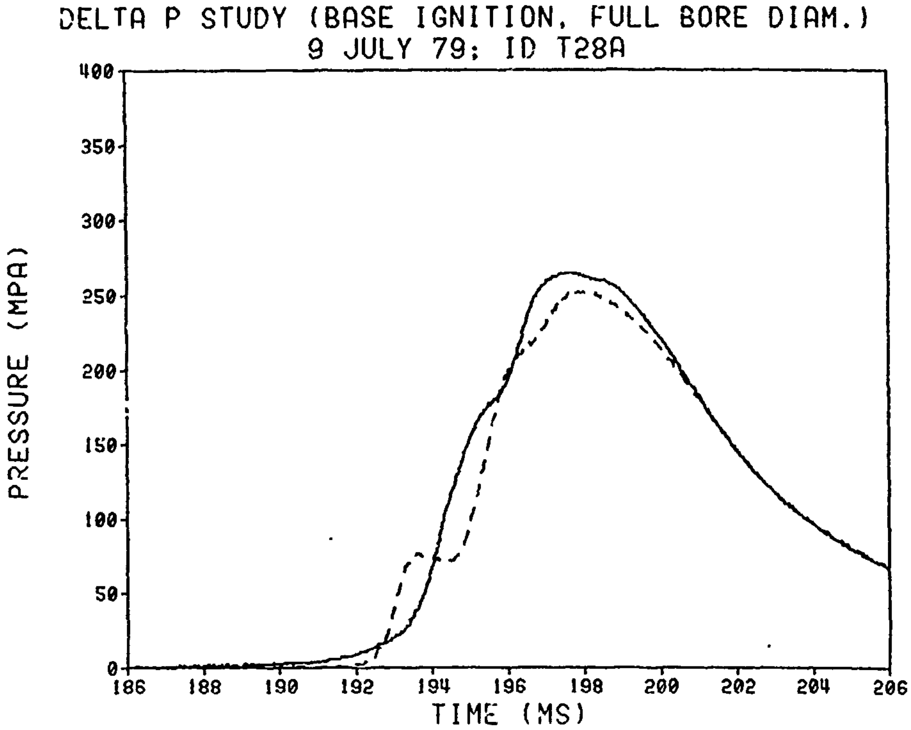
DELTA P STUDY (BASE IGNITION, FULL BORE DIAM.)
9 JULY 79; ID T28A
PRESSURE (MPA)
TIME (MS)
0
50
100
150
200
250
300
350
400
186
188
190
192
194
196
198
200
202
204
206

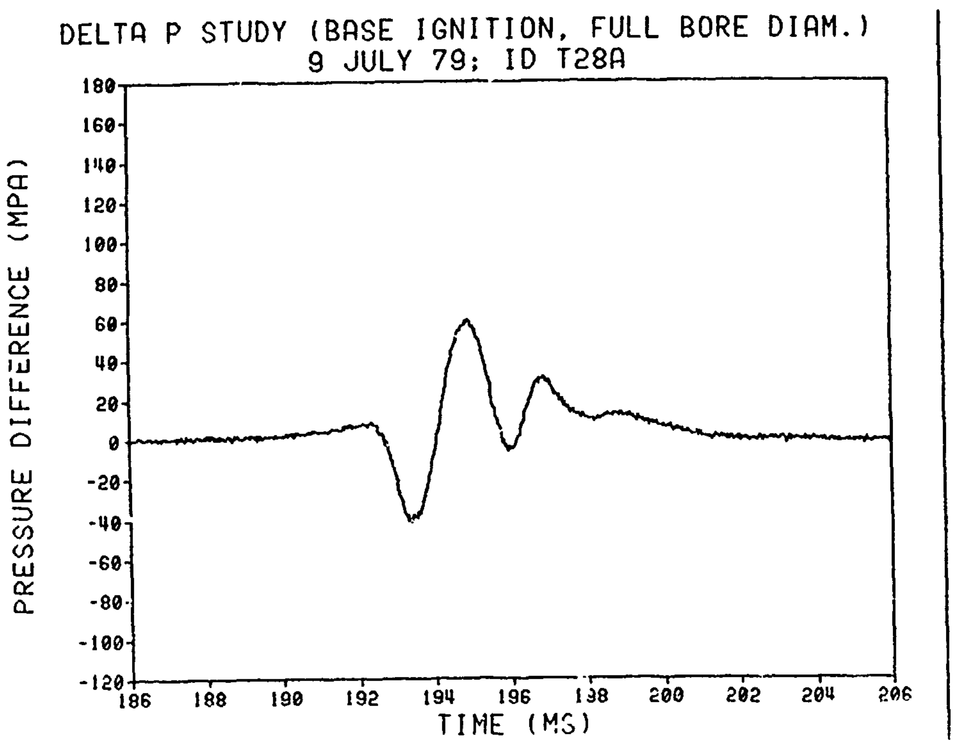
DELTA P STUDY (BASE IGNITION, FULL BORE DIAM.)
9 JULY 79; ID T28A
PRESSURE DIFFERENCE (MPA)
TIME (MS)
180
160
140
120
100
80
60
40
20
0
-20
-40
-60
-80
-100
-120
186
188
190
192
194
196
198
200
202
204
206

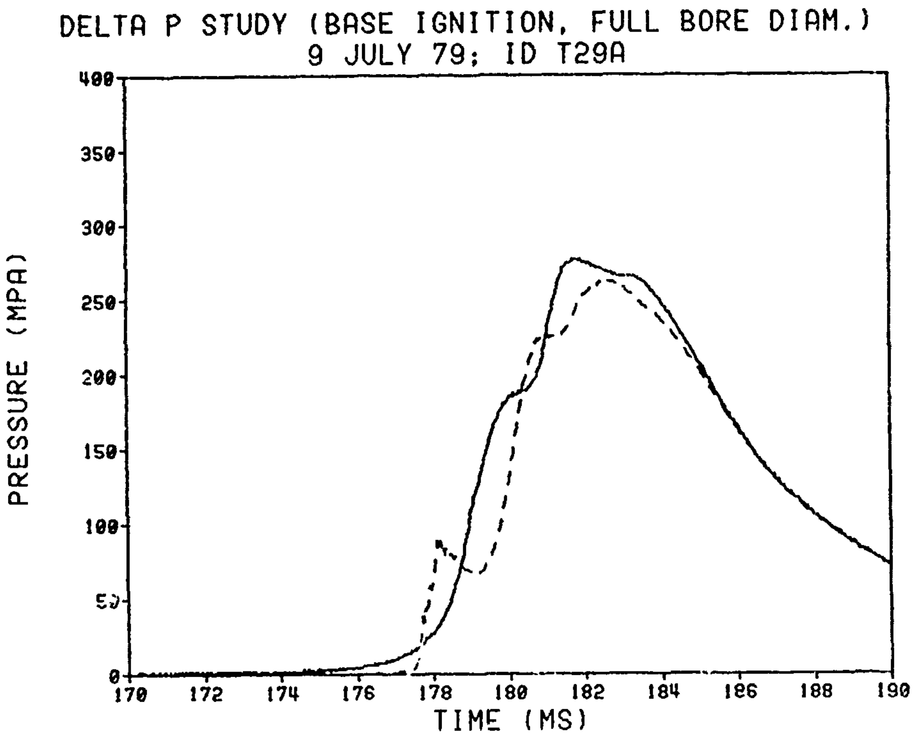
DELTA P STUDY (BASE IGNITION, FULL BORE DIAM.)
9 JULY 79; ID T29A
PRESSURE (MPA)
TIME (MS)
400
350
300
250
200
150
100
0
170
172
174
176
178
180
182
184
186
188
190

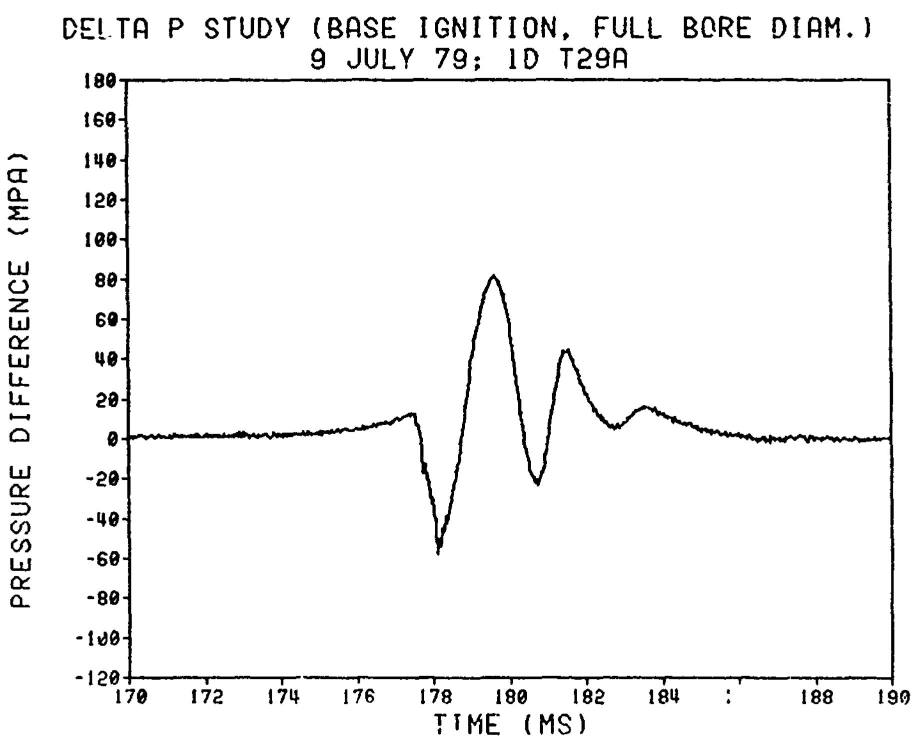
DELTA P STUDY (BASE IGNITION, FULL BORE DIAM.)
9 JULY 79; ID T29A
PRESSURE DIFFERENCE (MPA)
TIME (MS)
180
160
140
120
100
80
60
40
20
0
-20
-40
-60
-80
-120
170
172
174
176
178
180
182
184
188

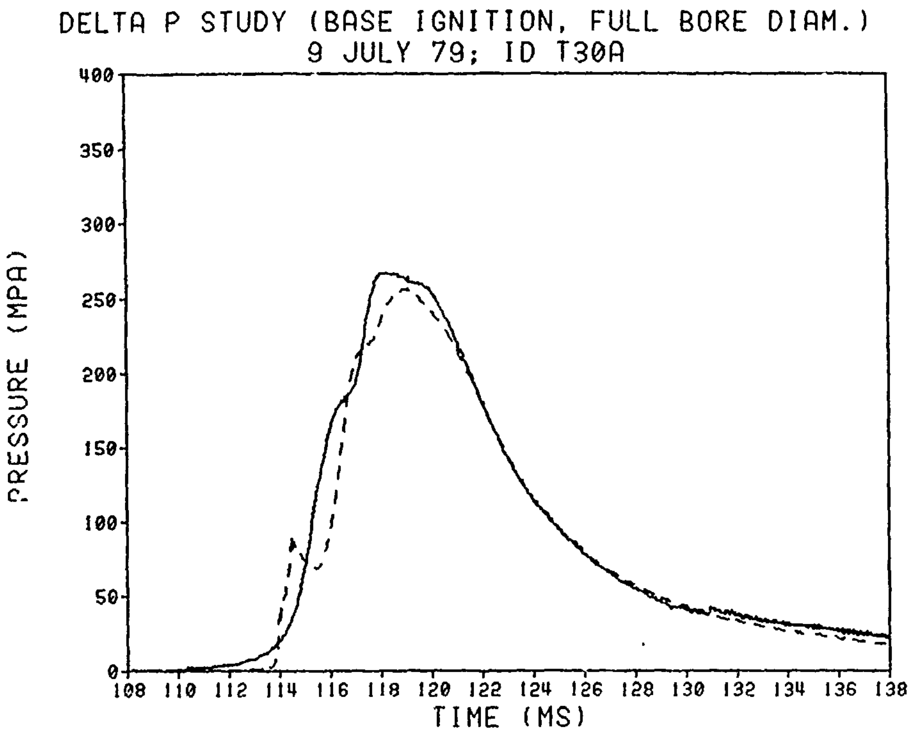
DELTA P STUDY (BASE IGNITION, FULL BORE DIAM.)
9 JULY 79; ID T30A
PRESSURE (MPA)
TIME (MS)
0
50
100
150
200
250
300
350
400
108
110
112
114
116
118
120
122
124
126
128
130
132
134
136
138

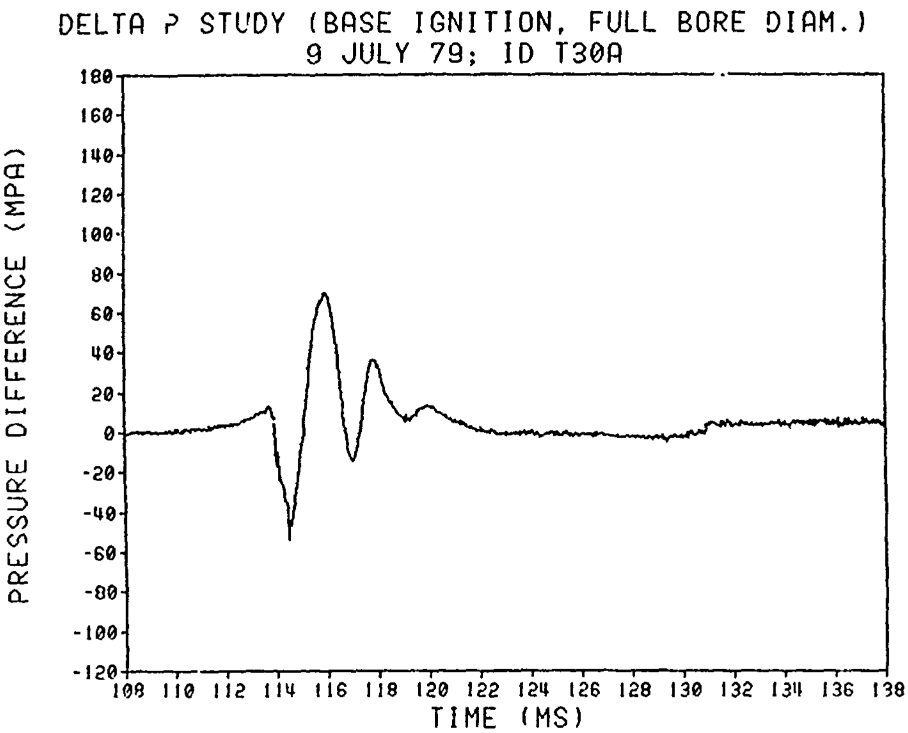
DELTA P STUDY (BASE IGNITION, FULL BORE DIAM.)
9 JULY 79; ID T30A
PRESSURE DIFFERENCE (MPA)
TIME (MS)
-120
-100
-80
-60
-40
-20
0
20
40
60
80
100
120
140
160
180
108
110
112
114
116
118
120
122
124
126
128
130
132
134
136
138

DELTA P STUDY (BASE IGNITION, FULL BORE DIAM.)
30 JULY 79; ID T37A

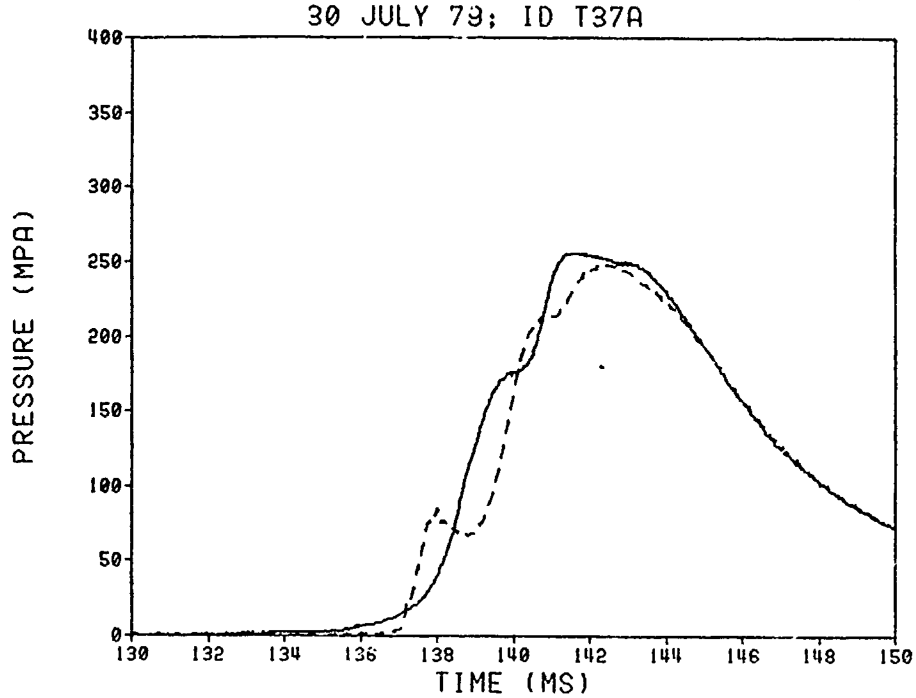

DELTA P STUDY (BASE IGNITION, FULL BORE DIAM.)
30 JULY 79; ID T37A

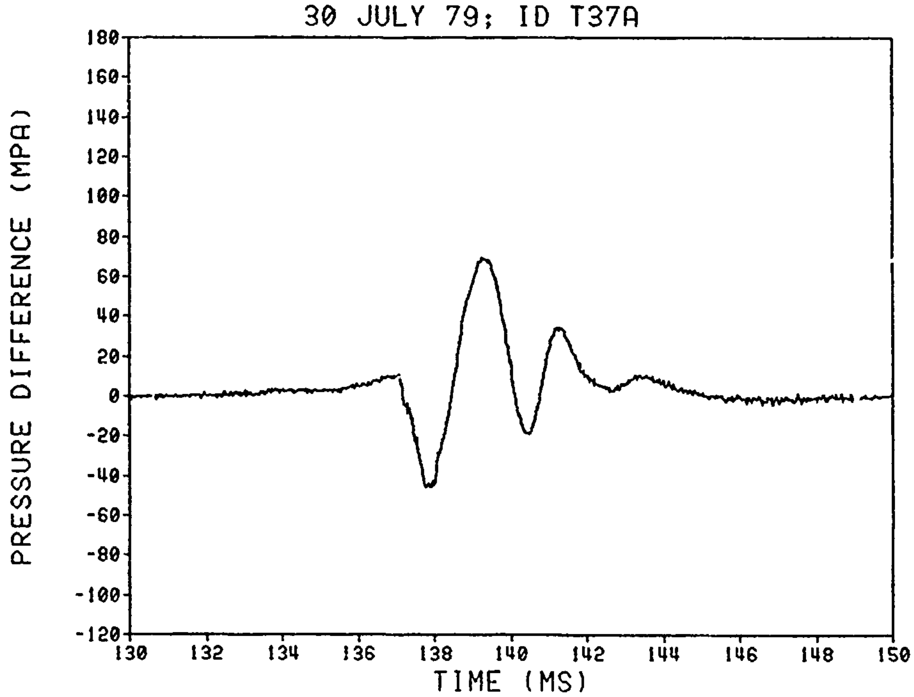

DELTA P STUDY (BASE IGNITION, FULL BORE DIAM.)
30 JULY 79; ID T38A

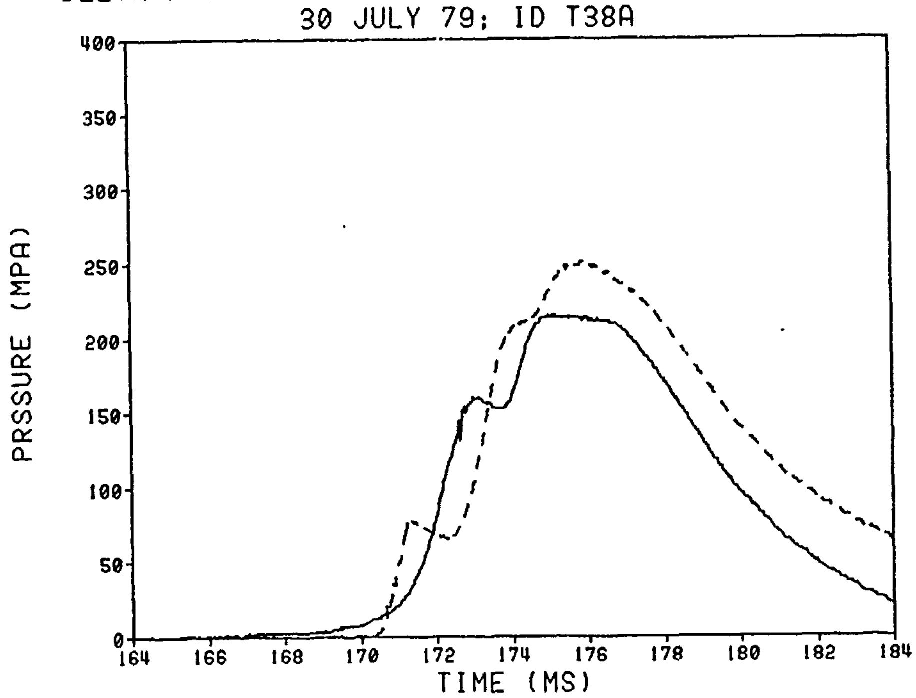

DELTA P STUDY (BASE IGNITION, FULL BORE DIAM.)
30 JULY 79; ID T38A

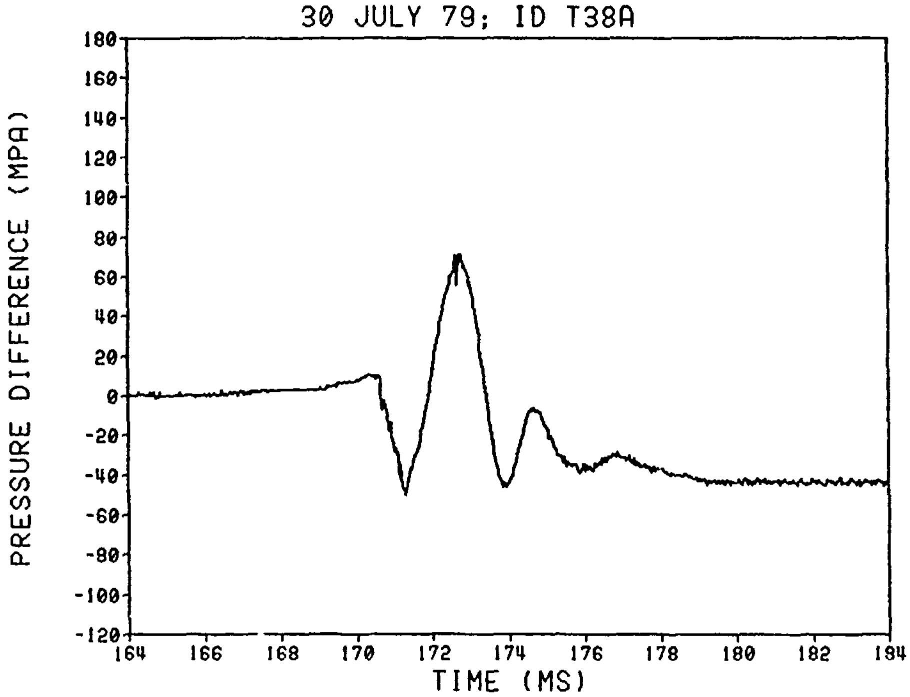

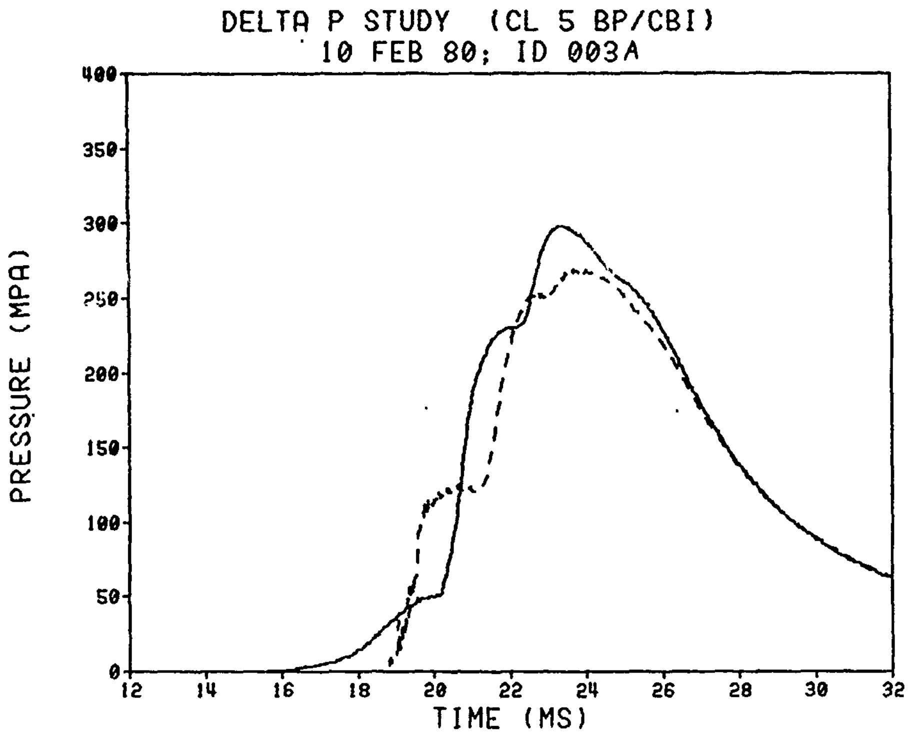
DELTA P STUDY (CL 5 BP/CBI)
10 FEB 80; ID 003A
PRESSURE (MPA)
0
50
100
150
200
250
300
350
400
12
14
16
18
20
22
24
26
28
30
32
TIME (MS)

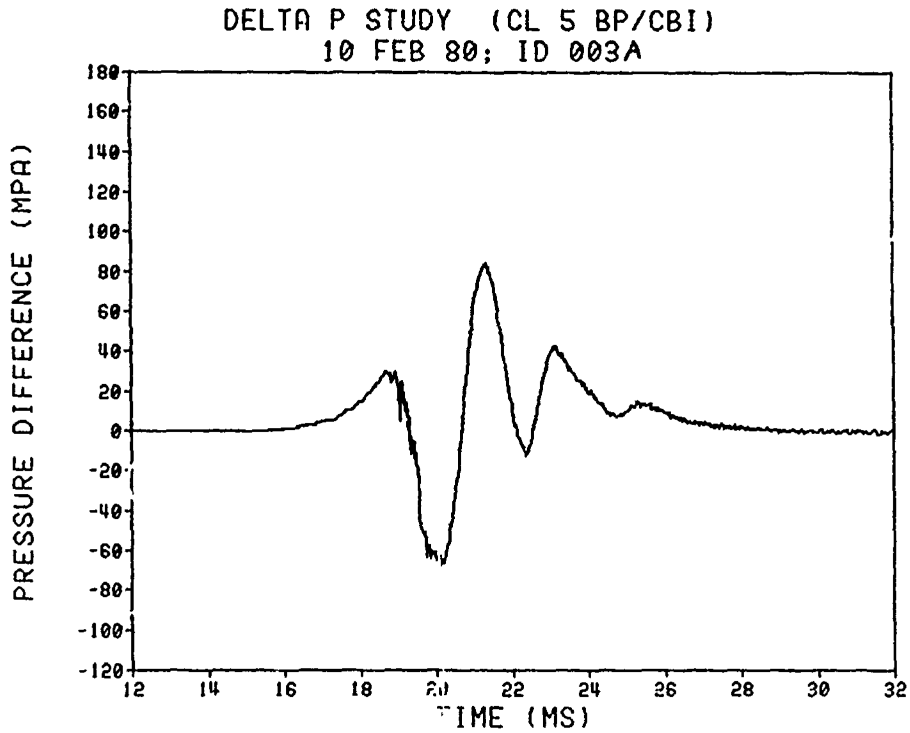
DELTA P STUDY (CL 5 BP/CBI)
10 FEB 80; ID 003A
PRESSURE DIFFERENCE (MPA)
180
160
140
120
100
80
60
40
20
0
-20
-40
-60
-80
-100
-120
12
14
16
18
22
24
26
28
30
32
IME (MS)

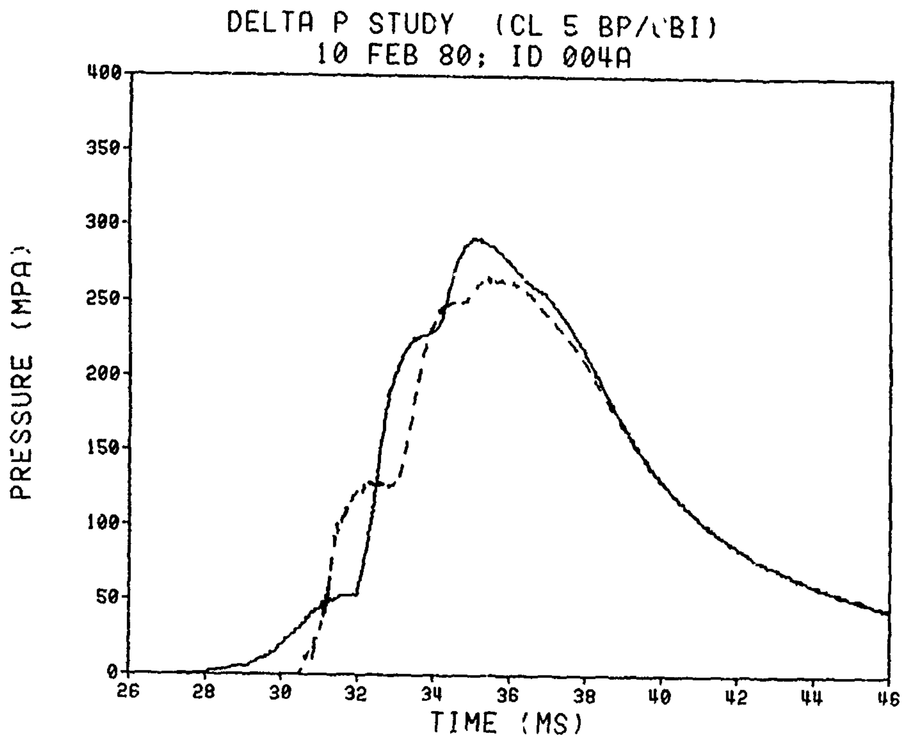
DELTA P STUDY (CL 5 BP/CBI)
10 FEB 80; ID 004A
PRESSURE (MPA)
TIME (MS)
400
350
300
250
200
150
100
50
0
26
28
30
32
34
36
38
40
42
44
46

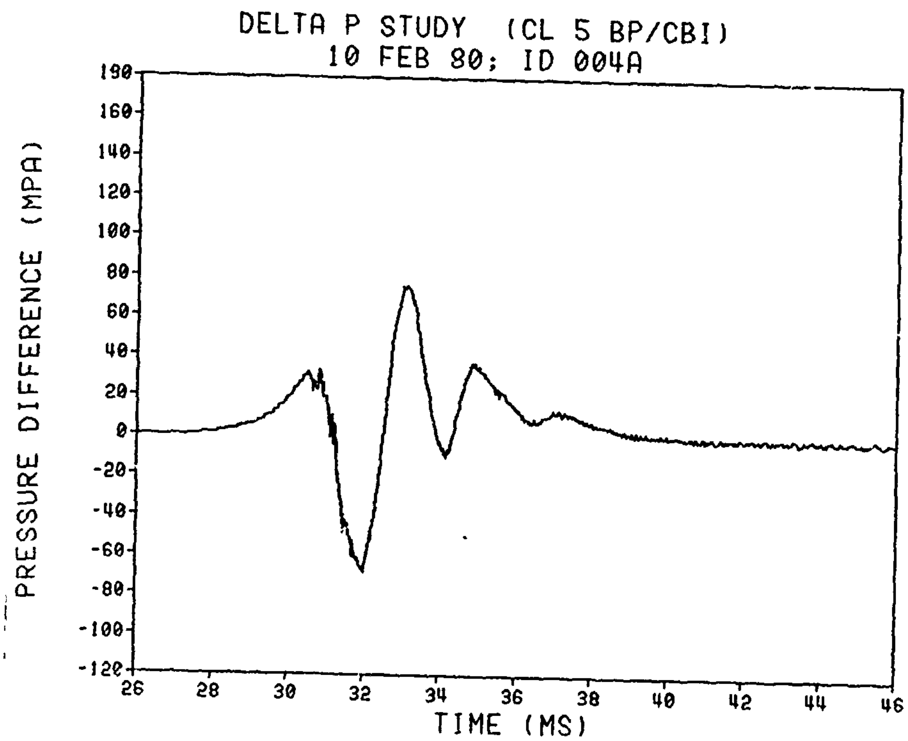
DELTA P STUDY (CL 5 BP/CBI)
10 FEB 80; ID 004A
PRESSURE DIFFERENCE (MPA)
TIME (MS)
180
160
140
120
100
80
60
40
20
0
-20
-40
-60
-80
-100
-120
26
28
30
32
34
36
38
40
42
44
46

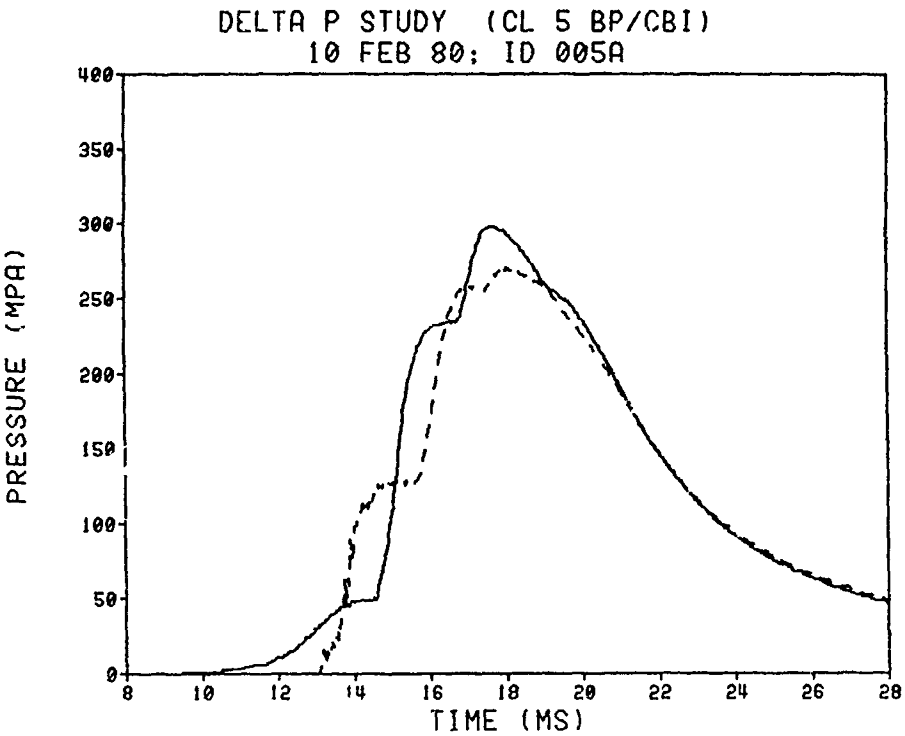
DELTA P STUDY (CL 5 BP/CBI)
10 FEB 80; ID 005A
PRESSURE (MPA)
TIME (MS)
400
350
300
250
200
150
100
50
0
8
10
12
14
16
18
20
22
24
26
28

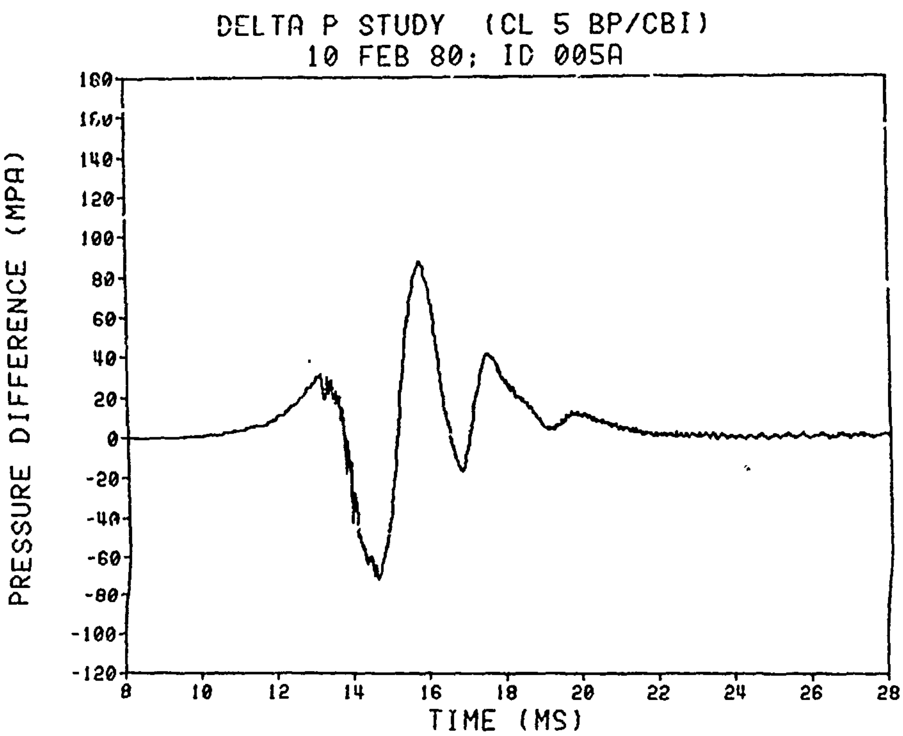
DELTA P STUDY (CL 5 BP/CBI)
10 FEB 80; ID 005A
PRESSURE DIFFERENCE (MPA)
TIME (MS)
180
160
140
120
100
80
60
40
20
0
-20
-40
-60
-80
-100
-120
8
10
12
14
16
18
20
22
24
26
28

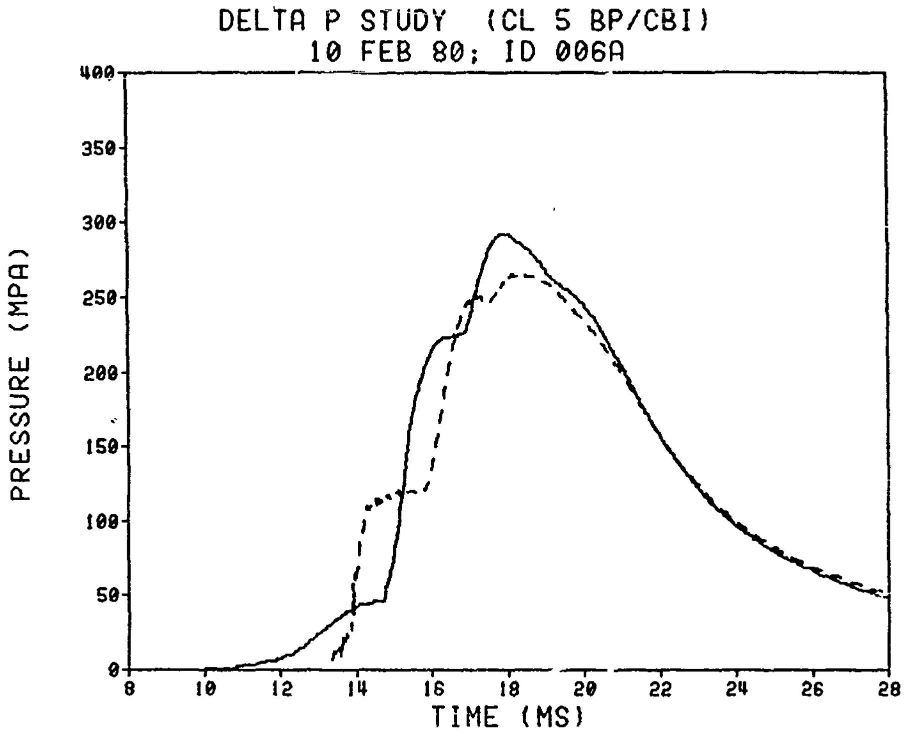
DELTA P STUDY (CL 5 BP/CBI)
10 FEB 80; ID 006A
PRESSURE (MPA)
TIME (MS)
400
350
300
250
200
150
100
50
0
8
10
12
14
16
18
20
22
24
26
28

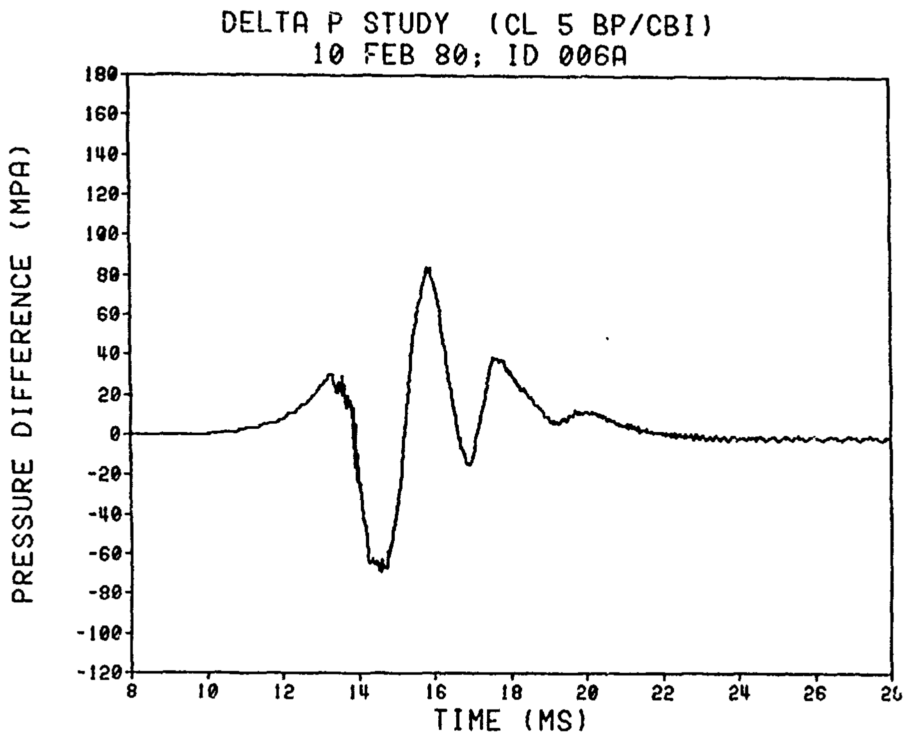
DELTA P STUDY (CL 5 BP/CBI)
10 FEB 80; ID 006A
PRESSURE DIFFERENCE (MPA)
TIME (MS)
180
160
140
120
100
80
60
40
20
0
-20
-40
-60
-80
-100
-120
8
10
12
14
16
18
20
22
24
26

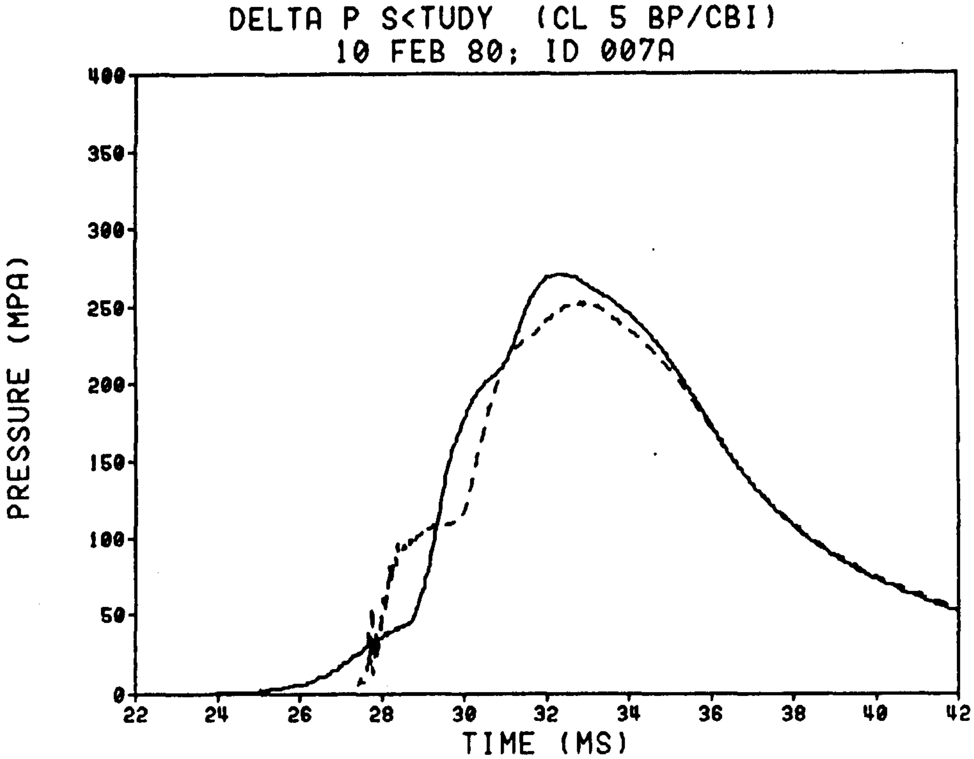
DELTA P S<TUDY (CL 5 BP/CBI)
10 FEB 80; ID 007A
PRESSURE (MPA)
400
350
300
250
200
150
100
50
0
22
24
26
28
30
32
34
36
38
40
42
TIME (MS)

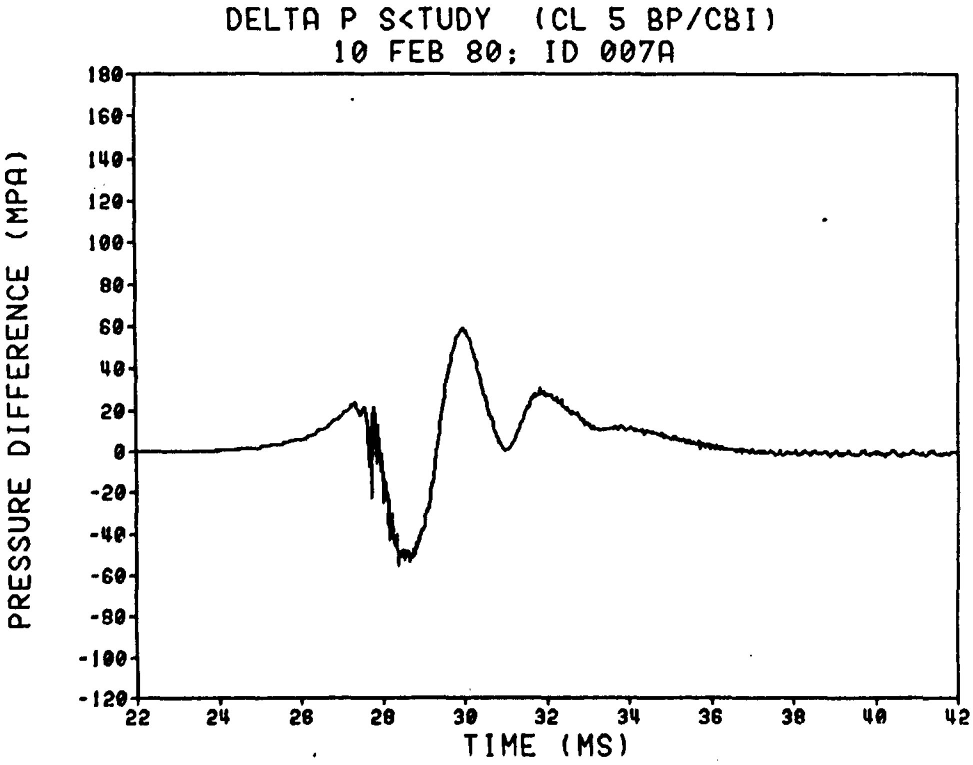
DELTA P S<TUDY (CL 5 BP/CBI)
10 FEB 80; ID 007A
PRESSURE DIFFERENCE (MPA)
180
160
140
120
100
80
60
40
20
0
-20
-40
-60
-80
-100
-120
22
24
26
28
30
32
34
36
38
40
42
TIME (MS)

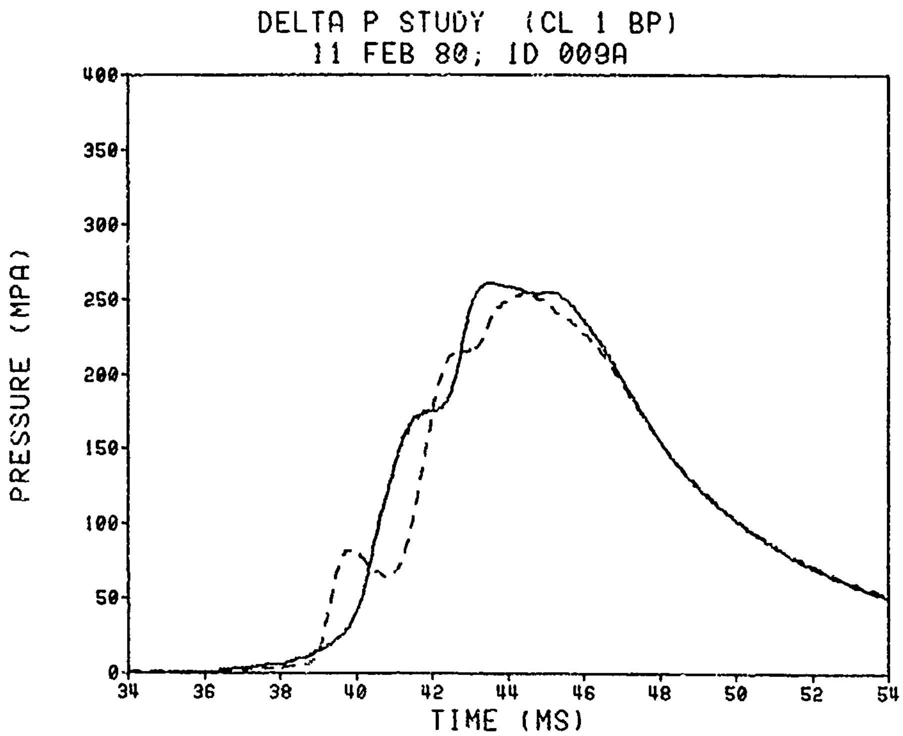
DELTA P STUDY (CL 1 BP)
11 FEB 80; ID 009A
PRESSURE (MPA)
TIME (MS)
400
350
300
250
200
150
100
50
0
34
36
38
40
42
44
46
48
50
52
54

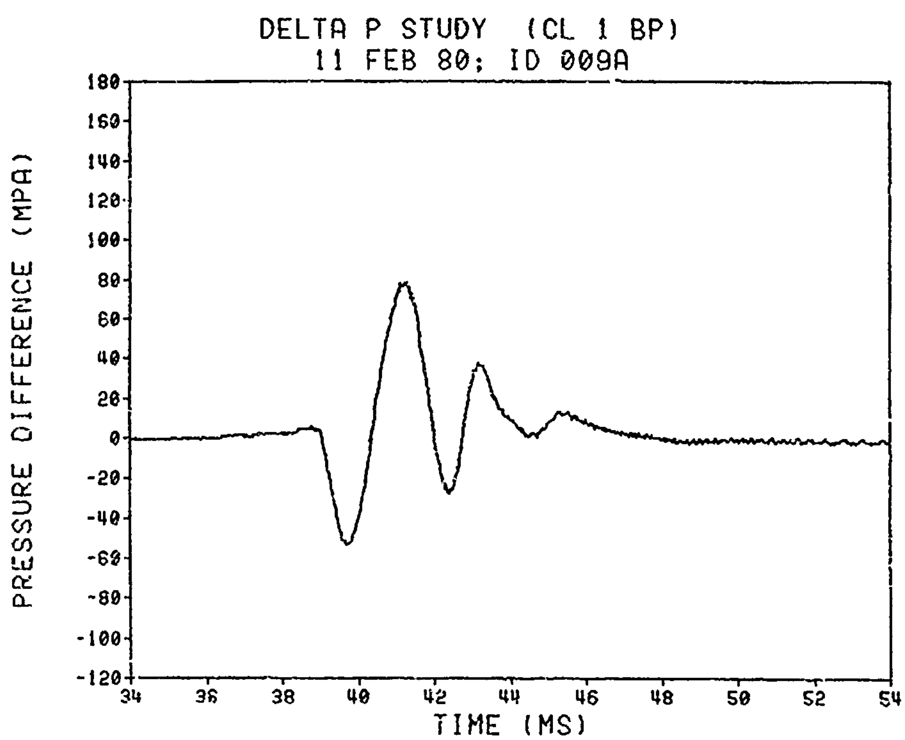
DELTA P STUDY (CL 1 BP)
11 FEB 80; ID 009A
PRESSURE DIFFERENCE (MPA)
TIME (MS)
180
160
140
120
100
80
60
40
20
0
-20
-40
-60
-80
-100
-120
34
36
38
40
42
44
46
48
50
52
54

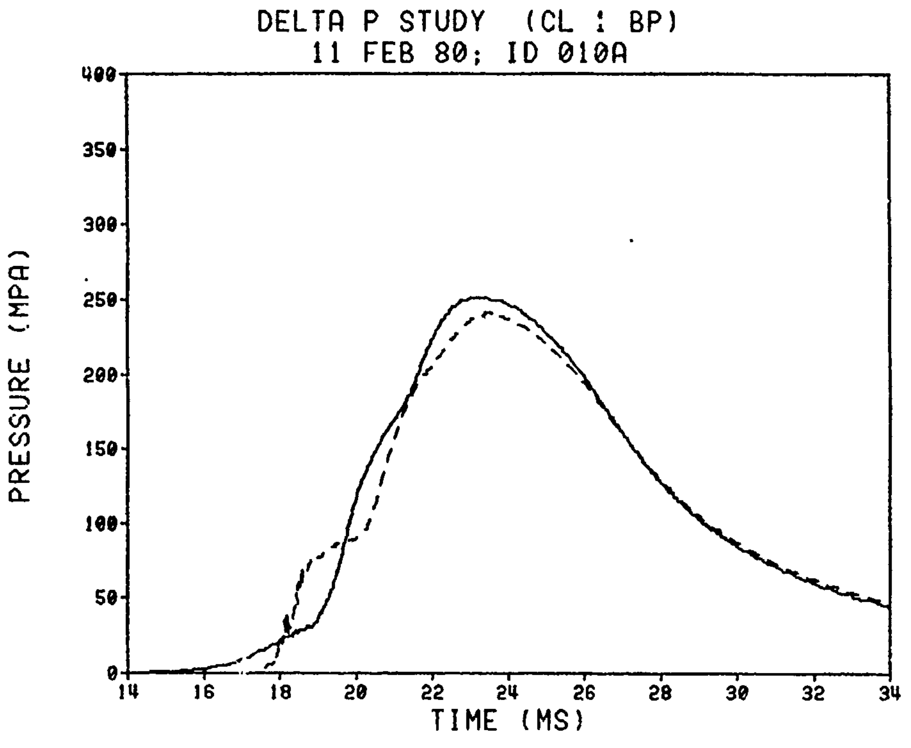
DELTA P STUDY (CL 1 BP)
11 FEB 80; ID 010A
PRESSURE (MPA)
TIME (MS)

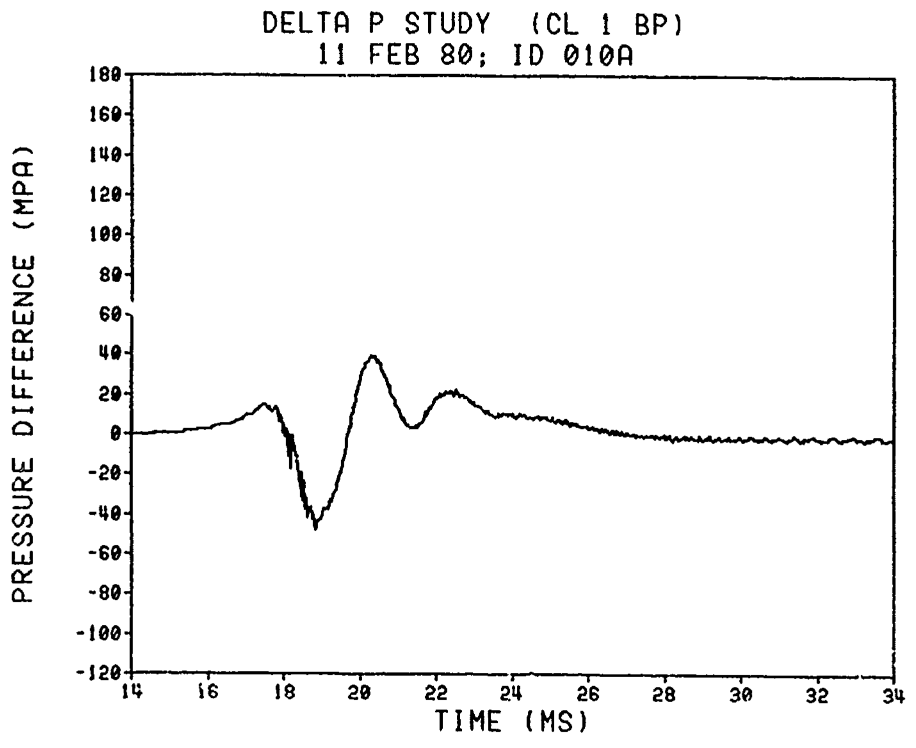
DELTA P STUDY (CL 1 BP)
11 FEB 80; ID 010A
PRESSURE DIFFERENCE (MPA)
TIME (MS)

DELTA P STUDY (CL 1 BP)
11 FEB 80; ID 011A

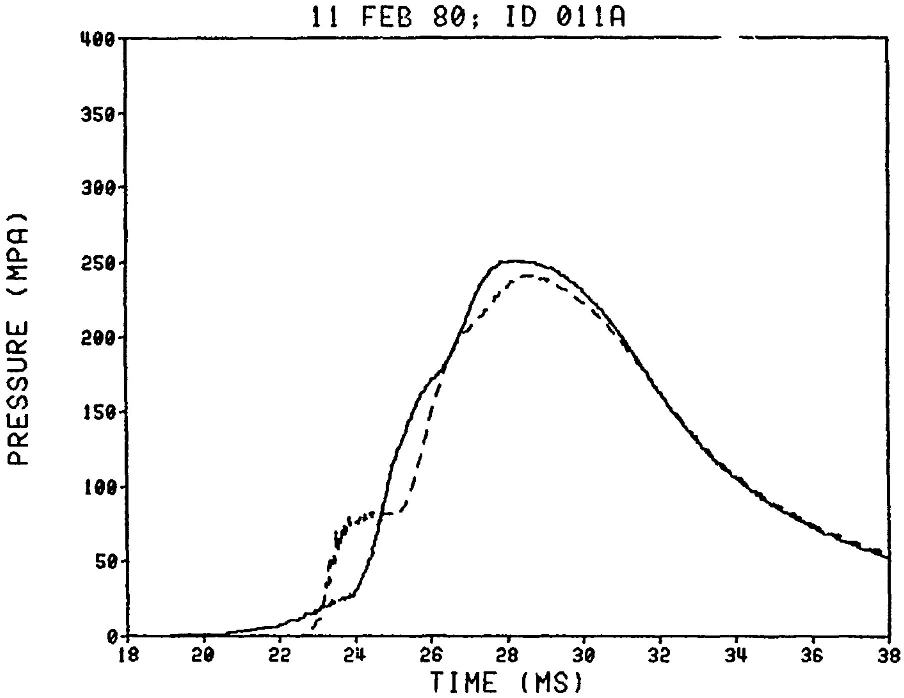

DELTA P STUDY (CL 1 BP)
11 FEB 80; ID 011A

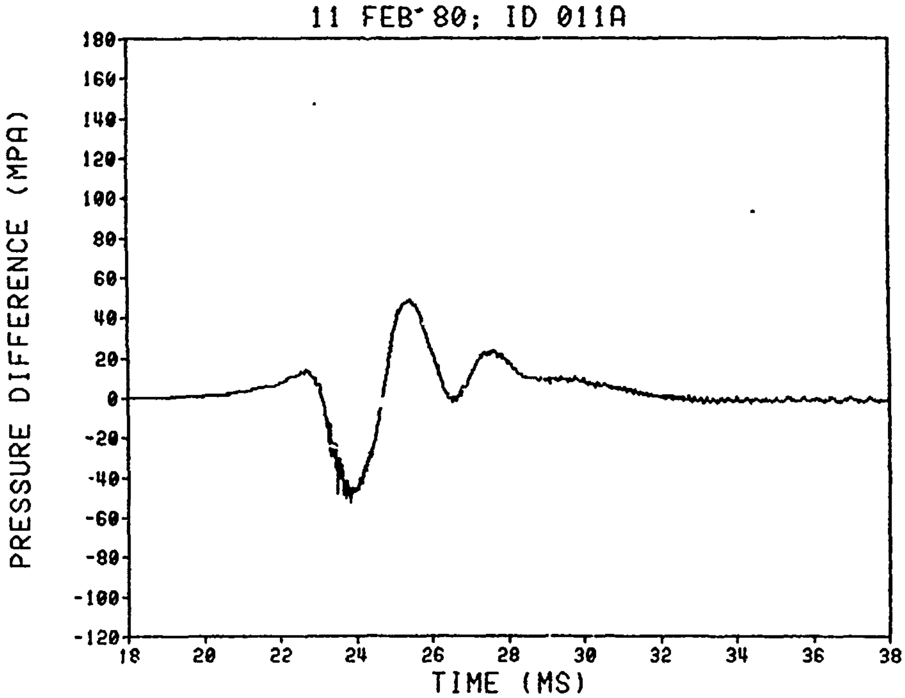

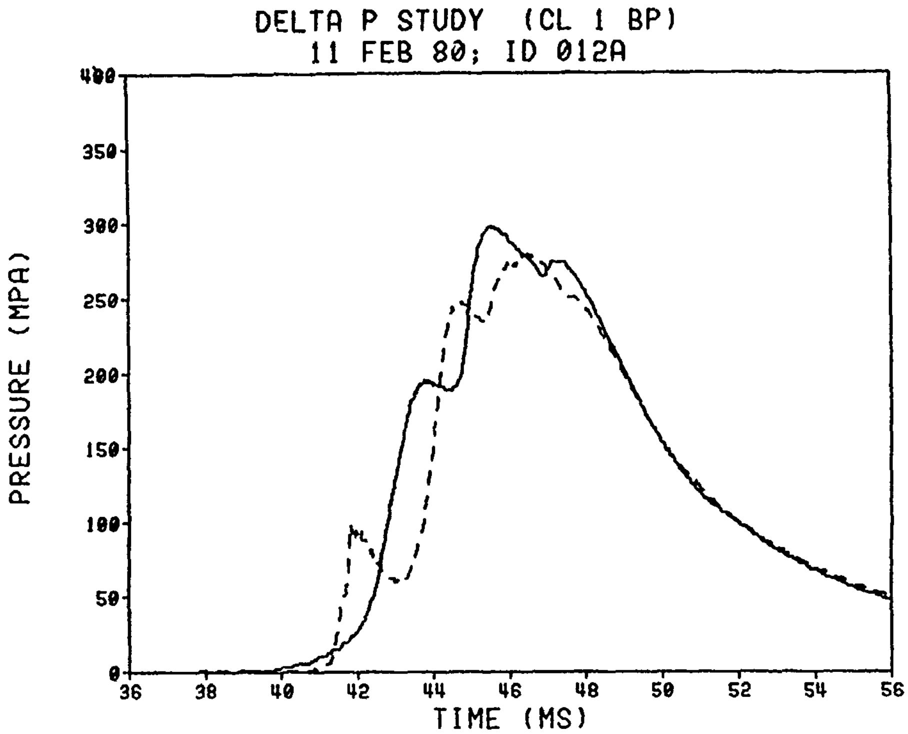
DELTA P STUDY (CL 1 BP)
11 FEB 80; ID 012A
PRESSURE (MPA)
TIME (MS)
0
50
100
150
200
250
300
350
400
36
38
40
42
44
46
48
50
52
54
56

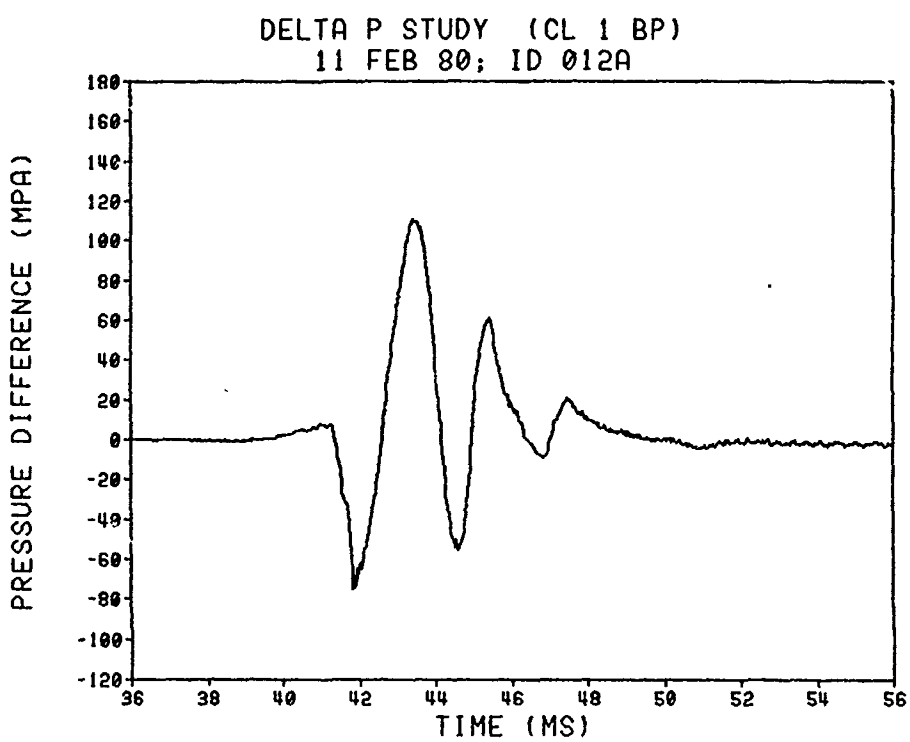
DELTA P STUDY (CL 1 BP)
11 FEB 80; ID 012A
PRESSURE DIFFERENCE (MPA)
TIME (MS)
180
160
140
120
100
80
60
40
20
0
-20
-40
-60
-80
-100
-120
36
38
40
42
44
46
48
50
52
54
56

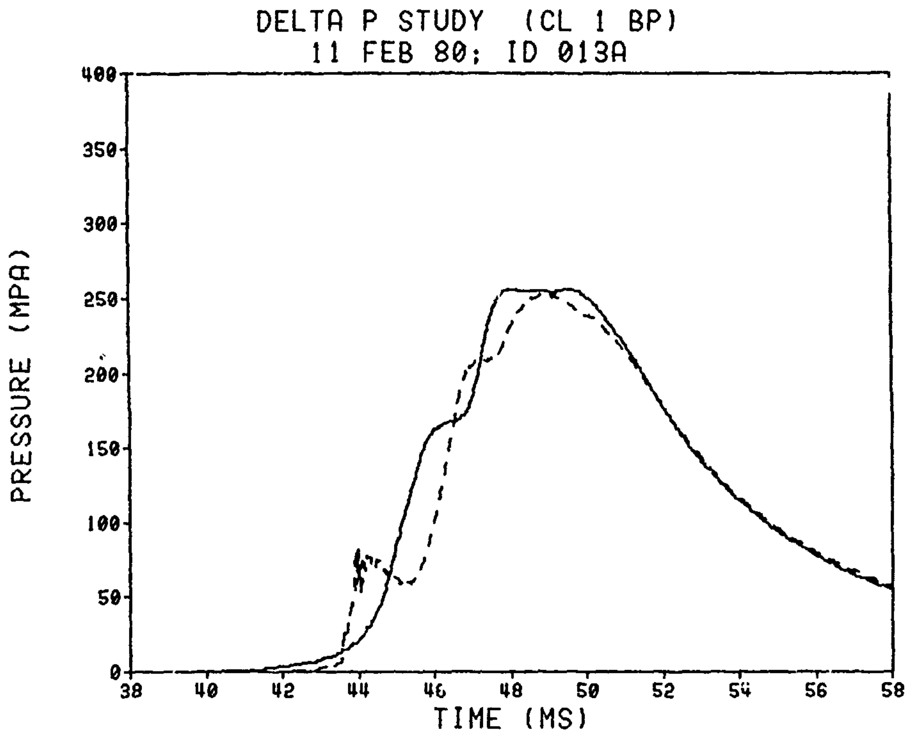
DELTA P STUDY (CL 1 BP)
11 FEB 80; ID 013A
PRESSURE (MPA)
400
350
300
250
200
150
100
50
0
38
40
42
44
46
48
50
52
54
56
58
TIME (MS)

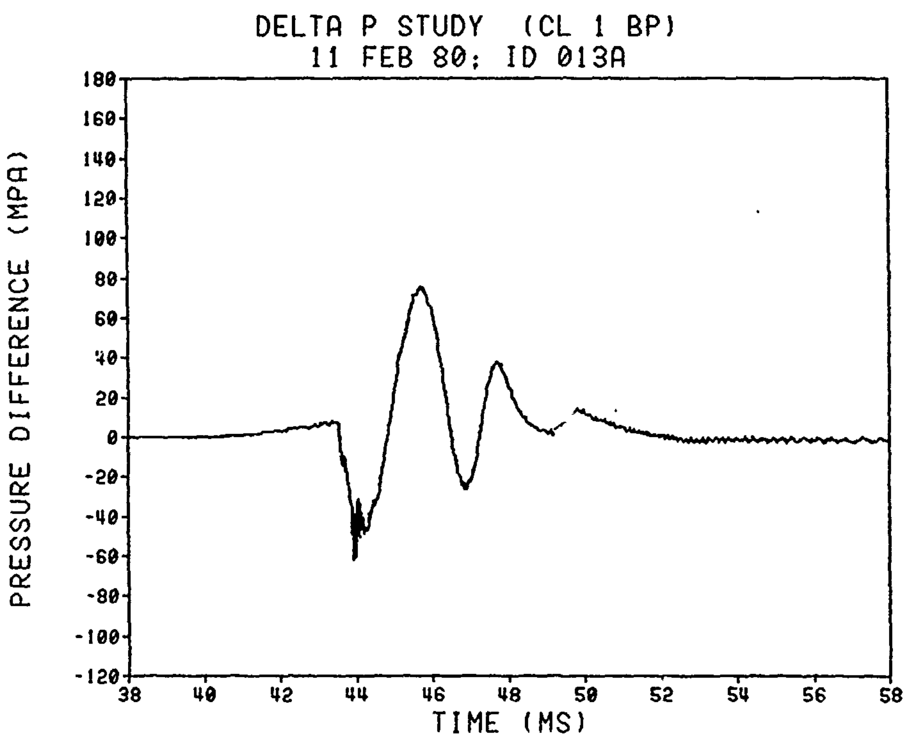
DELTA P STUDY (CL 1 BP)
11 FEB 80; ID 013A
PRESSURE DIFFERENCE (MPA)
180
160
140
120
100
80
60
40
20
0
-20
-40
-60
-80
-100
-120
38
40
42
44
46
48
50
52
54
56
58
TIME (MS)

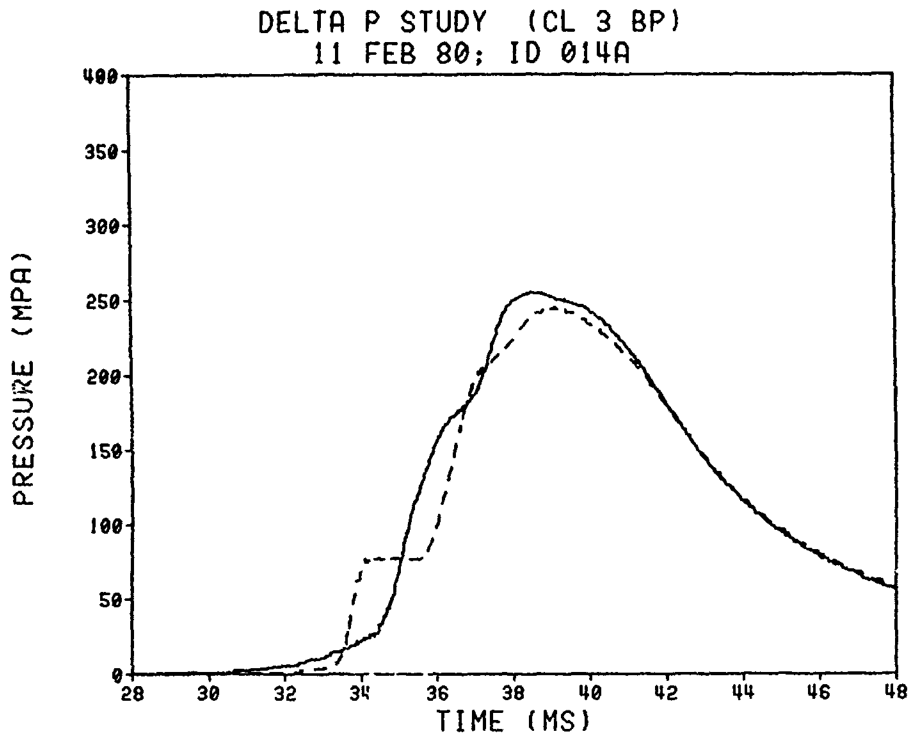
DELTA P STUDY (CL 3 BP)
11 FEB 80; ID 014A
PRESSURE (MPA)
TIME (MS)
400
350
300
250
200
150
100
50
0
28
30
32
34
36
38
40
42
44
46
48

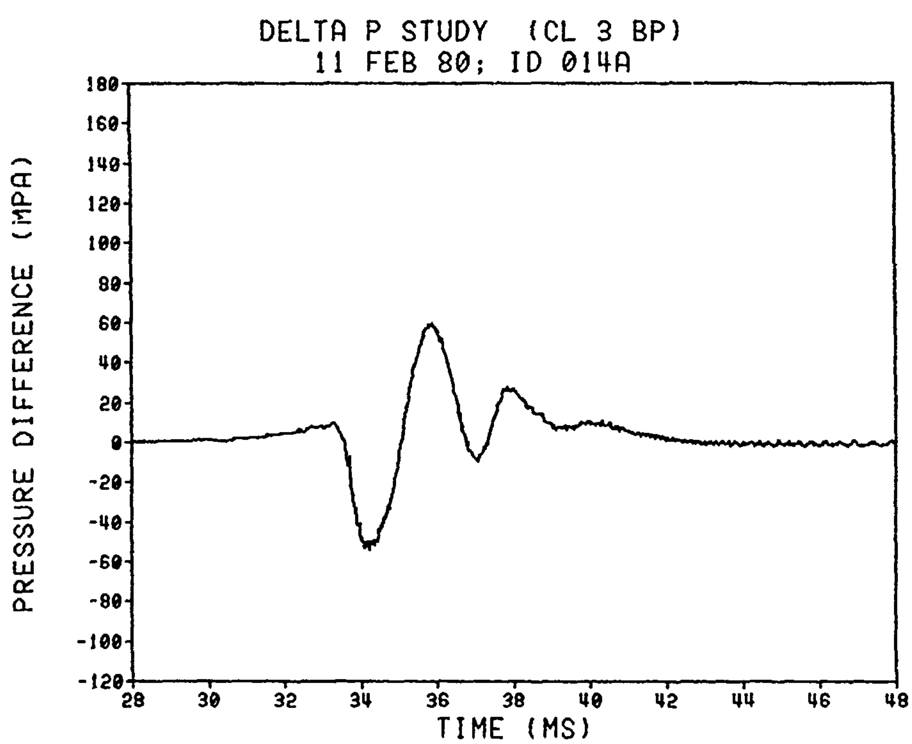
DELTA P STUDY (CL 3 BP)
11 FEB 80; ID 014A
PRESSURE DIFFERENCE (MPA)
TIME (MS)
180
160
140
120
100
80
60
40
20
0
-20
-40
-60
-80
-100
-120
28
30
32
34
36
38
40
42
44
46
48

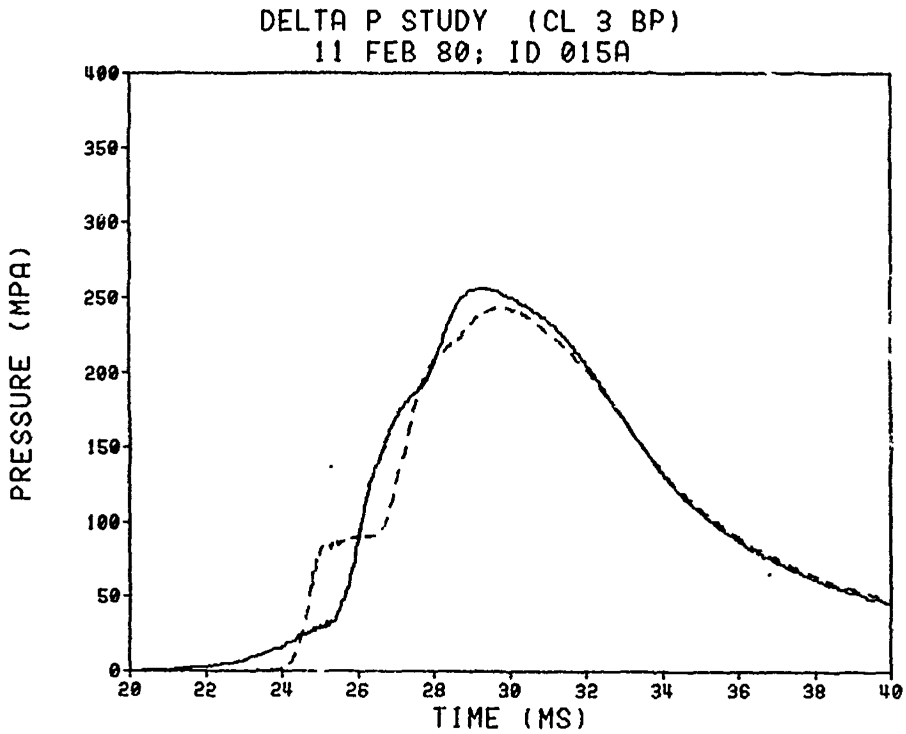

DELTA P STUDY (CL 3 BP)
11 FEB 80; ID 015A
PRESSURE (MPA)
400
350
300
250
200
150
100
50
0
20
22
24
26
28
30
32
34
36
38
40
TIME (MS)

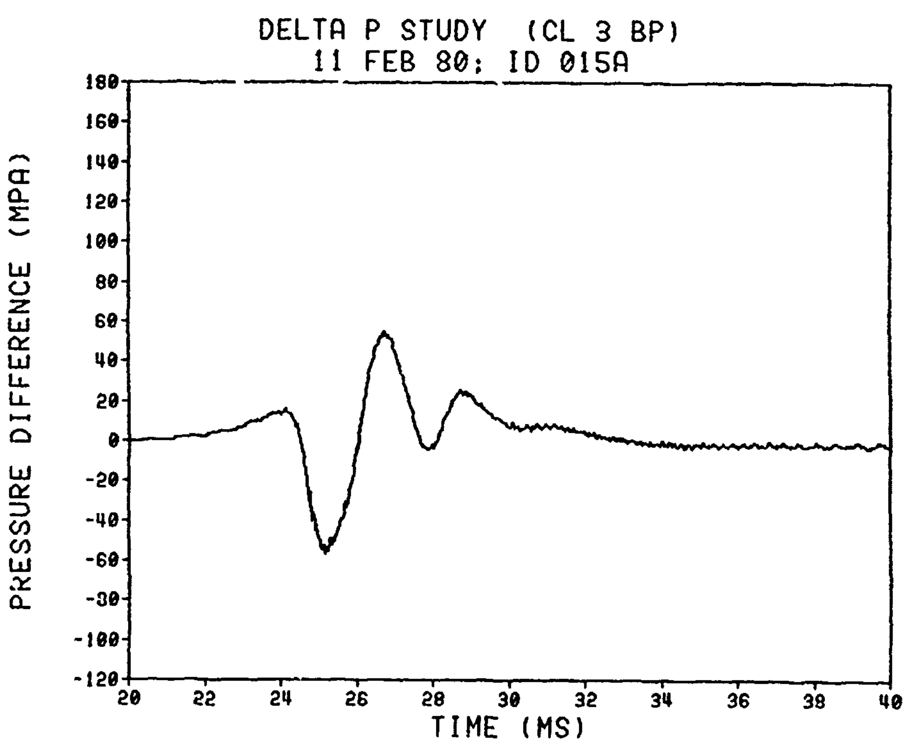

DELTA P STUDY (CL 3 BP)
11 FEB 80; ID 015A
PRESSURE DIFFERENCE (MPA)
180
160
140
120
100
80
60
40
20
0
-20
-40
-60
-80
-100
-120
20
22
24
26
28
30
32
34
36
38
40
TIME (MS)

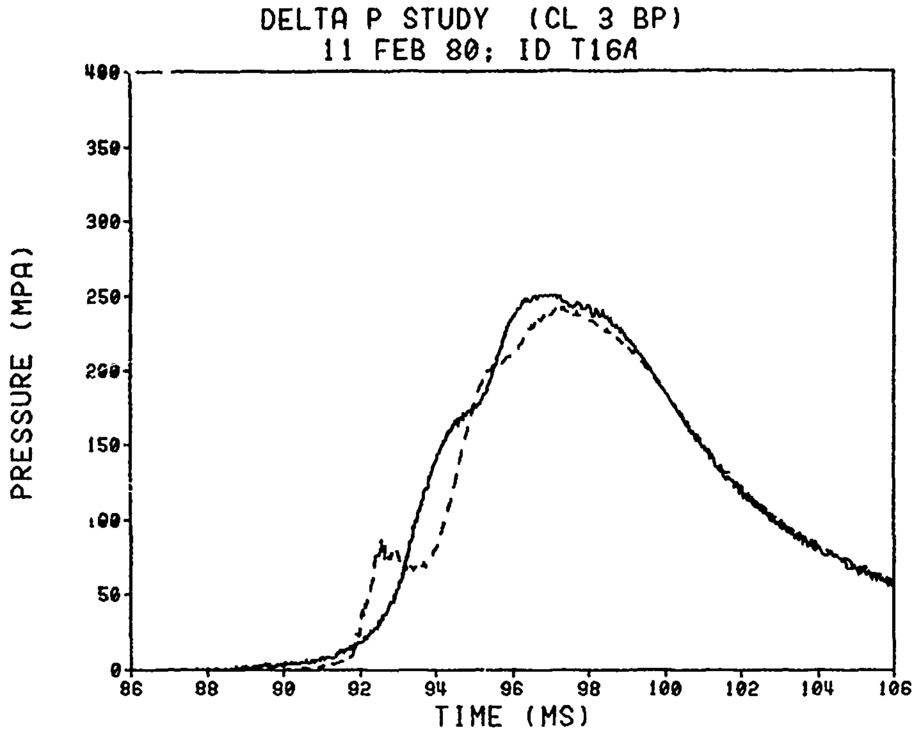
DELTA P STUDY (CL 3 BP)
11 FEB 80; ID T16A
PRESSURE (MPA)
400
350
300
250
200
150
100
50
0
86
88
90
92
94
96
98
100
102
104
106
TIME (MS)

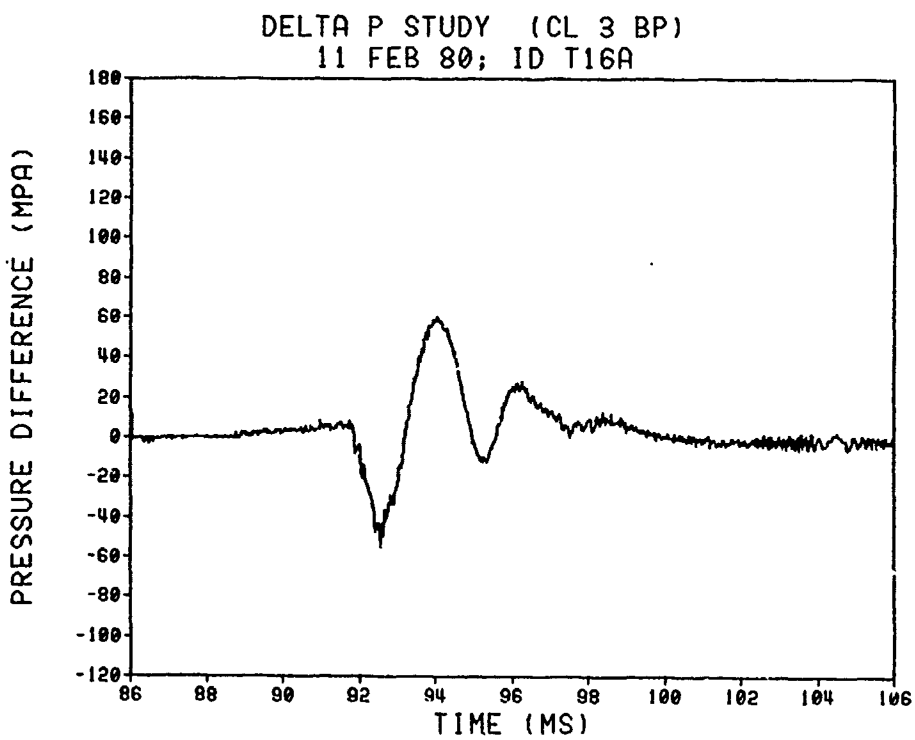
DELTA P STUDY (CL 3 BP)
11 FEB 80; ID T16A
PRESSURE DIFFERENCE (MPA)
180
160
140
120
100
80
60
40
20
0
-20
-40
-60
-80
-100
-120
86
88
90
92
94
96
98
100
102
104
106
TIME (MS)

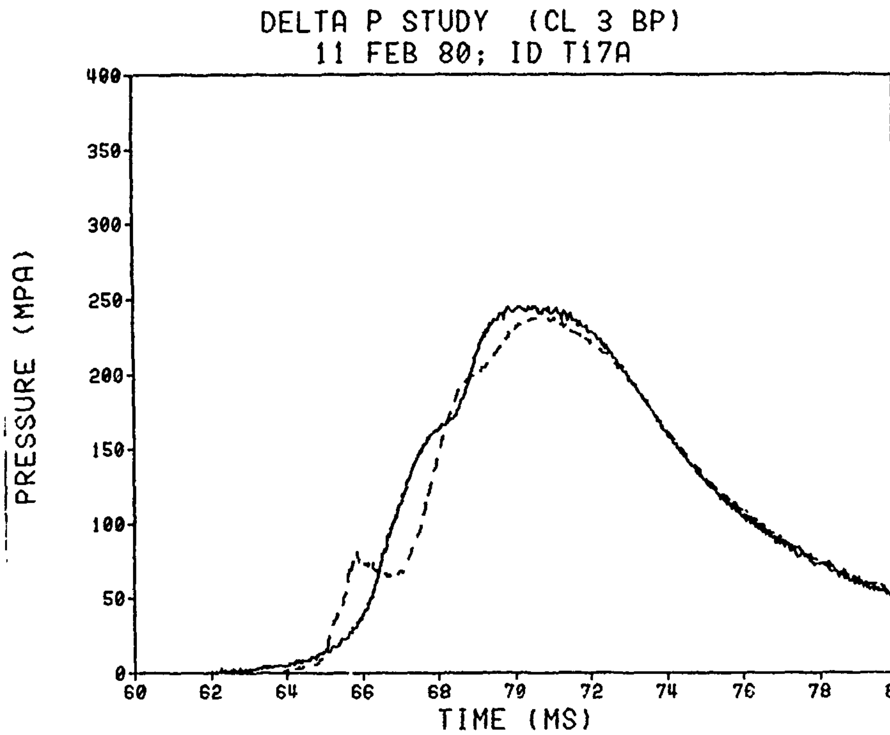
DELTA P STUDY (CL 3 BP)
11 FEB 80; ID T17A
PRESSURE (MPA)
400
350
300
250
200
150
100
50
0
60
62
64
66
68
70
72
74
76
78
80
TIME (MS)

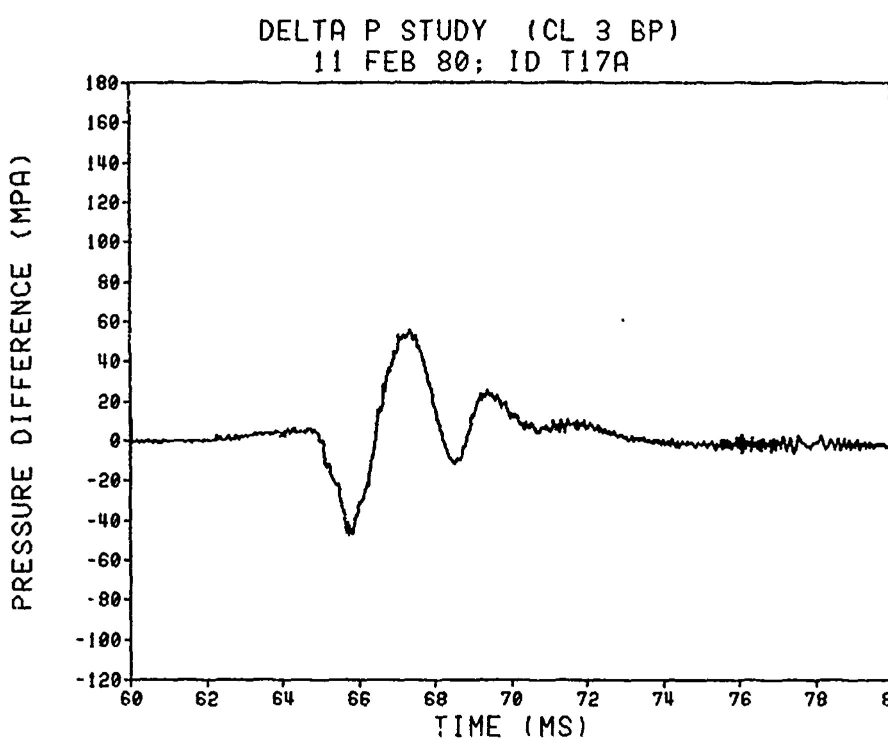
DELTA P STUDY (CL 3 BP)
11 FEB 80; ID T17A
PRESSURE DIFFERENCE (MPA)
180
160
140
120
100
80
60
40
20
0
-20
-40
-60
-80
-100
-120
60
62
64
66
68
70
72
74
76
78
80
TIME (MS)

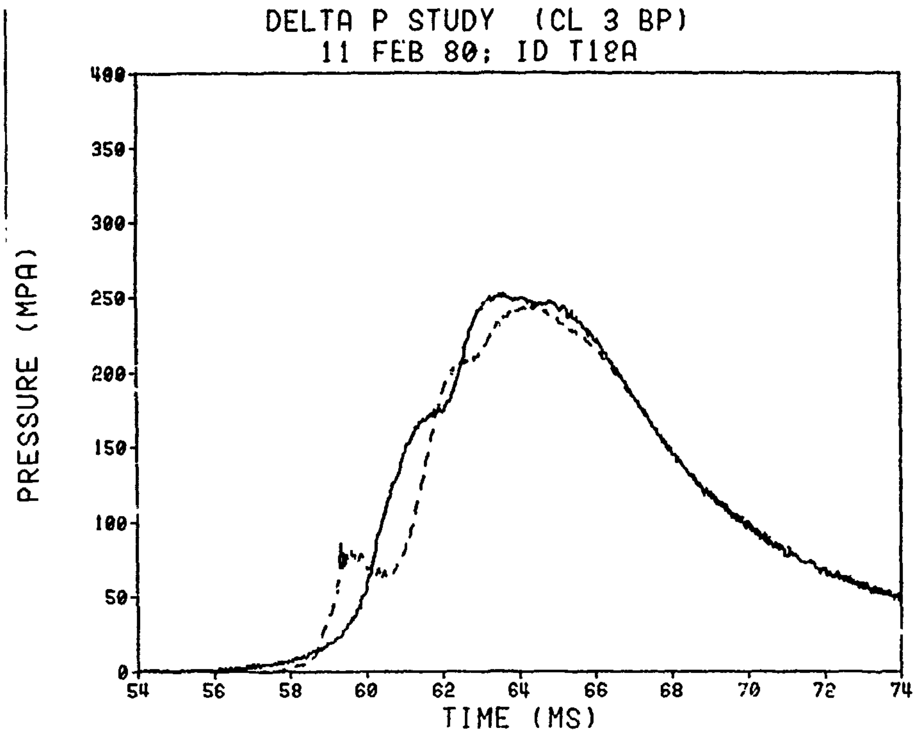
DELTA P STUDY (CL 3 BP)
11 FEB 80; ID T18A
PRESSURE (MPA)
TIME (MS)
400
350
300
250
200
150
100
50
0
54
56
58
60
62
64
66
68
70
72
74

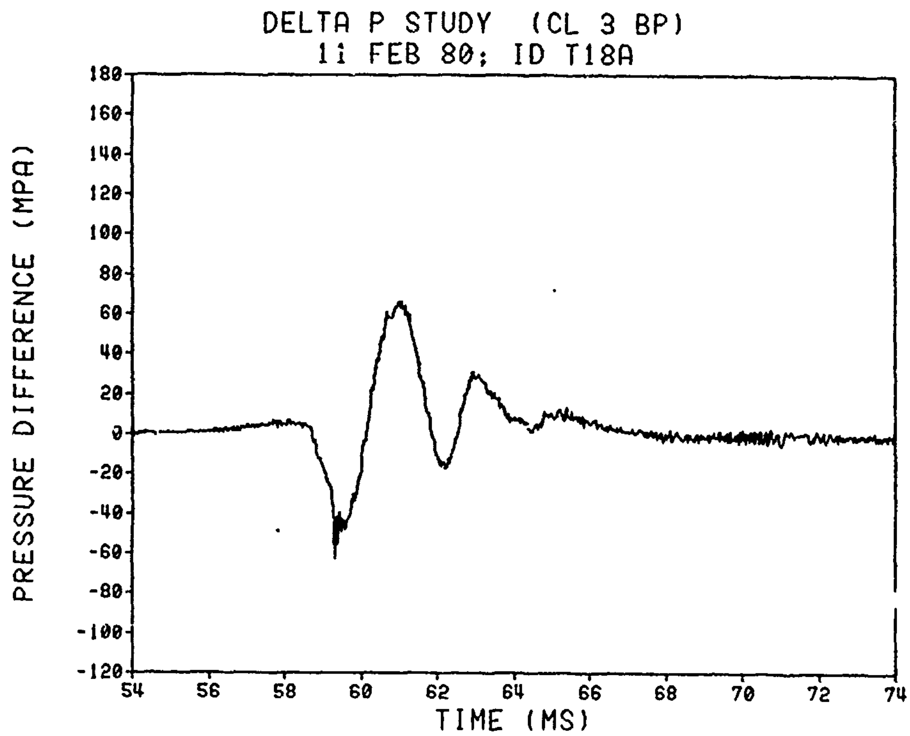
DELTA P STUDY (CL 3 BP)
11 FEB 80; ID T18A
PRESSURE DIFFERENCE (MPA)
TIME (MS)
180
160
140
120
100
80
60
40
20
0
-20
-40
-60
-80
-100
-120
54
56
58
60
62
64
66
68
70
72
74

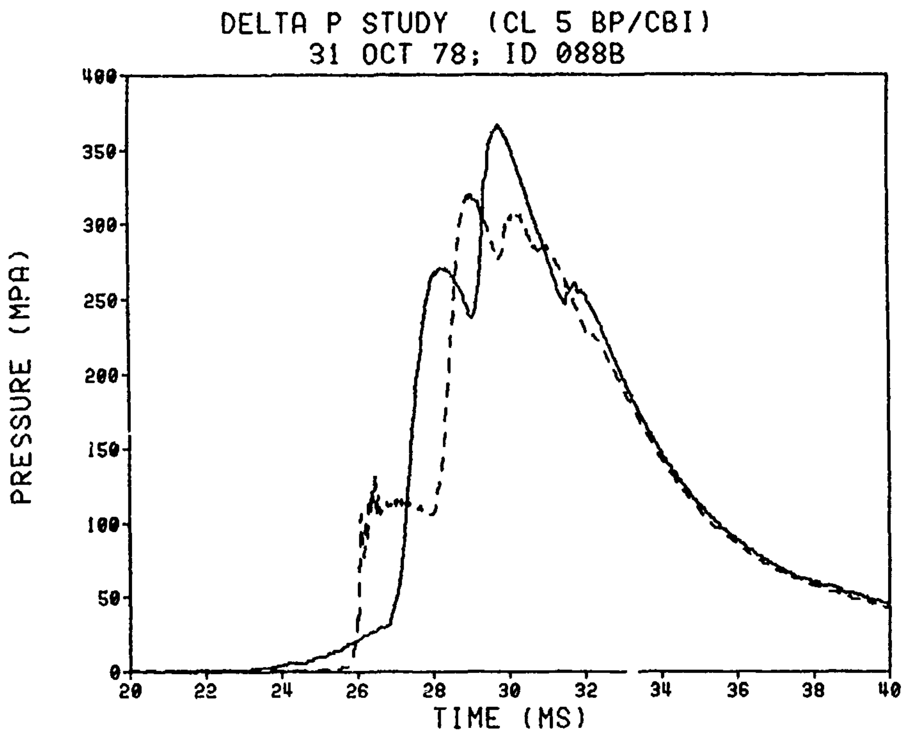
DELTA P STUDY (CL 5 BP/CBI)
31 OCT 78; ID 088B
PRESSURE (MPA)
TIME (MS)

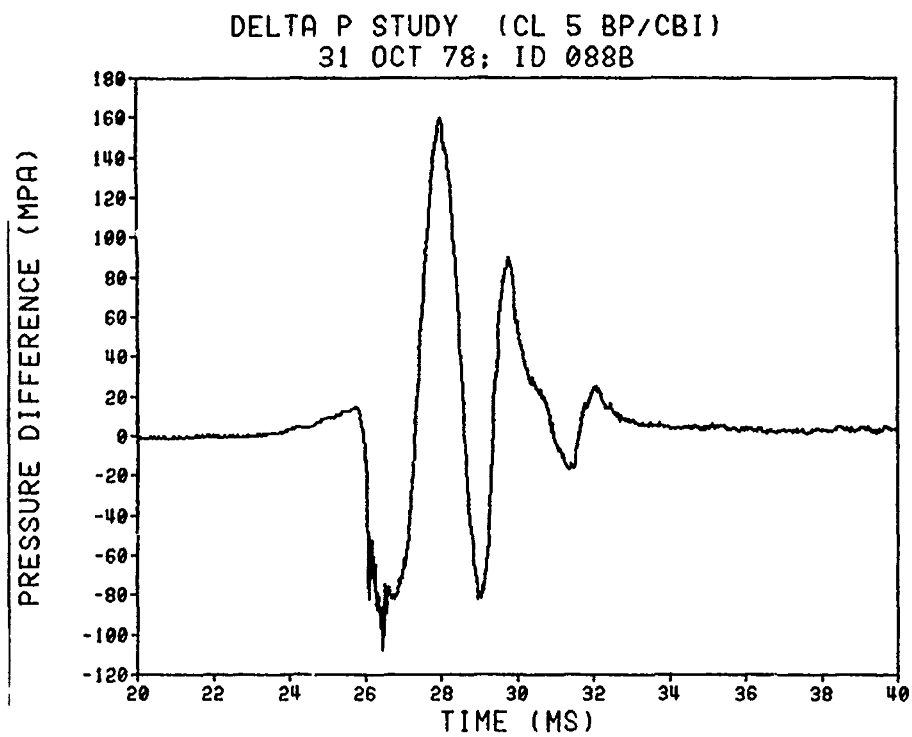
DELTA P STUDY (CL 5 BP/CBI)
31 OCT 78; ID 088B
PRESSURE DIFFERENCE (MPA)
TIME (MS)

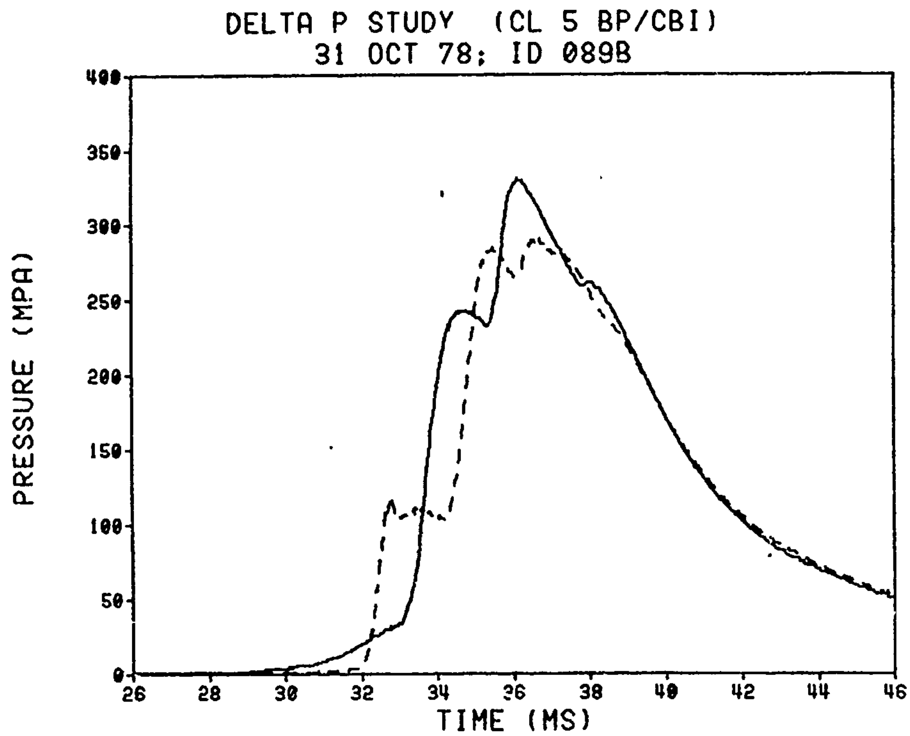
DELTA P STUDY (CL 5 BP/CBI)
31 OCT 78; ID 089B
PRESSURE (MPA)
TIME (MS)
400
350
300
250
200
150
100
50
0
26
28
30
32
34
36
38
40
42
44
46

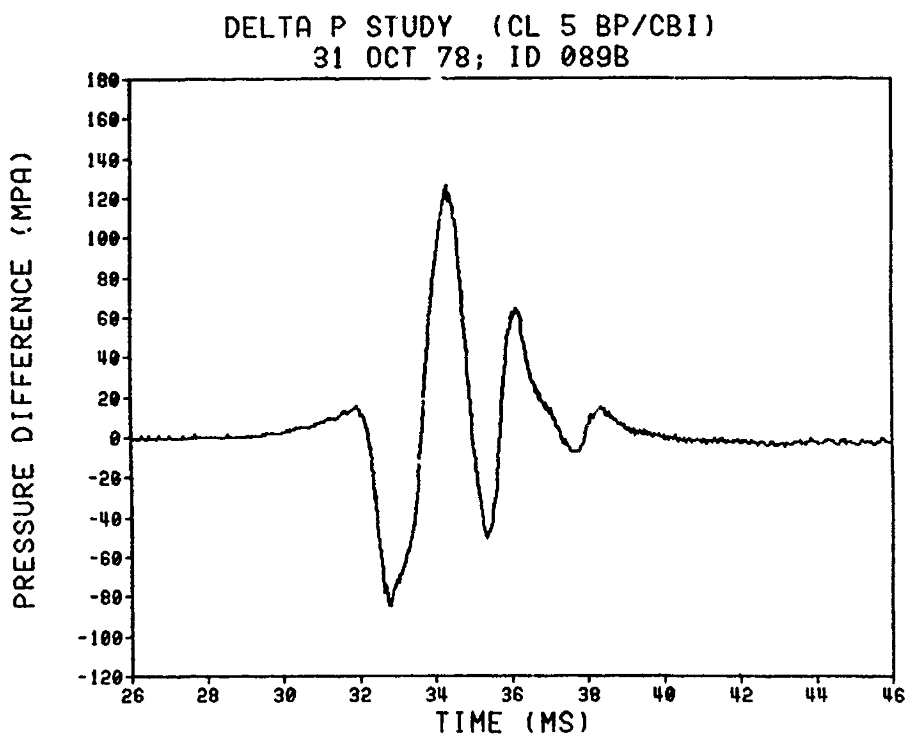
DELTA P STUDY (CL 5 BP/CBI)
31 OCT 78; ID 089B
PRESSURE DIFFERENCE (MPA)
TIME (MS)
180
160
140
120
100
80
60
40
20
0
-20
-40
-60
-80
-100
-120
26
28
30
32
34
36
38
40
42
44
46

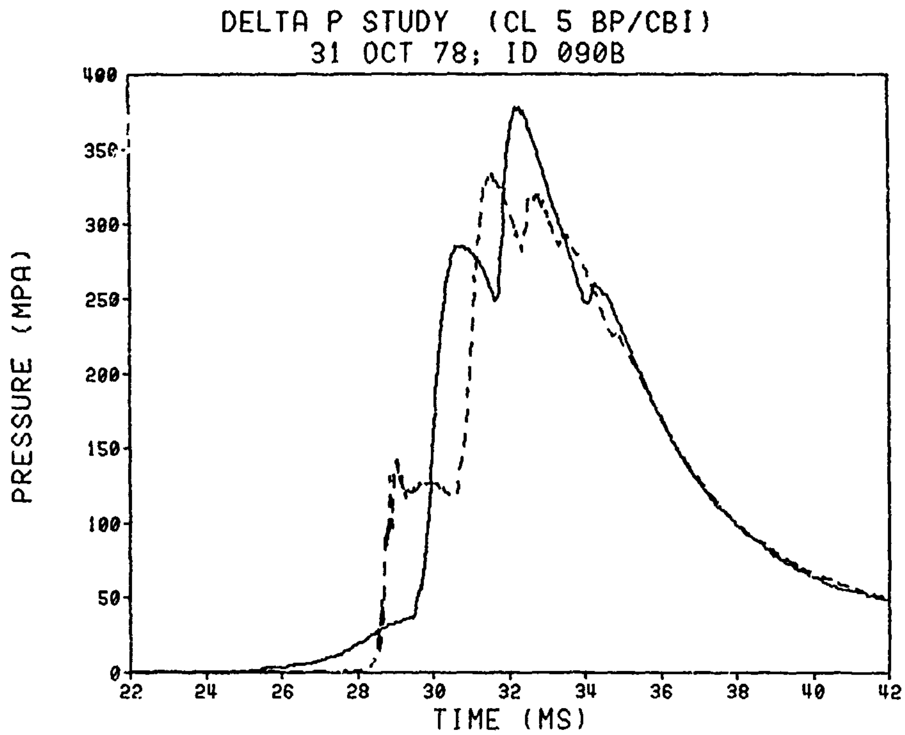
DELTA P STUDY (CL 5 BP/CBI)
31 OCT 78; ID 090B
PRESSURE (MPA)
TIME (MS)
0
50
100
150
200
250
300
350
400
22
24
26
28
30
32
34
36
38
40
42

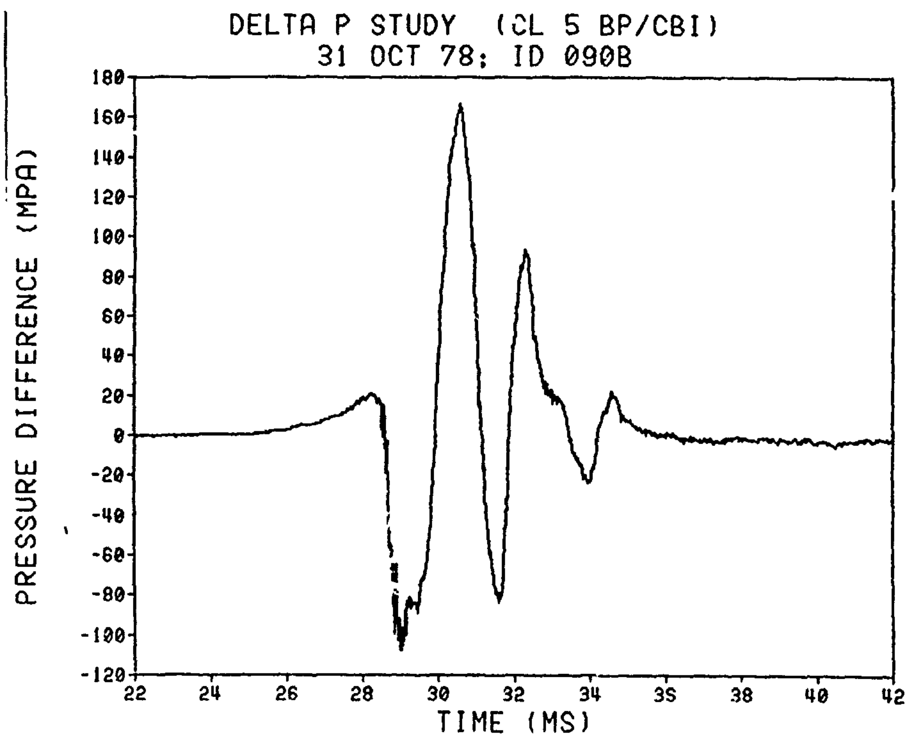
DELTA P STUDY (CL 5 BP/CBI)
31 OCT 78; ID 090B
PRESSURE DIFFERENCE (MPA)
TIME (MS)
180
160
140
120
100
80
60
40
20
0
-20
-40
-60
-80
-100
-120
22
24
26
28
30
32
34
36
38
40
42

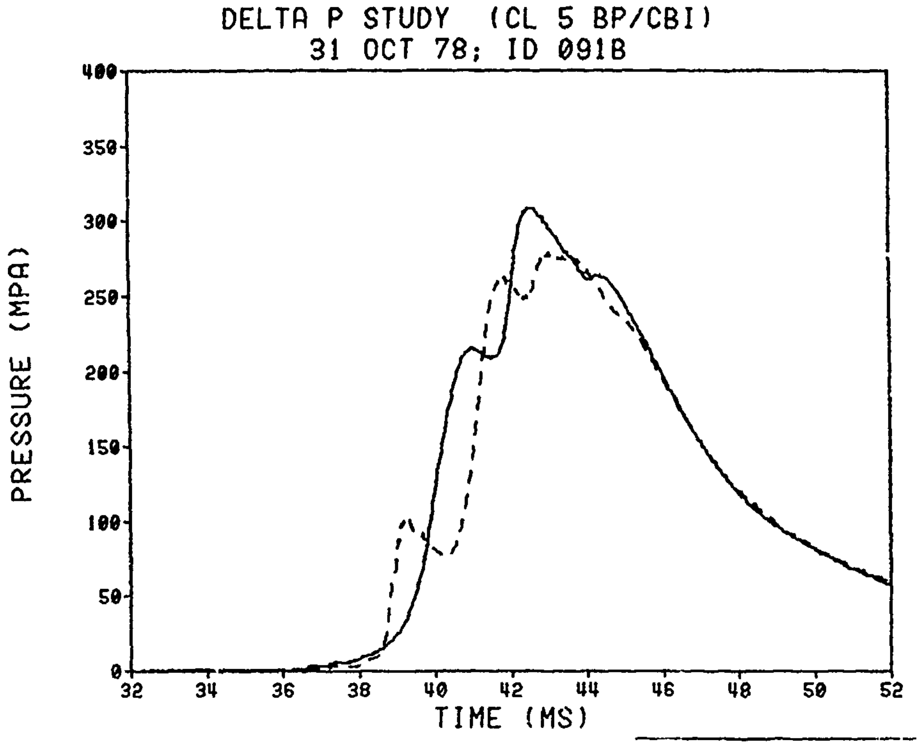
DELTA P STUDY (CL 5 BP/CBI)
31 OCT 78; ID 091B
PRESSURE (MPA)
TIME (MS)
400
350
300
250
200
150
100
50
0
32
34
36
38
40
42
44
46
48
50
52

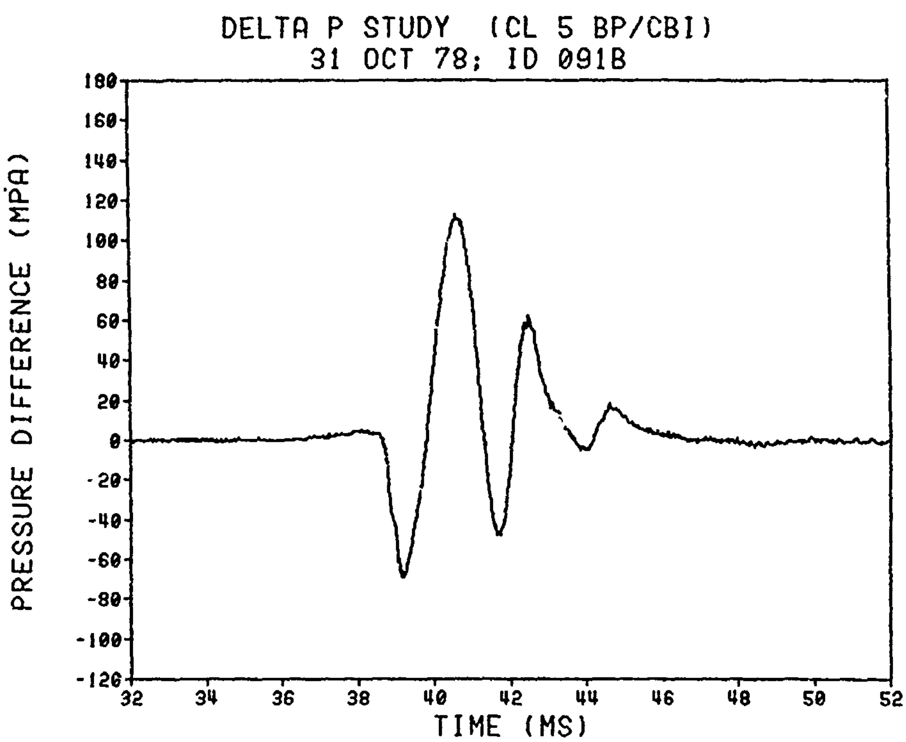
DELTA P STUDY (CL 5 BP/CBI)
31 OCT 78; ID 091B
PRESSURE DIFFERENCE (MPA)
TIME (MS)
180
160
140
120
100
80
60
40
20
0
-20
-40
-60
-80
-100
-120
32
34
36
38
40
42
44
46
48
50
52

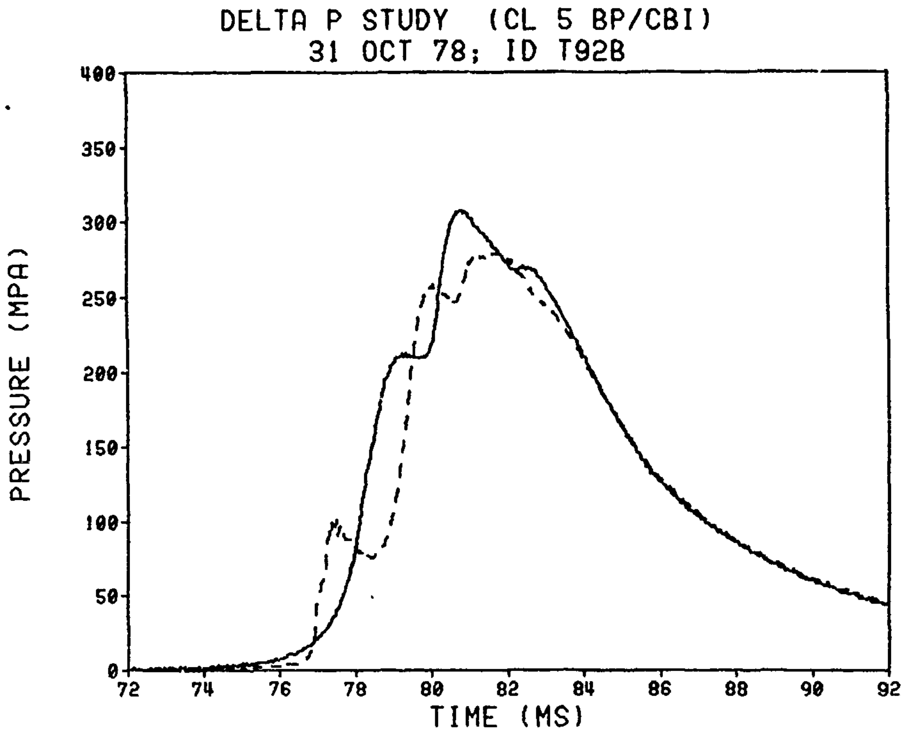
DELTA P STUDY (CL 5 BP/CBI)
31 OCT 78; ID T92B
PRESSURE (MPA)
TIME (MS)

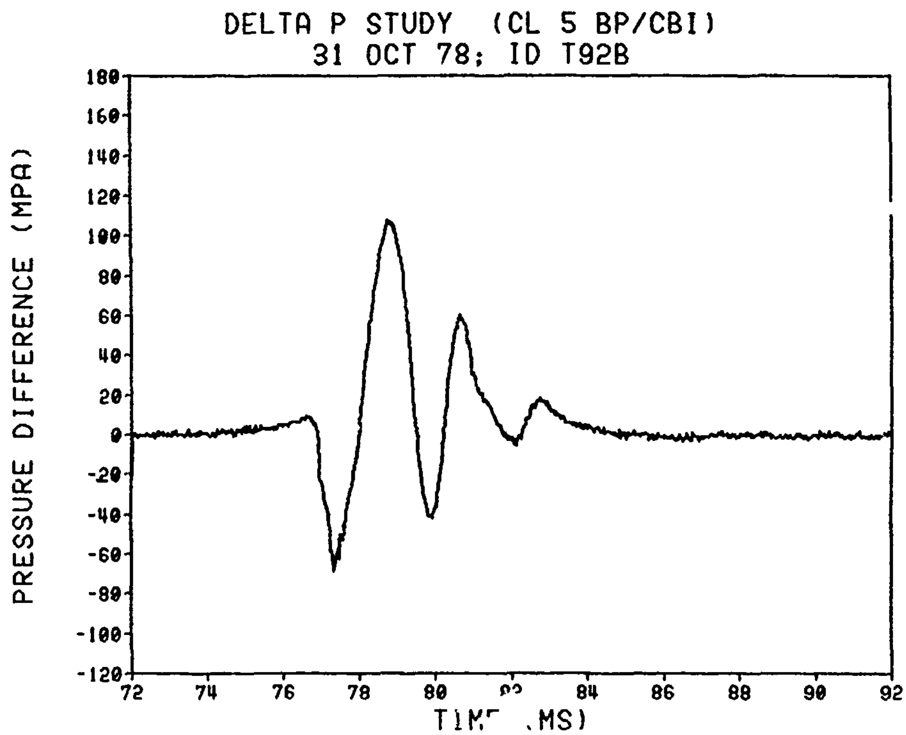
DELTA P STUDY (CL 5 BP/CBI)
31 OCT 78; ID T92B
PRESSURE DIFFERENCE (MPA)

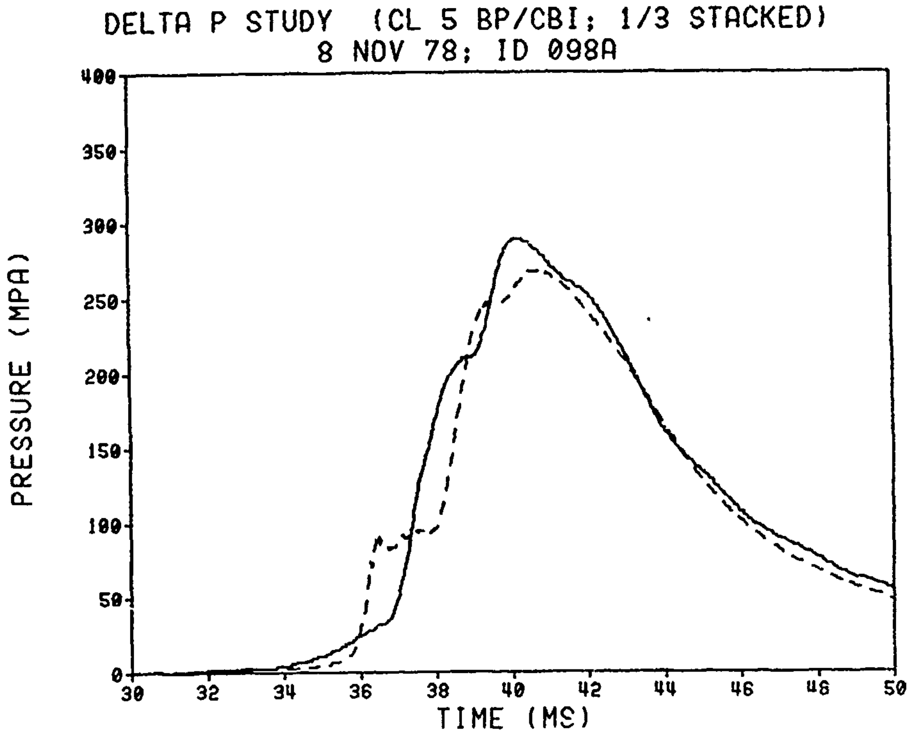
DELTA P STUDY (CL 5 BP/CBI; 1/3 STACKED)
8 NOV 78; ID 098A
PRESSURE (MPA)
TIME (MS)
0
50
100
150
200
250
300
350
400
30
32
34
36
38
40
42
44
46
48
50

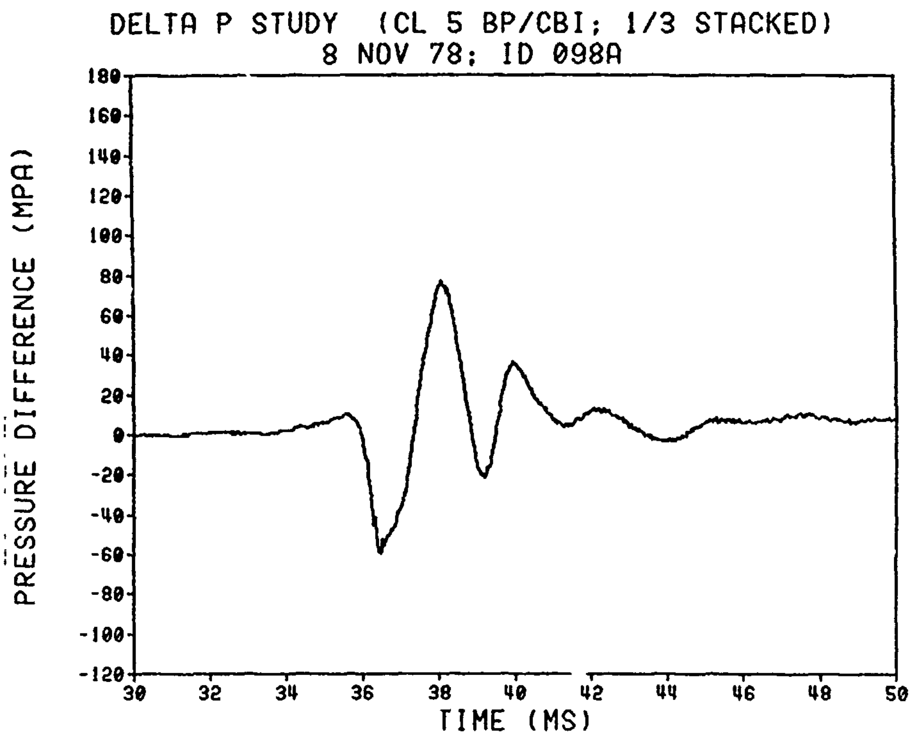
DELTA P STUDY (CL 5 BP/CBI; 1/3 STACKED)
8 NOV 78; ID 098A
PRESSURE DIFFERENCE (MPA)
TIME (MS)
180
160
140
120
100
80
60
40
20
0
-20
-40
-60
-80
-100
-120
30
32
34
36
38
40
42
44
46
48
50

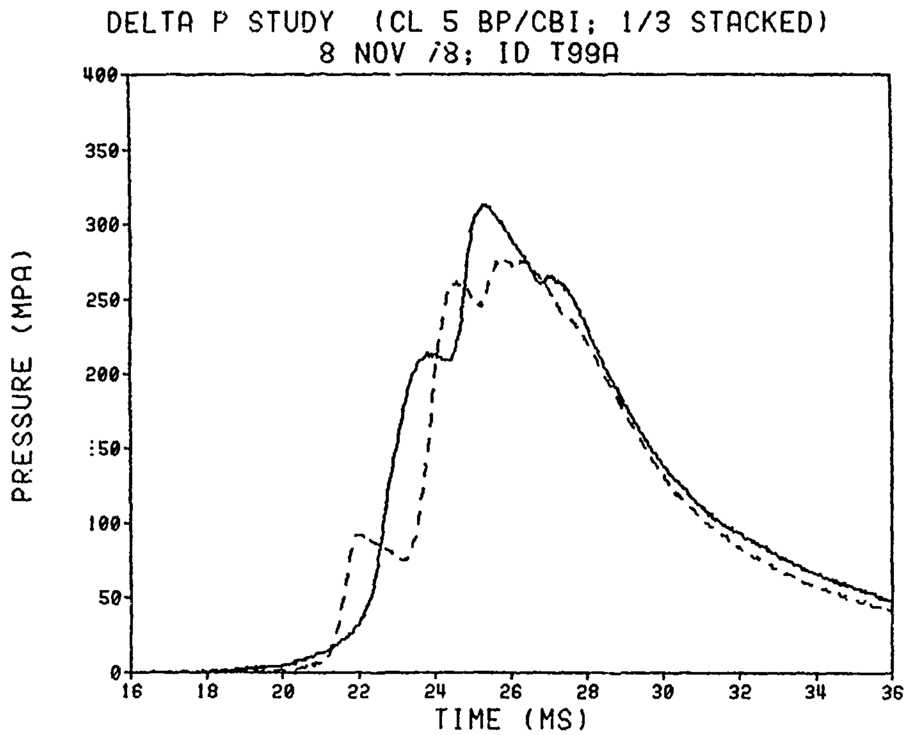

DELTA P STUDY (CL 5 BP/CBI; 1/3 STACKED)
8 NOV 78; ID T99A
PRESSURE (MPA)
400
350
300
250
200
150
100
50
0
16
18
20
22
24
26
28
30
32
34
36
TIME (MS)

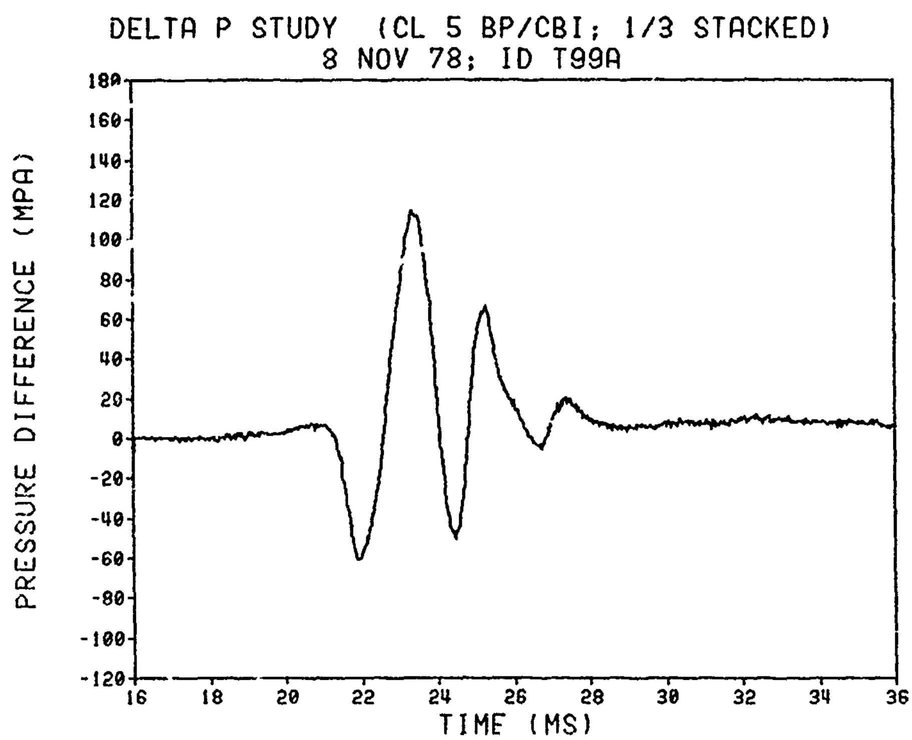

DELTA P STUDY (CL 5 BP/CBI; 1/3 STACKED)
8 NOV 78; ID T99A
PRESSURE DIFFERENCE (MPA)
180
160
140
120
100
80
60
40
20
0
-20
-40
-60
-80
-100
-120
16
18
20
22
24
26
28
30
32
34
36
TIME (MS)

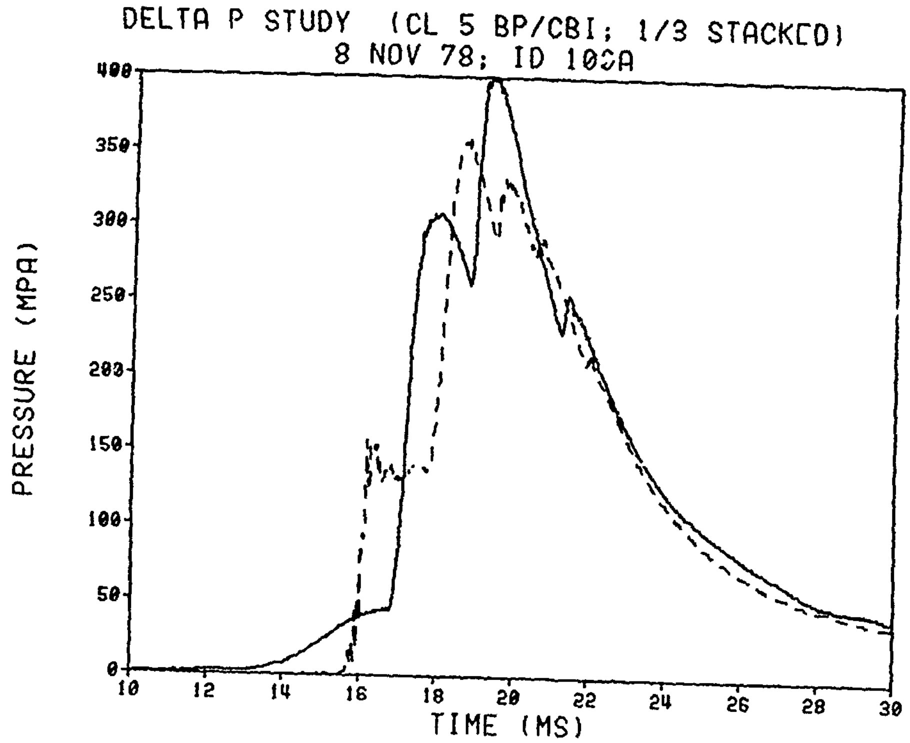
DELTA P STUDY (CL 5 BP/CBI; 1/3 STACKED)
8 NOV 78; ID 100A
PRESSURE (MPA)
TIME (MS)
400
350
300
250
200
150
100
50
0
10
12
14
16
18
20
22
24
26
28
30

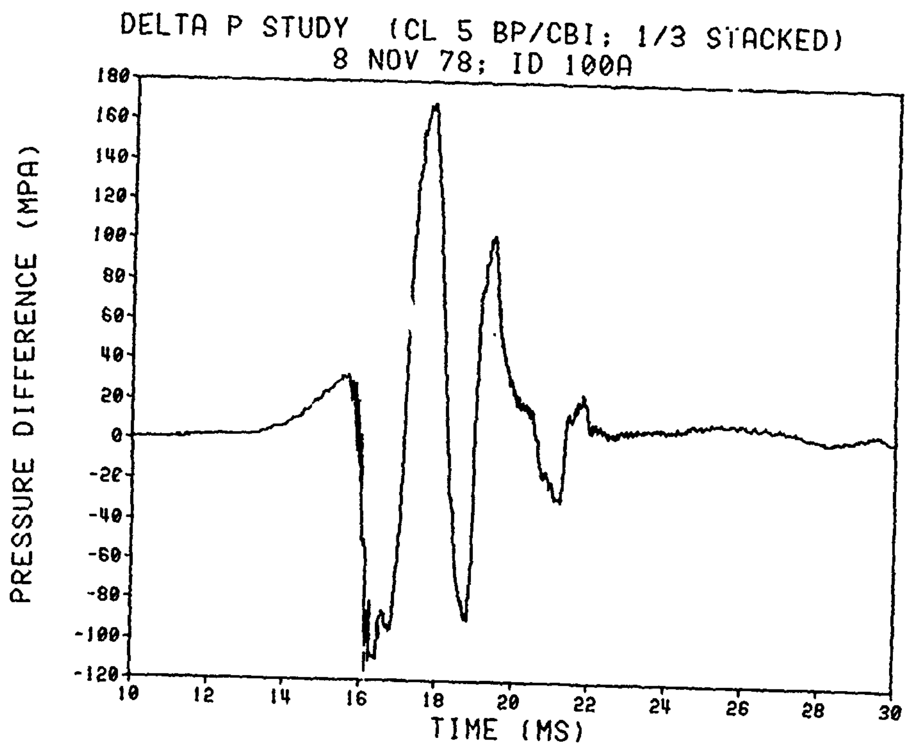
DELTA P STUDY (CL 5 BP/CBI; 1/3 STACKED)
8 NOV 78; ID 100A
PRESSURE DIFFERENCE (MPA)
TIME (MS)
180
160
140
120
100
80
60
40
20
0
-20
-40
-60
-80
-100
-120
10
12
14
16
18
20
22
24
26
28
30

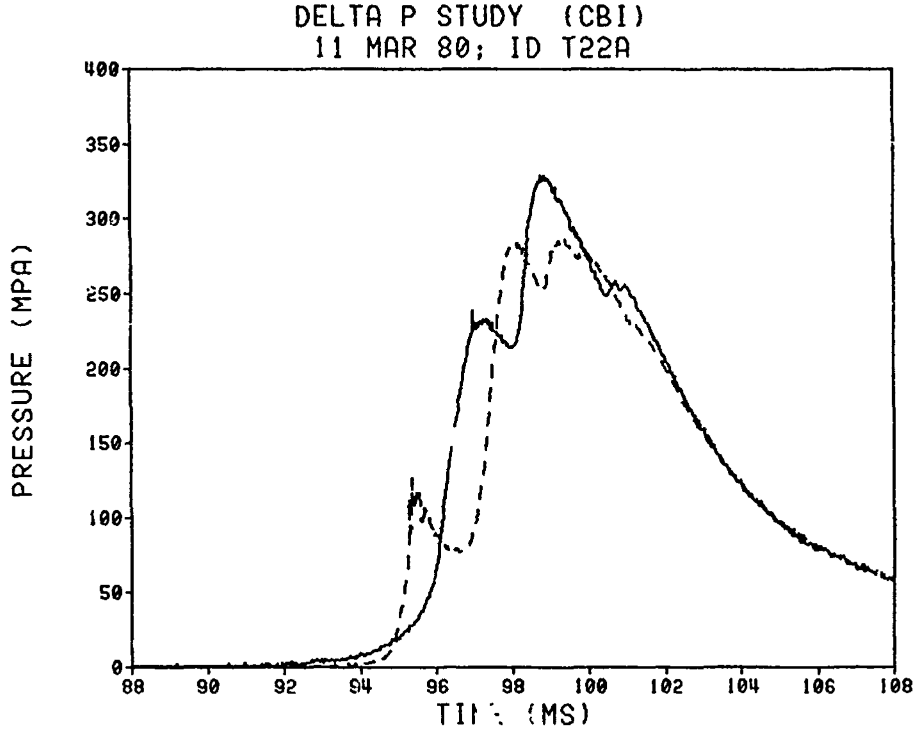
DELTA P STUDY (CBI)
11 MAR 80; ID T22A
PRESSURE (MPA)
TIME (MS)

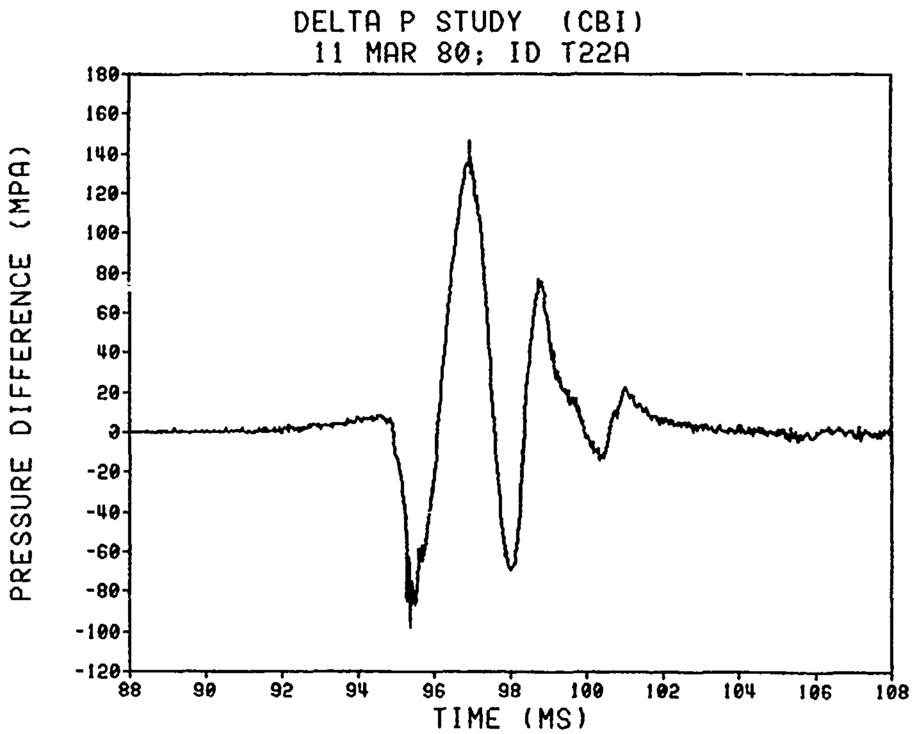
DELTA P STUDY (CBI)
11 MAR 80; ID T22A
PRESSURE DIFFERENCE (MPA)
TIME (MS)

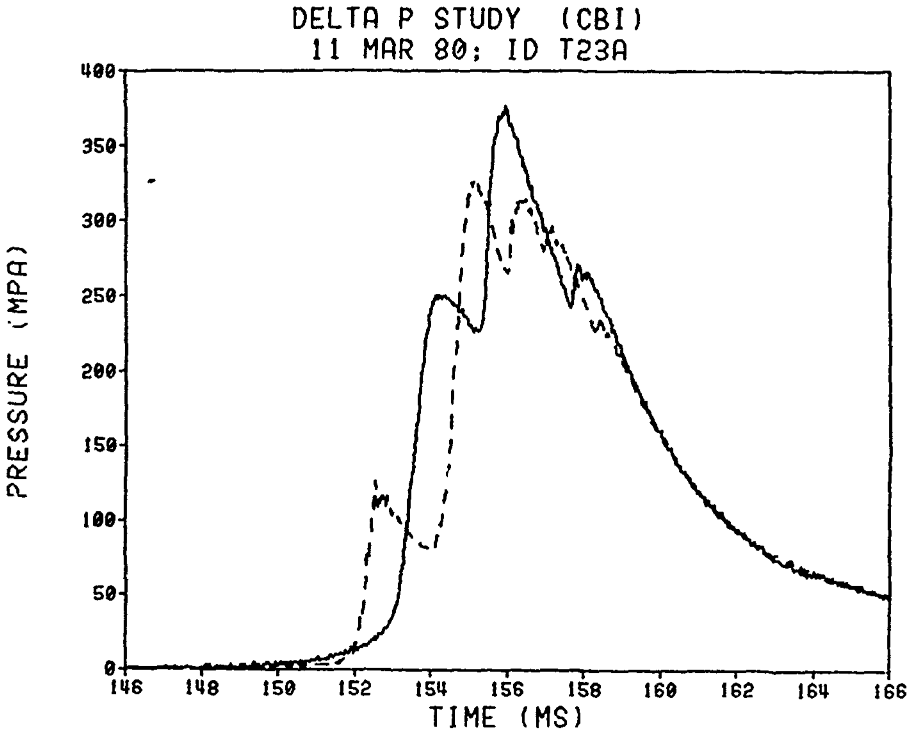

DELTA P STUDY (CBI)
11 MAR 80; ID T23A
PRESSURE (MPA)
400
350
300
250
200
150
100
50
0
146
148
150
152
154
156
158
160
162
164
166
TIME (MS)

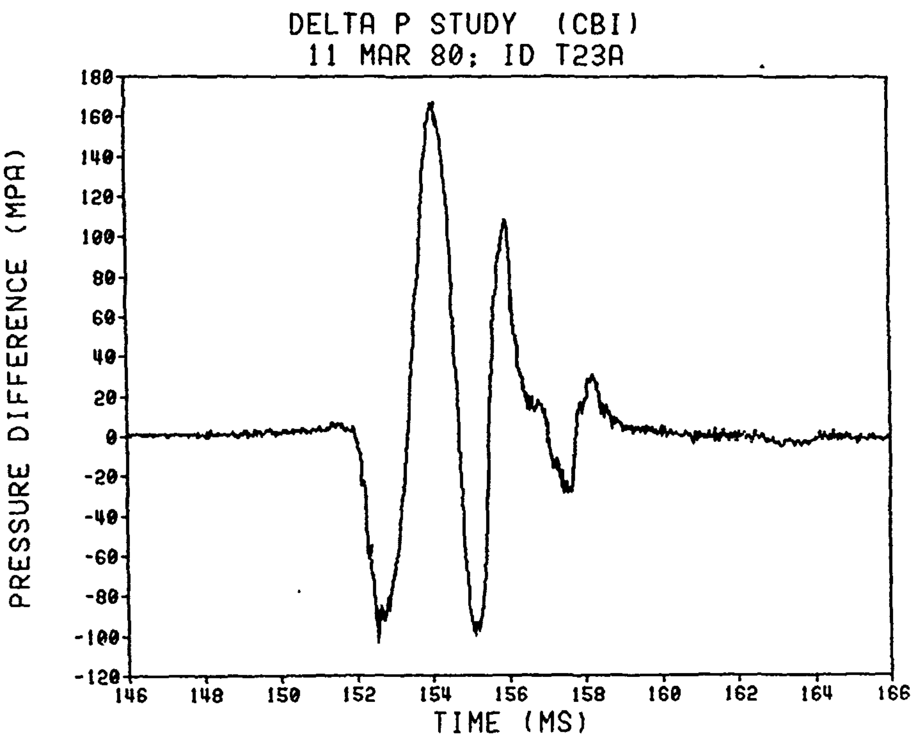

DELTA P STUDY (CBI)
11 MAR 80; ID T23A
PRESSURE DIFFERENCE (MPA)
180
160
140
120
100
80
60
40
20
0
-20
-40
-60
-80
-100
-120
146
148
150
152
154
156
158
160
162
164
166
TIME (MS)

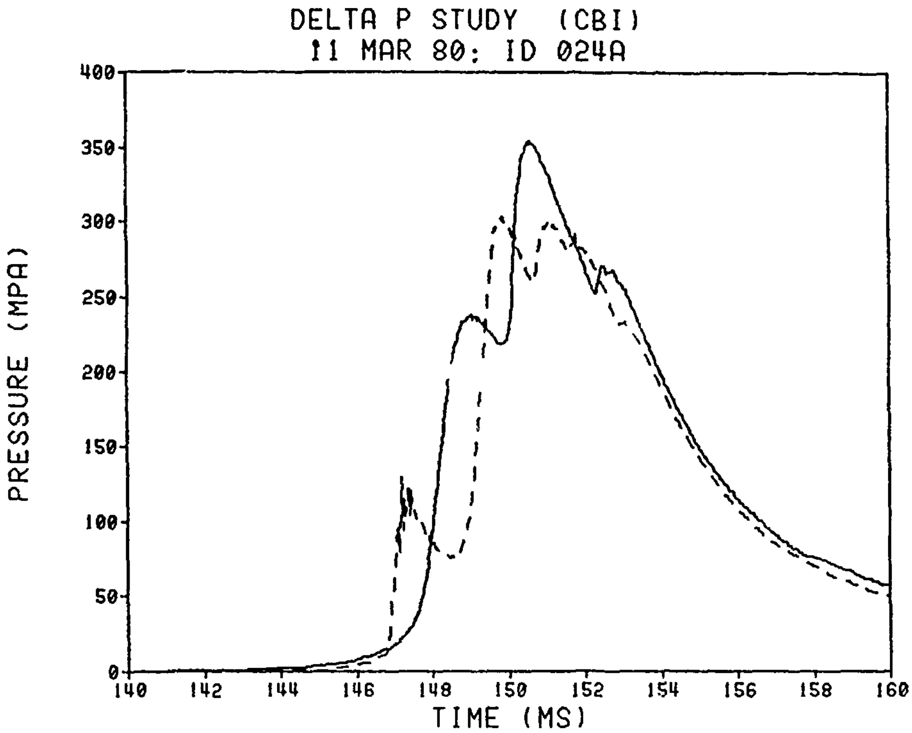

DELTA P STUDY (CBI)
11 MAR 80: ID 024A
PRESSURE (MPA)
TIME (MS)
0
50
100
150
200
250
300
350
400
140
142
144
146
148
150
152
154
156
158
160

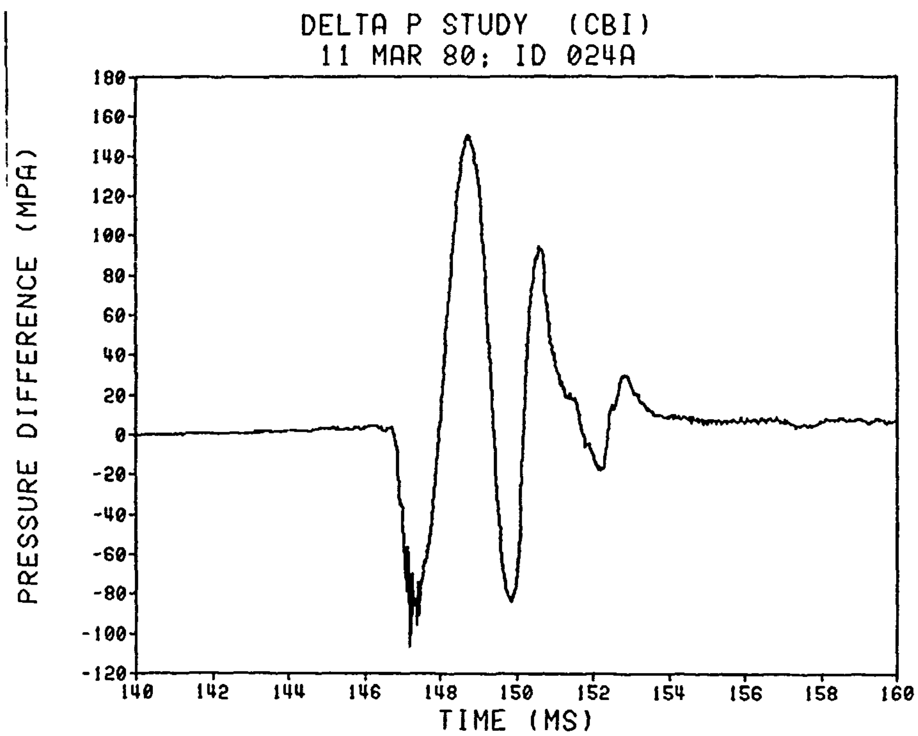

DELTA P STUDY (CBI)
11 MAR 80: ID 024A
PRESSURE DIFFERENCE (MPA)
TIME (MS)
-120
-100
-80
-60
-40
-20
0
20
40
60
80
100
120
140
160
180
140
142
144
146
148
150
152
154
156
158
160

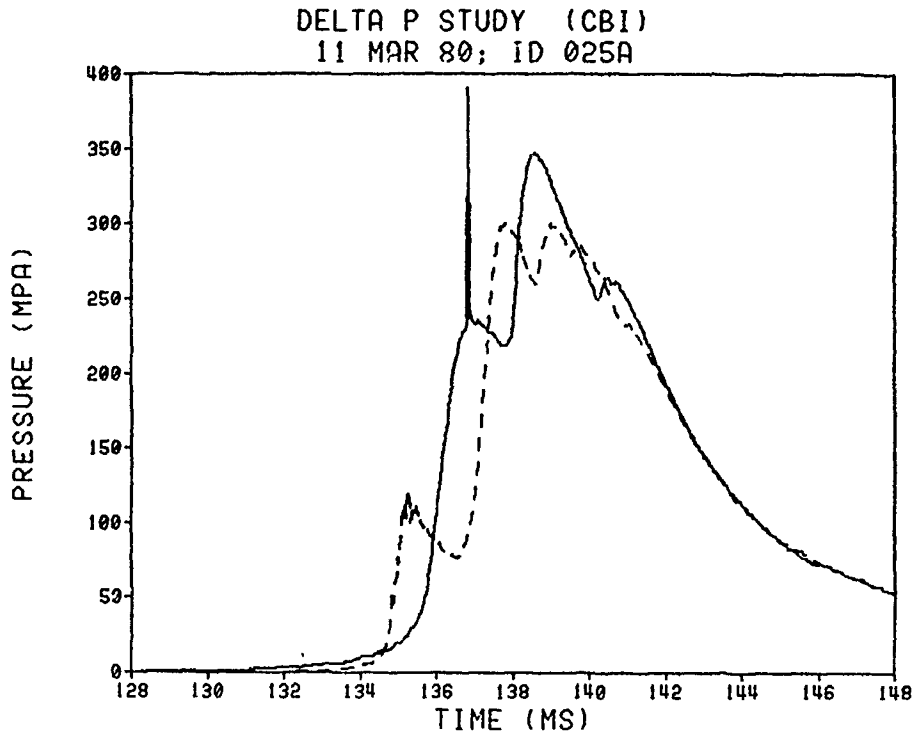
DELTA P STUDY (CBI)
11 MAR 80; ID 025A
PRESSURE (MPA)
0
50
100
150
200
250
300
350
400
TIME (MS)
128
130
132
134
136
138
140
142
144
146
148

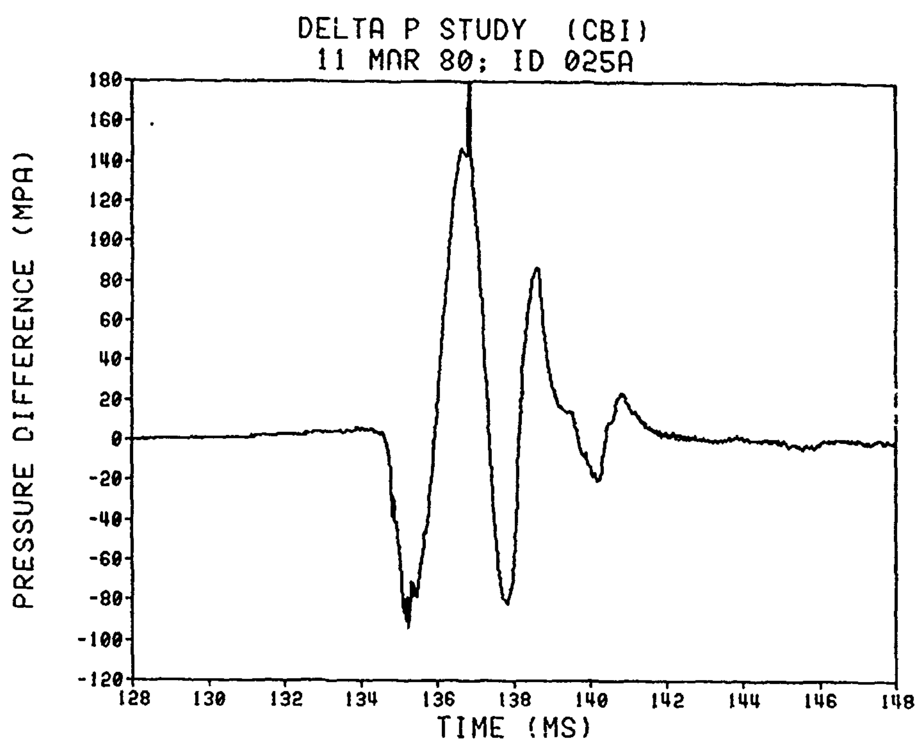
DELTA P STUDY (CBI)
11 MAR 80; ID 025A
PRESSURE DIFFERENCE (MPA)
-120
-100
-80
-60
-40
-20
0
20
40
60
80
100
120
140
160
180
TIME (MS)
128
130
132
134
136
138
140
142
144
146
148

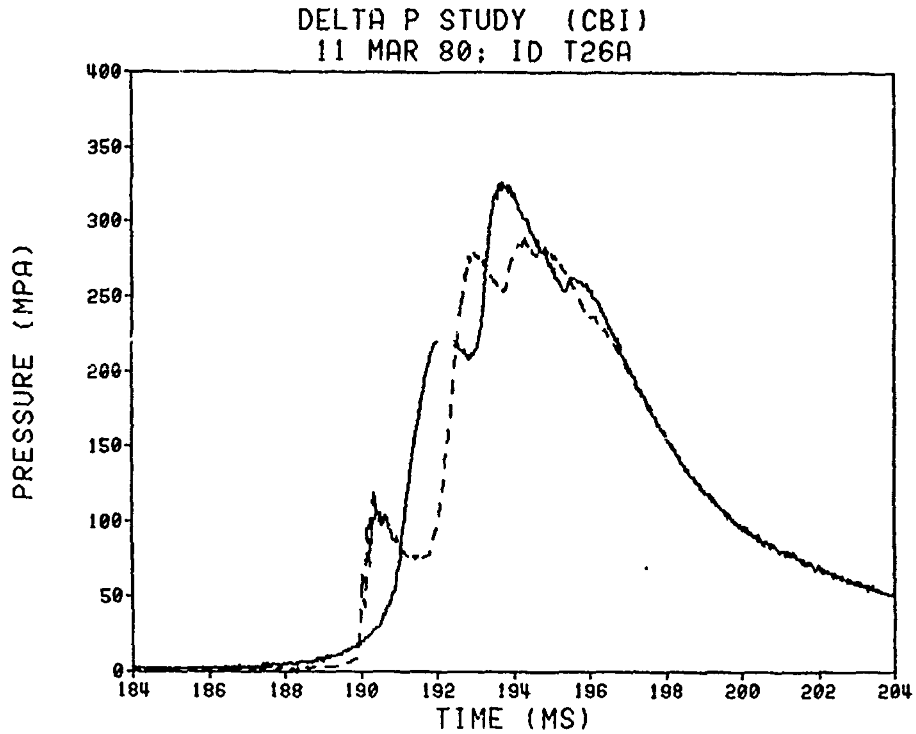
DELTA P STUDY (CBI)
11 MAR 80; ID T26A
PRESSURE (MPA)
400
350
300
250
200
150
100
50
0
184
186
188
190
192
194
196
198
200
202
204
TIME (MS)

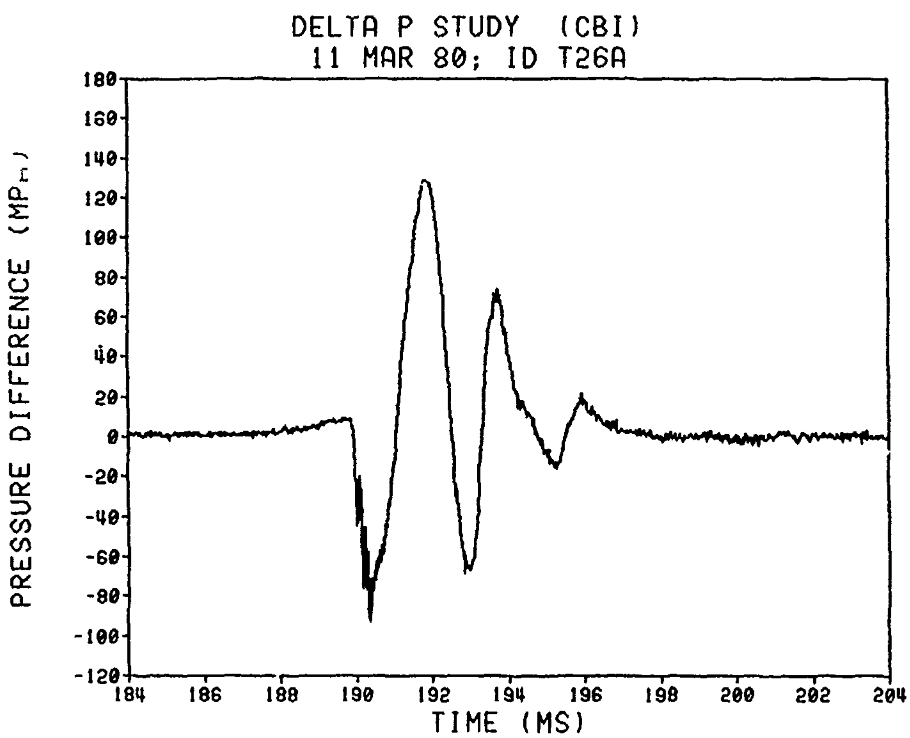
DELTA P STUDY (CBI)
11 MAR 80; ID T26A
PRESSURE DIFFERENCE (MPA)
180
160
140
120
100
80
60
40
20
0
-20
-40
-60
-80
-100
-120
184
186
188
190
192
194
196
198
200
202
204
TIME (MS)

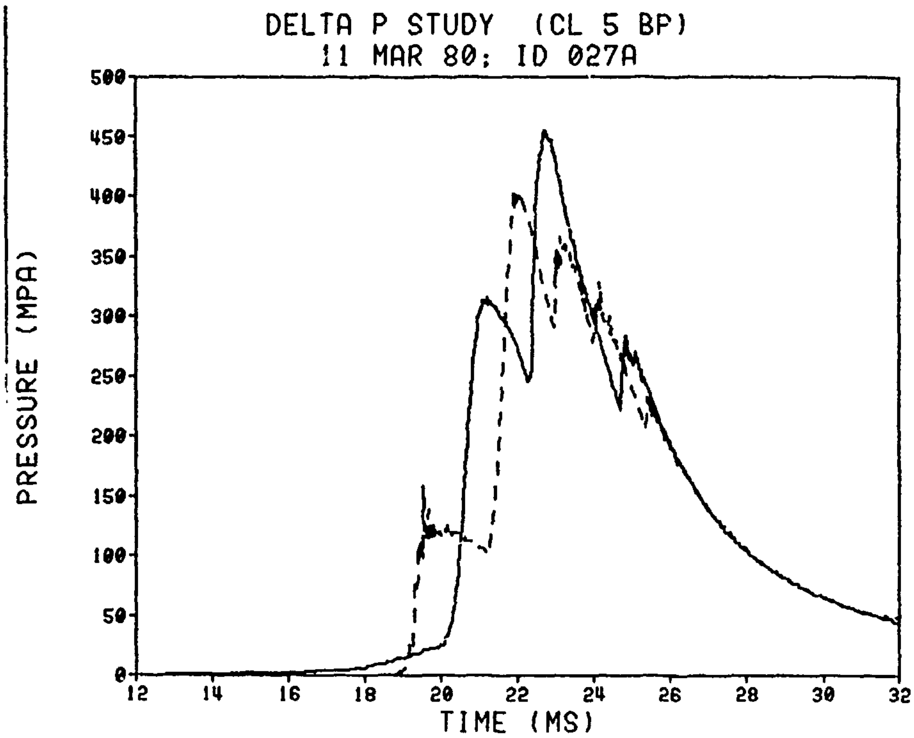
DELTA P STUDY (CL 5 BP)
11 MAR 80; ID 027A
PRESSURE (MPA)
TIME (MS)
500
450
400
350
300
250
200
150
100
50
0
12
14
16
18
20
22
24
26
28
30
32

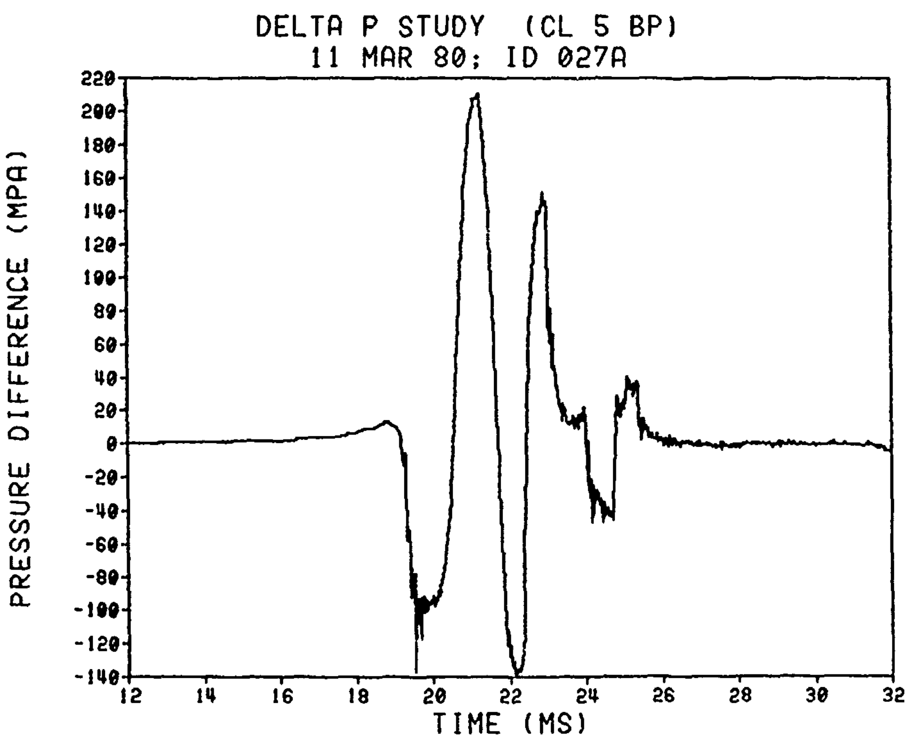
DELTA P STUDY (CL 5 BP)
11 MAR 80; ID 027A
PRESSURE DIFFERENCE (MPA)
TIME (MS)
220
200
180
160
140
120
100
80
60
40
20
0
-20
-40
-60
-80
-100
-120
-140
12
14
16
18
20
22
24
26
28
30
32

DISTRIBUTION LIST

No. of Copies	Organization
12	Commander Defense Technical Info Center ATTN: DTIC-DDA Cameron Station Alexandria, VA 22314
1	Commander US Army Materiel Development and Readiness Command ATTN: DRCDMD-ST 5001 Eisenhower Avenue Alexandria, VA 22333
1	Commander US Army Materiel Development and Readiness Command ATTN: DRCDE-DW 5001 Eisenhower Avenue Alexandria, VA 22333
1	Commander US Army Aviation Research and Development Command ATTN: DRDAV-E 4300 Goodfellow Blvd St. Louis, MO 63120
1	Director US Army ARRADCOM Benet Weapons Laboratory ATTN: DRDAR-LCB-TL Watervliet, NY 12189
2	Commander USA ARRADCOM ATTN: DRDAR-LCB, W. Austin J. Busuttil Watervliet Arsenal Watervliet, NY 12189
1	Director US Army Air Mobility Research and Development Laboratory Ames Research Center Moffett Field, CA 94035

No. of Copies	Organization
1	Commander US Army Electronics Research and Development Command Technical Support Activity ATTN: DELSD-L Fort Monmouth, NJ 07703
1	Commander US Army Communications Research and Development Command ATTN: DRDCO-PPA-SA Fort Monmouth, NJ 07703
2	Commander US Army Missile Research and Development Command ATTN: DRDMI-R DRDMI-YDL Redstone Arsenal, AL 35809
1	Commander US Army Tank Automotive Research and Development Command ATTN: DRDTA-UL Warren, MI 48090
10	Commander US Army Armament R&D Command ATTN: DRDAR-TSS (2 cys) DRDAR-LCA S. Bernstein D. Downs L. Schlosberg G. Bubb L. Rosendorf DRDAR-LCE-R. Walker DRDAR-SCA-L. Stiefel DRDAR-TSF-L. Goldsmith Dover, NJ 07801

DISTRIBUTION LIST

No. of Copies	Organization
2	Commander US Army Materials and Mechanics Research Center ATTN: DRXMR-ATL Tech Library Watertown, MA 02172
1	Commander US Army Natick Research and Development Command ATTN: DRXRE, D. Sieling Natick, MA 01762
1	Commander US Army Armament Materiel Readiness Command ATTN: DRDAR-LEP-L, Tech Library Rock Island, IL 61299
1	Commander US Army Watervliet Arsenal ATTN: SARWV-RD, R. Thierry Watervliet, NY 12189
1	Director US Army TRADOC Systems Analysis Activity ATTN: ATAA-SL, Tech Library White Sands Missile Range, NM 88002
1	Project Manager Cannon Artillery Weapons Systems ATTN: DRCPM-CAWS-AM, F. Menke Dover, NJ 07801
2	Commander US Army Materiel Testing Directorate ATTN: STEYP-MTC, W. Phillips J. Gallett Yuma Proving Ground Yuma, AZ 85364

No. of Copies	Organization
1	Director Tonapah Test Range Division 1173 ATTN: J. Patrick P.O. Box 871 Tonapah, NV 89049
2	Commander US Army Yuma Proving Ground ATTN: STEYP-MT, W. Taylor R. Bartlett Yuma, AZ 85364
2	Commander US Army Dugway Proving Ground ATTN: STEDP-MT, W. Dyer J. Deale Dugway, UT 84022
1	Commander US Army Materiel Testing Directorate ATTN: STEJP-MT, V. Gudkese Jefferson Proving Ground Madison, IN 47251
1	Commander Hawthorne Army Ammo Plant ATTN: V. Miller Hawthorne, CA 90250
1	Commander US Army Research Office ATTN: Tech Library P.O. Box 12211 Research Triangle Park, NC 27709
1	Chief Naval Research ATTN: Code 473, R. Miller 800 N. Quincy Street Arlington, VA 22217

DISTRIBUTION LIST

No. of Copies	Organization	No. of Copies	Organization
3	Commander US Naval Surface Weapons Center ATTN: Code G33, J. East D. McClure Code DX-21 Tech Library Dahlgren, VA 22448	1	Princeton Combustion Research Laboratories, Inc. ATTN: M. Summerfield 1041 US Highway One North Princeton, NJ 08540
2	Commander US Naval Surface Weapons Center ATTN: S. Jacobs/Code 240 Code 730 Silver Spring, MD 20910	1	General Electric Company Armament Systems Department ATTN: M. Bulman, Room 1311 Lakeside Avenue Burlington, VT 05402
2	Commander US Naval Weapons Center ATTN: Code 388, R. Derr C. Price China Lake, CA 93555	1	Lawrence Livermore Laboratory ATTN: M.S. L-355, A. Buckingham P.O. Box 808 Livermore, CA 94550
1	Superintendent US Naval Postgraduate School Dept. of Mechanical Engineering ATTN: A. Fuhs Monterey, CA 93940	1	Paul Gough Associates, Inc. ATTN: P. Gough P.O. Box 1614 Portsmouth, NH 03801
2	Commanding Officer US Naval Ordnance Station ATTN: P. Stang C. Smith Indian Head, MD 20640	1	Sandia Laboratories ATTN: Div 1548, W. Hartman Albuquerque, NM 87115
1	AFATL/DLDL ATTN: Dr. D. C. Daniel Eglin AFB, FL 32542	1	Battelle Memorial Institute ATTN: Tech Library 505 King Avenue Columbus, OH 43201
2	AFRPL (DYSC) ATTN: D. George J. Levine Edwards AFB, CA 93523	1	Johns Hopkins University Applied Physics Laboratory Chemical Propulsion Information Agency ATTN: T. Christian Johns Hopkins Road Laurel, MD 20810
1	Calspan Corporation ATTN: E. Fisher P.O. Box 400 Buffalo, NY 14221	1	Pennsylvania State University Dept. of Mechanical Engineering ATTN: K. Kuo University Park, PA 16802

DISTRIBUTION LIST

No. of Copies	Organization
1	James Forestal Campus Princeton University Dept. of Aerospace and Mechan- ical Science ATTN: M. Summerfield Princeton, NJ 08540
1	University of California Los Alamos Scientific Lab ATTN: T3, D. Butler Los Alamos, NM 87545

Aberdeen Proving Ground

Dir, USAMSAA
ATTN: DRXSY-D
DRXSY-MP, H. Cohen
Cdr, USATECOM
ATTN: DRSTE-TO-F
Dir, USACSL, Bldg. E3516, EA
ATTN: DRDAR-CLB-PA

USER EVALUATION OF REPORT

Please take a few minutes to answer the questions below; tear out this sheet, fold as indicated, staple or tape closed, and place in the mail. Your comments will provide us with information for improving future reports.

1. BRL Report Number ______________________________

2. Does this report satisfy a need? (Comment on purpose, related project, or other area of interest for which report will be used.)

____

____

____

3. How, specifically, is the report being used? (Information source, design data or procedure, management procedure, source of ideas, etc.) ______________________________

____

____

4. Has the information in this report led to any quantitative savings as far as man-hours/contract dollars saved, operating costs avoided, efficiencies achieved, etc.? If so, please elaborate.

____

____

5. General Comments (Indicate what you think should be changed to make this report and future reports of this type more responsive to your needs, more usable, improve readability, etc.) __________

____

____

____

6. If you would like to be contacted by the personnel who prepared this report to raise specific questions or discuss the topic, please fill in the following information.

Name: ______________________________

Telephone Number: ______________________________

Organization Address: ______________________________

____

____

— — — — — — — — — — — FOLD HERE — — — — — — — — — — —

Director
US Army Ballistic Research Laboratory
Aberdeen Proving Ground, MD 21005

OFFICIAL BUSINESS

PENALTY FOR PRIVATE USE, $300

NO POSTAGE
NECESSARY
IF MAILED
IN THE
UNITED STATES

BUSINESS REPLY MAIL

FIRST CLASS PERMIT NO 12062 WASHINGTON,DC

POSTAGE WILL BE PAID BY DEPARTMENT OF THE ARMY

Director
US Army Ballistic Research Laboratory
ATTN: DRDAR-TSB
Aberdeen Proving Ground, MD 21005

— — — — — — — — — — FOLD HERE — — — — — — — — — —